Generation of *in vitro* data to model dose dependent *in vivo* DNA binding of genotoxic carcinogens and its consequences:
-the case of estragole-

Alicia Paini

Thesis committee

Thesis supervisors
Prof. dr. ir. I.M.C.M. Rietjens
Professor of Toxicology
Wageningen University

Prof. dr. P.J. van Bladeren
Professor of Toxico-kinetics and Biotransformation
Division of Toxicology
Wageningen University

Thesis co-supervisor
Dr. G. Scholz
Project Manager – Chemical Food Safety - Quality & Safety Department
Nestlé Research Center
Lausanne, Switzerland

Other members
Prof. dr. B.J. Blaauboer (Utrecht University)
Dr. J.M. O'Brien (Nestlé Research Center, Lausanne, Switzerland)
Dr. M. Verwei (TNO, Zeist)
Prof. dr. R.F. Witkamp (Wageningen University)

Generation of *in vitro* data to model dose dependent *in vivo* DNA binding of genotoxic carcinogens and its consequences: -the case of estragole-

Alicia Paini

Thesis
submitted in fulfilment of the requirements for the degree of doctor
at Wageningen University
by the authority of the Rector Magnificus
Prof. dr. M.J. Kropff,
in the presence of the
Thesis Committee appointed by the Academic Board
to be defended in public
on Monday 26 March 2012
at 11 a.m. in the Aula.

What we do in life will echo in eternity (The Gladiator)

A Anna & Isa

Content

Chapter 1

General introduction, aim, outline of thesis

1.1 Short description and aim of the thesis

Our food contains several compounds which, when tested in isolated form at high doses in animal experiments, have been shown to be genotoxic and carcinogenic. At the present state-of-the-art there is no scientific consensus on how to perform the risk assessment of these compounds when present at low levels in a complex food matrix. In order to refine the evaluation of the risks associated with these food-borne genotoxic carcinogens, information on their mode of action (MOA) at low versus high doses, on species differences in toxicokinetics and toxicodynamics, including dose- and species- dependent occurrence of DNA damage and repair, and on effects on expression of relevant enzymes, is required. For modern Toxicology it is of importance to better understand the MOA of genotoxic carcinogens to which humans are exposed daily via the diet at low doses. Genotoxic compounds can be direct acting when the compound is reactive itself and binds to the molecular target, or may need to be bioactivated before interacting with the molecular target. Bioactivation of a compound usually proceeds by phase I and/or phase II enzymatic pathways. When a genotoxic compound binds covalently to DNA it can form adducts with the four bases of the double helix. For all of these compounds the biological effect is a sum of both kinetic (absorption, distribution, metabolism and excretion) and dynamic (ultimate reaction with the molecular target) mechanisms. The model genotoxic carcinogenic compound studied in the present thesis is estragole (Figure 1.1). Estragole is an alkenylbenzene, found in herbs and spices, to which humans are exposed at low doses via the diet. Once absorbed estragole can undergo detoxification and bioactivation through phase I and II enzymatic pathways, resulting in the compound being either excreted or converted to a reactive carbocation which binds covalently to DNA. Estragole is known to produce tumors in rodents exposed to high dose levels (Miller *et al.*, 1983) and it has been characterised as genotoxic and carcinogenic.
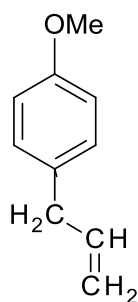
Figure 1.1 Estragole structure

The aim of the present thesis was to develop new strategies for low dose cancer risk assessment of estragole by extending the PBBK models previously defined for estragole to so-called physiologically based biodynamic (PBBD) models for DNA adduct formation, taking the approach one step closer to the ultimate endpoint of tumor formation. Such models will facilitate risk assessment because they facilitate extrapolation from high to low dose levels, between species including human and between individuals. Furthermore, building the PBBD models predicting *in vivo* DNA adduct formation based on only *in vitro* parameters contributes to the 3Rs (Replacement, Reduction and Refinement) for animal testing.

The following sections present an overview of the basic principles of importance for the present thesis including an introduction to chemical carcinogenesis, to cancer risk assessment strategies, to physiologically based biokinetic (PBBK) and physiologically based biodynamic (PBBD) models, and to estragole, the model compound used in the present thesis.

1.2 Chemical Carcinogenesis: a multi-step process

Cancer is an important disease in the western world. Important factors contributing to cancer development in the human population are lifestyle, dietary, occupational, and environmental factors; as well as genetic predisposition, functioning of the immune system, and hormone dependent modulations. The first link between external factors and tumor incidence was described in 1775 in London, where the physician Percival Pott related tumor incidence and environmental chemical agents when he noted a high incidence of scrotal cancer among chimney sweeps (Shimkin, 1975). His hypothesis was that this scrotal cancer among chimney sweeps was caused by their exposure to coals and tars. Since Pott's observations a wide range of chemicals, radiation sources, viruses and bacteria have been implicated in the development of tumors.

The induction of cancer by chemicals is a complex process that involves a series of steps, proceeding from the neoplastic conversion of a normal cell to the final malignant neoplasm. Cancer development has been divided into three stages including initiation, promotion, and progression, each of which may consist of several steps leading to cancer development being known as a multi step process. **Initiation**, which is considered an irreversible genetic change, involves direct DNA reactivity usually resulting in DNA damage and/or DNA adduct formation which, upon subsequent steps may ultimately lead to a gene mutation. The rate of initiation of a genotoxic event may vary between various chemicals in the same tissue and between the different tissues depending on enzymatic bioactivation, DNA damage formation and DNA repair in a cell and the growth rate of the cell (Barrett, 1993; van Gijssel 1999). The **promotion** step is a slow reversible process which needs continuous stimulation and during which cells generally change their enzyme expression patterns (Pitot, 1996). Cells are provoked to proliferate, involving a variety of cellular mechanisms, with an increased rate of proliferation or a decreased rate of apoptosis leading to clonal expansion/growth. Clonal expansion leads to tumor **progression,** the last stage of carcinogenesis, and this phase proceeds from a reversible stage to a (potentially malignant) irreversible stage (Barrett, 1993) forming metastasis and neoplasms (**tumors**).

1.2.1 Chemical Carcinogenesis: DNA damage and DNA adducts

The term 'DNA damage' defines a heterogeneous group of chemical and physical alterations of the DNA double helix. DNA damage may be caused by exogenous agents such as UV or radioactive irradiation or natural or man-made chemicals. These factors can cause various lesions, e.g. UV-induced crosslinks between adjacent cytosine and thymine bases, DNA strand breaks through ionising radiation, and a large variety of DNA bulky adducts induced by numerous industrial, environmental, or natural chemicals. Reactive electrophiles can form DNA adducts through covalent reactions with double stranded DNA by S_N1 or S_N2 mechanisms. Alkylating agents that react directly with biologic molecules follow an S_N1 mechanisms and the

S_N2 mechanism is for those alkylating agents that form a reactive intermediate, which then reacts with the biologic molecules (Colvin, 2000). Alkylating agents reacting by a S_N2 mechanism show greater affinity for the ring nitrogens in the DNA bases, being the most nucleophilic sites in the DNA bases (Osborne, 1984, Phillips 2007). When the S_N1 reaction occurs the reaction will be predominant on the exocyclic groups (reviewed in Philips, 2007). DNA adducts are structurally diverse and are not equally mutagenic, since the chemical compound can react with more than one DNA base and at different sites (Figure 1.2) resulting in different DNA adducts affecting different genes. Examples of such reactive sites in DNA bases are indicated by an arrow in Figure 1.2. Guanine is the DNA base that reacts more frequently, with interactions occurring most frequently at its N^2, N-3, O^6, N-7 and C-8 position. Adducts with adenine are formed at the N-1, N-3, N^6, N-7 position. For cytosine the preferential reaction sites are O^2, N-3, N^4, and C-5, and for thymine O^2 and O^4 (reviewed in Phillips, 2007). In addition to external factors, DNA damage can be caused by endogenous factors such as attack by reactive oxygen species produced by normal metabolic pathways or by products from lipid peroxidation such as hydroxynonenal, malonaldehyde, acrolein, or crotonaldehyde (De Bont and van Larebeke, 2004). There are four main types of damage to DNA due to endogenous cellular processes: oxidation of bases (e.g. 8-hydroxy-deoxyguanosine); alkylation of bases (methylation, ethylation), such as formation of N7-methylguanine; hydrolysis of bases, such as deamination, depurination and depyrimidination; mismatch of bases, due to DNA replication in which the wrong DNA base is stitched into place in a newly forming DNA strand. The background level for DNA oxidation in human has been found to range from 7 to 5279 adducts in 10^8 nucleotides (nt) (reviewed in De Bont and van Larebeke, 2004). DNA adducts formed by products from lipid peroxidation may result in background levels that range from 0.6 to 90 adducts in 10^8 nt. The background level of alkylated adducts in human DNA is thought to be at least 0.6-190 modification in 10^8 nt (reviewed in De Bont and van Larebeke, 2004) and similar levels of 10 to 100 modification in 10^8 nt were reported by Farmer *et al.* (2005). The general background is estimated to amount to 10-100 adducts in 10^8 nt (Williams, 2008; Farmer *et al.,* 2005; Farmer, 2008); adduct levels below this back ground level have been considered to be of no toxicological consequence (Williams, 2008).
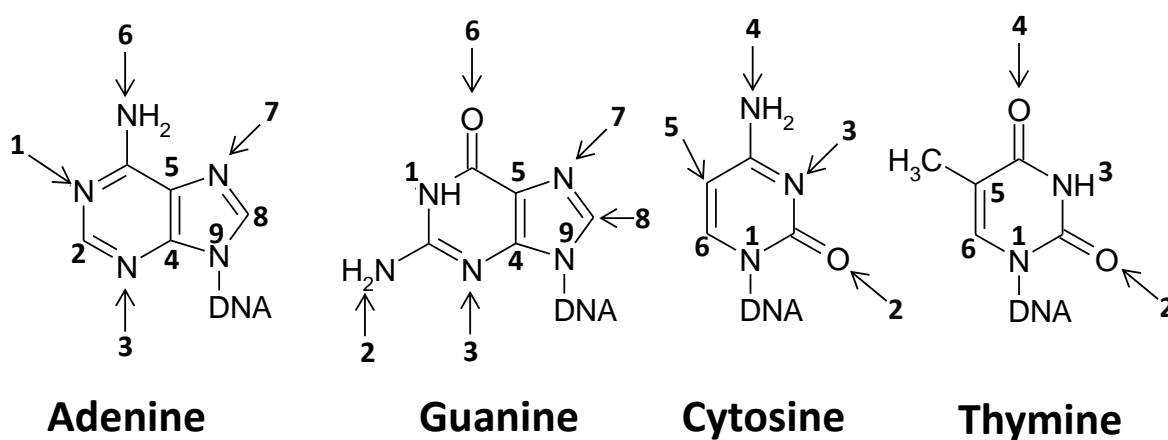

Figure 1.2. DNA bases and sites at which genotoxic compounds can covalently bind and form DNA adducts (adapted from Phillips, 2007).

1.2.2 Analytical methods to measure DNA adducts

Analytical techniques used to measure DNA adduct formation in different tissues, blood, and urine (e.g. 8-hydroxy-deoxyguanosine) are continuously improving, both qualitatively and quantitatively. The currently most used analytical methods in the field of DNA adduct measurements include: ^{32}P-postlabeling, immunoassays, HPLC/ECD, LC-MS/MS, GC-MS/MS, and accelerator mass spectrometry (Farmer *et al.*, 2005). Table 1.1 presents the techniques and their main characteristics with respect to sensitivity. ^{32}P-postlabeling is a highly sensitive method which needs only small amounts of DNA (Himmelstein *et al.*, 2009; Randerath *et al.*, 1981) and it is a widely applied method for the detection of DNA adducts. However a limitation of the ^{32}P-postlabeling method is the potential for underestimation of the adduct levels due to incomplete DNA digestion, submaximal efficiency of adduct labeling by polynucleotide kinase and/or loss of adducts during enrichment and chromatography stages (Phillips and Arlt, 2007). For example for aflatoxin B1 (AfB1), the N-7 guanine adduct is the predominant adduct formed, but this AfB1 adduct appears to be poorly labelled by ^{32}P-postlabeling, and a different analytical technique ^{3}H/HPLC, is required for its quantification (Phillips and Arlt, 2007).

Table 1.1 Analytical methods for detection of DNA adduct (Adapted from Farmer *et al.*, 2005).

	Maximum sensitivity (adduct/nucleotide)	Amount of DNA (µg)
Immunoassays	Ca $1/10^8$	1-100
Mass Spectrometry (MS):		
LC-MS/MS; GC-MS/MS.	Ca $1/10^8$	1-100
HPLC/ECD- Fluorescence	Ca $1/10^8$	1-100
^{32}P-postlabeling	Ca $1/10^{10}$	1-10
Accelerator MS (AMS)	Ca $1/10^{12}$	1-2000

Immunoassays, where antisera elicited against the carcinogen-DNA adduct are used, is a highly sensitive method but generally needs more DNA adducts as compared to the ^{32}P-postlabeling technique (Phillips, 2005; 2007). Mass Spectrometry (MS) is the most selective method for DNA adduct detection. LC-MS/MS or the variant GC-MS/MS, are the most popular methods used. By using stable isotope adducts as internal standards in the samples LC-MS/MS achieves accurate quantification of DNA adducts along with specific structural characterization (Phillips, 2005; 2007). LC-MS/MS is also the method used in the present thesis for quantification of the estragole DNA adducts. At present, Accelerator Mass Spectrometry (AMS) is the most sensitive technique available for detection of DNA adducts, since this technique can detect and quantify DNA adducts at levels of about 1 adduct in 10^{12} ($1/10^{12}$) nt (Farmer *et al.*, 2005).

1.2.3 DNA adduct data in Risk Assessment

As outlined in the previous section formation of DNA adducts can play a role in the mode of action of genotoxic carcinogens. However, although DNA adduct formation can be considered an important step in the initiation of carcinogenesis, and reduction of DNA adduct formation generally results in reduced tumor incidence (Adriaenssens *et al.*, 1983; Hecht, 2003) DNA adducts are generally considered to represent biomarkers of exposure rather than biomarkers of effect (Farmer 2004 a, b). Several attempts have been made to correlate the occurrence of DNA adducts with the carcinogenic outcome (see paragraph 1.5), but the significance of their formation in the risk assessment, especially with respect to the discussion and justification of possible thresholds is a matter of ongoing debate (Sander *et al.*, 2005; EFSA, 2005; Pottenger *et al.*, 2009). The potential for the use of DNA adduct data for risk assessment was addressed in an ILSI/HESI and ECETOC workshop in 2004 (Sander *et al.*, 2005) and in 2008 (Pottenger *et al.*, 2009). In addition, no consensus was reached with regards to the biological significance of low levels of DNA adducts in the EFSA meeting in Brussels in 2005. The meeting rather identified the need for more experimental data and new approaches to address this issue (EFSA, 2005; Barlow *et al.,* 2006).

1.2.4 Chemical Carcinogenesis: DNA repair

The first and most critical cellular response to DNA damage is the attempt to repair the DNA lesion (Figure 1.3). DNA repair does not proceed in isolation but occurs in the context of ongoing cellular processes such as gene transcription, DNA replication, chromatin organization and cell cycle progression. The manifestation of DNA lesions into mutations or chromosomal aberrations and finally into tumorigenic transformation essentially depends on the presence and efficiency of repair mechanisms. Cells are able to respond to DNA damage by various mechanisms, which depend on the type of lesion. DNA repair mechanisms are classified into the following types: mismatch repair (MMR); base excision repair (BER); nucleotide excision repair (NER); direct damage reversal (DDR) and DNA double strand break repair (DSBR).
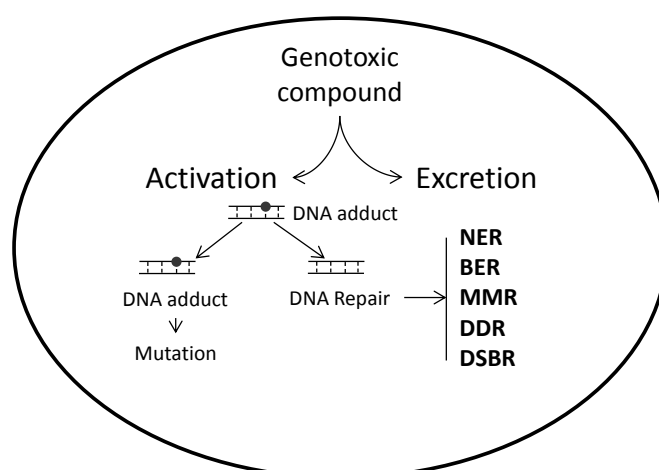

Figure 1.3. Schematic representation of bioactivation of a genotoxic compound followed by formation of DNA adducts which can result in a mutation if not repaired. DNA repair mechanisms include: mismatch repair (MMR); base excision repair (BER); nucleotide excision repair (NER); direct damage reversal (DDR) and DNA double strand breaks repair (DSBR).

However, repair mechanisms are not always completely effective, and residual DNA damage can lead to insertion of an incorrect base during replication followed by transcription and translation, leading to synthesis of altered/mutated protein (Klaunig and Kamendulis, 2007). The following text presents in brief a few examples of DNA damage and repair. Oxidative damage typically induces 8-hydroxy-deoxyguanosine, a marker of oxidative DNA damage, that is repaired by BER (Hwang and Bowen, 2007; Klaunig et al., 2010; Valavanidis et al, 2011). Methylated bases (caused by alkylating agents) at the N3 or N7 position can be removed by DNA glycosylases as part of BER (Wyatt and Pittman, 2006). Such N-alkylpurines are susceptible to spontaneous hydrolysis resulting in abasic sites, which are also repaired by BER. Methylation at the O6 position causes G-C to A-T mutations, and is recognized by the mismatch repair system (MMR). MMR also recognizes spontaneous mismatches, intra strand crosslinks, UV induced photoproducts, 8-oxoguanine and various chemical induced adducts (Wyatt and Pittman, 2006). Bulky adducts as well as crosslinks caused by UV light, intra strand crosslinks, single strand breaks, adducts of aflatoxin and benzo[a]pyrene are repaired by NER. NER repairs damage in longer strands of 2-30 bases, while BER recognizes especially damaged single nucleotides (Watson et al., 2004). Double-strand breaks (DSB), in which both strands in the double helix are detached, are particularly hazardous to the cell because they can lead to genome rearrangements. DSBs result from disruption of the phosphodiester backbone on both strands of the DNA double helix. They may be induced by ionizing radiation, x-rays, UV light, some chemicals, including anticancer drugs, or arise spontaneously during DNA replication. They may also result from programmed action of endonucleases or can occur as intermediates in DNA excision repair (Pastwa and Blasiak, 2003). Two DSBR mechanisms exist to repair DSB: homologous recombination (HR) and non-homologous end joining (NHEJ). HR is predominant in simple eukaryotes like yeast, whereas NHEJ is the main pathway in mammals (Christmann *et al.*, 2003).

1.2.5 Chemical Carcinogenesis: Gene and Protein regulation

Mechanisms leading to mutations and disease may be detected by changes in expression of genes and proteins. Changes in protein and gene expression profiles induced by a genotoxic compound play a role in signal transduction mechanisms, metabolic pathways and protective responses in a cell (Heijne, 2004). Distinguishing between gene and chromosome level DNA changes, or at least the extent of the DNA change involved in a mutation, does have some utility for predicting the shapes of the dose-response curves for inducing such effects (Swenberg *et al.,* 2008). For example, single gene mutations resulting from a base substitution or a small deletion or insertion (point mutations) can arise from the mishandling of an unrepaired DNA adduct (of the appropriate kind) during DNA replication. Of interest is to study the biological effects of DNA adduct formation by gene expression profiling with emphasis on expression of proteins involved in DNA repair mechanisms. The different DNA repair mechanisms (paragraph 1.2.4) are supported by 130 genes involved in different distinct repair processes (Wood *et al*, 2001). If not repaired, DNA lesions can be misread by DNA polymerases, leading to heritable mutations (La and Swenberg, 1996). Some DNA lesions directly induce the expression of specific cascade events. Insight in DNA adduct formation and DNA repair by applying gene and protein expression analysis will help to refine the knowledge on the MOA of genotoxic compounds.

1.3 Quantitative relationship between DNA adducts and tumor formation

In literature several papers attempt to find a quantitative relationship between DNA adducts and tumor formation. Poirier *et al.* (1992) compared the dose response relationships for tumor formation (chronic exposure) and specific DNA adduct levels (4-8 weeks exposure) in target organs in rodents for well-known genotoxic carcinogens. The correlations found were variable. The formation of DNA adducts seemed linear, or linear at low doses and saturable at high doses for most of the compounds, which did not necessarily correlate with the curves for tumor incidences. For instance, AfB1 and diethylnitrosamine (DEN) showed clearly correlated linear dose responses for both adducts and liver tumor incidence. The dose response for 2-acetylaminofluorene (2-AAF) was target organ specific: DNA adducts and tumor incidences in liver were linear and correlated, whereas in bladder, only the response for DNA adducts was linear, while the response for tumors was nonlinear. No tumors were found at low doses of 30 to 75 mg/kg in the diet of 2-AAF and tumors were only found at the highest doses of 100 and 150 mg/kg in diet. For 4-aminobiphenyl (4-ABP), DNA adduct formation was linear, but no tumors were found at low doses neither in liver nor in bladder. The response to 4-ABP was, furthermore, sex specific. Both the formation of tumors and DNA adducts showed saturable dose responses at 100 mg/L in drinking water in females only. In addition, the number of DNA adducts did not necessarily indicate the carcinogenic potency. The different responses between the genotoxic carcinogens were discussed to be potentially related to kinetics, to effective detoxification, metabolic saturation of bioactivation, different metabolic pathways at different doses, additional induction of cell proliferation or toxicity at high doses, and DNA repair (Poirier *et al.*, 1992). In another study by Otteneder and Lutz (1999), a correlation was found between DNA adduct levels in target organs and tumor incidences in both rats and mice for 27 well known hepatocarcinogens. In rat liver, the calculated adduct concentration 'responsible' for a 50% of liver tumor incidence ranged between 53 to 2083 adducts per 10^8 nt, in the following order for the adducts levels for AfB1 < tamoxifen < IQ, MeIQx < 2,4-diaminotoluene < dimethylnitrosamine. In mouse liver, the respective values were 812 to 5543 adducts per 10^8 nt, for the adduct levels for ethylene oxide, < dimethylnitrosamine < 4-aminobiphenyl < 2-acetylaminofluorene. The observed span (40-fold in rats, 7-fold in mice) reflects a difference between the various DNA adducts to lead to critical mutations (Otteneder and Lutz 1999). These studies highlight the necessity to address, besides tumor incidences and adduct levels, the MOA including bioactivation and detoxification, DNA damage and repair mechanisms, the kinetics and saturability of these reactions, the nature and potency of the adducts and also the different potential mechanisms underlying the tumor formation in different target organs and species.

1.4 The model compound of the present thesis: Estragole

Estragole ($C_{10}H_{12}O$), is an alkenylbenzene, the chemical structure consists of a benzene ring substituted with a methoxy group and a propenyl group (Figure 1.1). Estragole is a natural ingredient of several herbs and spices such as: basil, nutmeg, fennel, marjoram, tarragon and anise, and these provide one of the sources of human exposure. Since estragole containing extracts are used in food processing, exposure to this compound can also occur in food products containing the extracts (De Vincenzi *et al.*, 2000) or in food products containing the spices and herbs. For instance the main constituent of pesto sauce is basil, and the

amount of estragole found in this food item was in a range of 0.05 – 19.30 mg/kg (Siano *et al.*, 2003). Recently Van den Berg *et al.* demonstrated also that some basil-based food supplements may contain high levels of estragole, from 0.20 up to 241.56 mg/g basil food supplement (Van den Berg *et al.*, 2011).

The possible risk of estragole exposure for the consumer has attracted much interest because estragole was found to be carcinogenic when administered to rodents at high dose levels. However, when used at low dose levels as a flavour, estragole was considered to be generally recognized as safe (GRAS) in 1965 by the Expert Panel of the Flavour and Extract Manufacturer's Association (FEMA) and was approved by the US food and Drug Administration (FDA) for food use as a flavour. In 2002 the FEMA Expert Panel reviewed the safety of the use of estragole as a flavour and estimated that the average intake from natural flavouring complexes is approximately 0.01 mg/kg bw/day (Smith *et al.*, 2002). Estragole has also been evaluated by the European Scientific Committee on Food, with the final opinion pointing to the genotoxic and carcinogenic properties, and suggesting restrictions in its use in food (EFSA, 2001). In the evaluation of the European Committee on Food the estimated intake of estragole, calculated based on its proposed uses and use levels in various food categories, amounted to 0.07 mg/kg bw/day estragole (EFSA, 2001). Furthermore, the European Medicine Agency (EMA, 2005) concluded that the present exposure to estragole resulting from consumption of herbal medicinal products (short time use in adults at recommended posology) does not pose a significant cancer risk. Nevertheless, further studies are needed to define the nature of the dose response curve in rats at low levels of exposure to estragole and its implications for the human situation. The ultimate risk will depend on the dose and the frequency of use.

1.4.1 Estragole Metabolism

Upon oral intake estragole undergoes rapid and essentially complete absorption along the gastrointestinal tract (Anthony *et al.*, 1987). Abdo *et al.* reported that estragole could be already adsorbed in the stomach (Abdo *et al.*, 2001). Estragole itself is not reactive but upon its absorption in the gastrointestinal track the compound is transported to the liver, where it can be either bioactivated or detoxified (Smith *et al.*, 2002). Figure 1.4 presents an overview of the various phase I and phase II metabolites produced resulting in bioactivation or detoxification of estragole. Estragole is detoxified via O-demethylation to 4-allylphenol and via epoxidation to estragole 2,3-oxide (Phillips *et al.*, 1981; Smith *et al.*, 2002). The main pathway for bioactivation of estragole proceeds by hydroxylation on the allyl side chain by cytochrome P450 enzymes resulting in the formation of 1′-hydroxyestragole (Swanson *et al.*, 1981). Subsequent sulfonation of 1′-hydroxyestragole by sulfotransferases gives rise to formation of the unstable ultimate carcinogenic metabolite 1′-sulfooxyestragole which decomposes to generate the reactive carbocation which covalently binds to DNA and protein (Phillips *et al.,* 1981). 1′-Hydroxyestragole can be detoxified by glucuronidation or via oxidation to 1′-oxoestragole (Bock *et al.*, 1978; Iyer *et al.*, 2003; Phillips *et al.*, 1981). Cytochrome P450 mediated oxidation of the allyl side chain of estragole may also result in formation of 3′-hydroxyanethole that can be oxidized to 4-methoxycinnamic acid which in turn can further be oxidized to 4-methoxybenzoic acid. Glucuronosyl conjugates of 3′-hydroxyanethole have also been observed in urine of rats exposed to estragole (Anthony *et al.*, 1987), which indicates that glucuronidation of 3′-hydroxyanethole can occur as well (Anthony *et al.*, 1987; Punt *et al.*, 2008).
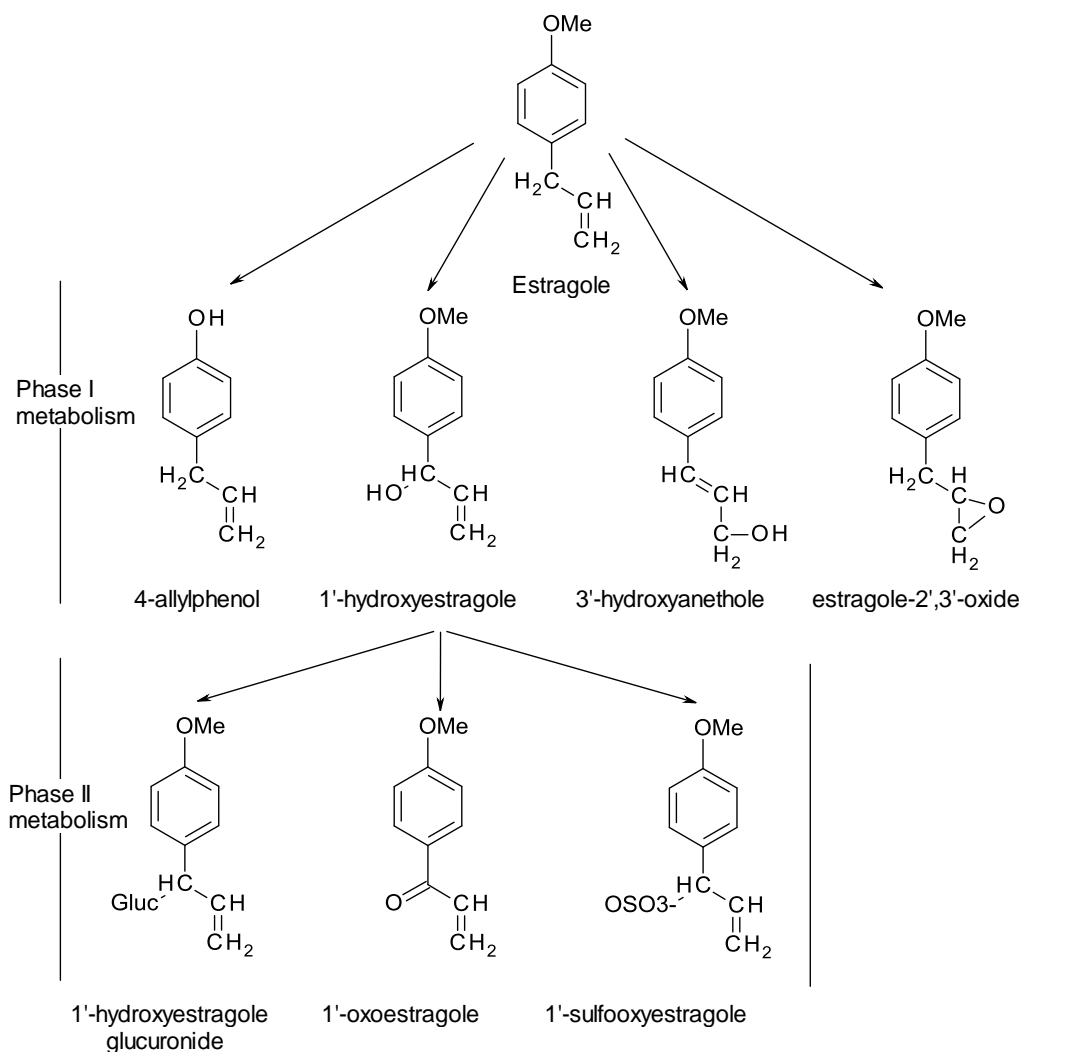
Figure 1.4. Estragole Metabolism, phase I and phase II metabolites formed in liver.

Several adducts are formed upon reaction of 1′-sulfooxyestragole with DNA (Figure 1.5). These adducts include N^2-(trans-isoestragol-3′-yl)-deoxyguanosine (E-3'-N^2-dG), N^2-(estragol-1′-yl)-deoxyguanosine (E-1'-N^2-dG), 7-(trans-isoestragol-3′-yl)-deoxyguanosine (E-3'-7-dG), 8-(trans-isoestragol-3′-yl)-deoxyguanosine (E-3'-8-dG), (Phillips *et al.*, 1981; Punt *et al.*, 2007) and N^6-(trans-isoestragol-3′-yl)-deoxyadenosine (E-3′-N^6-dA) (Phillips *et al.*, 1981). The major adduct formed with the guanine base is N^2-(trans-isoestragol-3′-yl)-deoxyguanosine (E-3′-N^2-dG) which is considered to play a role in the genotoxic and carcinogenic effects induced by estragole (Philips *et al.*, 1981; Smith *et al*, 2002). Recently it was reported that adducts between estragole and adenine (E-3′-N^6-dA) were formed to a significant extent in the liver of male rats (F344) exposed to estragole at a dose level of 600 mg/kg bw for 4 weeks (Phillips *et al.*, 1981; Ishii *et al.*, 2011). A study performed by Anthony *et al.* (1987) in rodents (mice and rats) which were exposed to different concentrations of estragole, and also a study by Zangouras *et al.* (1981) reported that with increasing doses a relative increase in excretion of the proximate carcinogenic metabolite 1'-hydroxyestragole was found, whereas *O*-demethylation became relatively less important. Thus, the extent of excretion of 1'-

hydroxyestragole, in the form of its glucuronide, after administration of estragole was found to be dose-dependent. In rats treated once by oral gavage the amount of 1'-hydroxyestragole glucuronide excreted increased from 1.3% - 5.4% of the dose for doses in the range from 0.05 –to 50 mg/kg bw to 11.4% - 13.7% for doses in the range from 500 to 1000 mg/kg bw (Anthony *et al.*, 1987). An explanation for these changes in metabolism with the dose could be a shift in phase I metabolism from *O*-demethylation at low doses to 1'-hydroxylation at higher dose (Anthony *et al.*, 1987). Recently, it was found that at increasing doses of estragole the 1'-hydroxylation pathway may became more important due to saturation of the *O*-demethylation pathway in lungs and kidneys (Punt *et al.*, 2008; Punt *et al.*, 2009).
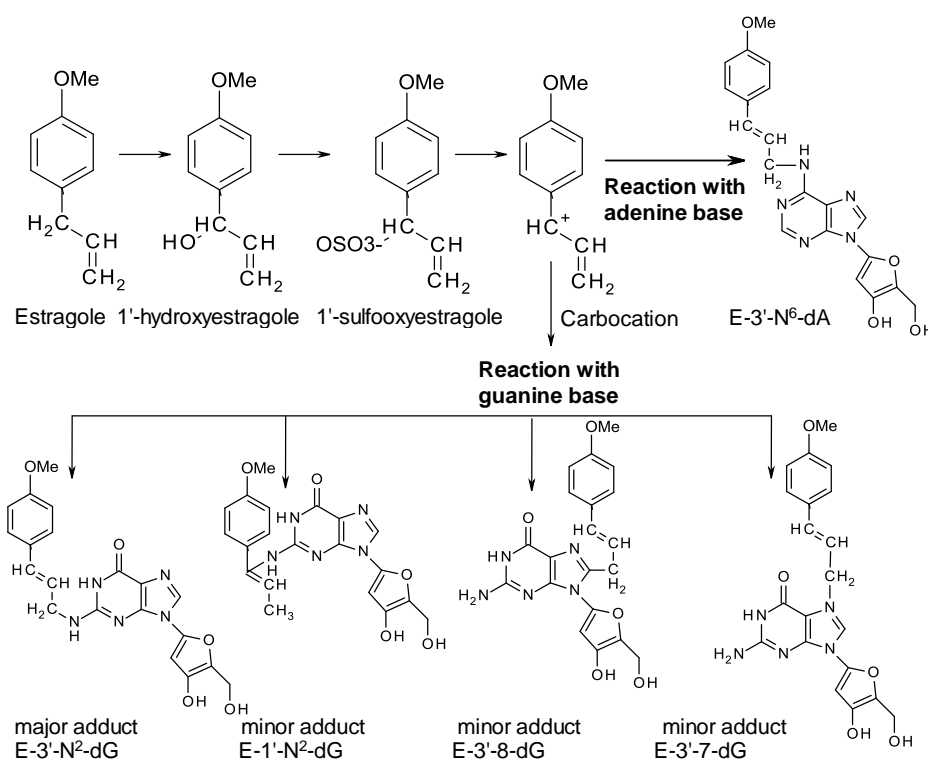
Figure 1.5. Estragole metabolism: hydroxylation and sulfonation leading to a reactive intermediate which covalently binds to DNA bases: guanine and adenine. Upon reaction with these bases different adducts are formed: N^2-(trans-isoestragol-3'-yl)-deoxyguanosine (E-3'-N^2-dG), N^2-(estragol-1'-yl)-deoxyguanosine (E-1'-N^2-dG), 7-(trans-isoestragol-3'-yl)-deoxyguanosine (E-3'-7-dG), 8-(trans-isoestragol-3'-yl)-deoxyguanosine (E-3'-8-dG), and N^6-(trans-isoestragol-3'-yl)-deoxyadenosine (E-3'-N^6-dA).

1.4.2 Estragole DNA adduct formation and tumor incidence studies

Several investigators have studied the mechanism of estragole carcinogenesis by examining DNA binding and characterizing DNA adducts formed by estragole and its reactive metabolites. Randerath *et al.* (1984) utilized ^{32}P-postlabeling to analyze DNA adduct formation in the livers of adult female CD-1 mice administered intra peritoneal (i.p.) injections of estragole, safrole, and other alkenylbenzenes. Estragole exhibited the strongest adduct formation to mouse liver DNA (200-300 pmol adducts/mg DNA, at a 10 mg dose per mouse, corresponding to a dose level of 400 mg/kg bw/day assuming a mouse weight of 0.025 kg). Phillips *et al.* (1984) found that estragole induced adducts to liver DNA of newborn male B6C3F1 mice treated by i.p. injection on day 1, 8, 15 and 22 after birth at doses of 0.25, 0.5, 1.0 and 3.0 µmol per animal

(with a final total dose of 4.75 µmol per animal). The DNA adduct levels observed in estragole-treated mice were 30.0, 14.8 and 9.4 pmol/mg DNA on days 23, 29 and 43, after birth respectively (Philips *et al.*, 1984). Ishii *et al.* (2011) confirmed estragole-specific dG and dA adduct formation *in vivo*, using an isotope dilution LC-ESI-MS/MS method for measuring E-3′-N^6-dA together with the two major dG adducts, E-3′-C^8-dG and E-3′-N^2-dG. The levels of these adducts measured in the livers of F344 rats treated with estragole at a probably carcinogenic dose of 600 mg/kg bw for 4 weeks were respectively 3.5 E-3′-C^8-dG adducts in 10^6 dG, 4.8 E-3′-N^2-dG adducts in 10^6 dG, and 20.5 E-3′-N^6-dA adducts in 10^6 dA. Furthermore, *in vitro* studies conducted in human hepatoma (HepG2) cells exposed for 24hrs to three concentration (50, 150, 450 µM) of estragole and measured by ^{32}P-postlabeling showed formation of the major E-3′-N^2-dG and minor E-1′-N^2-dG adducts (Zhou *et al.*, 2007). Jeurissen *et al.* (2007) measured by LC-MS/MS the formation of 130 E-3′-N^2-dG adducts in 10^{6}dG in HepG2 cells exposed to 50µM 1'-hydroxyestragole. These data indicate that both *in vivo* and *in vitro* estragole is able to form DNA adducts.

This section of the thesis presents the *in vivo* long-term rodent carcinogenicity studies of estragole (Table 1.2) and its metabolite 1′-hydroxyestragole (Table 1.3) available in literature. Three independent studies published in one publication by Miller *et al.* (1983) employed oral administration of estragole. In study 1 increasing levels of hepatocellular carcinomas were observed in female adult CD-1 mice administered estragole via the diet (Miller *et al.*, 1983). In both treated groups the incidence of hepatocellular carcinomas was statistically significantly different from control. In study 2 and 3 estragole induced hepatomas in 73% and 9% of newborn male and female CD-1 mice when administered estragole orally at a dose level of 370 mg/kg bw, for 2 times per week for 5 weeks (Miller et al., 1983).

Table 1.2. Carcinogenicity data from studies in mice performed using estragole.

Strain and Age	Sex	# of animals	Incidence	%	Lesion	Route/Dose/Duration	Sacrifice	Reference
CD1 (newborn)	M	51	6	12	Hpc	s.c. vehicle controls (Trioctanoin) – administered on day 1, 8, 15, and 22	12-15 m.	Drinkwater *et al.*, (1976)
CD1 (newborn)	M	60	14	14	Hpc	s.c. total dose 4.4 µmol (0.65mg) – administered on day 1, 8, 15, and 22	12-15 m.	Drinkwater *et al.,* (1976)
CD1 (newborn)	M	18	7	39	Hpc	s.c. total dose 5.2 µmol (0.77mg) – administered on day 1, 8, 15, and 22	12-15 m.	Drinkwater *et al.,* (1976)
CD1 (Preweanling)	M	49	36	73	Hpa	p.o. 370 mg/kg bw - 2x/wk for 5 w., from day 4 following birth	11-14 m.	Miller *et al*., (1983)
CD1 (Preweanling)	F	44	4	9	Hpa	p.o. 370 mg/kg bw - 2x/wk for 5 w., from day 4 following birth	11-14 m.	Miller *et al*., (1983)
CD1 (Preweanling)	M	46	7	15	Hpa	Untreated	12 m.	Miller *et al*., (1983)
CD1 (Preweanling)	M	42	11	26	Hpa	i.p. solvent control (Trioctanoin) administered on day 1, 8, 15, and 22	13 m.	Miller *et al*., (1983)
CD1 (Preweanling)	M	46	30	65	Hpa	i.p. total dose 9.45 µmol (1.4 mg) administered on day 1, 8, 15, and 22	14 m.	Miller *et al*., (1983)
B6C3F$_1$ (Preweanling)	M	82	23	28	Hpa	Untreated	13-18 m.	Miller *et al*., (1983)
B6C3F$_1$ (Preweanling)	M	58	24	41	Hpa	i.p. solvent control (Trioctanoin) administered on day 1, 8, 15, and 22	13-18 m.	Miller *et al*., (1983)
B6C3F$_1$ (Preweanling)	M	41	34	83	Hpa	i.p. total dose 4.75 µmol (0.70 mg) administered on day 1, 8, 15, and 22	113-8 m.	Miller *et al*., (1983)
CD1 (8 w. old)	F	50	0	0	Hpc	in diet for 12 months - control	20 m.	Miller *et al*., (1983)
CD1 (8 w.old)	F	48	27	56	Hpc	in diet for 12 months -0.23% (54 mg/kg bw)	20 m.	Miller *et al*., (1983)
CD1 (8 w. old)	F	49	35	71	Hpc	in diet for 12 months -0.46% (107 mg/kg bw)	20 m.	Miller *et al*., (1983)
A/J (8 w. old)	F	24	3	13	LA	i.p solvent control (Trioctanoin) - twice/week for 12 w	8 m.	Miller *et al*., (1983)
A/J (8 w. old)	F	18	1	6	LA	i.p. 42 mg/kg bw - twice/w. for 12 w	8 m.	Miller *et al*., (1983)
B6C3F$_1$ (12 days-old)	M	59	10	17	Hpa	i.p. solvent only (Trioctanoin) – single injection	10 m.	Wiseman *et al*., (1987)
B6C3F$_1$ (12 days-old)	M	40	38	95	Hpa	i.p. 111 mg/kg bw - single injection	11 m.	Wiseman *et al*., (1987)

M= male; F= female; Hpc= Hepatocarcinoma; Hpa= Hepatoadenoma; LA= Lung Adenoma; s.c= subcutaneous; i.p= intraperitonal; p.o= per oral, via stomach tube; d= day/s; m= month/s; w= week/s.

Additionally, four carcinogenicity studies administered estragole or its metabolites by intra peritoneal (i.p.) injection: two in newborn male B6C3F1 mice (Miller *et al*., 1983; Wiseman *et al*., 1987), one in newborn male CD-1 mice (Miller *et al*., 1983), and one in adult female A/J mice (Miller *et al*., 1983). Estragole administration by i.p. injection induced hepatomas (Miller *et al*., 1983; Wiseman *et al*., 1987). Administration of pentachlorophenol, a potent sulfotransferase inhibitor, by i.p. injection prior to treatment with estragole reduced the incidence of animals developing hepatomas to control levels, supporting the role for sulfotransferases activity in the bioactivation of estragole (Wiseman *et al*., 1987). Six percent of female A/J mice developed lung adenomas after i.p. injection of 148 mg/kg bw twice per week for 12 weeks (Miller *et al*., 1983). One bioassay administered estragole by subcutaneous (s.c) injection at a total dose of 0.65 or 0.77 mg prior to weaning, estragole induced hepatocarcinomas in 23 and 39% of the pups respectively (Drinkwater *et al*., 1976).

Several additional carcinogenicity studies which administered metabolites or derivatives of estragole, but not estragole itself, were conducted in both mice and rats, through various routes of administration. 1′-Hydroxyestragole (Table 1.3) induced hepatocellular carcinomas in mice treated by s.c. or i.p. injection, or via the diet, and examined after 8-20 months (Drinkwater *et al*., 1976; Wiseman *et al*., 1987; Miller *et al*., 1983). Susceptibility to hepatoma induction was influenced by mouse strain, sex, and age (Wiseman *et al*., 1987). It is important to underline that in studies performed by Miller *et al*., (1983) a group of 43 CD1 female mice were administered 0.25% of the metabolite 1′-hydroxyestragole in the diet, and the study was terminated at 20 months. The number of hepatoma-bearing mice amounted to 56%.

Table 1.3. Carcinogenicity data from studies in mice (and one in Fischer rat) performed using estragole metabolite 1'-hydroxyestragole.

Strain and Age	Sex	# of animals	Incidence	%	Lesion	Route/Dose/Duration	Sacrifice	Reference
CD1 (newborn)	M	51	6	12	Hpc	s.c. vehicle controls (Trioctanoin) – administered on day 1, 8, 15, and 22	12-15 m.	Drinkwater *et al*., (1976)
CD-1 (newborn)	M	51	35	70	Hpc	s.c. total dose 4.4 μmol (722 mg) – administered on day 1, 8, 15, and 22	12-15 m.	Drinkwater *et al*., (1976)
B6C3F$_1$ (prewealing)	M	35	5	15	Hpa	Untreated	12 m.	Miller *et al*., (1983)
B6C3F$_1$ (prewealing)	M	32	7	15	Hpa	i.p. control administered on days 1, 8, 15, and 22	12 m.	Miller *et al*., (1983)
B6C3F$_1$ (prewealing)	M	27	25	93	Hpa	i.p. 1.87 μmol (307 mg) administered on days 1, 8, 15, and 22	12 m.	Miller *et al*., (1983)
B6C3F$_1$ (prewealing)	M	82	23	28	Hpa	Untreated	13-18 m.	Miller *et al*., (1983)
B6C3F$_1$ (prewealing)	M	58	24	41	Hpa	i.p. control administered on days 1, 8, 15, and 22	13-18 m.	Miller *et al*., (1983)
B6C3F$_1$ (prewealing)	M	60	59	98	Hpa	i.p. 1.90 μmol (312 mg) - administered on days 1, 8, 15, and 22	13-18 m.	Miller *et al*., (1983)
B6C3F$_1$ (prewealing)	M	40	40	100	Hpa	i.p. 2.85 μmol (468 mg) - administered on days 1, 8, 15, and 22	13-18 m.	Miller *et al*., (1983)
B6C3F$_1$ (prewealing)	M	46	45	98	Hpa	i.p. 4.65 μmol (762 mg) - administered on days 1, 8, 15, and 22	13-18 m.	Miller *et al*., (1983)
CD 1 (8 w. old)	M	50	50	0	Hpc	in diet for 12 months - control	20 m.	Miller *et al*., (1983)
CD 1 (8 w. old)	M	43	24	56	Hpc	in diet for 12 months -0.25% (58 mg/kg bw)	20 m.	Miller *et al*., (1983)
A/J (8 w. old)	F	24	3	13	LA	i.p solvent control (Trioctanoin) - twice/12 w	8 m.	Miller *et al*., (1983)
A/J (8 w. old)	F	22	5	23	LA	i.p. 82 mg/kg bw - twice/12 w	8 m.	Miller *et al*., (1983)
B6C3F$_1$ (prewealing)	M	31	3	10	Hpa	i.p. solvent control (Trioctanoin) - administered on days 1, 8, 15, and 22	13 m.	Wiseman *et al*., (1987)
B6C3F$_1$ (prewealing)	M	47	24	51	Hpa	i.p 0.4 μmol (66 mg) - administered on days 1, 8, 15, and 22	13 m.	Wiseman *et al*., (1987)
B6C3F$_1$ (prewealing)	M	42	40	95	Hpa	i.p. 1.9 μmol (312 mg) - administered on days 1, 8, 15, and 22	13 m.	Wiseman *et al*., (1987)
B6C3F$_1$(12days-old)	M	40	9	22	Hpa	i.p. solvent control (Trioctanoin) – single injection	12 m.	Wiseman *et al*., (1987)
B6C3F$_1$(12days-old)	M	37	8	22	Hpa	i.p. 1.64 mg/kg bw – single injection	12 m.	Wiseman *et al*., (1987)
B6C3F$_1$(12days-old)	M	38	36	95	Hpa	i.p. 16.4 mg/kg bw – single injection	12 m.	Wiseman *et al*., (1987)
RAT Fischer (5 w. old)	M	20	1	5	Hpc	s.c. 0.05 mmol twice/w. for 10 w. (2.25 mg/kg bw)	24 m.	Miller *et al*., (1983)

M= male; F= female; Hpc= Hepatocarcinomas; Hpa= Hepatoadenoma; LA= Lung Adenoma; s.c= subcutaneous; i.p= intraperitonal; p.o= per oral, via stomach tube; d= day/s; m= month/s; w= week/s.

The three publications from Drinkwater *et al.* (1976), Wiseman *et al.* (1987), and Miller *et al.* (1983) give sufficient proof on the carcinogenicity of estragole and its metabolite 1′-hydroxyestragole in mice.

Recently a 3 month toxicity study by the NTP was published where rats and mice were exposed via gavage to estragole (37.5, 75, 150, 300, or 600 mg estragole/kg bw) and results indicated a potential for neoplastic transformation in rat liver (Bristol, 2011). The authors found that the incidences of hepatocellular hypertrophy and hepatocellular degeneration were significantly increased in 300 and 600 mg/kg bw male mice and 150 and 300 mg/kg bw female mice. Liver necrosis occurred in all 600 mg/kg bw female mice, along with a significant increase in the incidence of diffuse fatty change. Under the conditions of these 3-month studies, estragole showed carcinogenic activity based on the occurrence of two cholangiocarcinomas and one hepatocellular adenoma in the liver of three of 10 male F344/N rats in the high dose group. Because rats and mice were exposed for only 3 months, these studies do not access the full carcinogenic potential of estragole (Bristol, 2011).

1.5 Risk Assessment strategies for genotoxic carcinogens

Risk assessment, a scientifically based process, is a careful examination of what could cause harm to people. Risk assessment is achieved through the process of hazard identification, hazard characterization, exposure assessment, and risk characterization (EFSA, 2005). In the specific case of cancer risk assessment the goal is to predict the probability of tumor occurrence in people exposed to genotoxic and carcinogenic agents for instance from the diet. In the specific case of DNA reactive carcinogens it is presently assumed that it is not possible to establish safe levels of exposure due to the lack of a threshold. The preferred source of data would be from epidemiological studies that relate exposure to incidence in humans; however these studies are rare and when available mostly not sufficient to allow an adequate risk assessment. In cases where epidemiological studies are not available the prediction of human cancer risk may be based on data obtained in animal experiments. Krewski *et al.* (1991) reported that the prediction of human cancer risk could be carried out using laboratory carcinogenicity studies in experimental animals, assuming that animal carcinogens are presumptive human carcinogens. Allen *et al.* reported that some degree of correlation in carcinogenic potency exists between animals and humans (Allen *et al.*, 1988). However, the levels of administration used in animal studies are generally much higher than normal human exposure levels; high doses of the test compound are used in groups consisting of a limited number of experimental animals in order to optimize the potential cancer incidence. Thus, estimating human cancer risks based on animal data generally requires extrapolation from one species to another and from high to low dose levels. Interspecies scaling of physiological parameters and characteristics often implies extrapolation across routes of exposure, exposure times, and tumor induction mechanisms (van Leeuwen, 2003). Furthermore, when dealing with extrapolation from data in studies with experimental animals to the human situation one should also take into account that the human diet is a much more complex food matrix than what is used for the experimental exposure of rodents, where the test compound is often dosed by oral gavage as a pure compound dissolved in a carrier solvent. These issues complicate extrapolation from animal data to human. To obtain a quantitative risk assessment for human at realistic low dose levels, results obtained in animal studies at high doses are extrapolated to low dose levels using mathematical models. One of the mathematical approaches used to extrapolate from high to low doses is linear extrapolation from

the experimental data. However, there are several other approaches available that can be used to address the low-dose risk extrapolation that imply an assumed mathematical equation relating cancer risk to exposure (Krewski *et al.*, 1991). All of the models attempt to define the dose-response relationship on the basis of a particular extrapolation of the experimental data beyond the lowest data point. Due to the uncertainties concerning the low dose response and the shape of the dose response curve at low dose levels, numerical estimates for the quantitative risk at a certain dose level can vary by orders of magnitude depending on the mathematical model applied (COC, 2004; EFSA, 2005). In addition, mechanistic information on low dose effects and interspecies differences is difficult to assess and is often not taken into account when performing quantitative low dose extrapolations from animal data to the human situation. Discussions on low dose cancer risk extrapolation, low dose effects, species differences, matrix effects and thresholds for genotoxic carcinogens are therefore ongoing.

1.6 Physiologically based biokinetic models/ Physiologically based biodynamic model

Uncertainties in extrapolation from high doses used in animal studies to low-dose situations relevant for human exposure, and in the influences of species differences, genetic polymorphism and lifestyle factors on the ultimate risk, are not taken into account when extrapolating cancer risks using a conservative linear model or mathematical models. Physiologically based biokinetic and biodynamic (PBBK/BD) models may be helpful in characterising and better defining the dose- and species dependent influences on bioactivation, detoxification and possible adverse effects of genotoxic carcinogens thereby providing a basis for more reliable extrapolation from animal experimental data to the human situation. Krishnan and Andersen (2001) gave examples of what could be taken into account when PBBK/BD models are used with a compound that has a complex nature of toxicity: non/linearity in dose response, sex/species differences in tissue response, differential response of different tissues to chemical exposure, qualitative and/or quantitative responses to the same cumulative dose administered by different routes or exposure scenario. All these aspects can convey into one PBBK/BD model, which describes the toxicokinetics and/or toxicodynamics of a specific compound after ingestion or inhalation by using a computer simulation. PBBK models describe the body as a set of interconnected compartments, which represent the human organs and plasma, describing the absorption, distribution, metabolism, and excretion (ADME) (Krishnan and Andersen, 2001) characteristics of a compound within the body (Figure 1.6). PBBD models additionally include a description of the interaction of the chemical or its reactive metabolite with the toxicological receptor causing the adverse effect. A six step approach for the development of a basic PBBK/BD model was recently illustrated (Rietjens *et al.*, 2011). Briefly, these steps may include (i) definition of a conceptual model, which includes defining a simplified representation of the biological system and which model compartments can be included; (ii) translation of the conceptual model into a mathematical model by formulating a differential equation for each compartment; (iii) defining the values of the parameters in the equations either from literature or from experiments; (iv) solving the equations by calculating the concentrations of relevant compounds and their metabolites in the specific compartments, or the extent of their adverse reactions with the toxicological receptor; (v) evaluation of the model performance with ultimate improvements to the model when needed; and (vi) making predictions by performing simulations (Rietjens *et al.*, 2011). At the start of the work of the present thesis PBBK models

were available to simulate estragole bioactivation and detoxification in both rat (Punt *et al.*, 2008) and human (Punt *et al.*, 2009).

These PBBK models were defined based on literature data and *in vitro* metabolic parameters only, and provide possibilities to model metabolism of estragole at different oral doses in both species. These models provide more insight in relative dose- and species-dependent differences in bioactivation and detoxification of estragole, and are able to provide dose dependent predictions on the level of formation of the proximate and ultimate carcinogenic metabolites 1′-hydroxyestragole and 1′-sulfooxyestragole, respectively, in the target organ, the liver.

In order to extend PBBK models to PBBD models the overall toxic response and mode of action of a genotoxic compound should be described taking into account dynamics factors in addition to the kinetic factors. In the case of estragole, it is important to include in such a PBBD model dynamic responses such as DNA adduct formation, DNA repair, gene and protein expression, mutation modulation and ultimately tumor formation. Such PBBK and PBBD models will provide a new tool in the risk assessment process, enabling science based extrapolation not only from one species to another but also from high to low levels of exposure.
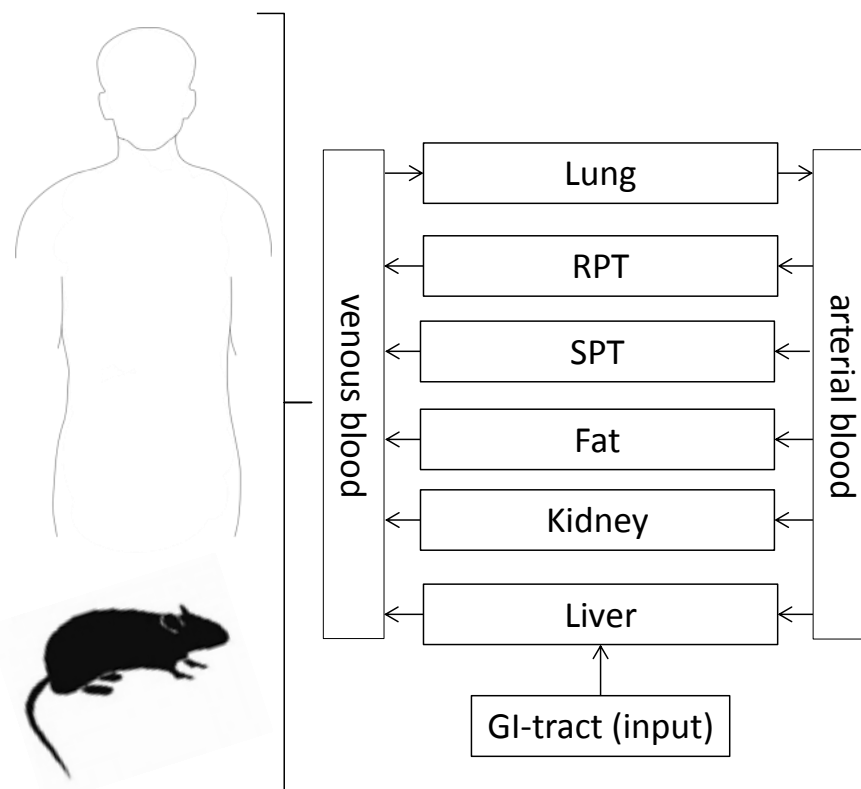

Figure 1.6. Basic schematic representation of so called physiologically based biokinetic and biodynamic models (PBBK/BD), for both rats and human, including the gastro-intestinal tract (GI) venous and arterial blood, and various organs including lung, rapidly perfuse tissue (RPT), slowly perfused tissue (SPT), fat, kidney, and liver.

1.7 Outline of the present thesis

The aim of the present thesis was to develop new strategies for low dose cancer risk assessment of estragole by extending the PBBK models previously defined for estragole to so-called physiologically based biodynamic (PBBD) models for DNA adduct formation, taking the approach one step closer to the ultimate endpoint of tumor formation. The work of the present thesis is presented in 7 chapters: **Chapter 1** presents an overview of the basic principles of importance for the present thesis including an introduction to cancer risk assessment strategies, physiologically based biokinetic (PBBK) and physiologically based biodynamic (PBBD) models, and to estragole, the model compound used in the present work. **Chapter 2** describes the development of a PBBD model predicting the *in vivo* dose dependent DNA adduct formation in rat liver based on *in vitro* data only. The model was based on the previously developed PBBK model that allowed prediction of the levels of 1′-hydroxyestragole and 1′-sulfooxyestragole in the liver of rat and an *in vitro* concentration response curve for DNA adduct formation in cultured rat primary hepatocytes exposed to 1′-hydroxyestragole. In **Chapter 3** the *in vivo* PBBD model was validated by quantifying the dose-dependent estragole DNA adduct formation *in vivo* in Sprague Dawley rat liver and the urinary excretion of 1′-hydroxyestragole glucuronide in rats exposed to increasing doses of estragole. The model allows prediction of dose dependent bioactivation, detoxification, and DNA adduct formation of estragole in rats. In **Chapter 4** the PBBD model for DNA adduct formation in rat liver was extended to human liver and it was investigated how variability in the human population would result in variability in levels of DNA adducts formed in human livers after exposure to average daily intake levels of estragole. Comparison of the predictions made by the human model to those of the rat model allows studying dose- and species-dependent effects on estragole detoxification, bioactivation and DNA adduct formation. The adduct levels predicted for human liver were also compared to average endogenous levels in order to improve our insight in the role of DNA adduct formation in the MOA for tumor formation by estragole in human. In **Chapter 5** further insight in the MOA of estragole was obtained by investigating gene and protein expression as well as DNA adduct formation and repair in hepatocytes exposed to estragole and to its proximate carcinogenic metabolite 1′-hydroxyestragole. **Chapter 6** describes a review in which, based on literature data and the Benchmark Dose (BMD) approach, the importance of DNA adduct formation for the ultimate cancer risk was evaluated in order to obtain insight in the role of DNA adduct formation in the MOA of different genotoxic carcinogens, including methyleugenol and safrole, alkenylbenzenes related to estragole. Data on *in vivo* DNA adduct formation and on tumor incidences were compared taking into account reported endogenous background levels of DNA adduct formation. Finally, **Chapter 7** summarizes the results described in the previous chapters, compiles the overall discussion and presents future perspectives to be addressed.

Reference

Abdo KM, Cunningham ML, Snell ML, Herbert RA, Travlos GS, Eldridge SR, and Bucher JR. (2001) 14-week toxicity and cell proliferation of methyleugenol administered by gavage to F344 rats and B6C3F1 mice. Food and Chemical Toxicology 39: 303-316.

Adriaenssens PI, White CM and Anderson MW. (1983) Dose response relationships for the binding of benzo[a]pyrene metabolites to DNA and protein in lung, liver, and fore stomach of control and butylated hydroxyanisole-treated mice. Cancer Res. 43: 3712–3719.

Allen BC, Crump KS, and Shipp AM. (1988) Correlation between Carcinogenic Potency of Chemicals in Animals and Humans. Risk Analysis 8: 531-544.

Anthony A, Caldwell J, Hutt AJ, and Smith RL. (1987) Metabolism of Estragole in Rat and Mouse and Influence of Dose Size on Excretion of the Proximate Carcinogen 1'-Hydroxyestragole. Food and Chemical Toxicology 25: 799-806.

Barlow S, Renwick AG, Kleiner J, Bridges JW, Busk L, Dybing E, Edler L, Eisenbrand G, Fink-Gremmels J, Knaap A, Kroes R, Liem D, Müller DJG, Page S, Rolland V, Schlatter J, Tritscher A, Tueting W, and Würtzen G. (2006) Risk assessment of substances that are both genotoxic and carcinogenic—Report of an international conference organized by EFSA and WHO with support of ILSI Europe. Food Chem Toxicol, 44: 1636–1650.

Barrett JC. (1993) Mechanisms of Multistep Carcinogenesis and Carcinogen Risk Assessment. Environmental Health Perspectives 100: 9-20.

Bristol DW. (2011) NTP 3-month toxicity studies of estragole (CAS No. 140-67-0) administered by gavage to F344/N rats and B6C3F1 mice. Toxic Rep Ser.82:1-111.

Bock KW, Brunner G, Hoensch H, Huber E, and Josting D. (1978) Determination of microsomal UDP-glucuronyltransferase in needle-biopsy specimens of human liver. Eur. J. Clin. Pharmacol., 14, pp. 367–373.

Christmann M, Tomicic MT, Roos WP, and Kaina B. (2003) Mechanisms of human DNA repair: an update. Toxicology 193 (1-2):3-34.

COC Committee on Carcinogenicity of chemicals in food, (2004) Guidance on a strategy for the risk assessment of chemical carcinogens. http://www.advisorybodies.doh.gov.uk/coc/guideline04.pdf.

Colvin DM. (2000) Alkylating Agents and Platinum Antitumor Compounds. Cancer Medicine. 5th edition. Bast RC Jr, Kufe DW, Pollock RE, *et al.*, editors. Hamilton (ON): BC Decker; 2000.

De Bont R, and van Larebeke N. (2004) Endogenous DNA damage in humans: a review of quantitative data. Mutagenesis.19(3):169-85.

De Vincenzi M, Silano M, Maialetti F, and Scazzocchio B. (2000) Constituents of aromatic plants: II.Estragole. Fitoterapia, 725-729.

Drinkwater NR, Miller EC, Miller JA, and Pitot HC. (1976) Hepatocarcinogenicity of Estragole (1-Allyl-4-Methoxybenzene) and 1'-Hydroxyestragole in Mouse and Mutagenicity of 1'-Acetoxyestragole in Bacteria. Journal of the National Cancer Institute 57: 1323-1331.

EFSA   European Food Safety Authority (2001) Opinion of the Scientific Committee on Food on Estragole (l-AUyl-4-methoxybenzene).

EFSA   European Food Safety Authority (2005) Opinion of the Scientific Committee on a request from EFSA related to A Harmonised Approach for Risk Assessment of Substances Which are both Genotoxic and Carcinogenic. The EFSA Journal 282: 1-31.

EMA European Medicines Agency (2005) PUBLIC STATEMENT ON THE USE OF HERBAL MEDICINAL PRODUCTS CONTAINING ESTRAGOLE Evaluation of Medicines for Human Use - London, 23 November 2005- Doc Ref: EMEA/HMPC/137212/2005.

Farmer PB. (2004a) Exposure biomarkers for the study of toxicological impact on carcinogenic processes, IARC Sci. Publ., vol. 157 ,in: P. Buffler, J. Rice, R. Baan, M. Bird, P. Boffetta, Editors, Mechanisms of Carcinogenesis. Contributions of Molecular Epidemiology, IARC, Lyon, pp. 71–90.

Farmer   PB. (2004b) DNA and protein adducts as markers of genotoxicity. Toxicol. Lett.,149:3–9.

Farmer PB, Brown K, Tompkins E, Emms VL, Jones DJ, Singh R, Phillips DH. (2005) DNA adducts: mass spectrometry methods and future prospects. Toxicol Appl Pharmacol. 207 (2):293- 301.

Farmer PB. (2008). Significance for risk assessment of increases in background levels of carcinogen-derived protein and DNA Aadducts. Toxicology Letters 180, S24-S24.

Himmelstein MW, Boogaard PJ, Cadet J, Farmer PB,Kim JH, Martin EA, Persaud R, Shuker DEG. (2009) Creating context for the use of DNA adduct data in cancer risk assessment: II. Overview of methods of identification and quantitation of DNA damage. Crit. Rev. Toxicol. 39:679-694.

Hecht SS. (2003) Tobacco carcinogens, their biomarkers and Tobacco-Induced Cancer. Nature Reviews 3:733-744.

Heflich RH. (1991) Chemical mutagens. In Genetic Toxicology (Li, A. P., and Heflich, R. H., Eds.) CRC Press, Boca Raton.

Heijne WHM. (2004) Toxicogenomics: applications of new functional genomics technologies in toxicology. PhD thesis ISBN 90-8504-121-X.

Hwang ES, and Bowen PE. (2007) DNA damage, a biomarker of carcinogenesis: its measurement and modulation by diet and environment. Crit Rev.Food Sci.Nutr. 47(1):27-50.

Iyer LV, Ho MN, Shinn WM, Bradford WW, Tanga MJ, Nath SS, Green CE. (2003) Glucuronidation of 1′-hydroxyestragole (1′-HE) by human UDP-glucuronosyltransferases UGT2B7 and UGT1A9. Toxicol. Sci.73:36-43.

Ishii Y, Suzuki Y, Hibi D, Jin M, Fukuhara K, Umemura T, Nishikawa A. (2011) Detection and Quantification of Specific DNA Adducts by Liquid Chromatography−Tandem Mass Spectrometry in the Livers of Rats Given Estragole at the Carcinogenic Dose. Chemical Research in Toxicology. 24(4): 532-541.

Jeurissen SMF, Bogaards JJP, Boersma MG, ter Horst JPF, Awad HA, Fiamegos YC, van Beek TA, Alink GM, Sudholter EJR, Cnubben NHP, and Rietjens IMCM. (2007) Human cytochrome P450 enzymes of importance for the bioactivation of methyleugenol to the proximate carcinogen 1 '-hydroxymethyleugenol. Chemical Research in Toxicology 20: 798-806.

Klaunig JE, and Kamendulis LM. (2007) Chapter 8: chemical carcinogenesis. In Casarett & Doull's Toxicology: The Basic Science of Poisons (C. D. Klaassen, ed.), 7th ed., pp. 329–80. McGraw-Hill, New York.

Klaunig, JE, Kamendulis, LM, and Hocevar BA. (2010) Oxidative Stress and Oxidative Damage in Carcinogenesis. Toxicologic Pathology 38: 96-109.

Krewski, D, Gaylor, D, and Szyszkowicz, M. (1991) A Model-Free Approach to Low-Dose Extrapolation. Environmental Health Perspectives 90, 279-285.

Krishnan K, and Andersen ME. (2001) Physiologically Based Pharmacikinetic modelling in Toxicology. In Principles and Methods of Toxicology (A. W. Hayes, ed., pp. 193-242. Taylor & Francis, Philadelphia).

La DK, and Swenberg J.A. (1996) DNA adducts: biological markers of exposure and potential applications to risk assessment. Mutat. Res., 365, 129–146.

Miller EC, Swanson AB, Phillips DH, Fletcher TL, Liem A, and Miller JA. (1983) Structure-Activity Studies of the Carcinogenicities in the Mouse and Rat of Some Naturally-Occurring and Synthetic Alkenylbenzene Derivatives Related to Safrole and Estragole. Cancer Research 43: 1124-1134.

Osborne MR. (1984) DNA interactions of reactive intermediates derived from carcinogens, in Searle, CE (ed) Chemical Carcinogens 2nd edition, Vol.1 pp 485-524 American Chemical Society, Washington DC.

Otteneder M, and Lutz WK. (1999) Correlation of DNA adduct levels with tumor incidence: carcinogenic potency of DNA adducts. Mutat. Res. 424:237-247.

Pastwa E, and Blasiak J. (2003) Non/homologous DNA end joining. Acta Biochimica Polonica. 50 (4): 891-908

Phillips DH, Miller JA, Miller EC, and Adams B. (1981) Structures of the DNA adducts formed in mouse liver after administration of the proximate hepatocarcinogen 1′-hydroxyestragole. Cancer Res. 41:176-186.

Phillips DH, Reddy MV, and Randerath K. (1984) 32P-post-labeling analysis of DNA adducts formed in the livers of animals treated with safrole, estragole and other naturally-occurring alkenylbenzenes. II. Newborn male B6C3F1 mice. Carcinogenesis 5:1623-1628.

Phillips DH. (2005) DNA adducts as markers of exposure and risk. Mutation Res. 577 (1-2): 284–292.

Phillips DH. (2007) The formation of DNA adducts. The cancer handbook 2nd edition Edited by Malcom R Alison. John Wiley & Sons, Ltd.

Phillips DH, and Arlt VM. (2007) The 32P-postlabeling assay for DNA adducts. Nature Protocols - 2772 – 278.

Pitot HC. (1996) Stage-specific gene expression during hepatocarcinogenesis in the rat. J Cancer Res. Clin. Oncol 122:257-265.

Poirier MC, and Beland FA. (1992) DNA adduct measurements and tumor-incidence during chronic carcinogen exposure in animal-models implications for DNA adduct-based human cancer risk assessment. Chem. Res. Toxicol. 5:749-755.

Pottenger LH, Carmichael N, Banton MI, Boogaard PJ, Kim J, Kirkland D, Phillips RD, van Benthem J, Williams GM, Castrovinci A. (2009) ECETOC workshop on the biological significance of DNA adducts: summary of follow-up from an expert panel meeting. Mutat Res. 678(2):152-7.

Punt A, Freidig AP, Delatour T, Scholz G, Boersma MG, Schilter B, van Bladeren PJ, Rietjens IMCM. (2008) A physiologically based biokinetic (PBBK) model for estragole bioactivation and detoxification in rat. Toxicol. Appl. Pharmacol. 231:248-259.

Punt A, Paini A, Boersma MG, Freidig AP, Delatour T, Scholz G, Schilter B, van Bladeren PJ, Rietjens IMCM. (2009) Use of physiologically based biokinetic (PBBK) modeling to study estragole bioactivation and detoxification in humans as compared with male rats. Toxicol. Sci. 110:255-   269.

Punt A, Delatour T, Scholz G, Schilter B, van Bladeren PJ, and Rietjens IMCM. (2007) Tandem mass spectrometry analysis of N^2-(trans-isoestragol-3'-yl)-2'-deoxyguanosine as a strategy to study species differences in sulfotransferase conversion of the proximate carcinogen 1'-hydroxyestragole. Chemical Research in Toxicology. 20, 991-998.

Randerath K, Reddy MV, and Gupta RC. (1981) P-32-labeling test for DNA damage. Proc. Natl Acad. Sci. US. 78:6126-6129.

Rietjens IMCM, Louisse J, and Punt A. (2011) Tutorial on physiologically based kinetic modelling in molecular nutrition and food research. Molecular Nutrition & Food Research 55(6): 941–956.

Sander M, Cadet J, Casciano DA, Galloway SM, Marnett LJ, Novak RF, Pettit SD, Preston RJ, Skare J, Williams GM, Van Houten B, Gollapudi BB. (2005) Proceedings of a workshop on DNA adducts: biological significance and applications to risk assessment Washington, DC, April 13–14, 2004. Toxicol. Appl. Pharmacol. 208:1–20.

Shimkin MB. (1975) Some historical landmarks in cancer epidemiology. In Cancer Epidemiology and Prevention, ed. D. Schottenfeld, pp. 60-75. Springfield, Ill: Thomas. 574 pp.

Siano F, Ghizzoni C, Gionfriddo F, Colombo E, Servillo L, and Castaldo D. (2003) Determination of estragole, safrole and eugenol methyl ether in food products. Food Chemistry 81: 469-475.

Smith RL, Adams TB, Doull J, Feron VJ, Goodman JI, Marnett LJ, Portoghese PS, Waddell WJ, Wagner BM, Rogers AE, Caldwell J, and Sipes IG. (2002) Safety assessment of allylalkoxybenzene derivatives used as flavouring substances - methyl eugenol   and estragole. Food and Chemical Toxicology 40: 851-870.

Swanson AB, Miller EC, and Miller JA. (1981) The Side-Chain Epoxidation and Hydroxylation of the Hepatocarcinogens Safrole and Estragole and Some Related-Compounds by Rat and Mouse-Liver Microsomes. Biochimica Et Biophysica Acta 673, 504-516.

Swenberg JA, Fryar-Tita E, Jeong YC, Boysen G, Starr T, Walker VE, and Albertini RJ. (2008). Biomarkers in toxicology and risk assessment: Informing critical dose-response relationships. Chemical Research in Toxicology 21, 253-265.

Valavanidis A, Vlachogianni T, and Fiotakis C. (2009) 8-hydroxy-2′-deoxyguanosine (8-OHdG):A Critical Biomarker of Oxidative Stress and Carcinogenesis. Journal of Environmental Science and Health, Part C. 27(2):120-139.

Van den Berg SJPL, Restani P, Boersma MG, Delmulle L, and Rietjens IMCM. (2011) Levels of genotoxic and carcinogenic ingredients in plant food supplements and associated risk assessment Food and Nutrition Sciences, Food and Nutrition Sciences 2, 989-1010.

Van Gijssel HE. (1999). Mechanisms of p53 (in)activation and hepatocarcinogenesis in the rat: the role of DNA adducts, mdm2, and Bcl-2. PhD thesis ISBN 90-9012578-7.

Van Leeuwen IMM. (2003) Mathematical Models in Cancer Risk Assessment. In Institute of Ecological Science, p. 164. Vrije Universiteit, Amsterdam.

Watson JD, Baker TA, Bell SP, Gann A, Levine M, and Losick R. (2004) Molecular Biology of the Gene 2004 Peason Benjamin Cummings; CSHL Press. 5th ed.

Williams GM. (2008). Application of mode-of-action consideration in human cancer risk assessment. Toxicol. Lett. 180, 75–80.

Wiseman RW, Miller EC, Miller JA, and Liem A. (1987) Structure-Activity Studies of the Hepatocarcinogenicities of Alkenylbenzene Derivatives Related to Estragole and Safrole on Administration to Preweanling Male C57Bl/6J X C3H-Hej F1-Mice. Cancer Research 47: 2275-2283.

Wood RD, Mitchell M, Sgouros J, and Lindahl T. (2001) Human DNA repair genes. Science, 291, 1284.

Wyatt MD and Pittman DL. (2006) Methylating agents and DNA repair responses: Methylated bases and sources of strand breaks. Chem.Res.Toxicol. 19 (12):1580-1594.

Zangouras A, Caldwell J, Hutt AJ, and Smith RL. (1981) Dose Dependent Conversion of Estragole in the Rat and Mouse to the Carcinogenic Metabolite, 1'-Hydroxyestragole. Biochemical Pharmacology 30: 1383-1386.

Zhou GD, Moorthy B, Bi J, Donnelly KC, and Randerath K. (2007) DNA adducts from alkoxyallylbenzene herb and spice constituents in cultured human (HepG2) cells. Environ Mol Mutagen. 48(9):715-21.

Chapter 2

Based on:

A physiologically based biodynamic (PBBD) model for estragole DNA binding in rat liver based on *in vitro* kinetic data and estragole DNA adduct formation in primary hepatocytes

By:

Paini A, Punt A, Viton F, Scholz G, Delatour T, Marin-Kuan M, Schilter B, van Bladeren PJ, Rietjens IMCM.

Abstract

Estragole has been shown to be hepatocarcinogenic in rodent species at high dose levels. Translation of these results into the likelihood of formation of DNA adducts, mutation, and ultimately cancer upon more realistic low dose exposures remains a challenge. Recently we have developed physiologically based biokinetic (PBBK) models for rat and human predicting bioactivation of estragole. These PBBK models, however, predict only kinetic characteristics. The present study describes the extension of the rat PBBK model to a so-called physiologically based biodynamic (PBBD) model predicting *in vivo* DNA adduct formation of estragole in rat liver. This PBBD model was developed using *in vitro* data on DNA adduct formation in rat primary hepatocytes exposed to 1′-hydroxyestragole. To define the PBBD model, the PBBK model was extended by linking the area under the curve for 1′-hydroxyestragole formation predicted by the PBBK model to the area under the curve for 1′-hydroxyestragole in the *in vitro* experiments. The outcome of the PBBD model revealed a linear increase in DNA adduct formation with increasing estragole doses up to 100 mg/kg bw. Although DNA adduct formation of genotoxic carcinogens is generally seen as a biomarker of exposure rather than a biomarker of response, the PBBD model now developed is one step closer to the ultimate toxic effect of estragole than the PBBK model described previously. Comparison of the rat PBBD model outcome to available data on *in vivo* DNA adduct formation showed that the model predicts the dose dependent level of DNA adduct formation for low levels of exposure up to a dose level shown to cause cancer in rodent bioassays providing a proof of principle for modeling a toxicodynamic *in vivo* endpoint on the basis of solely *in vitro* experimental data.

2.1 Introduction

The regular human diet is known to contain several compounds that have been shown to be genotoxic and carcinogenic when tested at high doses in rodents. Estragole is such a food-borne natural compound, which is known to be a genotoxic hepatocarcinogen in rodent studies at high dose levels (Miller *et al.*, 1983). Estragole itself is not reactive but upon its rapid absorption in the gastrointestinal track it is transported to the liver, where the compound is bioactivated (Smith *et al.*, 2002). Metabolism of estragole can follow different pathways (Figure 2.1). It is detoxified via *O*-demethylation to 4-allylphenol and epoxidation to estragole 2,3-oxide (Phillips *et al.*, 1981; Smith *et al.*, 2002). The main pathway for bioactivation of estragole proceeds by hydroxylation on the allyl side chain by P 450 enzymes resulting in the formation of 3′-hydroxyanethole and 1′-hydroxyestragole. 1′-Hydroxyestragole can be detoxified by glucuronidation or via oxidation to 1′-oxoestragole (Bock *et al.*, 1978; Iyer *et al.*, 2003; Phillips *et al.*, 1981). Alternatively, sulfonation of 1′-hydroxyestragole by sulfotransferases gives rise to formation of the unstable ultimate carcinogenic metabolite 1′-sulfooxyestragole which decomposes to generate the reactive carbocation which covalently binds to DNA and proteins (Gardner *et al.*, 1997). Several adducts are formed upon reaction of 1′-sulfooxyestragole with DNA: N^2-(*trans*-isoestragol-3′-yl)-2′-deoxyguanosine, N^2-(estragol-1′-yl)-2′-deoxyguanosine, 7-(trans-isoestragol-3′-yl)-2′-guanine, 8-(trans-isoestragol-3′-yl)-2′-deoxyguanosine (Phillips *et al.*, 1981; Punt *et al.*, 2007).
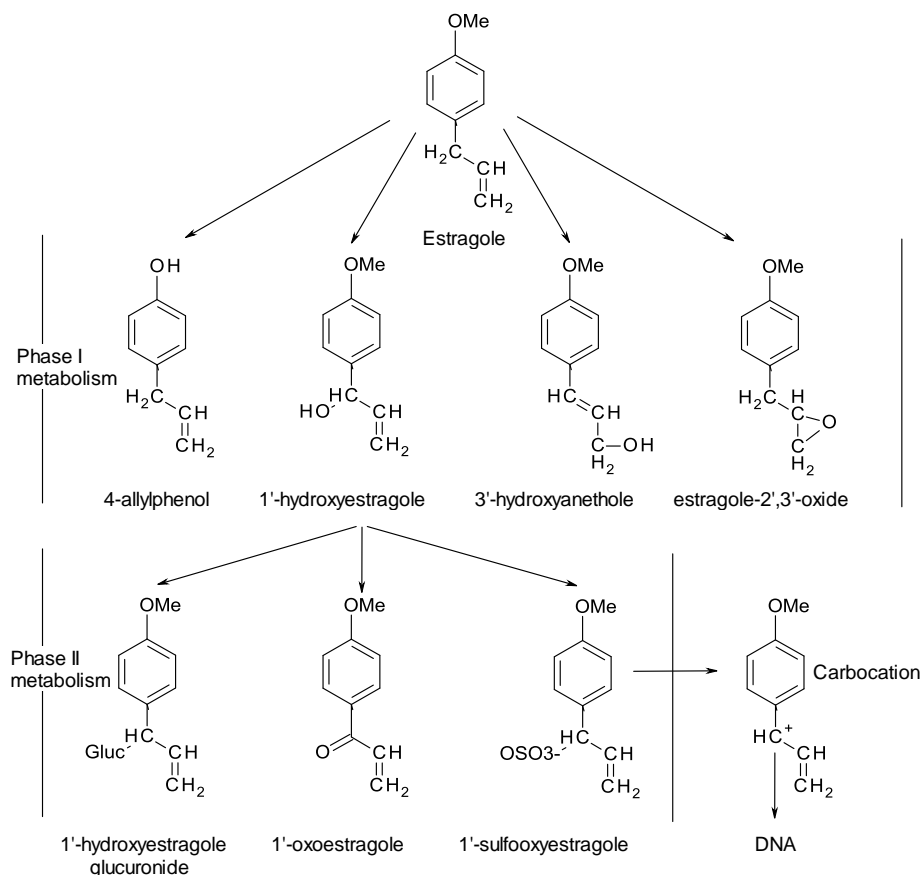

Figure 2.1. Metabolism of estragole (adapted from Punt et al., 2009).

The major adduct formed is N^2-(*trans*-isoestragol-3′-yl)-2′-deoxyguanosine (E-3′-N^2-dG) (Figure 2.1) which is considered to play a role in the genotoxic and carcinogenic effects induced by estragole (Philips *et al.*, 1981; Smith *et al*, 2002). A physiologically based biokinetic (PBBK) model is represented as a set of mathematical equations that together describe the absorption, distribution, metabolism and excretion of a compound of interest within an organism (Yang *et al.*, 2004). However, a toxic response *in vivo* will be determined by kinetic and dynamic characteristics. Therefore, integration of additional information on the subsequent reactions with target molecules or organs causing toxicity, i.e. toxicodynamic parameters, will give a more complete picture of the consequences of chemical exposure. It has been discussed that PBBK and physiologically based biodynamic (PBBD) models will give more insight from animal systems to reliably predict the likelihood and magnitude of adverse health effect in human (Coleman *et al.*, 2008; Mager *et al.*, 2009). Recently, a PBBK model was developed to simulate estragole bioactivation and detoxification in both rat (Punt *et al.*, 2008) and human (Punt *et al.*, 2009) based on *in vitro* metabolic parameters only, providing possibilities to model metabolism of estragole at different oral doses in both species. These models provide more insight in relative dose- and species-dependent differences in bioactivation and detoxification of estragole, and are able to provide dose dependent predictions on the level of formation of the proximate and ultimate carcinogenic metabolites 1′-hydroxyestragole and 1′-sulfooxyestragole, respectively, in the target organ, the liver. As a result these PBBK models allow improved extrapolation of kinetic characteristics for both detoxification as well as bioactivation from high to low dose levels as well as from one species to another including human (Rietjens *et al.*, 2009). However, formation of a DNA reactive metabolite cannot be directly extrapolated to the actual level of DNA binding since in addition to the level of 1′-sulfooxyestragole formed also other factors, including the rates of adduct formation and DNA repair will influence the ultimate DNA adduct formation. Although not all DNA adducts have a mutagenic effect (Bignold, 2004), the formation of DNA adducts is considered as a marker of exposure (Shuker and Farmer, 1992; Phillips, 2005) and has also been accepted as a hazard indication pointing at a potential cancer risk (Renwick and Walton, 2001), whereas the reduction of DNA adduct levels by for example chemoprevention can result in reduction of tumors (Preston and Williams, 2005; Sander *et al.*, 2005). The processes determining the level of DNA binding as possible key event in tumor induction are part of what is called the toxicodynamic phase.

The objective of the present study was to extend the previously developed PBBK model that allowed prediction of the levels of 1′-hydroxyestragole and 1′-sulfooxyestragole in the liver of rats with a description of pharmacodynamic interactions enabling prediction of the dose dependent levels of DNA binding in the liver of rat at varying oral dose levels of estragole. It is well recognized that the level of DNA adduct formation as such cannot predict a cancer risk since several steps in the process of cancer induction are not yet taken into account including the relationship of the DNA adducts formed with mutagenicity and carcinogenicity. However, the PBBD model can take into account the processes of DNA binding and DNA repair, thereby allowing evaluation of dose- and species-dependent differences in bioactivation of estragole at a level one step beyond the biokinetic phase.

2.2 Materials and Methods

2.2.1 Chemicals and reagents

Estragole was obtained from Acros Organics (Geel, Belgium). 2′-Deoxyguanosine was purchased from Sigma (Basel, Switzerland). 1,2,3,7,9-^{15}N$_5$-2′-Deoxyguanosine (^{15}N$_5$-dG) was obtained from Cambridge Isotope Laboratories (Cambridge, MA). ITS+ (Insulin, Transferrin, and Selenious acid), l-glutamine and matrigel were obtained from collaborative Biomedical Products (Bedford, MA). Penicillin/streptomycin was acquired from Gibco (Paisley, UK). Fetal bovine serum (FBS) was purchased from Hyclone (Logan, Utah). Earle's balanced salts solution (EBSS), William's E, William's E without phenol red, dexamethasone, ethylene glycol tetra acetic acid (EGTA), collagenase from Clostridium hystoliticum type IV-S, dimethyl sulfoxide (DMSO), Hepes, CaCl$_2$*2H$_2$O, MgCl$_2$*6H$_2$O, trypan blue, calf thymus DNA (ctDNA), methanol, zinc sulphate (heptahydrate), phosphodiesterase I from Crotalus adamanteus (venom phosphodiesterase), phosphodiesterase II from bovine spleen (spleen phosphodiesterase), and alkaline phosphatase were purchased from Sigma (Schnelldorf, Germany). Acetonitrile, formic acid, dichloromethane, HCl (1N), sodium carbonate (1M), ammonium bicarbonate, sodium sulphate, petroleum ether, ethyl acetate, sodium acetate, Tris-HCl, ethylenediamine tetra acetic acid (EDTA), ammonia 30%, and ethanol were purchased from Merck (Darmstadt, Germany). Nuclease P1 was obtained from MP Biochemicals (Aurora, OH). Triethylacetate ammonium buffer, acetic anhydride, and pyridine were purchased from Fluka (Buchs, Switzerland) and β-glucuronidase was purchased from Roche (Mannheim, Germany).

Both 1'-hydroxyestragole and 1'-acetoxyestragole are carcinogenic to rodents and should be handled accordingly.

2.2.2 Preparation and cultivation of primary rat hepatocytes

White male Sprague-Dawley rats, 8 weeks old, with a weight of 200-250 g were used to isolate fresh primary hepatocytes by perfusion. Rat primary hepatocytes were isolated and cultured according to Cavin *et al.*, (2007), based on a protocol first described by Sidhu *et al.* (1993). Briefly, the rat was anesthetized and the liver perfused with medium containing calcium free EBSS, 0.75 mM EGTA, and 100 U/mL penicilin/streptomycin, for 10 min at a flow rate of 20 mL/min. After this a switch was made to perfusion with medium containing EBSS, 100 mg collagenase, 10mM Hepes pH 7.4, 100 U/mL penicillin/streptomycin, 1.8 mM CaCl$_2$, and 0.8 mM MgCl$_2$; the flow rate was kept at 25 mL/min for 8 to 10 min depending on the liver size. The organ was rapidly excised and transferred to William's E medium containing phenol red, supplemented with 2 mM L-glutamine, 10 mM Hepes pH 7.4, 1% ITS+, 100U/mL penicillin/streptomycin, and 100 nM dexamethasone. After gentle shaking the cells were passed through a sterilized filter nylon membrane of 200 μm cutoff and centrifuged using an Allegra X-15R Centrifuge Beckman coulter (Nyon, Switzerland) for 2 min at 37 g (400 rpm). Cells were washed with William's E containing 2 mM l-glutamine, 10 mM Hepes pH 7.4, 100 U/mL penicillin/streptomycin, and 100 nM dexamethasone. After which cells were filtered with a cutoff membrane of 60 μm to obtain single cells. Viability of the isolated hepatocytes was determined by a trypan blue test, and was at least 90%. Cells were seeded at a density of 3,5*10^6 cells/plate on a 60 mm culture dish in 3.5 mL William's E medium containing phenol red, supplemented with 2mM L-

glutamine, 10 mM Hepes pH 7.4, 1% ITS+, 100 U/ml penicillin/streptomycin, 25 nM dexamethasone and 5% FBS. Hepatocytes were allowed to attach (at 37°C with 5% CO_2) for two to three hrs and then washed with EBSS to remove unattached cells. Fresh serum-free medium containing 25 nM dexamethasone was added and matrigel (233 µg/mL) was then applied. Cells were kept overnight at 37°C with 5% CO_2 before treatment with test compounds.

2.2.3 Exposure of primary rat hepatocytes to 1′-hydroxyestragole

Rat primary hepatocytes were exposed to 1′-hydroxyestragole. The test compound was dissolved in DMSO to 100 mM stock solution. Further dilution was made first in DMSO and then in exposure media with final concentrations in exposure media of 0 (only DMSO), 0.5, 1, 2.5, 5, 10, 25, 50, 100, 150 µM of 1′-hydroxyestragole, with the final concentration of DMSO not exceeding 1%, a concentration that did not result in cytotoxicity for the rat hepatocytes. Exposure to the test compound was for 2 hrs at 37°C with 5% CO_2. It is known that DNA adduct formation is a fast reaction but that also repair pathways in rat primary hepatocytes are active as self defense mechanism; assumption was made that the two pathway were active in parallel. A 2 hr incubation was selected, during which DNA adduct formation appeared to be higher than repair of the DNA adducts since DNA adduct formation could be detected (see result section). To obtain a sufficient amount of DNA all concentrations of 1′-hydroxyestragole were tested in quadruplicates using hepatocytes from the same liver, and pooled together before the digestion step. For biological replicates, hepatocytes isolated from four individual perfusions were used. The supernatants of the incubations were used to measure cytotoxicity by detecting lactate dehydrogenase (LDH) activity and for the measurement of residual 1′-hydroxyestragole as described below.

2.2.4 DNA extraction from primary hepatocytes and enzymatic digestion

DNA was extracted from primary rat hepatocytes exposed to the test compound using the Get pure DNA Kit-Cell protocol (Dojindo Molecular Technology Inc., Kumamoto, Japan) for $3*10^6$ to $1*10^7$ cells (following the manufacturer's instructions); the protocol was modified by doubling the quantity of all reagents. The final DNA pellet was dissolved in a volume of 100 µL MilliQ water. The yield and purity of the extracted DNA was determined using Nanodrop technique by measuring the absorbance ratio A260 nm / A280 nm. DNA samples with an absorbance ratio of 1.8-2 were considered sufficiently pure. The quantity of DNA per sample was calculated from the Nanodrop output in ng/mL using a molar extinction coefficient for double stranded DNA of 50 ($L*mol^{-1}cm^{-1}$). The method of digestion was adjusted based on Delatour et $al.,$ (2008) for the release of the nucleosides E-3′-N^2-dG. Per 50 µg DNA in 100 µL water, 20 µL buffer P1 (300 mM sodium acetate, 1 mM $ZnSO_4$, pH 5.3), 12 µL SPDE (spleen phosphodiesterase) solution (0.0004 U/µL in water), and 10 µL nuclease P1 (0.5 µg/µL in water) were added and the resulting solution was incubated for 4 hrs at 37°C. Following incubation, 20 µL PA buffer (500 mM Tris-HCl, 1 mM EDTA, pH 8.0), 13 µL VPDE (venom phosphodiesterase) solution (0.00026 U/µL in water), and 5 µL alkaline phosphatase (0.764 U/µL in water) were added and the mixture was incubated for 3 hrs at 37°C (Delatour et $al.,$ 2008). Samples were filtered using eppendorf tubes with a cutoff membrane of 5.000 NMWL (Millipore). The hydrolyzed sample was evaporated to dryness and reconstituted in 50 µL water. The completeness of the digestion was confirmed by agarose gel electrophoresis (data not shown).

2.2.5 Synthesis of 1′-hydroxyestragole

1′-Hydroxyestragole was synthesized based on a reaction described by Drinkwater *et al.* (1976) adapted from Borchert *et al.* (1973). 1′-Hydroxyestragole was formed by a Grignard reaction: Vinyl Grignard (34.52 mmol) was added drop wise to a solution of 4-methoxybenzaldehyde (28.77 mmol) in 20.0 mL of anhydrous tetrahydrofuran cooled down to 0°C and purged under argon. The reaction mixture was stirred in an ice/water cold bath for 3 hrs (temperature maintained below 10°C) and quenched by the addition of 10.0 mL of saturated NH_4Cl. The reaction medium was then diluted with 30 mL of ethyl acetate and 10 mL of water. The two phases were separated and the aqueous phase was extracted with 2*40 mL of ethyl acetate. The combined organic extracts were dried over Na_2SO_4, filtered and evaporated under vacuum to afford 5.90 g of yellow oily residue. This oily residue was purified by column chromatography over silica gel using a Biotage SP-1 equipment with a gradient of hexane/ethyl acetate (from 5% to 40% ethyl acetate). 3.75 g (22.85 mmoL, 80% isolated yield) of (±)-1′-hydroxyestragole were isolated as a yellow oil. Satisfactory purity was demonstrated by NMR (> 96%), HPLC (> 96%) and GC-Tof analysis (pure). NMR analysis of 1′-hydroxyestragole:

^{1}H-NMR ($CDCl_3$, 360 MHz): δ (ppm) 1.86 (d, 1H, J = 3.9 Hz, OH); 3.81 (s, 3H, OMe); 5.17 (bm, 1H, CH); 5.19 (dt, 1H, J = 10.3 Hz; J = 1.4 Hz, =CH); 5.34 (dt, 1H, J = 17.2 Hz, J = 1.4 Hz, =CH); 6.05 (ddd, 1H, J = 17.2 Hz, J = 10.3 Hz, J = 5.9 Hz, =CH); 6.89 (m, 2H, ArH); 7.30 (m, 2H, ArH).

^{13}C-NMR ($CDCl_3$, 90 MHz): δ (ppm) 58.12 (1C, OMe); 77.72 (1C, CH); 116.76 (2C, ArH); 117.61 (1C, =CH_2); 130.50 (2C, ArH); 137.64 (1C; C^{IV} Ar); 143.17 (1C, =CH); 162.05 (1C, C^{IV} OAr).

GC-Tof analysis was performed on a DB-5 GC column (Length 30 m; Int. Diameter 250 μm; Film thickness 0.25 μm) in split-less mode using helium as the carrier gas. Inlet purge time: 120 s; Inlet purge flow: 30 mL/min; Inlet total flow: 31.27 mL/min; Inlet temperature: 250°C. (±)-1′-Hydroxyestragole eluted in these conditions with a retention time of 20.2 min and the mass spectrum was in agreement with the structure of (±)-1′-hydroxyestragole. GC-Tof mass spectrum: m/z (rel. int. %): 55(100), 77(97), 109(79), 39 (63), 121(53), 94(45), 135(43), 65(40) 164(36), 137(31), 115(17), 147 (14).

2.2.6 Synthesis of 1′-acetoxyestragole

1′-Hydroxyestragole (46 mg, 0.280 mmol) was dissolved in 1 mL of dichloromethane and this solution was cooled down to 0-5°C in an ice/water bath. Subsequently 35 μL of acetic anhydride (0.375 mmol) and 200 μL pyridine (2.48 mmol) were added and the reaction mixture was stirred for 10-15 min at 0-5°C. The reaction mixture was further stirred for 24 hrs at room temperature. After 24 hr, 10 mL dichloromethane were added to the reaction mixture and this solution was extracted with 2 mL MilliQ water. The pH of the aqueous extract was controlled (pH 8). The dichloromethane solution was then extracted with 2 mL HCl 1N. Control of the aqueous extract pH showed a pH of 2-3. The dichloromethane solution was further extracted with 2 mL sodium carbonate (1M), then dried with sodium sulphate, filtered, and evaporated to dryness under vacuum to obtain 60 mg of 1'acetoxyestragole (0.242 mmol, 86% isolated yield). Purity of 1′-acetoxyestragole was verified by HPLC UV, NMR and GC-ToF. NMR analysis of 1′-acetoxyestragole:

^{1}H-NMR (CDCl$_3$, 360 MHz): δ (ppm) 2.23 (s, 3H, OAc); 3.81 (s, 3H, OMe); 5.26 (bm, 1H, =CH); 5.24-5.31 (dt, 1H, J = 28.2 Hz; J = 1.0 Hz; =CH); 6.05 (ddd, 1H, J = 17.2 Hz; J = 10.1 Hz; J = 6.0 Hz; =CH); 6.20 (bd, 1H, J = 5 Hz, CH); 6.91 (m, 2H, ArH); 7.30 (m, 2H, ArH).

^{13}C-NMR (CDCl$_3$, 90 MHz): δ (ppm) 24.80 (1C, CH$_3$, OAc); 58.12 (1C, OMe); 78.51 (1C, CH); 116.57 (2C, ArH); 118.80 (1C, =CH$_2$); 131.35 (2C, ArH); 134.01 (1C; C^{IV} Ar); 139.43 (1C, =CH); 162.34 (1C, C^{IV} OAr); 169.31 (1C, CO, OAc).

GC-Tof Mass spectrum: m/z (rel. int. %): 103(100), 164(67) 146(67), 131(67), 147(56), 135(44), 115(44), 163(22), 206(17).

2.2.7 Synthesis of E-3′-N^2-deoxyguanosine (E-3′-N^2-dG) and (^{15}N$_5$) E-3′-N^2-deoxyguanosine ((^{15}N$_5$) E-3′-N^2-dG)

E-3′-N^2-dG and (^{15}N$_5$) E-3′-N^2-dG were prepared as described by Punt *et al.*, (2007). Briefly, 250 µl of a 0.01g/mL solution of 1′-acetoxyestragole in DMSO were added to 2250 µL of 2.5 mM 2'-deoxyguanosine (non-labeled or labeled, respectively) dissolved in 2.5 mM ammonium bicarbonate at pH 7.6. The incubation was stirred for 60 hrs at 37°C. In order to obtain the adduct E-3'-N^2-dG, the reaction mixture was purified using HPLC UV (HP1090 with a UV detector HP 1090) according to Punt *et al.* (2007). The synthesized nucleotides E-3′-N^2-dG and (^{15}N$_5$) E-3′-N^2-dG were further purified using a Waters semi preparative column: C18 7.8 cm * 150 mm, 7 µm. The gradient was made with ultrapure water and 100% acetonitrile, with a flow rate of 2 mL/min. 200 µL of the crude nucleoside preparation were injected. For elution, a linear gradient was applied over 40 min from 20% to 30% acetonitrile, followed by an increase to 100% acetonitrile in 2 min, and keeping the gradient at 100% acetonitrile for one minute. Then acetonitrile was lowered to 20% in 2 min and the column was equilibrated with 20% acetonitrile for 10 min. Batches of 200 µL of the crude mixture were injected and each individual peak was collected. Under these conditions, peaks corresponding to E-3′-N^2-dG and (^{15}N$_5$) E-3′-N^2-dG eluted at a retention time of 7.5 min.

2.2.8 LC-ESI-MS/MS method for detection and quantification of E-3'-N^2-dG

The LC-ESI-MS/MS method was adapted from Punt *et al.* (2007). LC-ESI-MS/MS analysis was performed on an Agilent 1100 series (Agilent Technologies, Waldbronn, Germany) coupled to a TSQ Quantum triple quadruple mass spectrometer from Thermo Finnigan (San Jose, CA, USA). Samples were injected on an Agilent Zorbax Extend-C18 column, 2.1*50 mm, 3.5 Micron 80 Å (Basel, Switzerland), with a Zorbax guard column. The gradient was made with ultrapure water containing 0.1% (v/v) formic acid and 100% acetonitrile. The flow rate was set at 0.3 mL/min. A linear gradient was applied from 20% to 70% acetonitrile over 8 min, after which the percentage of acetonitrile was brought to 100% in 1 min, and kept at 100% acetonitrile over 2 min. The amount of acetonitrile was lowered to 20% over 1 min, and the column was equilibrated at these initial conditions for 8 min. E-3'-N^2-dG eluted at 4.94 min. The mass spectrometric analysis was done in positive ion mode. The electro-spray capillary voltage was set at 4kV and the capillary temperature at 250°C. The cone voltage was set to 20V; extractor voltage 3V; and the RF lens to 0.3V. Nitrogen was used as sheath gas with a pressure of 7 bar (100 psi). The collision gas pressure was set at 350 mbar (5 psi) in the collision cell. The dwell time per transition was 0.02s. A divert valve was used in order to discard the first 2 min and the gradient after elution of the peak. Sample analysis was carried out using selected reaction

monitoring (SRM) mode, and characteristic transitions were recorded. The most intense transition was used as quantifier and the second transition as qualifier: 414 → 298 m/z (qualifier), 414 → 164 m/z (quantifier), and 414 → 147 (qualifier) for E-3'-N²-dG; 419 → 303 m/z (qualifier), and 419 → 169 m/z (quantifier) for (¹⁵N₅) E-3'-N²-dG (table 2.1). The limit of detection (LOD) and limit of quantification (LOQ) were measured by adding to digested DNA from untreated rat hepatocytes a constant amount of the internal standard (0.012 nmol) and increasing amount of E-3'-N²-dG (0-0.0157-0.04-0.0785-0.12-0.14-0.16 nmol). The LOD was defined as three times over the background level and the LOQ was defined as 10 times above the background level.

Table 2.1. Transition reaction (m/z) and the collision energy used to obtain the daughter fragments by LC-ESI-MS/MS.

	Transition (m/z) (used for quantification)	Collision energy (eV)	Transition (m/z) (used for conformation)	Collision energy (eV)
E-3′-N²-dG	414→164	34	414→298 414→147	26 45
(¹⁵N⁵)E-3′-N²-dG	419→169	34	419→303	26

2.2.9 Quantification of nucleoside E-3′-N²-dG by isotope dilution

Samples of 50 µL of digested rat hepatocyte DNA were spiked with 10 µL of the internal standard (¹⁵N₅) E-3'-N²-dG to achieve 5 ng/µL (0.012 nmol) injection of the internal standard into the instrument using an injection volume of 10µL. In order to quantify the amount of adduct formed in the samples, a calibration curve was prepared using increasing concentrations of E-3'-N²-dG (0, 0.0157, 0.04, 0.0785, 0.12, 0.14, and 0.16 nmol) with a constant concentration of (¹⁵N₅) E-3'-N²-dG (0.012 nmol). Calibration curves were prepared plotting the ratio of the peak areas against the ratio of the concentrations of E-3'-N²-dG and the internal standard, (¹⁵N₅) E-3'-N²-dG. Furthermore, these calibration curves were injected before and after each sample sequence run to ensure that the instrument response did not vary during the run of the sample sequence. As reported by Delatour *et al.*, (2009) the response was considered linear when the response factor was lower than 15%. Data analysis of the calibration series and sample sequence was performed using Xcalibur software (Thermo Electron Corporation) and integrated using an excel spreadsheet developed internally (Nestlé Research Center), to comply with EU guidelines 2002/657/EC concerning the performance of analytical methods and the interpretation of results (EU guidelines: 2002/657/EC).

The amount of E-3′-N²-dG detected in the samples was related to the total amount of digested DNA detected in each sample and adjusted for the average Mw of DNA monophosporylated nucleotides (nt) of 327g/mol, in order to quantify the number of E-3′-N²-dG adducts per 1000 nt.

2.2.10 Determination of 1′-hydroxyestragole in primary rat hepatocytes supernatant

Primary rat hepatocytes were exposed to 50 µM and 100 µM of 1′-hydroxyestragole and incubated at 37°C at increasing time intervals up to 2 hrs. To quantify possible protein binding of 1′-hydroxyestragole, samples containing 50 µM of 1′-hydroxyestragole were incubated for the same time intervals without cells with bovine serum albumin at a concentration of either 1.25 mg/mL (physiological level) or 50 mg/mL (high level). Furthermore, chemical stability of 1′-hydroxyestragole was quantified by incubating 1′-hydroxyestragole without cells for increasing time intervals also up to 2 hrs. The supernatants and samples thus obtained were analyzed by HPLC-UV (HP1050 with a UV detector HP 1050) with detection at wavelengths of 220-260-275 nm in order to quantify the 1′-hydroxyestragole in the incubation medium. The gradient was made with ultra-pure water and acetonitrile, with a flow rate of 1 mL/min. A linear gradient was applied from 20% to 30% acetonitrile in 20 min, followed by an increase in acetonitrile in 2 min to 100%, and keeping acetonitrile at 100% for one minute. Acetonitrile was lowered to 20% in 2 min and the HPLC instrument was equilibrated to 80% water and 20% acetonitrile for 10 min. 20 µL of sample was injected onto a Supelcosil LC 18 DB 25 cm * 4,6 mm, 5 µm column with a Supelco guard column Sulpelco. The elution time of 1′-hydroxyestragole was at 9.9 min. Furthermore, 90 µL of each sample were incubated for 2 hrs at 37°C with 2.5 µL of β-glucuronidase (0.35U, 140 U/mL) and 10 µL of 1M potassium phosphate buffer (pH 6.2) followed by analysis described above by HPLC-UV to detect 1′-hydroxyestragole. and investigate to what extent the reduction in 1′-hydroxyestagole in the incubation media could be ascribed to formation of 1′-hydroxyestagole glucuronide, representing a detoxification pathway.

2.2.11 Cytotoxicity assay

Cytotoxicity was determined by measuring the activity of cytoplasmic lactate dehydrogenase (LDH) in cell culture supernatants reflecting leakage from the cytoplasm of damaged cells, using ENZYLINE™ LDH Optimise 10 (BioMerieux® SA, Lyon, France) solution measured with the Roche COBAS MIRA plus analyzer (Minnesota, USA). The LDH was assayed by following the consumption of NADH to NAD^+, during the conversion of pyruvate to lactate. Absorbance of NADH was recorded at a wavelength of 340 nm at a temperature of 37°C, with an extinction coefficient of 6.22 mM^{-1} cm^{-1} (at 340 nm and pH 7.1). In order to validate the measurements, commercially available quality controls were freshly prepared and run in parallel. The quality controls used were: zymotrol™ (BioMerieux® SA, Lyon, France), duotrol™, and duotrol abnormal™ (Biomed, Germany).

2.2.12 Physiologically based biodynamic modeling

The PBBD model for rats was developed based on the PBBK model developed by Punt *et al.*, (2008). The equation for DNA adduct formation was introduced into the PBBK rat model for estragole, and parameters were kept similar to those reported and used before (Punt *et al.*, 2008). The time of simulation by the model was shortened from 24 hrs to 2 hrs in order to match the incubation time of the treated hepatocytes with 1′-hydroxyestragole. In order to calculate the amount of DNA adducts formed at each external dose of estragole given the model was extended as follows. The mass balance equation for the level of 1′-

hydroxyestragole in the liver reported in Punt *et al.,* 2008 in the PBBK model was used to derive the AUC for 1′-hydroxyestragole in the liver within the first two hours of exposure.

Liver: $dAL_{HE}/dt = + V_{max,L\_HE} * CL_E/PL_E/(K_{m,L\_HE} + CL_E/PL_E) - V_{max,L\_OE} * CL_{HE}/PL_{HE}/(K_{m,L\_OE} + CL_{HE}/PL_{HE}) - V_{max,L\_HEG} * CL_{HE}/PL_{HE}/(K_{m,L\_HEG} + CL_{HE}/PL_{HE}) - V_{max,L\_HES} * CL_{HE}/PL_{HE}/(K_{m,L\_HES} + CL_{HE}/PL_{HE})$

$CL_{HE} = AL_{HE}/VL$

$dAUC_{HE}/dt = CL_{HE}$

where CL_{HE} is the 1'-hydroxyestragole concentration in the liver (µmol/L); CL_E is the concentration of estragole in the liver; PL_E is estragole liver/blood partition coefficient; VL volume of the liver (in Liters); AL_{HE} is the amount of 1'-hydroxyestragole in the liver (L) in µmol; PL_{HE} is the liver/blood partition coefficient of 1'-hydroxestragole; V_{max,L_M} and K_{m,L_M} are the maximum rate of formation and the Michaelis–Menten constant for the formation of 1'-oxoestragole (OE), 1'-hydroxyestragole (HE) and for the phase II metabolites 1'-hydroxyestragole glucuronide (HEG) and 1'-sulfooxyestragole (HES) in the liver (Punt *et al.,* 2008). AUC_{HE} (hr*µmol/L) is the area under the concentration-time curve of 1'-hydroxyestragole in the liver. Differential equations were integrated using the Berkley Madonna 8.0.1 software (Macey and Oster, UC Bekeley, CA, USA).

The following equation was added to the model to describe the formation of E-3′-N^2-dG DNA adducts as a function of the AUC for 1′-hydroxyestragole:

$$DNA_{dG} = A + B * AUC_{HE}$$

The DNA_{dG} (#adducts/1000nt) is the amount of DNA adduct formed due to the specific binding of 1′-hydroxyestragole to deoxyguanosine nucleoside, A and B are the intercept and the slope calculated based on the data from the *in vitro* experiments.

2.2.13 Sensitivity Analysis

A sensitivity analysis was performed by analyzing all model parameters to identify key parameters that influence the outcome of the PBBD model, the DNA adducts formation. Individual parameters were modified without changing the other model parameters, which were left at initial values. Normalized sensitivity coefficients (SC) for each parameter of the model were determined according to the following equation:

$$SC = (C'-C)/(P'-P)x(P/C),$$

Where C is the initial value of model output, C′ is the modified value of the model output resulting from an increase in parameter value, P is the initial parameter value, and P′ is the modified parameter value (Evans and Andersen, 2000). A 5 % increase in parameter values was chosen, to analyze the effect of a change in parameter on formation of DNA adducts in the rat hepatocytes.

2.3 Results

2.3.1 Cytotoxicity of 1′-hydroxyestragole in primary rat hepatocytes

Concentrations of 1′-hydroxyestragole tested for cytotoxicity ranged from 0 µM to 1000 µM (Figure 2.2). When primary rat hepatocytes were exposed to 1′-hydroxyestragole an increase in the medium of the LDH levels was observed above 200 µM (Figure 2.2), which is in line to what was reported by Chan and Caldwell, (1992) who measured cytotoxicity by LDH measurement in medium of hepatocytes exposed for 17 hrs to 1′-hydroxyestragole and observed cytotoxicity at concentrations higher than 100 µM. Based on these results 1′-hydroxyestragole concentrations selected for measuring DNA adduct formation in primary rat hepatocytes exposed to 1′-hydroxyestragole were chosen to be below 150 µM. Below 150 µM and at 2 hrs exposure time of the primary rat hepatocytes to 1′-hydroxyestragole no cytotoxicity was observed (data not shown).
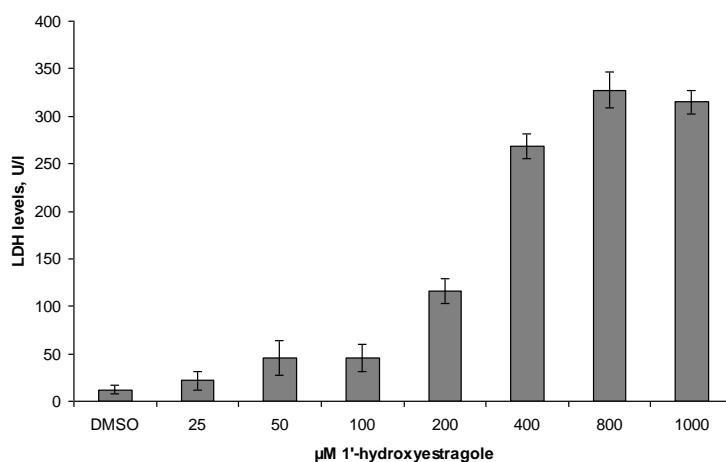

Figure 2.2. Cytotoxicity of 1′-hydroxyestragole towards isolated rat primary hepatocytes as detected by LDH leakage upon 2 hours exposure (extinction coefficient of NADH of 6.22 mM^{-1} cm^{-1}).

2.3.2 Quantification of E-3′-N^2-dG in primary rat hepatocytes exposed to 1′-hydroxyestragole by isotope dilution and LC-ESI-MS/MS

The reaction of the sulphate metabolite of 1′-hydroxyestragole with double strand DNA has been reported to produce four different adducts with the major one being E-3′-N^2-dG (Phillips *et al.*, 1981; Wiseman *et al.*, 1985; Wiseman *et al.*, 1987; Punt *et al.*, 2007). Via isotope dilution and LC-ESI-MS/MS analysis the amount of E-3′-N^2-dG DNA adducts formed in primary rat hepatocytes exposed to 1′-hydroxyestragole was quantified. Detection and quantification limits of the LC-ESI-MS/MS were 0.033 pmol and 0.08 pmol of E-3′-N^2-dG respectively. At concentrations above 0.5 µM 1′-hydroxyestragole formation of E-3′-N^2-dG DNA adducts was detected in the primary rat hepatocytes. Figure 2.3 presents the amount of E-3′-N^2-dG DNA adducts formed (expressed as # adducts/ 1000 nt) with increasing concentrations of 1′-hydroxyestragole (µM). These experimental data show a dose dependent increase in E-3′-N^2-dG DNA adduct formation at increasing concentrations of 1′-hydroxyestragole up to 150 µM, the highest non-cytotoxic dose level tested. At 150 µM 1′-hydroxyestragole the level of E-3′-N^2-dG DNA adducts formed amounted to 4.82

adducts/1000nt (average of four individual experiments). The results obtained reveal a linear relationship that passes through the origin between the concentration of 1′-hydroxyestragole and the level of E-3′-N^2-dG DNA adduct formation in the exposed rat primary hepatocytes.
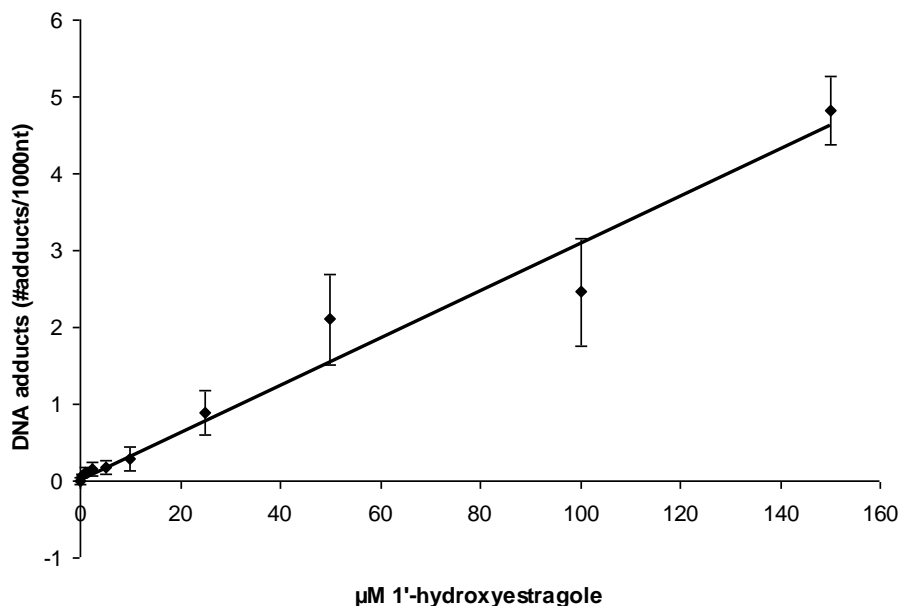

Figure 2.3. E-3′-N^2-dG adduct formation after 2 hours treatment in primary rat hepatocytes expressed in # adducts/1000nt as a function of different concentrations of 1′-hydroxyestragole, and quantified by LC-ESI-MS/MS using isotope dilution technique (average of four individual experiments).

2.3.3 Determination of 1′-hydroxyestragole in cell culture supernatants

To be able to define the AUC in order to link the PBBK model to the results from the *in vitro* studies on formation of DNA adducts in rat primary hepatocytes exposed to 1′-hydroxyestragole, the PBBK predicted AUC values for 1′-hydroxyestragole during the first two hours after *in vivo* exposure (AUC$_{HE}$) were linked to an equation defining the dependence of DNA adduct formation as a function of the AUC for 1′-hydroxyestragole as determined in the *in vitro* incubations (AUC$_{HE(in\ vitro)}$). To be able to define the AUC for 1′-hydroxyestragole in the *in vitro* model the time dependent changes in the level of 1′-hydroxyestragole in the medium of rat hepatocytes exposed to 1′-hydroxyestragole at different concentrations were quantified. The AUC$_{HE(in\ vitro)}$ was calculated using the generic formula of the area of the trapezoid: X = ba+b(c-a)/2 or X = b(c+a)/c. Figure 2.4A presents the time-dependent decrease in 1′-hydroxyestragole in the cell culture supernatants of hepatocytes exposed to 50 μM and to 100 μM 1′-hydroxyestragole up to 2 hrs. Control incubations in the absence of hepatocytes reveal no time dependent loss of the test compound (data not shown). In addition, control incubations in the absence of hepatocytes but in the presence of bovine serum albumin (BSA) resulted in about 10-20% loss of the test compound (data not shown), indicating a low level of protein binding. These results indicate that the compound is rapidly and effectively taken up and potentially metabolized by the cells. The majority of 1′-hydroxyestragole detoxification is known to occur through glucuronidation. In order to determine if the primary hepatocytes in our model are competent to metabolize
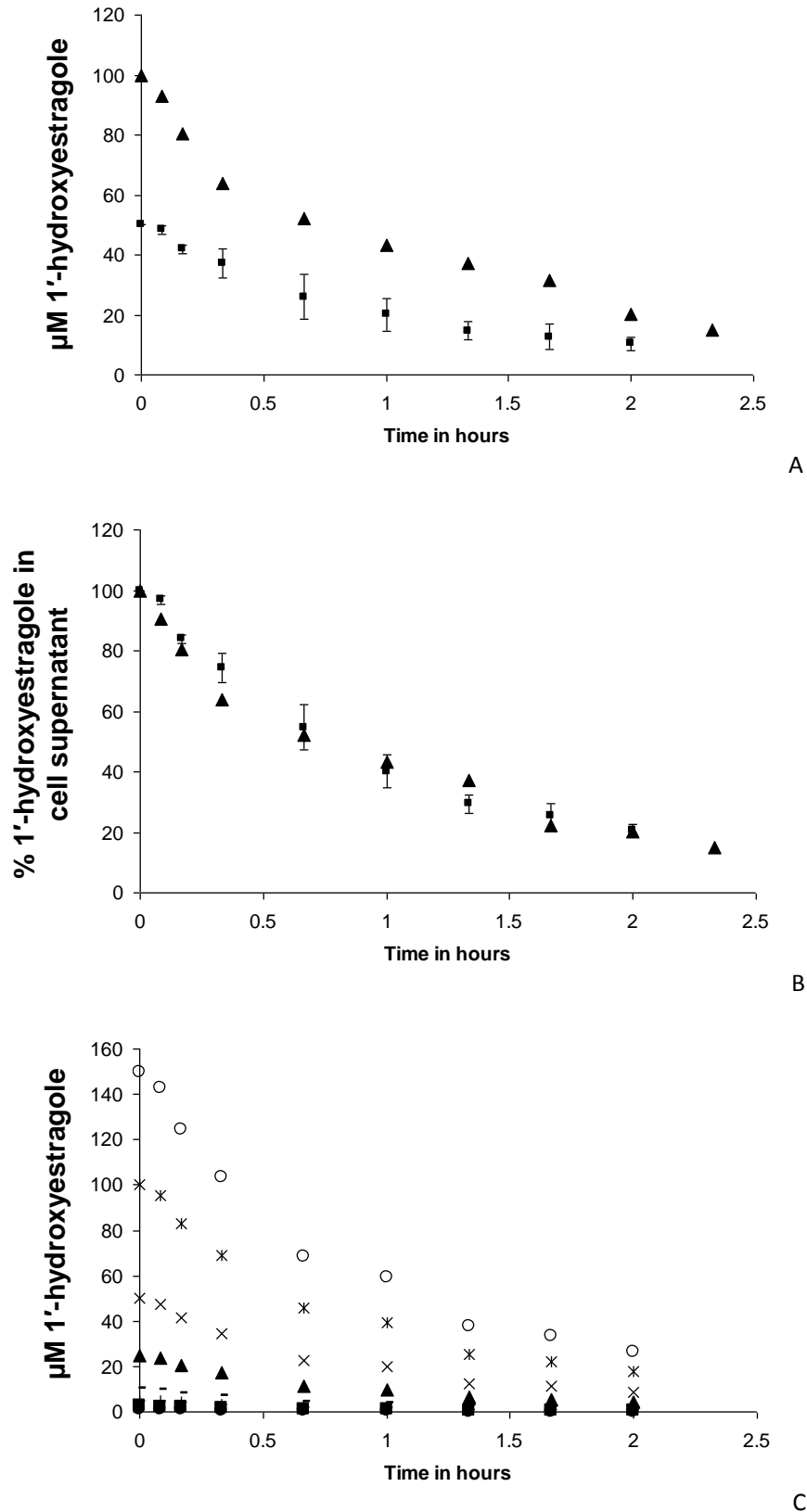
Figure 2.4. Time dependent decrease of 1'-hydroxyestragole in the media of primary rat hepatocytes exposed to either 50 (■) or 100 (▲) μM 1′-hydroxyestragole expressed in absolute concentrations (A) or as percentage of the starting concentration (B), and representation of the calculated time-dependent 1'-hydroxyestragole decrease in cell culture supernatant at each concentration tested 150μM (○), 100μM (*), 50μM (x), 25μM (▲), 10μM(−), 5μM (+), 2.5μM (■), 1μM (•) from which the respective $AUC_{HE(in\ vitro)}$ (hr*μmol/L) values were calculated (C).

1′-hydroxyestragole comparable to the *in vivo* situation, supernatants of the treated primary rat hepatocytes were treated with β-glucuronidase to release free 1′-hydroxyestragole from the glucuronic acid conjugates and reanalyzed for their 1′-hydroxyestragole levels. The results obtained revealed a recovery of more than 60-80% of 1′-hydroxyestragole upon treatment with β-glucuronidase (data not shown). This confirms that glucuronidation is a major pathway for conversion of 1′-hydroxyestragole in rat primary hepatocytes. Furthermore, taking into account that 10-20% of the originally added 1′-hydroxyestragole is lost due to possible protein binding it can be concluded that glucuronidation of 1′-hydroxyestragole accounts for most of the decrease in 1′-hydroxyestragole in the *in vitro* incubations, which would be in line with its metabolic fate in the *in vivo* situation. This confirms that the primary rat hepatocytes under these conditions are metabolically competent to form glucuronic acid conjugates as the major pathway for phase II metabolism of 1′-hydroxyestragole.

2.3.4 Definition of the PBBD model by linking *in vitro* data on DNA adduct formation to the PBBK model

From the experimental data on the decrease of 1′-hydroxyestragole as a function of time in the incubations with rat primary hepatocytes (Figure 2.4A) the $AUC_{HE(in\ vitro)}$ values were calculated. Experimental data obtained at 50 and 100 µM 1′-hydroxyestragole were also presented as the decrease in the percentage of the original concentration of the test compound (Figure 2.4B). This reveals that the time dependent decrease follows a similar pattern at both concentrations. From these experimental findings the time dependent decrease in the concentration of 1′-hydroxyestragole with other starting concentrations was modeled in line with these curves (Figure 2.4C) and this allowed calculation of the area under time curve ($AUC_{HE(in\ vitro)}$) values at all concentrations of 1′-hydroxyestragole tested.

In a next step these $AUC_{HE(in\ vitro)}$ values were used to replace the x-axis values in Figure 2.3 resulting in Figure 2.5. Figure 2.5 represent the level of E-3′-N^2-dG DNA adduct formation in the rat primary hepatocytes as a function of the AUC for 1′-hydroxyestragole ($AUC_{HE(in\ vitro)}$). In line with Figure 2.3 also Figure 2.5 reveals a linear relationship with an intercept at the origin. Thus, the curve presented in Figure 2.5 can be fitted by a linear equation passing through zero according to:

$$DNA_{dG} = 0.032 * AUC_{HE}$$

with $r^2 = 0.9635$, and DNA_{dG} representing the amount of E-3′-N^2-dG DNA adducts (#adducts/1000nt) formed in the hepatocytes at a certain $AUC_{HE(in\ vitro)}$ (hr*µmol/L) of 1′-hydroxyestragole.

By incorporating this equation in the PBBK model and defining that $AUC_{HE(in\ vitro)}$ should equal AUC_{HE} (hr*µmol/L) in the *in vivo* PBBK model defined by Punt *et al.,* (2008) a link between the AUC predicted in the PBBK model (AUC_{HE}) and the AUC from the hepatocyte incubations ($AUC_{HE(in\ vitro)}$) was established; ultimately providing a link between the PBBK model and the formula for DNA binding *in vitro* and defining a PBBD model that can predict DNA binding as a function of the estragole dose.
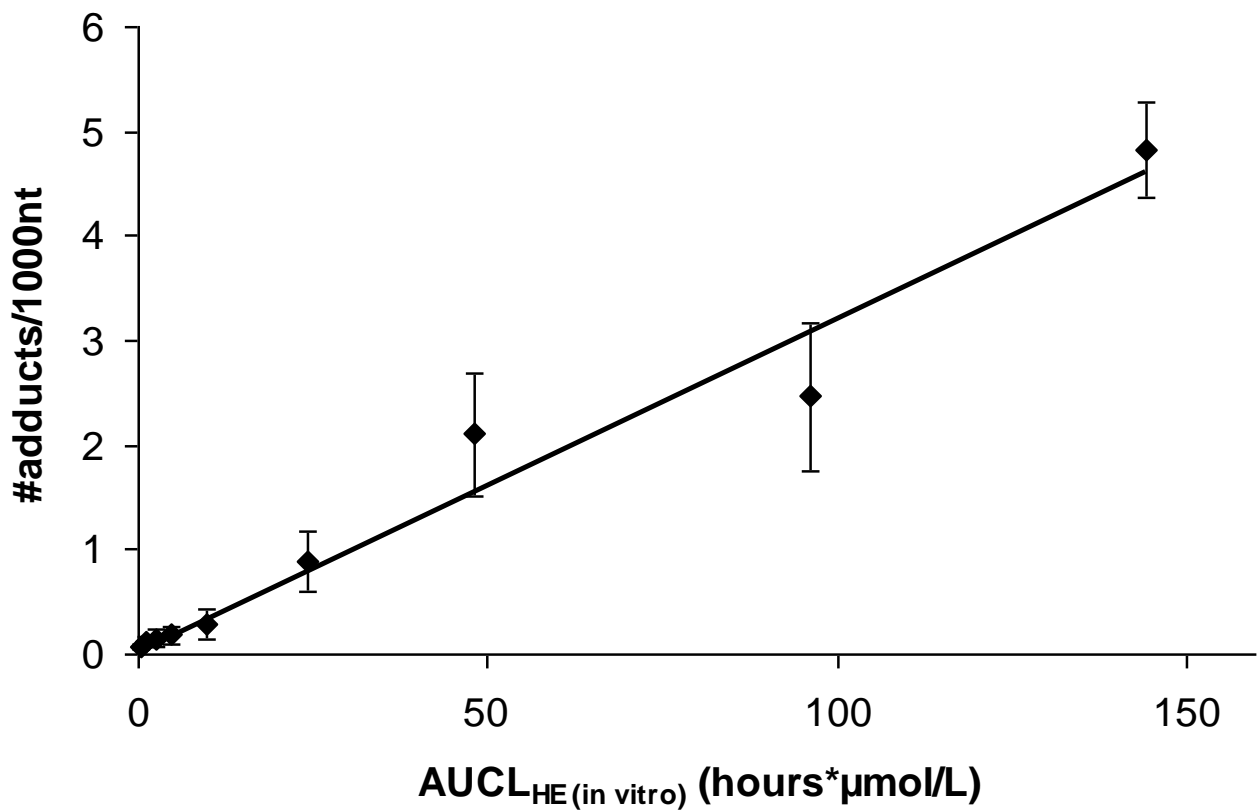
Figure 2.5. E-3'-N^2-dG adduct formation in primary rat hepatocytes expressed in #adducts/1000nt as a function of the AUC$_{HE(in\ vitro)}$ (hr*µmol/L) of 1'-hydroxyestragole, and quantified by LC-ESI-MS/MS using isotope dilution technique (average of four individual experiments).

2.3.5 Rat PBBD model predictions

The newly defined PBBD model was used to simulate the dose dependent DNA adduct formation in the liver of rat exposed to estragole. The results of this simulations are displayed in Figure 2.6 and reveals that up to dose levels of 100 mg/kg bw the E-3′-N^2-dG DNA adduct formation is predicted to be linear with increasing dose of estragole.

At a dose level of 0.01 mg/kg bw (Smith *et al.,* 2002), and 0.07 mg/kg bw estragole, (estimated daily human exposure for a 60 kg person reported by the Scientific Committee on food of the European Union) (SCF, 2001), the PBBK model predicted amounts of E-3′-N^2-dG DNA adduct formed of respectively 2, and 12.8 in 10^8 nt.

Figure 2.6. Dose dependent, PBBD model predicted DNA adduct formation (#adducts/1000nt) in the liver of rats exposed orally to estragole.

2.3.6 Sensitivity Analysis

Sensitivity analysis was performed at different estragole doses to identify the key parameters that can influence the DNA adduct formati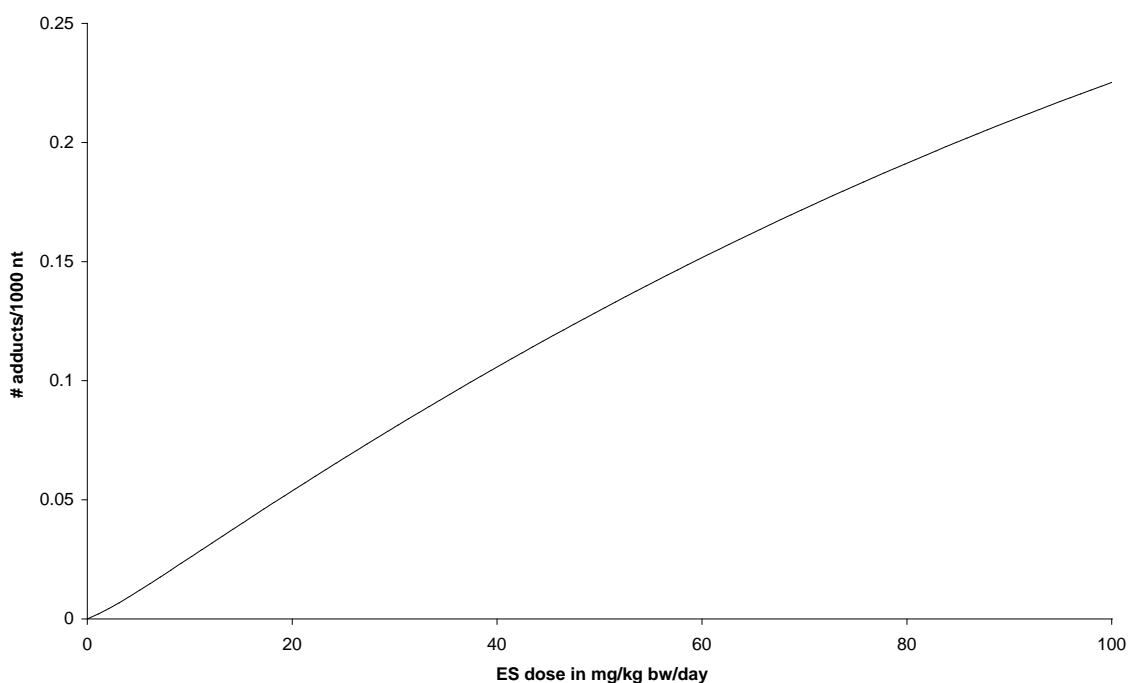on in the PBBD model outcome. The estragole doses set for sensitivity analysis were: 0.07 mg/kg bw (corresponding to the average daily intake for humans, SCF 2001), and 400 mg/kg bw (the dose used in the *in vivo* study by Randerath *et al.*, 1984). All parameters of the model were changed and only the ones which resulted in a normalized sensitivity coefficient higher than a 0.1 (in absolute value) were kept and displayed in Figure 2.7.

Figure 2.7 shows that the parameters with a major impact on the model prediction of the levels of DNA adducts were the slope of the DNA_{dG} versus $AUC_{HE(in\ vitro)}$ curve obtained from the *in vitro* hepatocyte data. Further, the kinetic parameters V_{max} and K_m for the glucuronidation of 1'-hydroxyestragole have a major impact. High sensitivity was found also when changing the liver/blood partition coefficient for 1'-hydroxyestragole (PLHE). Additionally, the dose played a role; at 0.07 mg/kg bw parameters such as body weight; volume Liver; blood through the liver; the uptake constant Ka; and the kinetic parameters V_{max} and K_m of the 1'-hydroxy metabolite had a higher impact than at 400 mg/kg bw. On the contrary at 400 mg/kg bw the blood through fat and the V_{max} of 1'-hydroxyestragole in the liver had a higher impact.
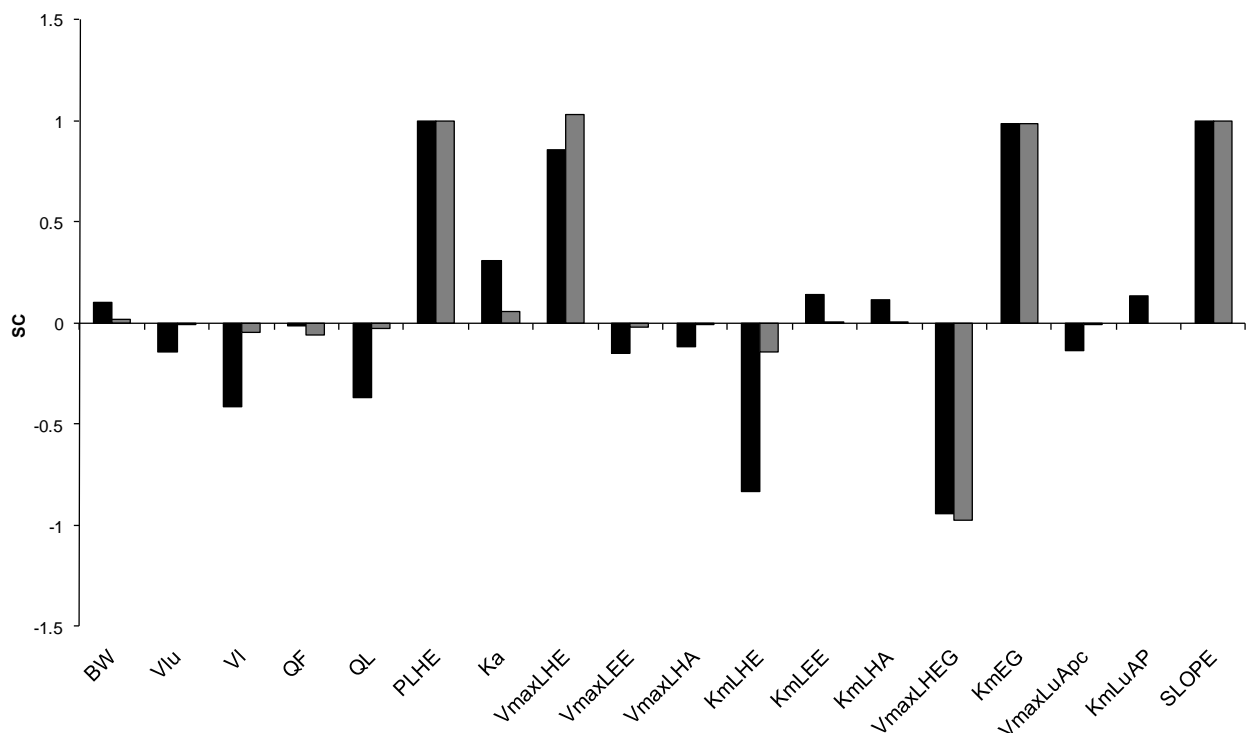
Figure 2.7. Sensitivity analysis of the PBBD model predictions at a dose of estragole of 0.07 mg/kg bw/day (black bars) and 400 mg/kg bw/day (grey bars). Model parameters evaluated include: the V_{max} and K_m of the different metabolites in the liver (L) and lung (Lu): 1'-hydroxyestragole (HE), estragole-2',3'-oxide (EE), 3'-hydroxyanethole (HA), 4-allylphenol (AP). 1'-hydroxyestragole glucuronide (HEG). Bw, body weight; VK, Volume kidney; VL, Volume Liver; QF, blood flow through fat; QL, blood flow through the liver; PLHE, liver/blood partition coefficient 1'-hydroxyestragole; and slope of the DNA_{dG} versus $AUC_{HE(in\ vitro)}$ curve.

2.4 Discussion

The present study illustrates the development of a physiologically based biodynamic (PBBD) model describing the dose dependent DNA adduct formation in liver of rats exposed to estragole. The PBBD model was developed based on combining our previously developed PBBK model for predicting *in vivo* formation of 1′-hydroxyestragole in the liver of rats exposed to estragole (Punt *et al.*, 2008) with *in vitro* data from experiments in which the formation of the major estragole DNA adduct, E-3′-N^2-dG, in isolated rat hepatocytes exposed to 1′-hydroxyestragole was quantified. In parallel, measurement of the time dependent decrease in 1′-hydroxyestragole in the medium of the exposed rat hepatocytes defined the concentration versus time area under the curve of each concentration of the test compound, $AUC_{HE(in\ vitro)}$. By defining the equation describing the E-3′-N^2-dG DNA adduct formation in rat primary hepatocytes as a function the $AUC_{HE(in\ vitro)}$, and by adding this equation to the PBBK model and defining the $AUC_{HE(in\ vitro)}$ to be equal to the AUC_{HE} already defined in the rat model it became possible to couple biokinetic with dynamic data and to extend the PBBK model to a PBBD model. The PBBD model allows estimation of the level of DNA adduct formation in rat liver upon different doses of estragole. This AUC approach was used previously in a paper on dynamical coupling of PBPK/PD and AUC-based toxicity models for arsenic *in vivo* in tilapia (Liao *et al.*, 2005). The PBBD model outcome showed a linear relationship between the level of E-3′-N^2-dG DNA adduct formation and the dose of estragole up to at least 100 mg/kg bw/day. At a dose level of 0.01 mg/kg bw/day (Smith *et al.*, 2002) and 0.07 mg/kg bw/day estragole (SCF, 2001), the PBBK model predicted amounts of E-3′-N^2-dG DNA adduct formed equal to respectively 2 and 12.8 in 10^8 nt. These levels of adducts were 2 to 3 order of magnitude below the background level of DNA damage of 1 adduct in 10^6 nt, which are of no known consequence (Williams, 2008). Furthermore levels are 1 to 2 order of magnitude lower when compared to the background levels of DNA adducts formed by low molecular weight alkylating agents, like for example N-nitrosamines, that are in a range of 1–10 adducts in 10^7 nucleotide (Farmer, 2005; Farmer, 2008).

To validate the newly developed PBBD model, *in vivo* experimental data on DNA adduct formation in rats exposed to estragole would be required but they are not available in the literature. Since generation of such *in vivo* data was beyond the objective of the present study the predicted PBBD model based outcomes were compared to data available in the literature on DNA adduct formation in the liver of mice exposed to estragole. Randerath *et al.* (1984) reported in female CD-1 mice the formation of 1 adduct in 10.000 – 15.000 DNA nucleotides after a single i.p. injection of 10 mg estragole per mouse. Assuming a mouse weight of 0.025 kg, the average intake dose was estimated to be 400 mg/kg bw/day. At this dose the PBBD model predicts the formation of E-3′-N^2-dG in the liver of rat at a level amounting to 4 adducts in 10.000nt. Taking into account that we quantified by LC-ESI-MS/MS the formation of only the E-3′-N^2-dG DNA adduct representing a major but not the only DNA adduct formed, whereas in the Randerath *et al.* (1984) DNA adducts were determined using ^{32}P-postlabelling detecting 1 adduct in 10.000nt, levels of DNA adduct formation in these two studies are within the same order of magnitude. The slight difference can be explained by the difference in the setup analysis of the two studies. In the present paper we used primary rat hepatocytes form male Sprague Dawley rats and the adducts were analyzed with the sensitive LC-ESI-MS/MS 2 hrs after exposure while Randerath *et al.* (1984) used female CD1 mice and analysis of samples was done by ^{32}P-postlabelling 24 hrs after treatment.

In risk assessment different mathematical models (ex. Linear model, Multistage model, Gamma model, Probit model, and Weibull model) can be used to extrapolate cancer risks from high dose animal exposure to cancer risks connected to low dose exposure relevant for the human situation. However, this approach to use mathematical models for high to low dose extrapolation of cancer risks is still a topic for considerable debate, since is not known whether or not these mathematical models take into account all biological process of relevant genotoxic carcinogenic compounds interacting with the body. PBBK models appear to provide a useful tool in risk assessment when modeling interspecies and high to low dose extrapolation of the ADME characteristics including bioactivation of genotoxic carcinogenic compound which are present in the human diet at low doses (Punt *et al.*, 2008; Punt *et al.*, 2009). Extension of the rat PBBK model to a rat PBBD model, by linking the area under the curve for 1′-hydroxyestragole formation predicted by the rat PBBK model to the area under the curve for 1′-hydroxyestragole in the culture medium of 1′-hydroxyestragole exposed rat primary hepatocytes, as reported in the present study, will give more insight on how the body reacts to the chemical at various dose levels. Clearly a limitation is that the present PBBD model predicts DNA adduct formation as the endpoint and does not yet allow prediction of estragole mutagenicity or carcinogencity, since for DNA adducts to induce mutations the cells must survive, proliferate, and replicate (Bailey *et al.*, 2009), which still is a long process before achieving the endpoint of actual tumor formation. However, although DNA adduct formation of genotoxic carcinogens is generally seen as a biomarker of exposure rather than a biomarker of response, the PBBD model now developed is one step closer to the ultimate toxic effect of estragole than the PBBK model for bioactivation and detoxification of estragole described previously. The PBBD model predicts the dose dependent level of $E-3′-N^2$-dG DNA adduct formation for low levels of exposure up to a dose level shown to cause cancer in the rodent bioassays and provides a proof of principle for modeling a toxicodynamic endpoint. Up to now only a few papers have described PBBD type models for genotoxic compounds. Conolly *et al.* (2004) reported a PBBD model for formaldehyde and Young *et al.* (2007) for acrylamide. However, both papers describe kinetic and dynamic modeling based on *in vivo* data, whereas the PBBD model of the present study is based solely on parameters from *in vitro* experimental data. Therefore, the present paper demonstrates for the first time that relatively reliable PBBD model linking doses to DNA adduct formation *in vivo* can be developed based solely on *in vitro* data. This provides a promising complement to the current risk assessment procedure, and may even have a substantial potential in the refinement, reduction or replacement of animals experimentation.

Reference

Bailey GS, Reddy AP, Pereira CB, Harttig U, Baird W, Spitsbergen JM, Hendricks JD, Orner GA, Williams DE, and Swenberg, JA. (2009) Nonlinear Cancer Response at Ultralow Dose: A 40800-Animal ED001 Tumor and Biomarker Study. Chem. Res. Toxicol. *22* (7): 1264–1276.

Bignold LP. (2004) Carcinogen-induced impairment of enzymes for replicative fidelity of DNA and the initiation of tumours. Carcinogenesis. 25(3): 299-307.

Borchert P, Wislocki PG, Miller JA, and Miller EC. (1973) The metabolism of the naturally occurring hepatocarcinogen safrole to 1′-hydroxysafrole and the electrophilic reactivity of 1′-acetoxysafrole. Cancer Res. 33: 575-589.

Bock KW, Brunner G, Hoensch H, Huber E, and Josting D. (1978) Determination of microsomal UDP-glucuronyltransferase in needle-biopsy specimens of human liver. Eur. J. Clin. Pharmacol. 14: 367–373.

Castegnaro M, Mohr U, Pfohl-Leszkowicz A, Estève J, Steinmann J, Tillmann T, Michelon J, Bartsch H. (1998) Sex- and strain-specific induction of renal tumors by ochratoxin A in rats correlates with DNA adduction. International Journal of Cancer. 77(1): 70-75.

Cavin C, Delatour T, Marin-Kuan M, Holzhäuser D, Higgins L, Bezencon C, Guignard G, Junod S, Richoz-Payot J, Gremaud E, Hayes JD, Nestler S, Mantle P, and Schilter B. (2007) Reduction in Antioxidant Defenses may Contribute to Ochratoxin A Toxicity and Carcinogenicity. Toxicol. Sci. 96(1): 30-39.

Chan VSW, and Caldwell J., (1992) Comparative induction of unscheduled DNA. synthesis in cultured rat hepatocytes by allylbenzenes and their 10-hydroxy metabolites. Food and Chemical Toxicology. 30: 831–836.

Coleman ME, Thran B, Morse SS, Hugh-Jones M, and Massulik S. (2008) Inhalation anthrax: dose response and risk analysis. Biosecurity and Bioterrorism: Biodefense Strategy, Practice, and Science. 6 (2): 147-159.

Conolly RB, Kimbell JS, Janszen D, Schlosser PM, Kalisak D, Preston J, and Miller FJ. (2003). Biologically motivated computational modeling of formaldehyde carcinogenicity in the F344 rat. Toxicol. Sci. 75: 432–47

Delatour T, Mally A., Richoz J, Ozden S, Dekant W, Ihmels H, Otto D, Gasparutto D, Marin-Kuan M, Schilter B, and Cavin C. (2008) Absence of 2′-deoxyguanosine-carbon 8-bound ochratoxin A adduct in rat kidney DNA monitored by isotope dilution LC-MS/MS. Mol. Nutr. Food Res. 52(4): 472-482.

Drinkwater NR, Miller EC, Miller JA, and Pitot HC. (1976) Hepatocarcinogenicity of estragole (1-allyl-4-methoxybenzene) and 1′-hydroxyestragole in the mouse and mutagenicity of 1′-acetoxyestragole in bacteria. J. Natl. Cancer Inst. 57: 1323–1331.

Evans MV, and Andersen ME. (1995) Sensitivity Analysis and the Design of Gas Uptake Inhalation Studies. Inhalation Tox., 7:7, 1075-1094.

Evans MV, and Andersen ME. (2000) Sensitivity analysis of a physiological model for 2,3,7,8-tetrachlorodibenzo-p-dioxin (TCDD): assessing the impact of specific model parameters on sequestration in liver and fat in the rat. Toxicol. Sci. 54: 71-80.

Farmer PB, Brown K, Tompkins E, Emms VL, Jones DJL, Singh R, and Phillips DH. (2005) DNA adducts: Mass spectrometry methods and future prospects. Toxicol. Appl. Pharmacol. 207: S293 – S301.

Farmer PB. (2008) Significance for risk assessment of increases in background levels of carcinogen-derived protein and DNA Adducts. Abstracts / Toxicology Letters 180S: S6–S27.

Gardner I, Wakazono H, Bergin P, de Waziers I, Beaune P, Kenna JG, and Caldwell J. (1997) Cytochrome P450 mediated bioactivation of methylglyoxal to 1′-hydroxymethyleugenol in Fischer 344 rat and human liver microsomes. Carcinogenesis. 18: 1775-1783.

Garg A, and Bathasar JP. (2007). Physiologically based pharmacokinetic (PBPK) model to predict IgG tissue kinetics in wild type and FcRn-knockout mice. J. Pharmacokinet. Pharmacodyn. 34: 687-709.

Iyer LV, Ho MN, Shinn WM, Bradford WW, Tanga MJ, Nath SS, and Green, CE. (2003) Glucuronidation of 1′-Hydroxyestragole (1′-HE) by Human UDP-Glucuronosyltransferases UGT2B7 and UGT1A9. Toxicol. Sci. 73: 36-43.

Liao CM, Liang HM, Chen BC, Singh S, Tsai JW, Chou YH, and Lin WT. (2005) Dynamical coupling of PBPK/PD and AUC-based toxicity models for arsenic in tilapia Oreochromis mossambicus from blackfoot disease area in Taiwan. Environ. Pollut. 135 (2): 221-33.

Mager DE, Woo S, and Jusko WJ. (2009) Scaling pharmacodynamics from *in vitro* and preclinical animal studies to humans. Drug Metab Pharmacokinet. 24(1): 16-24.

Miller EC, Swanson AB, Phillips DH, Fletcher TL, Liem A, and Miller JA. (1983) 'Structure-activity studies of the carcinogenicities in the mouse and rat of some naturally occurring and synthetic alkenylbenzene derivatives related to safrole and estragole. Cancer Res. 43: 1124-1134.

Phillips DH, Miller JA, Miller EC, and Adams B. (1981) Structures of the DNA adducts formed in mouse liver after administration of the proximate hepatocarcinogen 1′- hydroxyestragole. Cancer Res. 41: 176–186.

Phillips DH. (2005) DNA adducts as markers of exposure and risk. Mutation research. 577(1-2): 284-92.

Preston RJ, and Williams GM. (2005) DNA-reactive carcinogens: mode of action and human cancer hazard. Crit Rev. Toxicol. 35: 673-683.

Punt A, Delatour T, Scholz G, Schilter B, van Bladeren PJ, and Rietjens IMCM. (2007) Tandem mass spectrometry analysis of N^2-(trans-isoestragol-3′-yl)deoxyguanosine as a strategy to study species differences in sulfotransferase conversion of the proximate carcinogen 1′-hydroxyestragolen. Chem. Res. Tox. 20 (7): 991-998.

Punt A, Freidig AP, Delatour T, Scholz G, Schilter B, Boersma MG, van Bladeren PJ, and Rietjens IMCM (2008). A physiologically based biokinetic (PBBK) model for estragole bioactivation and detoxification in rat. Toxicol. Appl. Pharmacol. 231 (2): 248-259.

Punt A, Paini A, Boersma MG, Freidig AP, Delatour T, Scholz G, Schilter B, van Bladeren PJ, and Rietjens IMCM. (2009) Use of physiologically based biokinetic (PBBK) modeling to study estragole bioactivation and detoxification in humans as compared to male rats. Toxicol.   Sci. 110 (2), 255–269.

Randerath K, Haglund RE, Phillips DH, and Reddy MV. (1984) ^{32}P-Postlabelling analysis of DNA adducts formed in the livers of animals treated with safrole, estragole and other naturally-occurring alkenylbenzenes. I. Adult female CD-1 mice. Carcinogenesis. 5: 1613–1622.

Renwick AG, and Walton K. (2001) The use of surrogate endpoints to assess potential toxicity in humans. Toxicol. Lett. 120(1-3): 97-110.

Rietjens IMCM, Punt A, Schilter B, Scholz G, Delatour T, and Van Bladeren PJ. (2009) In-silico methods for physiologically based biokinetics (PBBK) models describing bioactivation and detoxification of coumarin and estragole; implication for risk assessment. Mol Nutr Food Res. 54(2), 195-207.

Sander M, Cadet J, Casciano DA, Galloway SM, Marnett LJ, Novak RF, Pettit SD, Preston RJ, Skare JA, Williams GM, Van Houten B, and Gollapudi BB. (2005) Proceedings of a workshop on DNA adducts: Biological significance and applications to risk assessment Washington, DC, April 13-14, 2004. Toxicol. Appl. Pharmacol. 208: 1-20.

SCF (Scientific Committee on Food). (2001) Opinion of the scientific committee on food on estragole (1-allyl-4-methoxybenzene, http://ec.europa.eu/food/fs/sc/scf/out104_en.pdf.

Shuker DEG. (1992) Relevance of urinary DNA adducts as markers of carcinogen exposure. Chem. Res. Toxicol. 5 (4): 450–460.

Sidhu JS, Farin FM, and Omiecinski CJ. (1993) Influence of extracellular matrix overlay on Phenobarbital-mediated induction of CYP 2B1, 2B2 and 3A1 genes in primary adult rat hepatocyte culture. Arch. Biochem. Biophys. 301: 103–113.

Smith RL, Adams TB, Doull J, Feron VJ, Goodman JI, Marnett LJ, Portoghese PS, Waddell WJ, Wagner BM, Rogers AE, Caldwell J, and Sipes IG. (2002) Safety assessment of allylalkoxybenzene derivatives used as flavouring substances - methyl eugenol and estragole. Food Chem. Toxicol. 40: 851-870.

Swenberg JA, Fryar-Tita E, Jeong Y, Boysen G, Vernon ST, Walker E, and Albertini RJ. (2008) Biomarkers in Toxicology and Risk Assessment: Informing Critical Dose–Response Relationships. Chem. Res. Toxicol. *21* (1): 253–265.

Tardif R, Droz PO, Charest-Tardif G, Pierrehumbert G, and Truchon G. (2002) Impact of human variability on the biological monitoring of exposure to toluene:I. Physiologically based toxicokinetic modeling. Toxicol. Lett. 134: 155-163.

Williams GM. (2008) Application of mode-of-action consideration in human cancer risk assessment. Toxicol. Lett. 180: 75-80.

Wiseman RW, Fennell TR, Miller JA, and Miller EC. (1985) Further characterization of the DNA adducts formed by electrophilic esters of the hepatocarcinogens 1′-hydroxysafrole and 1′-hydroxyestragole *in vitro* and in mouse liver *in vivo*, including new adducts at C-8 and N-7 of guanine residue. Cancer Res. 45: 3096-3105.

Wiseman RW, Miller EC, Miller JA, and Liem A. (1987) Structure-activity studies of the hepatocarcinogenicities of alkenylbenzene derivatives related to estragole and safrole on administration to preweanling male C57BL/6J x C3H/HeJ F_1mice. Cancer Res. 47: 2275-2283.

Yang RSH, El-Masri HA, Thomas RS, Dobrev I, Dennison Jr. JE, Bae DS, Campain JA, Liao KH, Reisfeld B, Andersen ME, and Mumtaz MM. (2004) Chemical mixture toxicology: from descriptive to mechanistic and going on to in silico toxicology. Environ. Toxicol. Pharmacol. 18: 65-81.

Young JF, Luecke RH, and Doerge DR. (2007) Physiologically Based Pharmacokinetic / Pharmacodynamic Model for Acrylamide and Its Metabolites In Mice, Rats, and Humans. Chem. Res. Toxicol. 20: 388-399.

Zhou G, Moorthy B, Bi J, Donnelly KC, and Randerath K. (2007) DNA adducts from alkoxyallylbenzene herb and spice constituents in cultured human (HepG2) cells. Environmental and Molecular Mutagenesis. 48 (9): 715–721.

Chapter 3

Based on:

***In vivo* validation of DNA adduct formation from estragole in rats predicted by physiologically based biodynamic (PBBD) modeling**

By:

Paini A, Gremaud E, Scholz G, Punt A, Spenkelink B, Alink G, Schilter B, van Bladeren PJ, Rietjens IMCM.

Abstract

Estragole is a naturally occurring food-borne genotoxic compound found in a variety of food sources, including spices and herbs. This results in human exposure to estragole via the regular diet. The objective of the present study was to quantify the dose-dependent estragole DNA adduct formation in rat liver and the urinary excretion of 1'-hydroxyestragole glucuronide in order to validate our recently developed physiologically based biodynamic (PBBD) model. Groups of male outbred Sprague Dawley rats (n=10, per group) were administered estragole once by oral gavage at dose levels of 0 (vehicle control), 5, 30, 75, 150, and 300 mg estragole/kg bw and sacrificed after 48hrs. Liver, kidney and lungs were analyzed for DNA adducts by LC-MS/MS. Results obtained revealed a dose-dependent increase in DNA adduct formation in the liver. In lungs and kidneys DNA adducts were detected at lower levels than in the liver confirming the occurrence of DNA adducts preferably in the target organ, the liver. The results obtained showed that the PBBD model predictions for both urinary excretion of 1'-hydroxyestragole glucuronide and the guanosine adduct formation in the liver were comparable within less than an order of magnitude to the values actually observed *in vivo*. The results obtained provide the first data set available on estragole DNA adduct formation in rats and confirm their occurrence in metabolically active tissues, i.e. liver, lung and kidney, while the significantly higher levels found in liver are in accordance with the liver as the target organ for carcinogenicity. This opens the way towards future modeling of dose dependent estragole liver DNA adduct formation in human.

3.1 Introduction

The human diet is highly complex and a variety of naturally occurring genotoxic carcinogens can be found in food. One common mechanism and a presumed prerequisite for the carcinogenicity of most genotoxic compounds is the formation of DNA adducts (Preston and Williams, 2005). Analysis of DNA adducts has been used to complement data on carcinogen exposure, metabolism, mutation, and tumor formation. The difficulties in assessing the risk of naturally occurring genotoxic carcinogens are well illustrated by the case of estragole. Estragole is present in spices and herbs such as basil, anise, fennel, bay leaves, and tarragon and their essential oils and thus present in a variety of foods with a long history of human use, traditionally considered as safe. However, estragole is known to be hepatocarcinogenic at high doses in rodents (Miller *et al.,* 1983). Estragole itself is not reactive but upon its rapid absorption in the gastrointestinal track it is transported to the liver, where the compound is bioactivated (Smith *et al.,* 2002). Metabolism of estragole can follow different pathways (Figure 3.1).
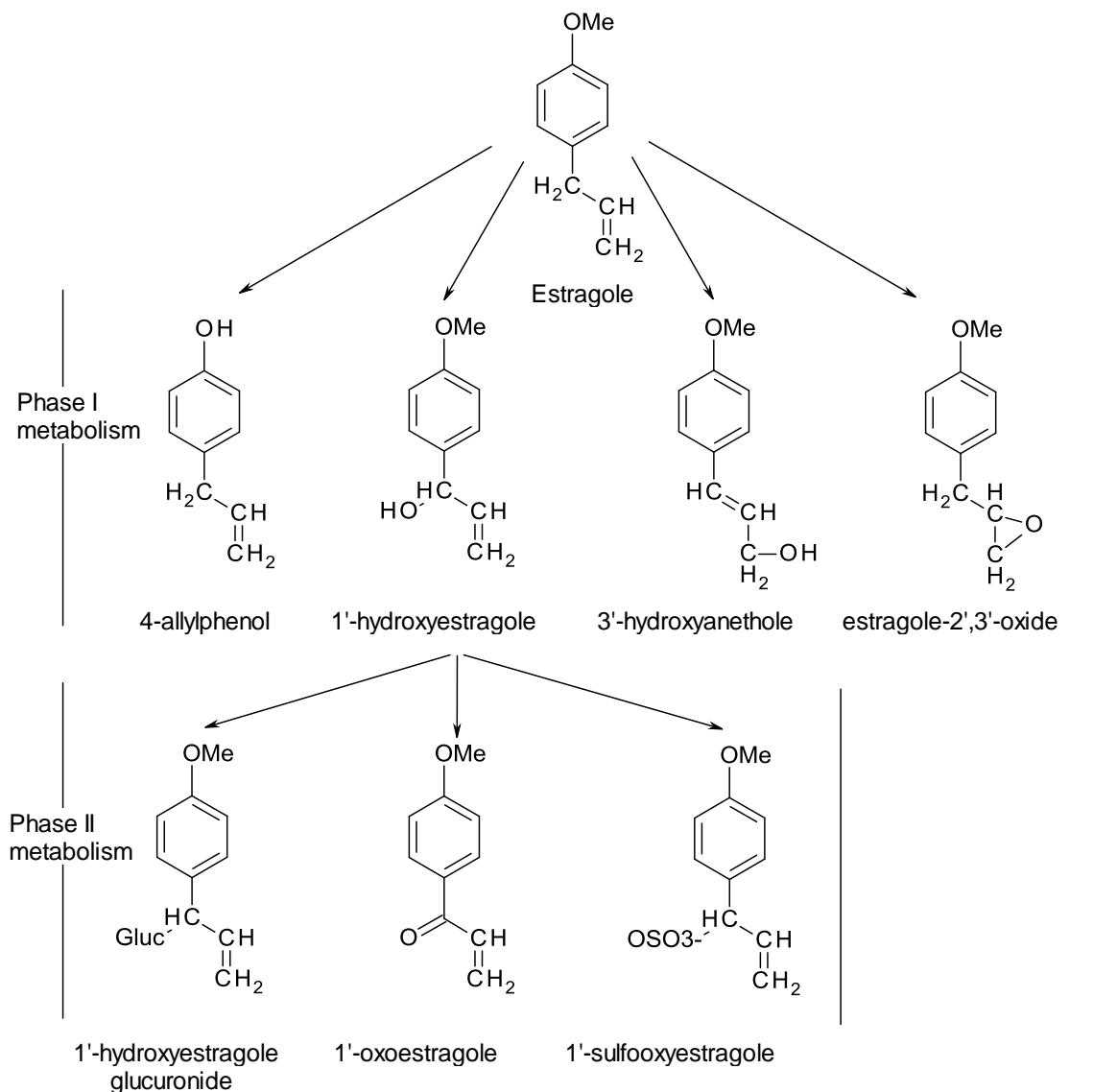

Figure 3.1. Metabolism of estragole (adapted from Punt *et al.*, 2009).

Estragole is detoxified via O-demethylation to 4-allylphenol or epoxidation to estragole 2',3'-oxide and subsequent swift conversion of the epoxide by epoxide hydrolase and/or glutathione S-transferases (Smith *et al.,* 2002; Phillips *et al.*, 1981). Estragole can also be converted to 3'-hydroxyanethole which can be glucuronidated and excreted in urine (Anthony *et al.,* 1987) or oxidized to 4-methoxycinnamic acid and in a follow up step form 4-methoxybenzoic acid. The main pathway for bioactivation of estragole proceeds by initial hydroxylation on the allyl side chain by cytochrome P450 enzymes resulting in the formation of 1'-hydroxyestragole, the proximate carcinogenic metabolite. 1'-Hydroxyestragole can be detoxified by glucuronidation or via oxidation (Phillips *et al.,* 1981; Iyer *et al.*, 2003). The glucuronidation of 1'-hydroxyestragole is present both in rat and human, being more dominant in rat than in human (Punt *et al.,* 2009), whereas the oxidation of 1'-hydroxyestragole to 1'-oxoestragole has been demonstrated to represent a major pathway in human but not in rat (Punt *et al.*, 2009).

Alternatively, sulfonation of 1'-hydroxyestragole by sulfotransferases gives rise to the unstable metabolite 1'-sulfooxyestragole which decomposes to generate the reactive carbocation which covalently binds to DNA, RNA and protein (Phillips *et al.*, 1981; Gardner *et al.*, 1996). Several adducts are formed upon reaction of 1'-sulfooxyestragole with the guanine base in DNA including N^2-(*trans*-isoestragol-3′-yl)-2′-deoxyguanosine, N^2-(estragol-1′-yl)-2′-deoxyguanosine, 7-(trans-isoestragol -3′-yl)-2′-guanine, 8-(trans-isoestragol-3′-yl)-2′-deoxyguanosine (Phillips *et al.*, 1981; Punt *et al.*, 2007). The major guanine adduct formed is N^2-(*trans*-isoestragol-3′-yl)-2′-deoxyguanosine (E-3′-N^2-dG) (Figure 3.1) which is considered to play a role in the genotoxic and carcinogenic effects induced by estragole (Smith *et al.,* 2002; Phillips *et al.*, 1981). The dG modifications have generally been reported as major adducts formed upon reaction of electrophiles with DNA because dG is the most potent nucleophilic nucleoside that can efficiently react with the electrophilic carbocation form (Singh *et al.,* 2006; Pfau *et al.,* 1994). Recently it was reported that adducts between estragole and adenine may also be formed to a significant extent (Ishii *et al.,* 2011).

Several investigators have studied the mechanism of estragole carcinogenesis by examining DNA binding and characterizing DNA adducts formed by estragole in mouse models. Randerath *et al.* (1984) utilized ^{32}P-postlabeling to analyze DNA adduct formation in the livers of adult female CD-1 mice administered intraperitoneal (ip) injections of estragole, safrole and other alkenylbenzenes. Estragole and safrole exhibited the strongest binding to mouse liver DNA (200-300 pmol adduct/mg DNA, at a 10 mg dose). Phillips *et al.* (1984) found that estragole, methyleugenol and safrole induced adducts to liver DNA of newborn male B6C3F1 mice treated by i.p. injection on day 1, 8, 15 and 22 after birth at doses of 0.25, 0.5, 1.0 and 3.0 μmol per animal. At day 23 upon dosing the adduct levels with methyleugenol (72.7 pmol/mg DNA) were higher than those with estragole (30.0 pmol/mg DNA) and safrole (14.7 pmol/mg DNA) (Phillips *et al.,* 1984).

Recently we defined a physiologically based biodynamic (PBBD) model to predict the dose-dependent DNA binding of estragole in rat liver (Chapter 2) by extending the previously published physiologically based biokinetic (PBBK) model for rat (Punt *et al.,* 2008). The PBBD model predicts the DNA adduct formation in the liver of rats at variable doses of estragole based on *in vitro and in silico* data only. However, the performance of the PBBD model developed could at the time not be evaluated due to the lack of *in vivo* data on DNA adduct formation in rats exposed to estragole. DNA adduct formation *in vivo* has to date only been studied in mice treated with estragole (Randerath *et al.,* 1984). Therefore the objective of the present study was to quantify the dose-dependent estragole DNA adduct formation in rat liver and the urinary excretion of

1'-hydroxyestragole glucuronide in order to validate our recently developed physiologically based biodynamic (PBBD) model. This PBBD model quantifies the dose-dependent bioactivation and adduct formation in liver of male rats based on *in vitro* experimental data on DNA adduct formation. The results obtained provide the first data set available on estragole DNA adduct formation in rats and confirm DNA adduct formation in the metabolically active organs liver, lung and kidney, and also indicate that the DNA adduct formation in the liver of estragole exposed rats can be modeled within one order of magnitude accuracy using PBBD modeling.

3.2 Methods and Materials

3.2.1 Materials

Estragole was obtained from Acros Organics (Geel, Belgium). 2′-Deoxyguanosine was purchased from Sigma (Basel, Switzerland). 1,2,3,7,9-$^{15}N_5$-2′-Deoxyguanosine ($^{15}N_5$-dG) was obtained from Cambridge Isotope Laboratories (Cambridge, MA). Alamethicin, β-glucuronidase, methanol, zinc sulphate (heptahydrate), phosphodiesterase I from Crotalus adamanteus (venom phosphodiesterase), phosphodiesterase II from bovine spleen (spleen phosphodiesterase), uridine 5'-diphospho-glucuronic acid (UDPGA) and alkaline phosphatase were purchased from Sigma (Schnelldorf, Germany). Acetonitrile, formic acid, dichloromethane, hydrochloric acid (37%), sodium carbonate , ammonium bicarbonate, sodium sulphate, petroleum ether, ethyl acetate, sodium acetate, tris (hydroxymethyl) aminomethane (Tris), ethylenediamine tetra acetic acid (EDTA), ammonia 30%, and ethanol were purchased from Merck (Darmstadt, Germany). Nuclease P1 was obtained from MP Biochemicals (Aurora, OH). Triethylacetate ammonium buffer, acetic anhydride, and pyridine were purchased from Fluka (Buchs, Switzerland) and β-glucuronidase was purchased from Roche (Mannheim, Germany). Heparin lithium tubes were purchased from Gosselin. Carboxymethyl cellulose (CMC; sodium salt, low viscosity - 42.0 mPa s) was purchased by Calbiochem. Animal feed Teklad 2914C was purchased from Harlan Laboratories.

Synthesis of E-3′-N^2-deoxyguanosine (E-3′-N^2-dG) and ($^{15}N_5$) E-3′-N^2-deoxyguanosine (($^{15}N_5$) E-3′-N^2-dG) were done as reported in Chapter 2.

3.2.2 Determination of kinetic constants for glucuronidation of 1′-hydroxyestragole

Incubation with different batches of male Sprague Dawley (SD) rat liver S9 were performed to determine the V_{max} and K_m for glucuronidation of 1'-hydroxyestragole. Three batches were purchased from BD Bioscience (cat # 452591 pooled SD rat liver S9 - Batch 1. Lot #61642; Batch 2. Lot #74099 ; Batch 3. Lot #88875). The incubation mixtures were performed as previously described (16) using a final volume of 200 µL, containing (final concentrations) 10 mM UDPGA and 0.2 mg mL-1 S9 protein in 0.2 M Tris-HCL (pH 7.4) containing MgCl2. The incubation mixture was pretreated on ice for 15 min with 0.025 mg/mL (final concentration) of alamethicin added from a 200 times concentrated stock solution in methanol (Fisher *et al.,* 2000; Lin *et al.,* 2002). The incubation reactions were started after pre-incubation of 1 min by the addition of 1'-hydroxyestragole at final concentrations varying from 50 to 2000 µM added from 200 times concentrated stock solutions in DMSO. The incubations were carried out for 10 min at 37°C and terminated by adding 50 µL of cold acetonitrile. Blank incubations were performed without the cofactor UDPGA. 1'-Hydroxyestragole

glucuronide was quantified on HPLC. Samples were centrifuged (16,000 g for 5 min) and 50 μL of supernatant of each were injected on an Alltima C18 5u column, 150*4.6 mm (Grace Alltech, Breda, The Netherlands) coupled to a HPLC-DAD system: a Waters 2695 Alliance system with a Waters 2996 photodiode array detector (Waters, Etten-Leur, The Netherlands). The gradient was made with ultrapure water containing 0.1% of acetic acid and acetonitrile. The flow rate was set a 1 mL/min and a linear gradient was applied from 10 to 25 % of acetonitrile over 30 min, after which the percentage of acetonitrile was increased in 2 min to 100% and kept at 100% for 2 min. 1'-Hydroxyestragole glucuronide and 1'-hydroxyestragole were quantified using a calibration curve of 1'-hydroxyestragole detected at a wavelength of 225 nm. For each batch V_{max} and K_m were determined in duplicate. The final V_{max} and K_m were calculated as the average of the three newly determined values and two data sets previously reported in the literature (Punt *et al.,* 2008; Alhusainy *et al.,* 2010).

3.2.3 Physiologically based biodynamic modeling

The PBBD model was developed based on the PBBK model developed by Punt *et al.*, (2008) and described in detail previously (Chapter 2). As presented in the result section some PBBK model parameters were defined specifically for the present study including the parameters for body weight and organ weights which were based on the actual data obtained for the rats of the present study. The kinetic parameters for glucuronidation of 1'-hydroxyestragole were defined in more detail using different batches of liver microsomes. The kinetics of 1'-hydroxyestragole glucuronidation appeared to have a major impact on the PBBK/BD model outcomes obtained and previous studies revealed a significant batch-to-batch variation for these kinetic parameters (Punt *et al.,* 2008; Alhusainy *et al.,* 2010). Other parameters were kept similar to those reported and used before (Punt *et al.,* 2007; Punt *et al.,* 2008).

3.2.4 Animals

The animal studies were in compliance to the Dutch Act on animal experimentation (Stb, 1977, 67; Stb 1996, 565), revised February 5, 1997. The study was approved by the ethical committee on animal experimentation of Wageningen University. All procedures were considered to avoid and minimize animal discomfort. Male SD rats, 6 weeks old were purchased from Harlan laboratories (The Netherlands). Rats were housed in type IV cages with Lignocel bedding (Lignocel BK 8/15), accommodating 3 rats per cage. Enrichment was provided, i.e. tissue, for each cage. Animal cages were cleaned according to the standard protocols. A photoperiod of 12 hrs light/dark cycle for the rats was applied during the animal acclimatization period and treatment period. Temperature (21°C ±1°C) and humidity (55% ±10%) were monitored daily. Teklad 2914C pellet feed and tap water was provided *ad libitum* during the overall period of the study (from arrival at the facility to sacrifice).

3.2.5 Time response study

The total number of animals for the time response study was 25 white male outbred SD rats, 6 weeks old (174 g; Stdev ± 6). Upon arrival animals were split randomly into cages and weighted 24 hrs after arrival at the facility, 7 days after arrival, and 12 days after arrival. After a 12 days acclimatization period in type IV cages in groups of 3 animals per cage, animals were put into metabolic cages 24 hrs prior to gavage and were kept in the metabolic cages up to time of sacrifice. Animals were treated with a single dose of estragole

of 300 mg/kg bw by gavage using a solution of estragole of 130 mg/mL in 0.5% carboxymethyl cellulose (CMC) (0.5 g CMC in 100 mL distillated water), with the volume of gavage not exceeding 10 mL/kg. Animal average weight was 242.3 g (Stdev ± 9.5) at treatment and 241.3 g (Stdev ± 10.9) at sacrifice. After the treatment animals were sacrificed at 2, 6, 24, or 48 hrs. For the 48 hrs time point a control was also introduced with 5 rats receiving only the vehicle control 0.5% CMC. Anesthesia was done with a mixture of isoflurane and oxygen, blood was removed after which the liver was harvested, weighted and cut into pieces, snap frozen in liquid nitrogen and stored at -80°C until further processing.

3.2.6 Dose-response study

The total number of animals for the dose response study was 60 white male outbred SD rats, 6 weeks old (177.1 g; Stdev ± 4.4). Upon arrival animals were split randomly into cages and weighted 24 hrs after arrival at the facility, 7 days after arrival, and 12 days after arrival. After a 12 days acclimatization period in type IV cage in groups of 3 animals per cage, animals were put into metabolic cages 24 hrs prior to gavage and were kept in the metabolic cages up to time of sacrifice. The following doses were administrated once to the rats; 0 mg/kg bw (vehicle control 0.5% CMC), 5, 30, 75, 150, or 300 mg/kg bw of estragole using a solution of estragole of 2.5, 15, 37, 76, and 150 mg/mL in 0.5% CMC, respectively. The volume of gavage did not exceed 10 mL/kg. Urines were collected twice a day (morning and afternoon) and were stored at -80°C until further analysis. Rats were sacrificed after 48 hrs. Average weight at treatment was 255.3 g (Stdev ± 9.8) and at sacrifice it amounted to 263.0 g (Stdev ± 10.23). After anesthesia of the animals with a mixture of isoflurane and oxygen, blood was removed after which liver, kidney and lungs were harvested, weighted and cut into pieces, snap frozen in liquid nitrogen and stored at -80°C until further processing. Blood was collected before removing organs in heparin tubes (4 mL), kept on ice and centrifuged (2000 rpm for 20 min, Sigma 2D centrifuge) plasma was stored at -80°C in aliquots for further analysis.

3.2.7 Tissue DNA extraction and digestion

DNA was extracted from liver, kidney, and lungs using the Get pure DNA Kit-Cell protocol (Dojindo Molecular Technology Inc., Kumamoto, Japan) for tissue (following the manufacturer's instructions). Briefly, three samples of each tissue were taken randomly from all organs, around 50-100 mg of each organ were put into a 2 mL eppendorf tube, and 800 µL of the lysis buffer with 20 µL of proteinase K solution were added. Homogenization of tissue was done using a Fast Prep cell disruptor instrument. The homogenized samples were further processed by following the manufacturer's protocol (Dojindo Molecular Technology Inc., Kumamoto, Japan). The final DNA pellet was dissolved in a volume of 100 µL MilliQ water. The yield and purity of the extracted DNA were determined using the Nanodrop technique by measuring the absorbance ratio A260 nm / A280 nm. DNA samples with an absorbance ratio of 1.8-2 were considered sufficiently pure. The quantity of DNA per sample was calculated from the Nanodrop output in ng/mL using a molar extinction coefficient for double stranded DNA of 50 ($L*mol^{-1}cm^{-1}$). The method of digestion was modified from Delatour *et al.* (2008) for the release of the nucleosides E-3′-N^2-dG. Briefly, per 50 µg DNA in 100 µL water, 20 µL buffer P1 (300 mM sodium acetate, 1 mM $ZnSO_4$, pH 5.3), 12 µL spleen phosphodiesterase solution (0.0004 U/µL in water), and 10 µL nuclease P1 (0.5 µg/µL in water) were added and the resulting solution was incubated for 4 hrs at 37°C. Following incubation, 20 µL PA buffer (500 mM Tris-HCl, 1 mM EDTA, pH 8.0),

13 µL venom phosphodiesterase solution (0.00026 U/µL in water), and 5 µL alkaline phosphatase (0.764 U/µL in water) were added and the mixture was incubated for 3 hrs at 37°C (Chapter 2). The hydrolyzed sample was evaporated to dryness and reconstituted in 50 µL water.

3.2.8 Isotope dilution quantification of E-3'-N^2-dG

Quantification of nucleoside E-3′-N^2-dG by isotope dilution was done as reported in Chapter 2. Briefly, 50 µL of digested DNA from rat tissue were spiked with 10 µL of the internal standard (^{15}N$_5$) E-3'-N^2-dG to achieve 5 ng (0.012 nmol) injection of the internal standard into the instrument using an injection volume of 10 µL. In order to quantify the amount of adduct formed in the samples, a calibration curve was prepared using increasing concentrations of E-3'-N^2-dG with a constant concentration of (^{15}N$_5$) E-3'-N^2-dG.

3.2.9 LC-MS/MS method for detection and data analysis of E-3'-N^2-dG

LC-MS/MS analysis was performed on a Perkin Elmer 200 Series HPLC System (Perkin Elmer, Waltham, Massachusetts) coupled to a API 3000 system (Applied Biosystem, Foster City, California). Samples were injected on an Agilent Zorbax Extend-C18 column, 2.1*50 mm, 3.5 Micron 80 Å (Basel, Switzerland), with a Zorbax guard column. The gradient was made with ultrapure water containing 0.1% (v/v) formic acid and 100% acetonitrile. The flow rate was set at 0.3 mL/min. A linear gradient was applied from 10% to 50% acetonitrile over 3 min, after which the percentage of acetonitrile was brought to 100% in 1 min, and kept at 100% acetonitrile over 2 min. The amount of acetonitrile was lowered to 10% over 1 min, and the column was equilibrated at these initial conditions for 8 min. E-3'-N^2-dG eluted at 2.88 min. The mass spectrometric analysis was performed with the following settings: Nebulizer gas (air) was set a 15 psi, Curtain gas (Nitrogen, which is used to keep the analyzer region clean) was set a 10 psi, ion spray voltage 4700V, collision energy (CE) 15eV, ion source temperature 300°C, declustering potential set at 37V, focusing potential was set at 200V, entrance potential at 9V, and collision cell exit was set at 12V. Nitrogen was used as sheath gas turbo, ion spray, with a pressure of 7000 L/h. The dwell time per transition was 0.05 sec. A divert valve was used in order to discard the gradient after elution of the peak. Quantification of the DNA adduct was carried out using selected-ion detection in the multiple reaction-monitoring mode (MRM), recording the following characteristic transitions: for the E-3′-N^2-dG 414 m/z → 298 m/z (CE= 18eV); 414 m/z → 164 m/z (CE= 37eV); and 414 m/z → 147 m/z (CE= 40eV); and for the (^{15}N$_5$) E-3'-N^2-dG 419 m/z → 303 m/z (CE= 18eV); 419 m/z → 169 m/z (CE= 37eV). Figure 3.2 shows the chromatograms of the E-3′-N^2-dG (414 → 298, quantifier) adduct formed in the three organs 48 hrs after a dose of 300 mg/kg bw, along with the qualifier transition (414 → 164) and the peak of (^{15}N$_5$) E-3'-N^2-dG (419 → 303).

Data analysis of the calibration series and sample sequence was performed using Analyst software (Applied Biosystem) and integrated using an Excel spreadsheet developed internally (Nestlé Research Center), to comply with EU guidelines 2002/657/EC concerning the performance of analytical methods and the interpretation of results (EU guidelines: 2002/657/EC). The amount of E-3′-N^2-dG detected in the samples was related to the total amount of digested DNA detected in each sample and adjusted for the average molecular weight of DNA monophosphorylated nucleotides (nt) of 327 g/mol, in order to quantify the number of E-3′-N^2-dG adducts per 1000 nt. For samples resulting in a negative value or below the LOD a zero value was applied; and for samples resulting in a value below the LOQ, the LOD value was applied.
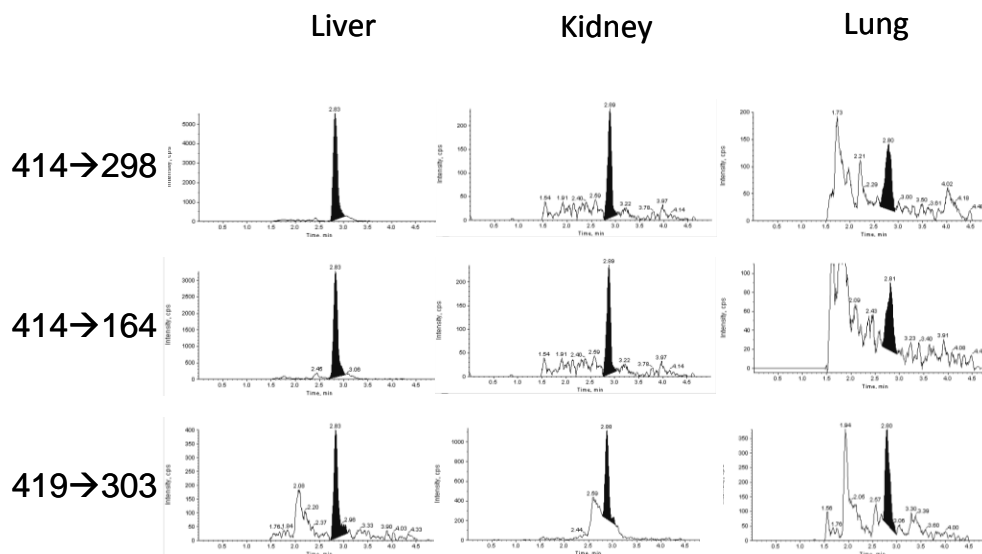
Figure 3.2. Chromatograms representing the E-3'-N^2-dG adduct formed in liver, kidney, and lungs at the quantifier transition (414→ 298), qualifier transition (414 → 164) and the peak of the internal standard (^{15}N$_5$) E-3'-N^2-dG (419 → 303). The highlighted peak reflects the presence of the adduct.

3.2.10 Quantification of urinary excretion of the biomarker 1'-hydroxyestragole glucuronide

Preparation and analysis of urines were done following the protocol reported by Zeller *et al*. (21). Urines were analyzed, randomly for 8 rats for each dose group. The vehicle control group was not analyzed, since for each rat a urine sample was collected 24 hrs before treatment which served as control. Briefly, to 50 µL urine sample 10 µL β-glucuronidase (0.36 U, 145700 U/mL) in phosphate buffer (pH 5) were added. Samples were incubated at 37°C for 2 hrs. Subsequently the metabolites were extracted using 500 µL ethylether (twice), the sample thus obtained was centrifuged and transferred to a new Eppendorf tube, after which the sample was dried using a speed vacuum and reconstituted with 200 µL water. An isotope dilution technique was used to measure the amount of 1'-hydroxyestragole released from 1′-hydroxyestragole glucuronide compared to the internal standard D-1'-hydroxyestragole (21). D-1′-hydroxyestragole was prepared by AltanChim Pharma (Nantes, France). LC-MS/MS analysis was performed on a Perkin Elmer 200 Series HPLC System (Perkin Elmer, Waltham, Massachusetts) coupled to an API 3000 system (Applied Biosystem, Foster City, California). Samples were injected on an Agilent Zorbax Extend-C18 column, 2.1*50 mm, 3.5 Micron 80 Å (Basel, Switzerland), with a Zorbax guard column. The gradient was made with ultrapure water containing 0.1% (v/v) formic acid and 100% acetonitrile. The flow rate was set at 0.3 mL/min. A linear gradient was applied from 10% to 50% acetonitrile over 3 min, after which the percentage of acetonitrile was brought to 100% in 1 min, and kept at 100% acetonitrile over 2 min. The amount of acetonitrile was lowered to 10% over 1 min, and the column was equilibrated at these initial conditions for 8 min. 1'-Hydroxyestragole eluted at 3.30 min. The mass spectrometric analysis was performed with the following settings: Nebulizer gas (air) was set a 15 psi, Curtain gas (Nitrogen, which is used to keep the analyzer region clean) was set a 12 psi, ion spray voltage 2200V, collision energy (CE) 15eV, ion source temperature 300°C, declustering potential set at 28V, focusing potential was set at 200V, entrance potential

at 12V, and collision cell exit was set at 27V. Nitrogen was used as sheath gas turbo, ion spray, with a pressure of 7000 L/h. The dwell time per transition was 0.05 sec. A divert valve was used in order to discard the gradient after elution of the peak. Quantification of the 1'-hydroxyestragole was carried out using selected-ion detection in multiple reaction-monitoring mode (MRM) recording the following characteristic transitions: for 1′-hydroxyestragole 147.2 m/z → 91.1 m/z (CE= 18eV); 147.2 m/z → 115.1 m/z (CE= 37eV); and 147.2 m/z → 131.2 m/z (CE= 40eV); and for D-1'-hydroxyestragole 150.2 m/z → 93.1 m/z (CE= 18eV); 150.2 m/z → 118.1 m/z (CE= 37eV); 150.2 m/z → 134.2 m/z (CE= 40eV).

3.2.11 Statistical analysis

T-test was performed using Excel (Microsoft Office 2010). Correlation analysis was performed using GraphPad Prism 5 (Version 5.04, 2010; GraphPad Software, Inc.). V_{max} and K_m were obtained using Graph pad Prism 5 (La Jolla, CA, USA), by selecting XY analyses – nonlinear regression and fitting the data to the standard Michaelis-Menten equation.

3.3 Results

3.3.1 Refinement of the physiologically based biodynamic (PBBD) model

Previously we developed a physiologically based biodynamic (PBBD) model for estimation of *in vivo* estragole DNA adduct formation based on experimental data on DNA adduct formation in primary hepatocytes (Chapter 2). This PBBD model allows estimation of the level of DNA adduct formation in rat liver upon different doses of estragole. To make the PBBD model as accurate as possible some adjustments were made to the model previously described. These included first of all a precise definition of the body and organ weights taking into account the actual values of the male SD rats used in the present study. Previously we applied as average body weight for male rats 250g, and values for liver, kidney and lung weight of respectively 8.5 g, 1.75 g, and 1.25 g (Punt *et al.,* 2008). In the present study the average body weight (for 60 animals) amounted to 263 g (Stdev ± 10.25) and the organ weights were: 11.32 g (±0.75), 1.70 (±0.14), and 1.42 (±0.09) for liver, kidney, and lung respectively. Furthermore, the PBBD model (Chapter 2) was run for 2 hrs which was extended to respectively 24 hrs or 48 hrs in the present study in order to make a correct comparison with the *in vivo* experimental data, since 24 hrs was the time used for urine collection and 48 hrs was the time between dosing and sacrifice used in the *in vivo* DNA adduct dose response study. Finally the kinetic parameters V_{max} and K_m for glucuronidation of 1'-hydroxyestragole were quantified for different batches of liver microsomes (table 3.1). This was done because the sensitivity analysis of the model previously indicated these parameters to be of significant influence on the outcomes obtained (Chapter 2) whereas they appeared to vary with the batch of liver microsomes analyzed and between different experimentalists, as shown in table 3.1. The average of five batches of male liver microsomes (three analyzed and two found in literature Punt *et al.*, 2008; Alhusainy *et al.*, 2010) resulted in values for the kinetic parameters for glucuronidation of 1′-hydroxyestragole that amounted to a V_{max} of 51.5 (Stdev ± 56) nmol min^{-1} (mg S9 protein)$^{-1}$ and a K_m of 203.4 (Stdev ± 40) µM (table 3.1). These values were incorporated in the PBBD model of the present study. In order to validate the PBBD model the *in vivo* study was performed in two steps: first a time response study was carried out to determine the time point at which the level of DNA

adducts in the target organ (liver) was maximal. Following this time dependent study a dose response study was performed using the time point determined in the first study, characterizing the dose dependent formation of DNA adducts in the liver and non-target organs (kidney and lungs) as well as the level of urinary excretion of 1'-hydroxyestragole glucuronide.

Table 3.1. Kinetic parameters for 1′-HE glucuronide formation (from literature (Punt *et al.,* 2008; Alhusainy *et al.,* 2010) and from experimental results using several batches of pooled male SD S9 fraction).

Kinetic parameters	Punt *et al.* (2008)	Alhusainy *et al.* (2010)	Batch 1	Batch 2	Batch 3	Average	Average All
V_{max} [nmol min^{-1} (mg S9 protein)$^{-1}$]	7.0	151	32.55	34.59	32.62	32.35	**51.5**
K_m (µM)	137	241	201.2	211.1	226.7	209.5	**203.4**

Batches were purchased at BD (cat # 452591 pld SD rat liver S9), for each batch the values are the average of 2 technical replicates. Batch 1. Lot #61642 ; Batch 2. Lot #74099 ; Batch 3. Lot #88875.

3.3.2 Time-dependent DNA adduct formation *in vivo*

Levels of DNA adducts in SD rats exposed by oral gavage to 300 mg/kg bw of estragole were measured in liver over time up to 48 hrs. Six random parts of each liver (50-100mg) were used to extract the E-3′-N^2-dG adduct. The limit of detection of the adduct in the liver was 0.001 adduct/1000 nt (1 in 10^6 nt). Figure 3.3 shows the DNA adduct formation in liver over time after a dose of 300 mg/kg bw, which was found to be time dependent. The amount of adduct formed in the liver at 48 hrs was significantly higher (p=0.003 by t-test) than the amount formed at 24 hrs and the value at 48 hrs was also significantly (p<0.0001 by t-test) increased compared to time zero (control). No adducts where detected in the control group, confirming that adduct formation is treatment related. Based on the results obtained 48 hrs post dosing was selected as the time point for analysis of DNA adduct formation in the subsequent dose-response study.
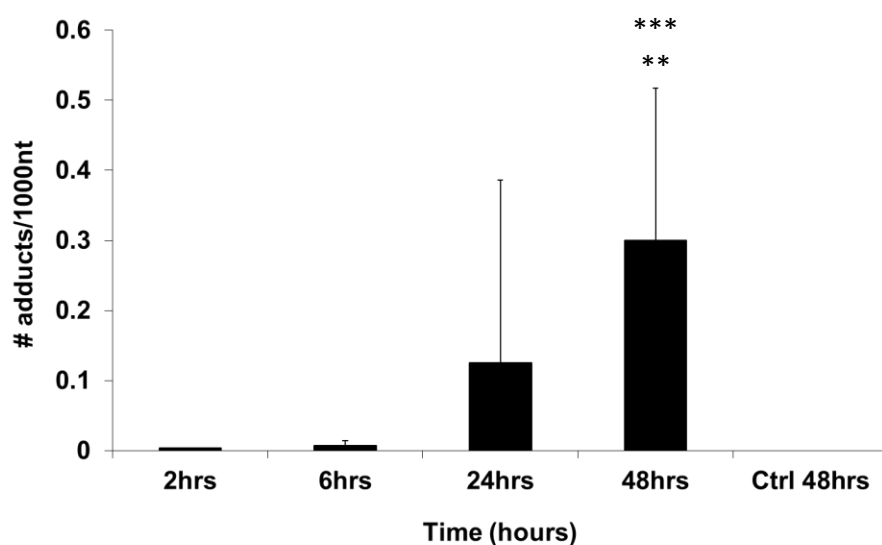

Figure 3.3. Time dependent DNA adduct formation in liver. DNA adducts are expressed as number of adducts in 1000 nt. T-test was used to test for significant difference in maximal DNA adduct formation between the 24 hrs and the 48 hrs groups (** p <0.01;*** p <0.001); data represent the average and Stdev of 5 rats, from which 3 technical replica were done.

3.3.3 Dose-dependent DNA adduct formation *in vivo*

Levels of DNA adducts in male SD rats exposed once by oral gavage to increasing doses (0, 5, 30, 75, 150 and 300 mg/kg bw) of estragole were measured in liver, kidney, and lungs 48 hrs after dosing (Figure 3.4). In the supplementary file values for each individual rat are reported, the results show for each dose group high variability between individuals. The limit of detection of the adduct was 0.001 adduct/1000 nt (1 in 10^6 nt) for liver and kidney, and 0.004 adduct/1000 nt (4 in 10^6 nt) for lung. In the liver a clear dose dependent increase in E-3′-N^2-dG formation was found (Figure 3.4A). The level of DNA adducts detected 48 hrs after a dose of 300 mg/kg bw in this experiment can be compared to the value obtained in the time response experiment. This revealed for the level of DNA adduct detected in the liver a somewhat higher amount of DNA adducts detected in the time response experiment, amounting to 0.28 (Stdev ± 0.20) adducts/1000 nt (Figure 3.3) versus 0.10 (Stdev ±0.08) adducts/1000 nt (Figure 3.4A) detected in the dose response experiment, but the difference was not statistically significant. In lungs DNA adducts were detected only at the two highest doses of estragole of 150 mg/kg bw and 300 mg/kg bw (Figure 3.4B). In kidney a dose response in DNA adduct formation was not observed, and levels were highest at the two highest dose levels (Figure 3.4C), with a statistically significant increase at the two highest dose levels. At 300 mg/kg bw the amount of DNA adducts in the liver was 9 times higher than in kidney and 5 times higher than in lungs.

3.3.4 Comparison of the *in vivo* urinary excretion of 1'-hydroxyestragole glucuronide to the levels predicted by the PBBD model

Urines were collected in order to measure 1′-HE glucuronide excretion and validate the outcomes of the PBBD model predicting the dose dependent formation of this urinary metabolite. In the supplementary file the urinary excretion of the 1′-HE glucuronide measured for each dose group for 8 individual rats from 0 to 24 hrs and from 0 to 48 hrs is reported. The results show for each dose group high variability between rats in excretion of the metabolite 1′-HE glucuronide. Further, the results show that increasing the dose of estragole given to the rats by gavage an increase in the biomarker, 1′-HE glucuronide, was measured in the urines. For each dose the cumulative amount of 1'-hydroxyestragole glucuronide formed was calculated by the PBBD model. Figure 3.5 shows the results obtained. Figure 3.5 also presents the data previously reported for urinary excretion of 1'-hydroxyestragole glucuronide by estragole exposed female Wistar albino rats by Anthony *et al.* (1987). The results obtained reveal that our data obtained for estragole exposed male SD rats match those reported by Anthony *et al.* (1987) for female Wistar albino rats. The results also reveal that the PBBD model based predictions match the experimentally observed values within less than an order of magnitude. The PBBD model predictions at 24 hrs upon dosing appear to overestimate the urinary 1′-hydroxyestragole glucuronide excretion by a factor of 4.6 to 7.7 fold.
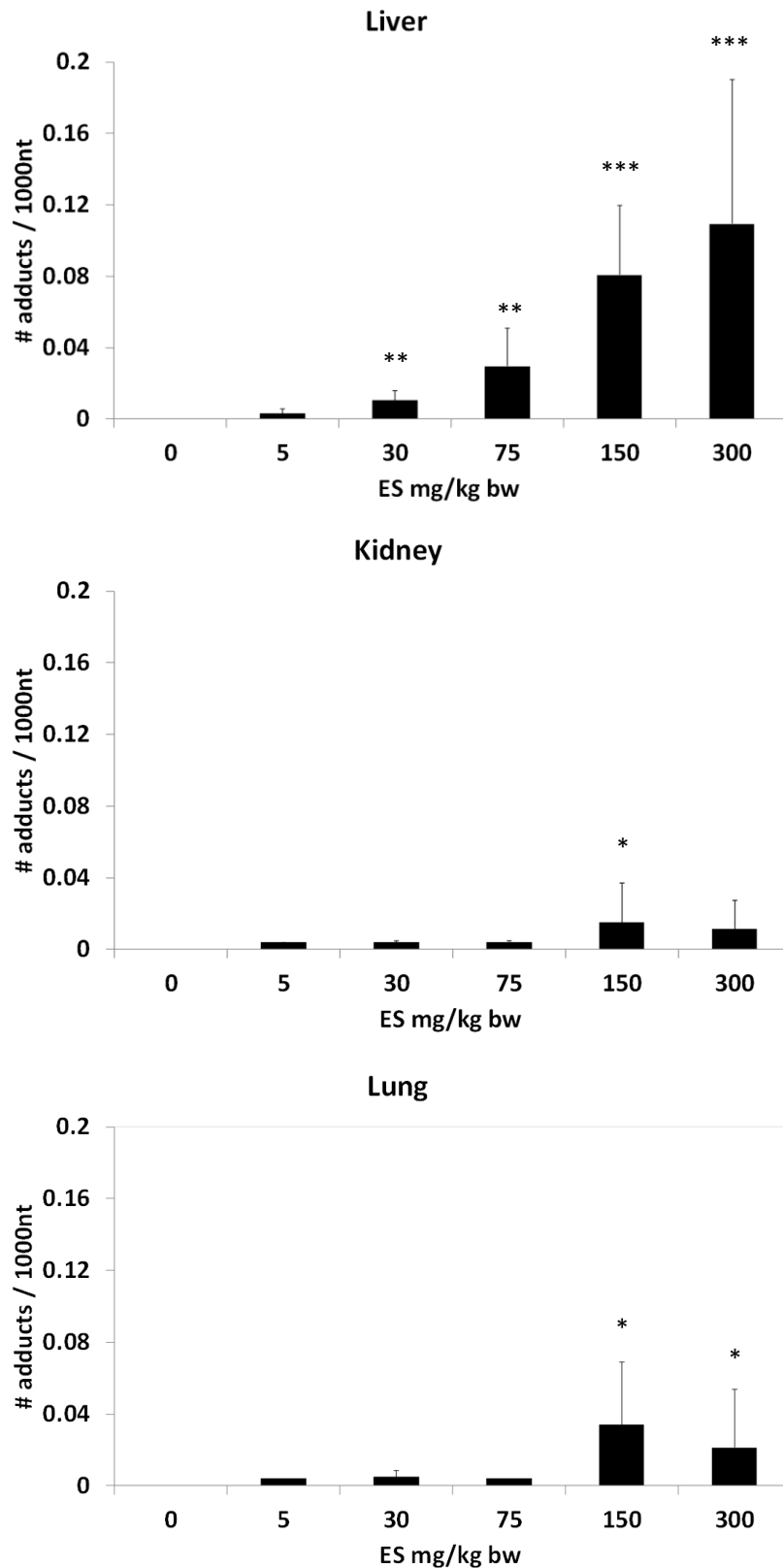
Figure 3.4. Dose dependent DNA adduct formation in liver, kidney and lungs, DNA adducts are expressed as number of adducts in 1000 nt. T-test was used to test for significant difference between treatment groups versus control group (p* <0.05, ** p <0.01, *** p<0.001); data represent the average and Stdev of 10 rats, from which 3 technical replica were done.

3.3.5 Comparison of the *in vivo* results obtained to the levels of DNA adduct formation predicted by the PBBD model

Figure 3.6 presents a comparison between the dose dependent formation of estragole DNA adduct formation in the liver of male SD rats as experimentally determined in the present study and as predicted by the PBBD model. The results also reveal that the PBBD model based predictions match the experimentally observed values within less than an order of magnitude. The PBBD model predictions at 48 hrs upon dosing appear to overestimate the DNA adduct formation by a by a factor of 1.9 to 2.3 fold.
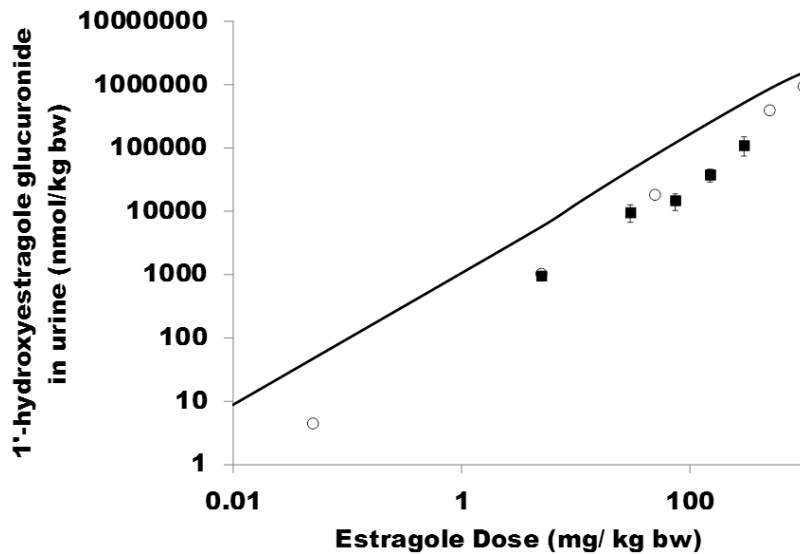
Figure 3.5. PBBD model predicted (solid line) and experimentally determined 24 hrs urinary levels of 1'-HE glucuronide at increasing oral doses of estragole. Data presented as black squares are the results of the present study whereas those presented as open circles are those reported by Anthony *et al.*, (1987) for female Wistar albino rats. Data represent the average and Stdev of 8 rats.
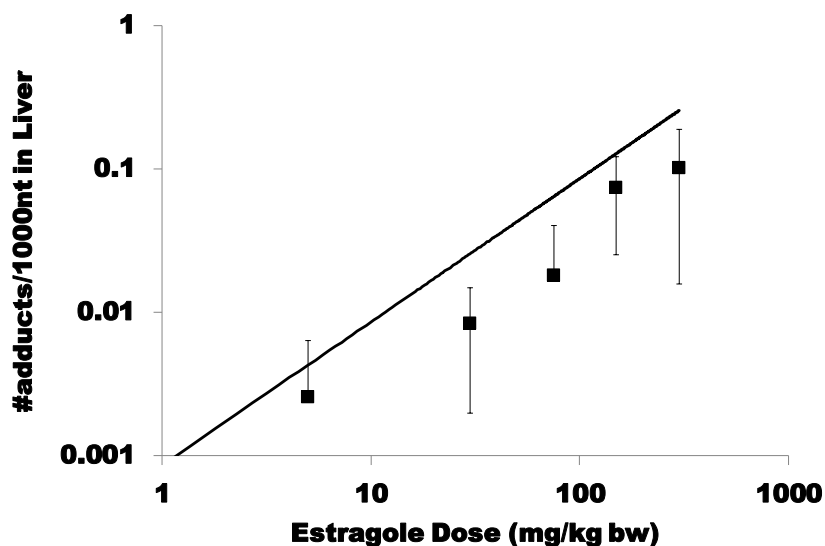
Figure 3.6. *In vitro* PBBD model (solid line) prediction of the DNA adduct formation at 48 hrs versus the DNA adduct measured *in vivo* (black square) at different oral doses of estragole. Data represent the average and Stdev of 10 rats.

3.3.6 Correlation of DNA adduct formation and the urinary biomarker 1'-hydroxyestragole-glucuronide

Figure 3.7 displays for each dose the relation between the amount of DNA guanine adducts formed (# adduct/1000 nt) in liver and the amount of 1'-HE (nmol/kg bw) excreted in urine as glucuronide conjugate. A significant positive correlation was found with increasing estragole dose between the number of DNA adducts and the concentration of 1'-HE glucuronide in the urine after 48 hrs (R^2 = 0.90; Pearson coefficient p= 0.95; P= 0.0118; n = 5 data points each representing the average of 8 rats).
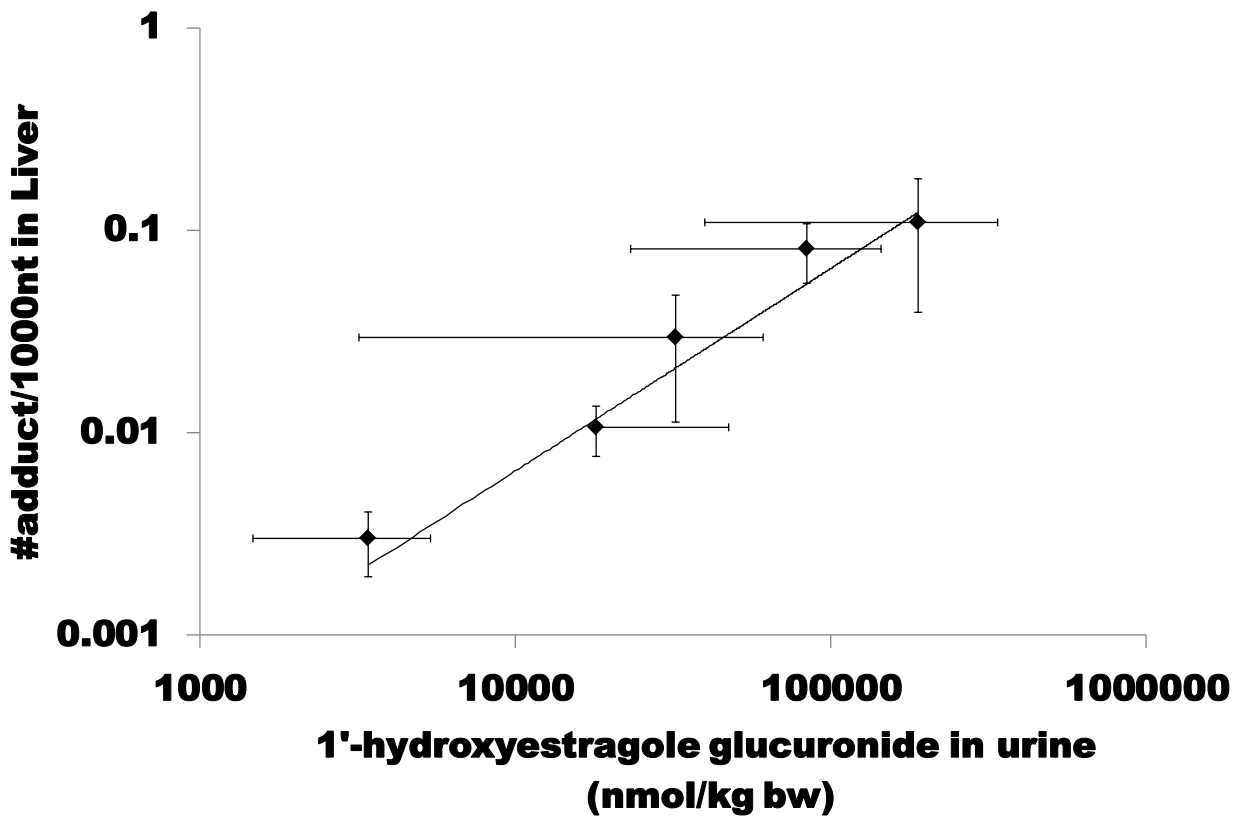
Figure 3.7. Correlation between 1'-HE glucuronide urinary excretion and estragole DNA adducts in the liver at increasing estragole doses, (R^2 = 0.90; Pearson coefficient p= 0.95; P= 0.0118 ; n = 5 data points each representing the average of 8 rats).

3.4 Discussion

The aim of the present study was to quantify the dose-dependent estragole DNA adduct formation in male SD rat liver and the levels of urinary excretion of 1'-hydroxyestragole glucuronide in order to validate the *in vitro* physiologically based biodynamic (PBBD) model previously built (Chapter 2). The adduct measured and predicted in the present study was E-3'-N^2-dG, which was previously reported to be the most abundant adduct formed by estragole (Singh *et al.,* 2006; Pfau *et al.,* 1994). Recently it was reported that adducts between estragole and adenine may also be formed to a significant extent (Ishi *et al.,* 2011). However, the formation of additional adducts to the E-3'-N^2-dG taken into account in the present study will not affect the outcomes of the present study since our measurements as well as the predictions focused on formation of E-3'-N^2-dG.

The first validation step of the PBBD model in the present study was based on the dose-dependent urinary excretion of 1'-hydroxyestragole glucuronide. The results acquired reveal that our data obtained for estragole exposed male SD rats match those reported by Anthony *et al.* (1987) for female Wistar albino rats. The results also reveal that the PBBD model based predictions match the experimentally observed values within less than an order of magnitude. Differences between the present data and those reported by Anthony *et al.* (1987) may be caused by differences in the animal strain and sex. Animals used in Anthony *et al.* (1987) study were female Wistar albino rats and those in the present study male outbred SD rats. The PBBD model predicted somewhat higher levels of the 1'-hydroxyestragole glucuronide compared to *in vivo* data, which was also found previously by Punt *et al.* (2008), but deviations were generally within one order of magnitude. Given this result it is important to stress that deviations within one order of magnitude are generally considered acceptable within the present state-of-the-art of PBBK modeling (Rietjens *et al.,* 2008). One explanation for the deviation in predicted urinary levels of 1'-hydroxyestragole glucuronide could be that the actual bioavailability of estragole is lower than 100%. Another reason could be that in the present PBBK model excretion and further extra hepatic metabolism of 1'-hydroxyestragole are not included, which may result in some overestimation of the levels of 1'-hydroxyestragole in the liver and thus of 1'-hydroxyestragole glucuronide and 1'-sulfooxyestragole predicted to be formed, and subsequently of the predicted urinary levels of 1'-hydroxyestragole glucuronide and DNA adducts formed. The match between experimentally observed and predicted value is also considered adequate when it is taken into consideration that the current PBBD model was based on *in vitro* data only, whereas most current physiologically based kinetic or dynamic models use *in vivo* data to optimize parameters in the model and improve the fit (Rietjens *et al.,* 2011, and references therein). DNA adducts are known to be a biomarker of genotoxic exposure and urinary excretion of metabolites are early biomarker of exposure (Gyorffy *et al.,* 2008). Thus a comparison between the experimental data for urinary excretion of 1'-HE glucuronide and DNA adduct formation in the liver was made revealing a positive correlation. This suggests that with increasing dose of estragole a proportional increase in bio-activation occurs in the liver, which is reflected by an increased level of urinary excretion of 1'-HE glucuronide. In the second step the PBBD model based predictions for formation of estragole DNA adducts in the liver of male rats were compared to the experimental data obtained. Using the optimized new parameters the PBBD model based predictions for the levels of adduct formation were within the same order of magnitude as the *in vivo* measurements. Data on DNA adduct levels in rats exposed to estragole have not

been reported before. Thus the results of the present study can only be compared to data obtained in estragole exposed mice. Randerath *et al.* (1984) reported in female CD-1 mice the formation of 1 adduct in 10,000–15,000 DNA nucleotides after a single i.p. injection of 10 mg estragole per mouse. Assuming a mouse weight of 0.025 kg, the average intake dose was estimated to be 400 mg/kg bw/day. At our highest dose tested *in vivo* (300 mg/kg bw/day) we obtained 1 adduct in 10,000 nt which is comparable to the value reported by Randerath *et al.* (1984) although this value was obtained using a different technique for quantification of the DNA adduct levels, in a different species and at a different dose level. The amount of E-3′-N^2-dG adducts at a daily human exposure level of 0.01 mg/kg bw/day (Smith *et al.,* 2002) and 0.07 mg/kg bw/day estragole (EU-SCF, 2001), was predicted to be respectively 0.44 and 3.1 in 10^8 nt. These levels of adducts are orders of magnitude below the background level of DNA damage of 100 adduct in 10^8 nt, which are of no known consequence (Williams, 2008).

Furthermore, it is of interest to note that the present study shows formation of DNA adducts in not only the liver, but also the kidney and lung of male SD rats treated with estragole. The lower amount of DNA adducts detected in these organs reflects the low metabolic conversion of estragole to 1′-HE found in these organs by Punt *et al.* (2008), although the data may indicate that these organs do contain the relevant cytochromes P450 and conjugating enzymes needed for bioactivation of estragole to some extent. To the best of our knowledge this is the first time DNA adduct levels for estragole treated rats were measured and detected in liver, lung and kidney. Interestingly the DNA adducts were detected *in vivo* in all three organs. DNA adduct formation appeared to be highest in the liver known to be the target organ.

In conclusion the present study reveals a dose-dependent increase in estragole guanine DNA adduct formation in the liver of rats exposed to estragole, and also corroborates that the now optimized PBBD model can provide a tool to examine dose-dependent DNA adduct formation in the liver of rats exposed to estragole. Extending this rat PBBD model to the human situation will provide a way to extrapolate from rats to the human situation including extrapolation from the high dose rat experimental dose levels to low dose levels that are more realistic for human exposure regimens. This will provide further insight in species and dose dependent differences or similarities in DNA adduct formation in the liver upon exposure to estragole.

Reference

Alhusainy WAAM, Paini A, Punt A, Louisse J, Spenkelink B, Vervoort JJM, Delatour T, Scholz G, Schilter B, Adams TB, van Bladeren PJ, Rietjens IMCM. (2010) Identification of nevadensin as an important herb-based constituent inhibiting estragole bioactivation and physiology-based biokinetic modeling of its possible in vivo effect. Toxicol. and Appl. Pharmacol. 245 (2), 179 - 190.

Anthony A, Caldwell J, Hutt AJ, and Smith RL. (1987) Metabolism of estragole in rat and mouse and influence of dose size on excretion of the proximate carcinogen 1'-hydroxyestragole. Food Chem. Toxicol. 25, 799–806.

Delatour T, Mally A, Richoz J, Ozden S, Dekant W, Ihmels H, Otto D, Gasparutto D, Marin-Kuan M, Schilter B, and Cavin C. (2008) Absence of 2'-deoxyguanosine-carbon 8-bound ochratoxin A adduct in rat kidney DNA monitored by isotope dilution LC-MS/MS. Mol. Nutr. Food Res. 52 (4), 472-482.

EU-SCF (Scientific Committee on Food) (2001) Opinion of the scientific committee on food on estragole (1-allyl-4-methoxybenzene), http://ec.europa.eu/food/fs/sc/scf/out104_en.pdf.

Fisher MB, Campanale K, Ackermann BL, Van den Branden M, and Wrighton SA. (2000) In vitro glucuronidation using human liver microsomes and the pore-forming peptide alamethicin. Drug Metab. Dispos. 28, 560–566.

Gardner I, Bergin P, Stening P, Kenna JG, Caldwell J. (1996) Immunochemical detection of covalently modified protein adducts in livers of rats treated with methyleugenol. Crit. Rev. Toxicol. 9 (4), 713–721.

Gyorffy E, Anna L, Kovács K, Rudnai P, Schoket B. (2008) Correlation between biomarkers of human exposure to genotoxins with focus on carcinogen-DNA adducts. Mutagenesis 23 (1), 1-18.

Iyer LV, Ho MN, Shinn WM, Bradford WW, Tanga MJ, Nath SS, and Green CE. (2003) Glucuronidation of 1'-hydroxyestragole (1'-HE) by human UDP- glucuronosyltransferases UGT2B7 and UGT1A9. Toxicol. Sci. 73, 36–43.

Ishii Y, Suzuki Y, Hibi D, Jin M, Fukuhara K, Umemura T, and Nishikawa A (2011) Detection and Quantification of Specific DNA Adducts by Liquid Chromatography−Tandem Mass Spectrometry in the Livers of Rats Given Estragole at the Carcinogenic Dose. Chem. Res. Toxicol. 24 (4), 532-541.

Lin JH, and Wong BK. (2002) Complexities of glucuronidation affecting in vitro in vivo extrapolation. Curr. Drug Metab. 3 (6), 623-646.

Miller EC, Swanson AB, Phillips DH, Fletcher TL, Liem A, and Miller JA. (1983). Structure–activity studies of the carcinogenicities in the mouse and rat of some naturally occurring and synthetic alkenylbenzene derivatives related to safrole and estragole. Cancer Res. 43, 1124–1134.

Pfau W, Brockstedt U, Söhren KD, and Marquardt H. (1994) ^{32}P-post-labelling analysis of DNA adducts formed by food derived heterocyclic amines: Evidence for incomplete hydrolysis and a procedure for adduct pattern simplification. Carcinogenesis 15,877–882.

Phillips DH, Miller JA, Miller EC, and Adams B. (1981) Structures of the DNA adducts formed in mouse liver after administration of the proximate hepatocarcinogen 1'-hydroxyestragole, Cancer Res. 41, 176–186.

Phillips DH, Reddy MV, and Randerath K. (1984) P-32 Post-Labeling Analysis of DNA Adducts Formed in the Livers of Animals Treated with Safrole, Estragole and Other Naturally-Occurring Alkenylbenzenes. II. Newborn Male B6c3f1 Mice. Carcinogenesis 5, 1623-1628.

Preston RJ and Williams GM.(2005)DNA-reactive carcinogens: mode of action and human cancer hazard. Crit.Rev.Toxicol.35,673–683.

Punt A, Delatour T, Scholz G, Schilter B, Van Bladeren PJ, and Rietjens IMCM. (2007) Tandem Mass Spectrometry Analysis of N^2-(trans-Isoestragol-3'-yl)-2'-deoxyguanosine as a strategy to study species differences in sulfotransferase conversion of the proximate carcinogen 1'-hydroxyestragole. Chem. Res. Toxicol. 20, 991–998.

Punt A, Freidig AP, Delatour T, Scholz G, Schilter B, Boersma MG, van Bladeren PJ and Rietjens IMCM. (2008) A physiologically based biokinetic (PBBK) model for estragole bioactivation and detoxification in rat. Toxicol. Appl. Pharmacol. 231 (2), 248–259.

Punt A, Paini A, Boersma MG, Freidig AP, Delatour T, Scholz G, Schilter B, van Bladeren PJ, and Rietjens IMCM. (2009) Use of physiologically based biokinetic (PBBK) modeling to study estragole bioactivation and detoxification in humans as compared to male rats. Toxicol. Sci. 110 (2), 255–269.

Randerath K, Haglund RE, Phillips DH, and Reddy MV. (1984) 32P-postlabelling analysis of DNA adducts formed in the livers of animals treated with safrole, estragole and other naturally-occurring alkenylbenzenes. I. Adult female CD-1 mice. Carcinogenesis 5, 1613–1622.

Rietjens IMCM, Boersma MG, Zaleska M, and Punt A. (2008) Differences in simulated liver concentrations of toxic coumarin metabolites in rats and different human populations evaluated through physiologically based biokinetic (PBBK) modeling. Toxicology in vitro 22 (8), 1890-1901.

Rietjens IMCM, Louisse J, and Punt A. (2011) Tutorial on physiologically based kinetic modeling in molecular nutrition and food research. Mol. Nutr. Food Res. 55 (6), 941-56.

Singh R, Gaskell M, Le Pla RC, Kaur B, Azim-Araghi A, Roach J, Koukouves G, Souliotis VL, Kyrtopoulos SA, and Farmer PB. (2006) Detection and quantification of benzo[a]pyrene-derived DNA adducts in mouse liver by liquid chromatography-tandem mass spectrometry: comparison with ^{32}P-postlabeling. Chem. Res. Toxicol. 19, 868–878.

Smith RL, Adams TB, Doull J, Feron VJ, Goodman JI, Marnett LJ, Portoghese PS, Waddell WJ, Wagner BM, Rogers AE, Caldwell J, and Sipes IG. (2002) Safety assessment of allylalkoxybenzene derivatives used as flavouring substances—methyleugenol and estragole, Food Chem. Toxicol. 40, 851–870.

Williams GM. (2008) Application of mode-of-action consideration in human cancer risk assessment, Toxicol. Lett. 180, 75–80.

Zeller A, Horst K, and Rychlik M. (2009) Study of the metabolism of estragole in humans consuming fennel tea. Chemical Research in Toxicology. 22 (12), 1929-1931.

Chapter 4

Based on:

Evaluation of interindividual human variation in bioactivation and DNA binding of estragole in liver predicted by physiologically based biodynamic (PBBD) and Monte Carlo modeling

By

Paini A, Scholz G, Boersma MG, Spenkelink B, Schilter B, van Bladeren PJ, Rietjens IMCM, Punt A.

Abstract

Estragole is known to be hepatocarcinogenic in rodents at high doses. Metabolic conversion of estragole into the DNA reactive metabolite 1′-sulfooxyestragole, has been suggested to be involved in the Mode of Action (MOA) for formation of liver tumors. The aim of the present study was to model possible levels of DNA adduct formation in human liver upon exposure to estragole at realistic human dietary intake levels. Estimates of DNA adduct formation in human liver upon exposure to estragole were made based on i) a previously defined PBBK model for estragole detoxification and bioactivation in humans, ii) new data on interindividual variation in the kinetics for the major biotransformation enzymes influencing formation of 1′-sulfooxyestragole and iii) an equation describing the relationship between 1′-sulfooxyestragole formation and DNA adduct formation derived from a PBBK model and an *in vivo* study on DNA adduct formation in rats. Interindividual differences in the V_{max} and K_m for the major biotransformation enzymes influencing formation of 1′-sulfooxyestragole were determined using liver samples from 22 individual donors. With the individual kinetic constants obtained differences in 1′-sulfooxyestragole and DNA adduct formation could be modeled, indicating a 25-fold variation between the 22 individuals. In addition, a Monte Carlo simulation was performed to evaluate differences in formation of 1′-sulfooxyestragole and formation of estragole DNA adducts in the whole population. These analyses revealed that at an estimated daily intake of 0.01 mg/kg bw/day the DNA adduct levels are predicted to be below 40 adducts per 10^8 nucleotides. These levels would be within the endogenous DNA adduct level of 10-100 adducts per 10^8 nt suggested before to be of no biological consequence. These levels are below the value of 490 adducts per 10^8 nt estimated, based on data from rodent studies, as the value required for statistically significant tumorigenesis potential of alkenylbenzene DNA adducts. In conclusion the results of the present study suggest a negligible cancer risk for the average human population at the currently estimated daily intake levels of estragole.

4.1 Introduction

Estragole, is an alkenylbenzene, naturally present in herbs and spices, and thus present in the human diet. Estragole is known to be hepatotoxic and to induce hepatocarcinomas in rodents at high dose levels (Miller *et al.*, 1983). Metabolic conversion of estragole into a genotoxic metabolite which is capable to form DNA adducts, has been suggested to be involved in the formation of liver tumors (Swanson *et al.*, 1979; Wiseman *et al.*, 1987). Metabolism of estragole occurs by reaction in the liver by phase I and phase II enzymes, and has been extensively reviewed by Smith *et al.* (2002). There are three metabolic pathways for estragole in phase I metabolism: *O*-demethylation, epoxidation, and hydroxylation. These pathways are catalyzed by cytochromes P450 (Jeurissen *et al.*, 2007). The *O*-demethylated metabolite, 4-allylphenol, is not involved in tumor formation, the metabolite resulting from epoxidation, estragole-2',3'-oxide, has been found to form DNA adducts *in vitro*, but not *in vivo*, the latter due to efficient detoxification by epoxide hydrolase and/or glutathione S-transferases (Luo *et al.*, 1992; Guenthner and Luo, 2001). The major metabolic route leading to the ultimate carcinogenic metabolite is hydroxylation to 1′-hydroxyestragole followed by sulfonation by sulfotransferases, leading to the transient 1′-sulfooxyestragole. Detoxification of 1′-hydroxyestragole can proceed by its oxidation to 1′-oxoestragole (Phillips *et al.*, 1981), or by conjugation to form 1′-hydroxyestragole glucuronide. Due to its unstable nature 1′-sulfooxyestragole becomes a carbocation that is capable to react with DNA (Phillips *et al.*, 1981; Punt *et al.*, 2007). Several adducts can be formed with the guanine base of the DNA helix, the major one being N^2-(trans-isoestragol-3′-yl)deoxyguanosine (E-3′-N^2-dG) (Phillips *et al.*, 1981; Smith *et al.*, 2002). Recently also adducts with adenine were reported to be abundant in liver of male rats (F344) exposed to estragole at a dose level of 600 mg/kg bw for 4 weeks (Ishii *et al.*, 2011). The formation of DNA adducts can be considered a marker of exposure (Shuker and Farmer, 1992; Swenberg *et al.*, 2008) and gives insight in the Mode of Action (MOA) of a carcinogenic compound. Analysis of DNA adducts is often used to complement data in risk assessments on exposure, metabolism, mutation, and tumor formation (Williams, 2008).

In order to assess the risks of estragole at low dose human exposure levels, knowledge on the levels of DNA adduct formation in the liver in humans at normal dietary levels of intake would be valuable. Therefore the aim of the present study was to obtain insight in DNA adduct formation in human liver upon exposure to estragole at realistic human dietary intake levels, taking interindividual variability in bioactivation of estragole to its ultimate carcinogenic metabolite 1′-sulfooxyestragole within the human population into account. To gain insight in the dose-dependent formation of DNA adducts in rats we have recently developed a physiologically based biodynamic (PBBD) model that predicted DNA adduct formation in the liver at different oral doses of estragole (Chapter 2). For evaluation of the performance of this model, the formation of E-3′-N^2-dG was also measured *in vivo* in rats exposed to estragole at different oral doses, revealing that predictions were overall only 1.9- to 2.3-fold different from the levels actually observed *in vivo* (Chapter 3). In the present study these data were used to define an equation quantifying the fraction of 1′-sulfooxyestragole formed in the liver that would end up in E-3′-N^2-dG adducts. This information and the PBBK model previously developed for detoxification and bioactivation of estragole in humans (Punt *et al.*, 2008) were applied to estimate the dose-dependent DNA adduct formation in humans at realistic dietary intake of estragole. Realistic daily intake levels of estragole have been estimated to range from 0.01 mg/kg bw/day (Smith *et al.,* 2002) to 0.07 mg/kg

bw/day (SCF, 2001). Due to interindividual differences in bioactivation and detoxification of estragole the levels of 1′-sulfooxyestragole and consequently of DNA adducts formed at these exposure levels will vary in the population. The previously developed PBBK model for estragole in humans showed that kinetic constants for sulfonation and oxidation of 1′-hydroxyestragole are the key parameters that affect the ultimate formation of 1′-sulfooxyestragole in the liver (Punt *et al.*, 2009). Therefore, in making the estimates for DNA adduct formation in human liver interindividual differences in these two key enzymes determining the interindividual differences in formation of 1′-sulfooxyestragole need to be taken into account. This was done by developing individual human models based on the V_{max} and K_m for these two key reactions as determined in incubations with individual human liver S9 obtained from 22 individual donors, as representative for the human population. In addition, a Monte Carlo simulation was performed to evaluate differences in formation of 1′-sulfooxyestragole and resulting into E-3′-N^2-dG in the population as a whole. The results obtained provide insight in levels of DNA adducts that can be formed in human livers after exposure to low average daily intake levels of estragole and their biological relevance as compared to endogenous levels of DNA adducts known to be present in liver tissue.

4.2 Method and materials

4.2.1 Materials

Two individual human liver S9 homogenates were purchased from Celsis (Brussels, Belgium). Twenty (20) individual human liver S9 homogenates were purchased from Xenotech (Lenexa, Kansas, USA). 2′-Deoxyguanosine was purchased from Sigma (Basel, Switzerland). 1,2,3,7,9-$^{15}N_5$-2′-Deoxyguanosine ($^{15}N_5$-dG) was obtained from Cambridge Isotope Laboratories (Cambridge, MA). Glutathione (GSH), and 3'-phosphoadenosine-5'-phosphosulfate (PAPS) were purchased from Sigma-Aldrich (Schnelldorf, Germany). Acetonitrile, formic acid, HCl (1N), and Tris-HCl were purchased from VWR (Darmstadt, Germany). Nicotinamide adenine dinucleotide (NAD+) was purchased from Roche Diagnostics (Mannheim, Germany).

The methods used for synthesis of 1′-hydroxyestragole, E-3′-N^2-dG, and ($^{15}N_5$) E-3′-N^2-dG were described previously (Chapter 2).

4.2.2 Determination of sulfonation of 1′-hydroxyestragole in incubations with S9 fractions

To characterize the kinetics for sulfonation of 1′-hydroxyestragole incubations with the 22 individual human liver S9 homogenates (1 mg protein/mL final concentration) were performed as previously described by Punt *et al.* (2007) in 0.1 M Tris-HCl (pH 7.4). Briefly, in the presence of different concentrations of the substrate 1′-hydroxyestragole, at final concentrations of 10-2000 μM (added from 100 times concentrated stock solutions in DMSO) using PAPS (1 mM final concentration) as cofactor, and 2′-deoxyguanosine (1 mM final concentration) as trapping agent of the transient 1′-sulfooxyestragole. The final volume of the incubation was 200 μL. The reaction was started, after 1 min pre-incubation at 37°C by adding PAPS, and all incubations were carried out for 1 hr at 37°C. The reaction was terminated by adding 50 μL acetonitrile, after which incubations were centrifuged for 5 min at 16,000g to precipitate the S9 proteins. The supernatant was collected, speed vacuum dried and reconstituted in 100μL water. Blanks were made without the addition of PAPS and the amount of E-3′-N^2-dG formed in the samples was corrected for the amount formed in these

blank incubations. Formation of E-3′-N²-dG was quantified by LC-MS/MS performed as described previously (Chapter 3) based on a method by Punt *et al.,* (2007).

4.2.3 Determination of 1′-hydroxyestragole oxidation in incubations with S9 fractions

Twenty-two (22) individual human liver S9 homogenates (1 mg protein/mL final concentration) were used for incubations to study the kinetics for oxidation of 1′-hydroxyestragole. As previously reported by Punt *et al.* (2009) the incubations (200 µL, final volume) were done in the presence of different concentrations of the substrate 1′-hydroxyestragole (added to a final concentration of 25-1000 µM from 100 times concentrated stock solutions in DMSO) dissolved in 0.2 M Tris-HCl (pH 7.4), with NAD (3 mM final concentration) as cofactor and GSH (2 mM final concentration) as trapping agent for the reactive 1′-oxoestragole. The reaction was started, after 1 min pre-incubation of the samples at 37°C by adding the substrate 1′-hydroxyestragole. All incubations were carried out for 10 min at 37°C. The reaction was terminated by adding 50 µL acetonitrile, after which incubations were centrifuged for 5 min at 16,000g to precipitate the S9 proteins. The supernatant was collected and analyzed by UPLC-DAD. Ten (10) µL samples were injected into an Acquity column BEH C18 1.7 µm 2.1*50 mm, with a guard column filter (Acquity, Waters). The runs were performed on an Acquity (Waters) UPLC system coupled to a DAD detector. The flow was 0.6 mL/min and the gradient started with 100% of 0.1% acetic acid in nanopure water and 0% of acetonitrile. After 1.2 minutes the amount of acetonitrile was increased to 25% and kept at 25% for 0.2 minutes, after which the acetonitrile amount was increased to 100% and kept at 100% for 30 seconds, after which starting conditions were reset. At these conditions 1′-oxoestragole eluted at 0.97 min. Blanks, without the addition of NAD were performed for each individual batch of human S9. The amount of 1′-oxoestragole formed in the different samples was corrected for the amount formed in blank incubations.

4.2.4 Evaluation of interindividual variability in sulfonation and in resulting E-3′-N²-dG formation using PBBK models and Monte Carlo simulation

In order to create models to study interindividual differences in formation of 1′-sulfooxyestragole the average V_{max} and K_m for sulfonation and for oxidation in the human PBBK model (Punt *et al.*, 2009) were replaced by the values obtained for each of the 22 individual humans creating 22 separate models. Levels of variation in 1′-sulfooxyestragole that could occur in the population as a whole were analyzed with a Monte Carlo simulation, assuming that the 22 individual are representative for the population as a whole. For this analysis, a total of 10,000 simulations were performed, where in each simulation, the V_{max} and K_m value for both formation of 1′-sulfooxyestragole and for oxidation of 1′-hydroxyestragole were randomly taken from a log-normal distribution. The V_{max} and K_m values for the different metabolic reactions were assumed to vary independently. For this simulation, the mean μ_w and standard deviation σ_w describing the log-normal distribution of each V_{max} and K_m value were derived from the 22 individual human subjects of the present study using the following equations:

$$\mu_W = Ln(\mu_X/\sqrt{1+CV^2_X}) \text{ and } \sigma^2_W = Ln(1+CV^2_X)$$

where μ_x is the mean and CV_x is the coefficient of variation of the non–ln-transformed V_{max} and K_m values of the different metabolic reactions as observed with the 22 individual human subjects of the present study

(Punt *et al.*, 2010). The following equations were added for both sulfonation and oxidation to the human PBBK model in order to perform the Monte Carlo simulation:

$$V_{max(HES)} = init \ (exp \ (normal \ (\mu_{w(VmaxHES)}, \sigma_{w(VmaxHES)}))$$

$$K_{m(HES)} = init \ (exp \ (normal \ (\mu_{w(KmHES)}, \sigma_{w(KmHES)}))$$

$$V_{max(OE)} = init \ (exp \ (normal \ (\mu_{w(VmaxOE)}, \sigma_{w(VmaxOE)}))$$

$$K_{m(OE)} = init \ (exp \ (normal \ (\mu_{w(KmOE)}, \sigma_{w(KmOE)}))$$

The V_{max} of sulfonation ($V_{max(HES)}$) or oxidation ($V_{max(OE)}$) are expressed in nmol/min/mg microsomal S9 protein and the Km of sulfonation ($K_{m(HES)}$) or oxidation ($K_{m(OE)}$) are expressed in µM. Model equations were coded and numerically integrated in Berkeley Madonna 8.0.1 (Macey and Oster, UC Berkeley, CA), using the Rosenbrock's algorithm for stiff systems. To prevent the Berkeley Madonna software to take new values from the defined distributions at each integration step of the simulation, only the initial (init) value, taken from the distribution at time zero, was used to define the V_{max} and K_m values for individual human subjects in the Monte Carlo simulation. Using the previously developed rat PBBK model the levels of 1′-sulfooxyestragole were predicted at different estragole doses and related to the levels of DNA adduct measured in vivo in SD rats (Chapter 3), and an equation was derived to translate the amount of 1′-sulfooxyestragole to the amount of E-3′-N^2-dG adducts. Based on this equation the levels of 1'-sulfooxyestragole predicted by the human PBBK model were converted to the amount of E-3′-N^2-dG formed for each individual. The equation derived for this conversion from the rat data relates PBBK-model predicted levels of 1′-sulfooxyestragole, expressed as nmol/g liver to E-3′-N^2-dG adduct formation, expressed as number of adducts in 10^8 nt. To provide an indication of the percentage of 1′-sulfooxyestragole that is converted to E-3′-N^2-dG adducts, the measured E-3′-N^2-dG adduct formation was also expressed as nmol E-3′-N^2-dG/g liver. Conversion to this unit was done using an average DNA molecular weight of 327 g/mol and an average measured DNA level of 1.8 mg/g liver obtained in the *in vivo* study (Chapter 3). This value of 1.8 mg DNA/g liver, is in line with published values for male Sprague Dawley rat amounting to 1.8-2 mg DNA/g liver (Coughlin *et al.*, 1987).

4.3 Results

4.3.1 Kinetics for sulfonation and oxidation of 1′-hydroxyestragole by human individual S9 fractions

Table 4.1 shows the kinetic constants, V_{max} and $K_{m,}$ for sulfonation and oxidation of 1′-hydroxyestragole for 22 human individuals, derived experimentally by incubating liver S9 homogenates with the relevant cofactors and increasing concentrations of 1′-hydroxyestragole. V_{max} and K_m values for sulfonation of 1′-hydroxyestragole for the 22 human individuals ranged between 0.0006 and 0.020 (nmol / (min*mg S9 protein)) and between 70 and 3321 µM, respectively.

V_{max} and $K_{m,}$ values for oxidation of 1′-hydroxyestragole to 1′-oxoestragole for the 22 human individuals ranged between 1.42 and 5.47 (nmol / (min*mg S9 protein)) and between 325 and 894 µM, respectively. The catalytic efficiency calculated as the ratio between V_{max} / K_m (µL/(mg protein * min)) was quantified for individual S9 fractions, for both sulfonation and oxidation of 1′-hydroxyestragole (table 4.1). These catalytic

efficiencies ranged between 0.01 and 0.24 µL/(mg protein*min) for sulfonation of 1′-hydroxyestragole and between 1.98 and 10.02 µL/(mg protein*min) for oxidation of 1′-hydroxyestragole. The average catalytic efficiency values for oxidation were on average 133-fold higher than those for sulfonation indicating oxidation of 1′-hydroxyestragole to be preferred over sulfonation, which is in agreement with previous observations using pooled human liver fractions (Punt *et al.*, 2009).

Table 4.1. Kinetics values of sulfonation (HES) and oxidation (OE) of 1′-hydroxyestragole in human individual. Depict is the fraction S9 code, description of the fraction, sex, sufonation and oxidation kinetic values.

Code	Supplier	Age	Gender	Sulfonation			Oxidation		
				$V_{max(HES)}$	$K_{m(HES)}$	CE	$V_{max(OE)}$	$K_{m(OE)}$	CE
H0354	X	0	F	0.0011	175	0.01	1.42	716	1.98
H0236	X	17	M	0.0016	108	0.01	3.12	672	4.64
H0322	X	1	M	0.0065	243	0.03	2.47	541	4.56
H0420	X	42	M	0.0006	70	0.01	2.04	421	4.84
H0291	X	18	F	0.0028	389	0.01	3.32	677	4.91
H0346	X	3	M	0.0016	91	0.02	3.64	751	4.85
M0963	C	72	M	0.0104	316	0.03	3.11	627	4.95
H0422	X	69	M	0.0097	128	0.08	2.47	499	4.95
H0120	X	57	F	0.0204	3321	0.01	3.34	581	5.74
H0442	X	49	M	0.0068	133	0.05	2.48	447	5.56
H0441	X	63	M	0.0017	48	0.04	3.19	556	5.73
H0270	X	0	M	0.0032	379	0.01	3.36	547	6.14
F0962	C	44	F	0.0052	360	0.01	3.14	488	6.43
H0251	X	42	F	0.0050	52	0.10	5.47	894	6.12
H0438	X	56	M	0.0151	187	0.08	2.22	345	6.44
H0432	X	60	M	0.0059	25	0.24	3.86	534	7.22
H0133	X	17	M	0.0048	92	0.05	3.05	358	8.52
H0393	X	30	F	0.0078	120	0.07	3.30	364	9.07
H0311	X	21	M	0.0054	166	0.03	3.73	398	9.38
H0428	X	57	F	0.0059	165	0.04	4.91	498	9.87
H0297	X	4	F	0.0031	102	0.03	3.47	346	10.0
H0280	X	36	F	0.0030	22	0.14	3.24	325	9.99

Code = S9 fraction code of supplier; C = Celsis; X = Xenotech; H = Human;F = Female; M= Male; V_{max} expressed as nmol min^{-1} (mg protein^{-1}); K_m expressed as µM; CE = Catalytic efficiency (V_{max}/K_m - expressed as µL min^{-1} (mg protein^{-1}). V_{max} and K_m are average of 3 independent experimental incubations.

4.3.2 Effect of inter-individual human variation in sulfonation and oxidation of 1′-hydroxyestragole on the predicted formation of 1′-sulfooxyestragole

Using the human PBBK model and the individual V_{max} and K_m values for each of the 22 individuals, the formation of 1′-sulfooxyestragole at an oral dose of 0.01 mg/kg bw of estragole (Smith *et al.*, 2002), was modelled for each individual. The results obtained are depicted in Figure 4.1. The difference in levels of 1′-sulfooxyestragole in the 22 humans was 25-fold (between lowest value 0.002 and highest value 0.05 nmol/g liver). In a next step, to investigate possible interindividual variation in formation of 1′-sulfooxyestragole in the

liver for the whole population, a Monte Carlo simulation was performed. The probability distribution used for this Monte Carlo simulation was derived from the V_{max} and K_m values for sulfonation and oxidation of 1′-hydroxyestragole as characterized in the present study. Parameters used to calculate the mean μ_w and standard deviation σ_w describing the log-normal distribution of each V_{max} and K_m for the Monte Carlo simulation are shown in table 4.2.
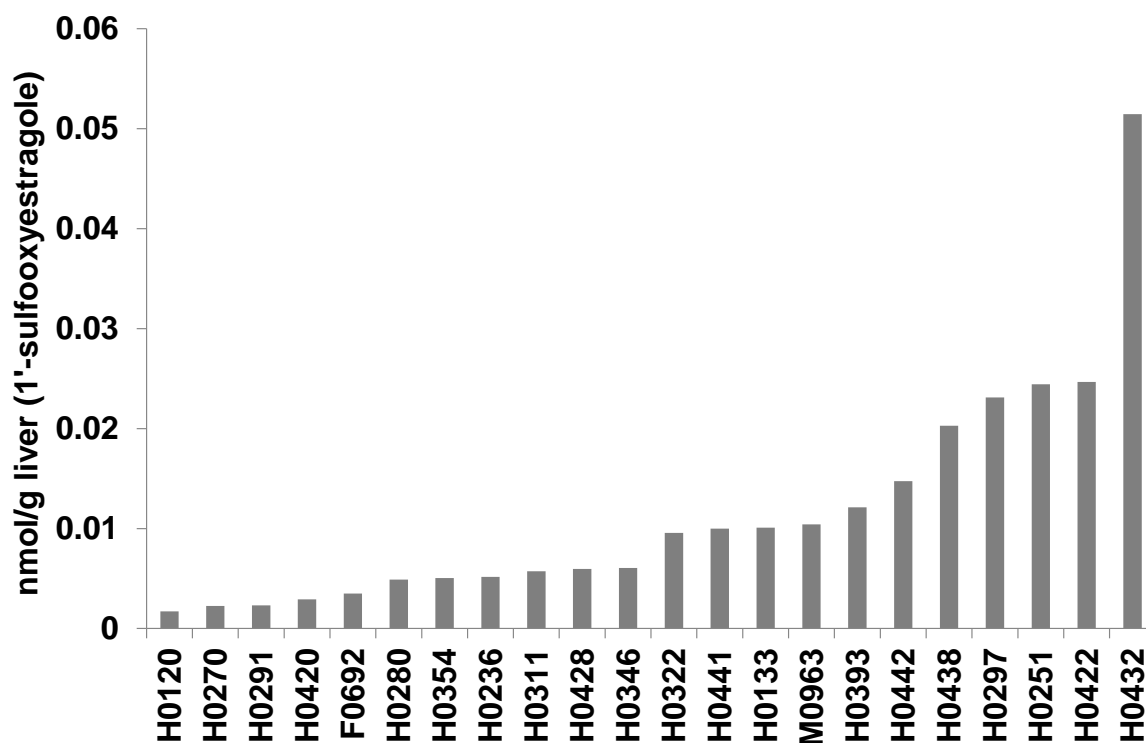
Figure 4.1. Predicted formation of 1′-sulfooxyestragole (nmol/g liver) in liver using the 22 individual human PBBK models, at an estragole dose of 0.01 mg/kg bw.

Table 4.2. Input for Monte Carlo simulation, for both sulfonation (HES) and oxidation (OE).

	$V_{max(HES)}$	$K_{m(HES)}$	$V_{max(OE)}$	$K_{m(OE)}$
Mean	0.006	304.2	3.20	526.6
Stdev	0.005	683.0	0.88	150.9
CV%	0.821	2.245	0.28	0.287
min	0.0006	21.90	5.47	894.3
max	0.0204	3321	3.85	2.750
fold variation	35	152	4	3
μw	-5.41	4.82	1.13	6.23
σw	0.72	1.34	0.27	0.28

Figure 4.2 shows the outcome of the Monte Carlo simulation and the 5th, 50th, and 95th percentiles of the 1′-sulfooxyestragole levels formed at an estragole dose of 0.01 mg/kg bw. The level of variation in 1′-sulfooxyestragole formation between the 5th and 95th percentiles and the 50th and the 95th percentile were found to be 19.9- and 4.5-fold respectively. From the Monte Carlo simulation that describes variability in formation of 1′-sulfooxyestragole in human liver a chemical-specific adjustment factor (CSAF) for interindividual variation in toxicokinetics can be derived, as previously done by Punt *et al.,* (2010), by dividing the 95th by the 50th percentile. The CSAF for interindividual variation in bioactivation of estragole to 1'-sulfooxyestragole thus obtained was 4.5 which is similar to the value of 4 derived using Monte Carlo simulations based on studies with pooled human samples in Punt *et al.,* (2010), and comparable to the default factor of 3.16 for interindividual kinetic variability (Gentry *et al.*, 2002; IPCS, 2005).
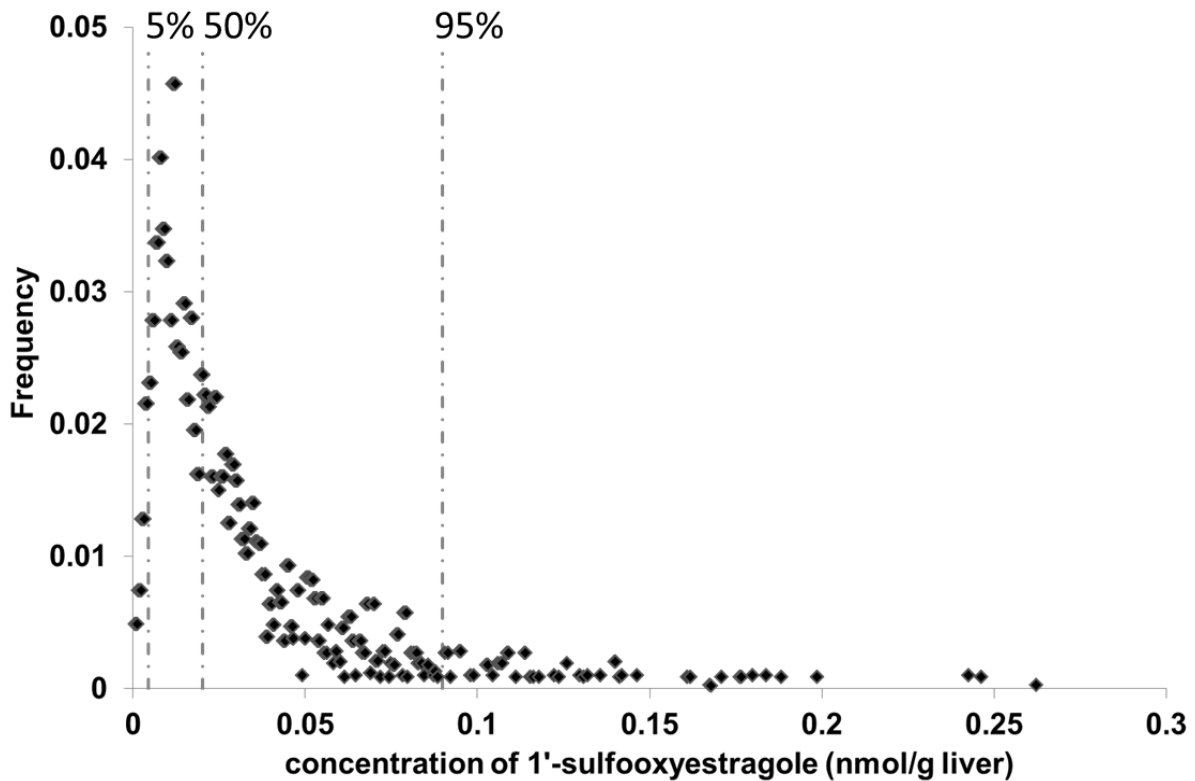
Figure 4.2. Results from a Monte Carlo simulation (10000 simulations) predicting the frequency distribution of 1'-sulfooxyestragole levels for the general population at an estragole dose of 0.01 mg/kg bw. Highlighted with a vertical straight line are the 5th, 50th, and 95th percentiles.

4.3.3 Equation describing E-3′-N^2-dG adduct formation as a function of PBBK predicted levels of 1'-sulfooxyestragole

Figure 4.3 presents the levels of the E-3′-N^2-dG adduct in 10^8 nt measured *in vivo* in rats (Chapter 3) plotted against the PBBK-predicted levels of 1′-sulfooxyestragole (nmol/g liver) that are formed in rat liver at increasing doses of estragole (5, 30, 75, 150 and 300 mg/kg bw). From these levels of E-3′-N^2-dG it can be calculated (see Paragraph 4.2.4) that the overall percentage of 1′-sulfooxyestragole that is converted to E-3′-N^2-dG adducts at the different dose levels corresponds to 0.71%, 0.32%, 0.33%, 0.42%, 0.28% at dose

levels of respectively 5, 30, 75, 150 and 300 mg estragole/kg bw, resulting in an average value of 0.41±0.18%. Furthermore, assuming linearity, the linear equation obtained when fitting the data in Figure 4.3 (y=629.87x) can be used to calculate the level of E-3′-N^2-dG adduct formation based on the PBBK-based predictions of 1′-sulfooxyestragole formation in the liver.
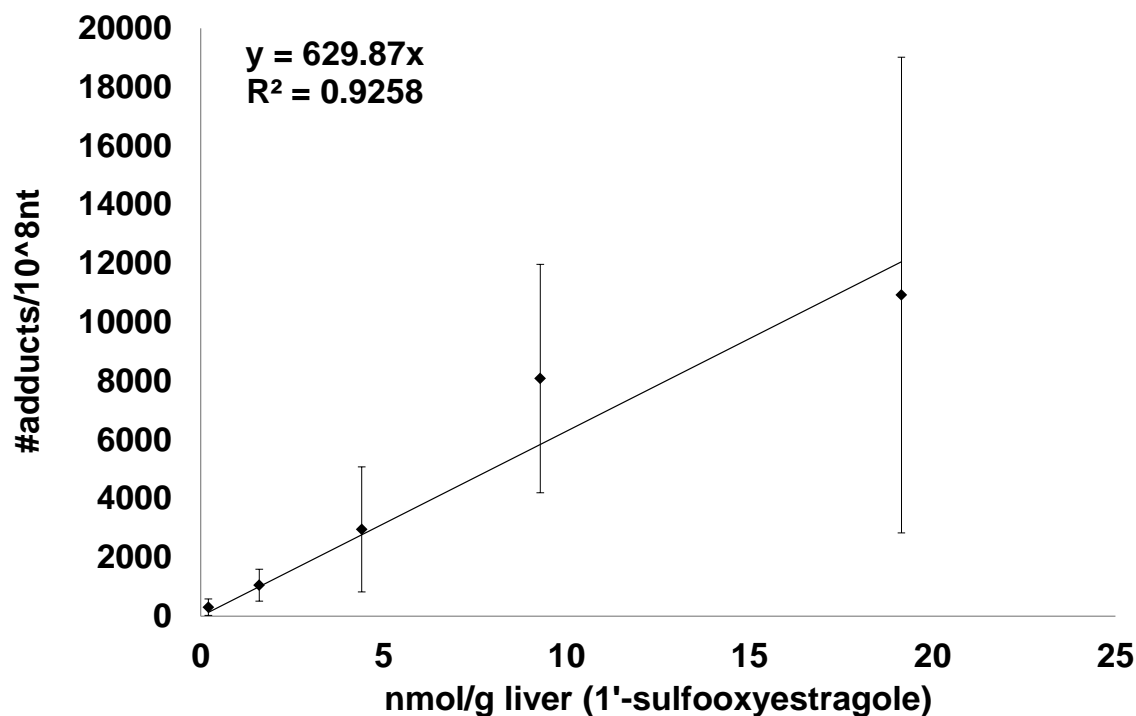
Figure 4.3. Formation of E-3′-N^2-dG adducts in 10^8 nt *in vivo* in male Sprague Dawley rats versus the levels of 1′-sulfooxyestragole (nmol/g liver) predicted by the rat PBBK model.

4.3.4 Evaluation of inter-individual human variation in DNA binding of estragole

Using the equation defined above based on the rat data, (assuming that the conversion to 1′-sulfooxyestragole to DNA adduct and repair mechanisms are similar in both rat and human), and the human PBBK model for predicting the dose-dependent formation of 1′-sulfooxyestragole, the resulting amount of E-3′-N^2-dG adducts formed in the 22 human individuals, at an estragole dose of 0.01 mg/kg bw can be determined and appeared to range between 1.2 and 31.5 E-3′-N^2-dG in 10^8nt (Figure 4.4A), corresponding to a 25-fold difference between the 22 individuals. The results show that the levels of E-3′-N^2-dG in 10^8 nt formed are generally below the reported endogenous background level of DNA adducts set at 10-100 adducts in 10^8 nt (Williams, 2008; Farmer *et al.*, 2005; Farmer, 2008). Additionally, from the formation of 1′-sulfooxyestragole for the whole population obtained by the Monte Carlo simulation, at a dose level of 0.01 mg estragole/kg bw, the amount of E-3′-N^2-dG adducts was determined. The results obtained (Figure 4.4B) show that the levels of E-3′-N^2-dG in 10^8 nt formed for 99% of the population are within the reported endogenous background level of DNA adducts set at 10-100 adducts in 10^8 nt (Williams, 2008; Farmer *et al.*, 2005; Farmer, 2008).

A

B
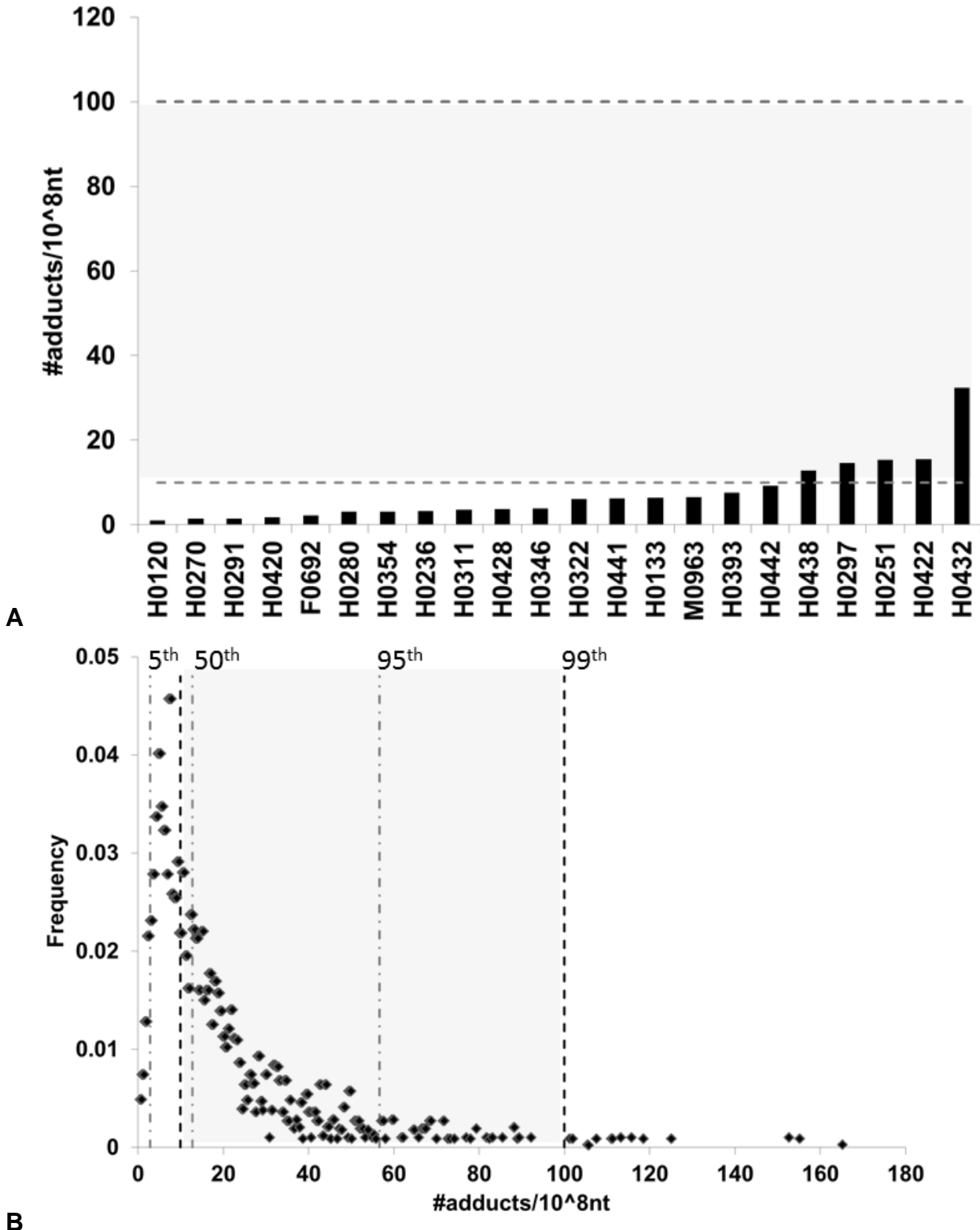
Figure 4.4. A) Number of E-3′-N^2-dG adducts in 10^8 nt formed at the levels of 1′-sulfooxyestragole predicted by the human PBBK model for the 22 human individuals and B) Monte Carlo distribution of 10,000 simulations of E-3′-N^2-dG adduct levels at an estragole dose of 0.01 mg/kg bw. In Figure B the dashed lines represents the 5th, 50th, 95th, and 99th percentiles. In both figures the grey area represents the endogenous background levels for DNA adducts (10-100 adducts in 10^8 nt, Williams, 2008; Farmer et al., 2005; Farmer, 2008).
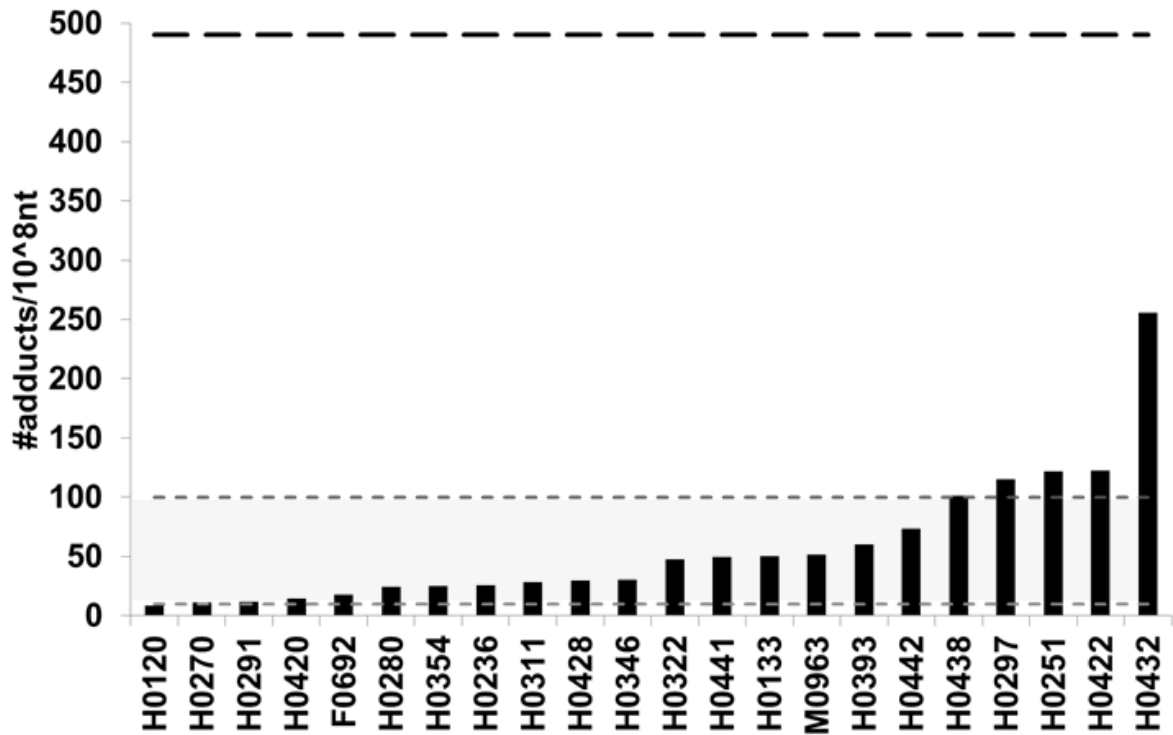
A
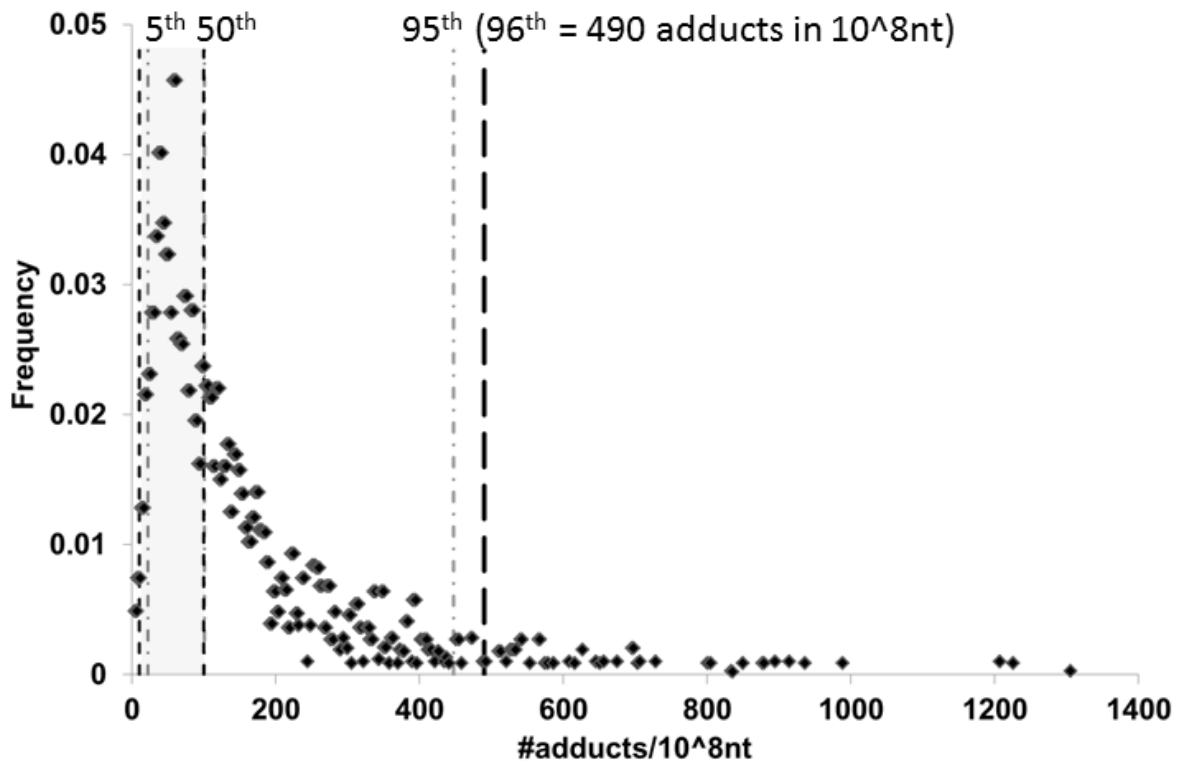
B

Figure 4.5. A) Number of E-3′-N^2-dG adducts in 10^8 nt formed at the levels of 1′-sulfooxyestragole predicted by the human PBBK model after applying a safety factor of 7.9, for the 22 human individuals, and B) Monte Carlo distribution of 10,000 simulations of E-3′-N^2-dG adduct levels at an estragole dose of 0.01 mg/kg bw. In figure B. dashed line represents the 5th, 50th, 95th, and 96th percentile. In both figures the grey area represents the endogenous background levels for DNA adducts (10-100 adducts in 10^8 nt, Williams, 2008; Farmer et al., 2005; Farmer, 2008). In Figure A The horizontal black dashed line represents the level of 490 adduct in 10^8 nt found in vivo in male mice by Philips et al. (1984) to be required for statistically-significant tumor formation (Philips et al., 1984); in Figure B this level of 490 adducts in 10^8 nt is represented by the vertical black dashed line.

4.3.5 Considerations on additional uncertainty factors to be taken into account.

As described above, the equation used to convert 1′-sulfooxyestragole levels to E-3′-N^2-dG adduct formation in the human subjects and the population as a whole was based on data obtained in rats. One might argue that the adduct formation and subsequent repair of the E-3′-N^2-dG adducts in human liver might not exactly resemble these processes in rat liver and that for this reason uncertainty factors for interspecies differences in these processes have to be taken into account. The default uncertainty factor used in risk assessment for interspecies extrapolation of 10 is made up of a factor for differences in biokinetics of 4-fold and a factor for differences in biodynamics of 2.5-fold (IPCS, 2005). Given that by using rat and human specific PBBK models, species differences in biokinetics are already taken into account, an uncertainty factor of 2.5 might be applied to the predicted DNA adduct levels to account for differences between rat and human in the biodynamics processes influencing DNA adduct formation and repair. In addition in the current Monte Carlo simulation only the interspecies differences in biokinetics are taken into account, leaving an extra uncertainty factor of 3.16 for interindividual differences in biodynamics in the human population, given that the default factor of 10 in this case is made up of a factor for differences in biokinetics of 3.16-fold and a factor for differences in biodynamics of 3.16-fold (IPCS, 2005).

This implies that an overall extra uncertainty factor of 2.5 times 3.16 (7.9) could be applied to our data presented in Figure 4.4 in order to take interspecies differences in biodynamics (2.5) and human interindividual differences in biodynamics (3.16) into account (IPCS, 2005). Figure 4.5 presents the data from Figure 4.4 multiplied by this uncertainty factor of 7.9, comparing the data obtained again with the endogenous background levels of DNA adducts. The results obtained reveal that the levels of DNA adducts formed are above the background level of 10-100 adducts in 10^8 nt for 4 out of the 22 individuals (Figure 4.5A) and for 50% of the population as a whole (Figure 4.5B). Additionally, a level of 490 adducts in 10^8 nt (15 pmol adducts/mg DNA) was added for comparison. This level was added since in an *in vivo* study using male mice exposed to estragole, safrole, methyleugenol, and other related alkenylbenzene (for 4 times resulting in a total dose of 4.75 μmol) performed by Phillips *et al.* (1984) it was concluded that alkenylbenzene-DNA adduct levels of at least 15 pmol/mg DNA (490 adducts in 10^8 nt) at 23 days were required for statistically significant tumorigenesis potential (Phillips *et al.*, 1984; FAO/WHO, 2009). The results show that at an estragole dose of 0.01 mg /kg bw the levels of E-3′-N^2-dG adduct formed after 48hr from the 22 individuals will not reach 490 adducts in 10^8 nt (Figure 4.5A), also when applying the safety factor of 7.9. However, when applying this safety factor for the whole population, 4% of the population will have DNA adduct formation above the level of 490 adducts in 10^8 nt (Figure 4.5B).

4.3.6 Estimates of DNA adduct formation in the human population at higher dose levels.

An analysis of DNA adduct formation at high levels of human exposure to estragole was also made. Although the addition of estragole as a pure compound in food was restricted (European Commission (EC), 2008), its presence in plant based food other than herbs and spices and in food supplements can still be expected. Recently, estragole levels up to 183.85 mg/g supplement have been measured in basil-based plant food supplements, resulting in an estimated average daily intake of up to 4.78 mg/kg bw (van den Berg *et al.*, 2011). Using the approach developed in the present study, it can be calculated that at 4.78 mg/kg bw the level of DNA adducts predicted to be formed would amount to 3000 E-3′-N^2-dG adduct in 10^8nt. This

amount of adducts is 30 times higher than the endogenous background level of 100 adducts in 10^8nt, and may indicate a risk for tumor formation. This latter conclusion is corroborated by the fact that a dose of 4.78 mg/kg bw would be comparable to the estimated BMD_{10} for tumor formation in mice of 4.7 to 8 mg/kg bw/day, resulting in a margin of Exposure (MOE) of 1-2 (van den Berg *et al.*, 2011).

4.4 Discussion

The objective of the present study was to obtain insight in possible levels of DNA adduct formation in human liver upon exposure to estragole at realistic human dietary intake levels, taking interindividual variability in bioactivation of estragole to its ultimate carcinogenic metabolite 1′-sulfooxyestragole within the human population into account. Intake levels of estragole have been estimated to range between 0.01 mg/kg bw (Smith *et al.,* 2002) and 0.07 mg/kg bw (SCF, 2001). Given that at present addition of estragole as a pure compound to individual food categories is no longer allowed in the European Union (European Commission, 2008), the value of 0.01 mg/kg bw/day resulting mainly from consumption of herbs and spices (Smith *et al.,* 2002) was considered representative for current levels of dietary human intake. Due to interindividual differences in bioactivation and detoxification the levels of 1′-sulfooxyestragole and consequently the levels of DNA adducts formed upon estragole exposure levels will vary in the population. This indicates the importance of characterizing these interindividual differences as was done in the present study.

A sensitivity analysis previously reported for the human PBBK model showed that formation of 1′-sulfooxyestragole mainly depends on the kinetic constants for the conversion of 1′-hydroxyestragole to 1′-oxoestragole and the kinetic constants for conversion of 1′-hydroxyestragole to 1′-sulfooxyestragole itself (Punt *et al.*, 2009). By determining the V_{max} and K_m values for these metabolic reactions experimentally for a set of liver S9 fractions from 22 human individuals, interindividual human variation in formation of 1′-sulfooxyestragole could be modeled for these 22 individuals as well as for the population as whole, the latter using a Monte Carlo simulation for 10,000 subjects. In a next step, the predicted liver levels of 1′-sulfooxyestragole were linked to E-3′-N^2-dG adduct formation by obtaining an equation from the available rat data that relates PBBK-model predicted levels of 1′-sulfooxyestragole to E-3′-N^2-dG adduct formation. Using the same equation for the human data assumes that DNA adduct formation and repair in rat and human are similar. Based on the equation obtained it could be calculated that on average only 0.41±0.18% of the 1′-sulfooxyestragole formed is actually converted to E-3′-N^2-dG adduct. This implies that the remaining 99.6% of 1′-sulfooxyestragole binds to GSH, protein and/or RNA, or, to a small extent, to other sites of the guanine base or other bases of the DNA (Miller and Miller, 1983; Fennell *et al.*, 1984; Fennell *et al.,* 1985; Phillips *et al.,* 1984; Ishii *et al.,* 2011). The results also imply that from the amount of estragole dosed only 0.0004±0.0001% is on average converted to E-3′-N^2-dG adducts.

The results of the present study reveal that predictions of DNA adduct formation at an estimated human daily intake of 0.01 mg estragole/kg bw were generally below the background level of DNA adducts reported to amount to 10-100 adducts in 10^8nt (Williams *et al.*, 2008; Farmer *et al.*, 2005; Farmer 2008), for all 22 individuals. For the 22 individuals the lowest value amounted to 1.2 E-3′-N^2-dG adducts in 10^8 nt and the highest value to 31.5 E-3′-N^2-dG adducts in 10^8nt, indicating a 25-fold variation between the 22 individuals. Additionally a Monte Carlo simulation revealed that for 99% of the whole population the predicted levels of

the E-3′-N^2-dG adduct formed remained within the endogenous background level. Because the equation used to convert levels of 1′-sulfooxyestragole formation to E-3′-N^2-dG adduct levels was based on rat data, the human data were also analyzed taking an extra uncertainty factor for interindividual and species differences in biodynamics into account. This uncertainty factor amounted to 7.9 corresponding to 2.5 for interspecies differences in biodynamics and 3.16 for interindividual differences in biodynamics. Upon applying this safety factor of 7.9 levels of E-3′-N^2-dG adduct formation for the 22 individuals were generally still within background levels four individuals having values that are somewhat higher, although these values did not reach the level of 490 adducts in 10^8 nt. This level of 490 adducts in 10^8nt was included in the analysis since it was concluded by Phillips *et al.,* (1984), based on data from rodent studies, that alkenylbenzene-DNA adduct levels of at least 15 pmol/mg DNA (490 adducts in 10^8 nt) were required for statistically significant tumorigenesis potential. Although this level of adducts is derived from rodent studies at a different exposure scenario than used to model the DNA adduct formation in humans it provides some indication of the level of DNA adducts needed for tumor formation. Possible differences between species and interindividual human variation in the tumorigenic potential of the DNA adducts can be taken into account by applying an uncertainty factor of 7.9 to the data. When applying this uncertainty factor to the 10000 individuals of the Monte Carlo simulation fifty percent of the whole population displayed a level of adduct formation above the endogenous background level (10-100 adducts in 10^8 nt), with 4% of the whole population having a value above the 490 adducts in 10^8 nt pointing at a higher risk for these individuals to develop tumors.

The present study also presented an estimate of DNA adduct formation at higher levels of human estragole intake. Recently an intake of 4.78 mg/kg bw, was reported based on the use of certain plant based food supplements (PFS) (van den Berg *et al.,* 2011). At this level of intake E-3′-N^2-dG adduct formation was predicted to be significantly (30-fold) above endogenous background levels, suggesting that DNA adduct formation could contribute to carcinogenicity at these dose levels. These high levels of estragole in PFS were similar to the lowest BMD$_{10}$ dose levels from mice (van den Berg *et al.,* 2011), pointing at a possible high risk upon daily exposure. Altogether it can be concluded that at the currently estimated daily intake levels resulting mainly from consumption of herbs and spices (0.01 mg/kg bw/day) the E-3′-N^2-dG adduct levels in humans are predicted to be within the endogenous DNA adduct levels and below the value of 490 adducts in 10^8 nt reported by Phillips *et al.,* (1984) to be required for statistically significant tumorigenesis potential of alkenylbenzene DNA adducts. Altogether these data point at a negligible risk for the average human population at the current levels of intake of estragole.

Reference

Coughlin JP, Austen WG, Donahoe PK, and Russell WE. (1987) Liver Regeneration during Immunosuppression. *J Pediatr Surg* 22, 566-570.

European Commission (EC). (2008) Regulation (EC) no 1334/2008 of the European Parliament and of the Council of 16 December 2008 on Flavourings and Certain Food Ingredients with Flavouring Properties for Use in and on Foods and Amending Council Regulation (EEC) No 1601/91, Regulations (EC) No 2232/96 and (EC) No 110/2008 and Directive 2000/13/EC. (http://eurlex.europa.eu/LexUriServ/LexUriServ.do?uri=OJ:L:2008:354:0034:0050:en: PDF).

FAO/WHO. (2009) Evaluation of certain food additives: sixty-ninth report of the joint FAO/WHO expert committee on food additives. World Health Organization, Geneva, Switzerland. WHO Technical Report 952.

Farmer PB, Brown K, Tompkins E, Emms VL, Jones DJL, Singh R, and Phillips DH. (2005) DNA adducts: Mass spectrometry methods and future prospects Toxicology and Applied Pharmacology. 207 (2005) S293 – S301

Farmer PB. (2008) Significance for risk assessment of increases in background levels of carcinogen-derived protein and DNA Adducts. Abstracts / Toxicology Letters 180S: S6–S27.

Fennell TR, Miller JA, and Miller EC. (1984) Characterization of the biliary and urinary glutathione and N-acetylcysteine metabolites of the hepatic carcinogen 1′-hydroxysafrole and its 1′-oxo metabolite in rats and mice. Cancer Res. 44:3231-3240.

Fennel TR, Wiseman RW, Miller JA, and Miller EC. (1985) Major role of hepatic sulfotransferase activity in the metabolic activation DNA adduct formation, and carcinogenicity of 1'-hydroxy-2',3'-dehydroestragole in infant male C57BL/6J x C3H/HeJ F1 mice. Cancer Res. 45;5310-5320.

Gentry PR, Hack CE, Haber L, Maier A, and Clewell HJ the III. (2002) An approach for the quantitative consideration of genetic polymorphism data in chemical risk assessment: Examples with warfarin and parathion. Toxicol. Sci. 70, 120–139.

Guenthner TM, and Luo G. (2001) Investigation of the role of the 2',3'- epoxidation pathway in the bioactivation and genotoxicity of dietary allylbenzene analogs. Toxicology 160, 47–58.

IPCS International Programme on Chemical Safety. (2005) Chemicalspecificadjustment factors for interspecies differences and human variability: Guidance document for use of data in dose/concentration-response assessment. Available at: http://whqlibdoc.who.int/publications/2005/ 9241546786_eng.pdf. Accessed November 28, 2009.

Ishii Y, Suzuki Y, Hibi D, Jin ML, Fukuhara K, Umemura T, and Nishikawa A. (2011) Detection and Quantification of Specific DNA Adducts by Liquid Chromatography-Tandem Mass Spectrometry in the Livers of Rats Given Estragole at the Carcinogenic Dose. Chem. Res. Toxicol. 24, 532-541.

Jarabek AM, Pottenger LH, Andrews LS. et al. (2009). Creating context for the use of DNA adduct data in cancer risk assessment: I. Data organization. Crit. Rev. Toxicol. 39, 659–678.

Jeurissen SMF, Punt A, Boersma MG, Bogaards JJP, Fiamegos YC, Schilter B, van Bladeren PJ, Cnubben NHP, and Rietjens IMCM. (2007) Human cytochrome p450 enzyme specificity for the bioactivation of estragole and related alkenylbenzenes. Chem. Res. Toxicol. 20, 798-806.

Luo G, Qato MK, and Guenthner TM. (1992) Hydrolysis of the 2',3'- allylic epoxides of allylbenzene, estragole, eugenol, and safrole by both microsomal and cytosolic epoxide hydrolases. Drug Metab. Dispos. 20,440–445.

Miller JA, and Miller EC. (1983) The metabolic acitvation and nucleic acid adducts of naturally-occuring carcinogens: Recent results with ethyl carbamate and the spice flavors safrole and estragole. Br. J. Cancer 48:1-15.

Miller EC, Swanson AB, Phillips DH, Fletcher TL, Liem A, and Miller JA. (1983) Structure-Activity Studies of the Carcinogenicities in the Mouse and Rat of Some Naturally-Occurring and Synthetic Alkenylbenzene Derivatives Related to Safrole and Estragole. Cancer Res. 43, 1124-1134.

Phillips DH, Miller JA, Miller EC, and Adams B. (1981) Structures of the DNA Adducts Formed in Mouse-Liver after Administration of the Proximate Hepatocarcinogen 1'-Hydroxyestragole. Cancer Res. 41, 176-186.

Phillips DH, Reddy MV, and Randerath K. (1984) ^{32}P-Postlabeling Analysis of DNA Adducts Formed in the Livers of Animals Treated with Safrole, Estragole and Other Naturally-Occurring Alkenylbenzenes. 2. Newborn Male B6c3f1 Mice. Carcinogenesis 5, 1623-1628.

Phillips DH, and Arlt VM. (2007) The P-32-postlabeling assay for DNA adducts. Nature Protocols 2, 2772.

Punt A, Delatour T, Scholz G, Schilter B, van Bladeren PJ, and Rietjens IMCM. (2007) Tandem mass spectrometry analysis of N-2-(trans-isoestragol-3'-yl)-2'-deoxyguanosine as a strategy to study species differences in sulfotransferase conversion of the proximate carcinogen 1'-hydroxyestragole. Chem. Res. Toxicol. 20, 991-998.

Punt A, Freidig AP, Delatour T, Scholz G, Boersma MG, Schilter B, van Bladeren PJ, and Rietjens IMCM. (2008). A physiologically based biokinetic (PBBK) model for estragole bioactivation and detoxification in rat. Toxicology and Applied Pharmacology 231, 248-259.

Punt A, Jeurissen SM, Boersma MG, Delatour T, Scholz G, Schilter B, van Bladeren PJ, and Rietjens IMCM. (2010). Evaluation of Human Interindividual Variation in Bioactivation of Estragole Using Physiologically Based Biokinetic Modeling. Toxicol. Sci. 113, 337-348.

Punt A, Paini A, Boersma MG, Freidig AP, Delatour T, Scholz G, Schilter B, van Bladeren PJ, and Rietjens IMCM. (2009). Use of Physiologically Based Biokinetic (PBBK) Modeling to Study Estragole Bioactivation and Detoxification in Humans as Compared with Male Rats. Toxicol. Sci. 110, 255-269.

SCF Scientific Committee on Food of the European Union. (2001) Opinion of the Scientific Committee on Food on Estragole (1-allyl-4-methoxybenzene). http://ec.europa.eu/food/fs/sc/scf/out104_en.pdf.

Shuker DEG, and Farmer PB. (1992) Relevance of Urinary DNA Adducts as Markers of Carcinogen Exposure. Chem. Res. Toxicol. 5, 450-460.

Smith RL, Adams TB, Doull J, Feron VJ, Goodman JI, Marnett LJ, Portoghese PS, Waddell WJ, Wagner BM, Rogers AE, Caldwell J, and Sipes IG. (2002) Safety assessment of allylalkoxybenzene derivatives used as flavouring substances - methyl eugenol and estragole. Food and Chemical Toxicology 40, 851-870.

Swanson AB, Chambliss DD, Blomquist JC, Miller EC, and Miller JA. (1979) Mutagenicities of Safrole, Estragole, Eugenol, Trans-Anethole, and Some of Their Known or Possible Metabolites for Salmonella-Typhimurium Mutants. Mutation Research 60, 143-153.

Swenberg JA, Fryar-Tita E, Jeong YC, Boysen G, Starr T, Walker VE, and Albertini RJ. (2008) Biomarkers in Toxicology and Risk Assessment: Informing Critical Dose–Response Relationships. Chem. Res. Toxicol. 21, 253–265

van den Berg S, Restani P, Boersma MG, Delmulle L, Rietjens IMCM. (2011) Levels of genotoxic and carcinogenic ingredients in plant food supplements and associated risk assessment. Food and Nutrition Sciences, Food and Nutrition Sciences, 2, 989-1010.

Williams GM. (2008) Application of mode-of-action considerations in human cancer risk assessment. Toxicology Letters 180, 75-80.

Wiseman RW, Miller EC, Miller JA, and Liem A. (1987) Structure-Activity Studies of the Hepatocarcinogenicities of Alkenylbenzene Derivatives Related to Estragole and Safrole on Administration to Preweanling Male C57Bl/6J X C3H-Hej F1-Mice. Cancer Res. 47:2275-2283.

Chapter 5

Based on:

DNA damage response induced by 1'-hydroxyestragole in rat primary hepatocytes

By

Paini A, Scholz G, Guignard G, Bezencon C, Latado H, Schilter B, van Bladeren, PJ, Rietjens IMCM, Marin-Kuan M.

Submitted to DNA Repair

Abstract

Estragole is a flavouring substance widely present in herbs and spices and human dietary exposure is, therefore, widespread. Estragole is hepatocarcinogenic at high doses in rodents and is considered to be genotoxic due to its capability to form DNA adducts after metabolic activation. However, detailed information on its Mode of Action (MOA) to induce carcinogenic transformation is lacking. The aim of the present study was, therefore, to study the possible implications of DNA damage and repair mechanisms in the MOA of estragole and its active metabolite 1'-hydroxyestragole, using primary rat hepatocytes. The present study shows that significantly increased levels of DNA adducts are induced upon two hour incubation of hepatocytes with 50µM 1'-hydroxyestragole, and that the level of adducts rapidly decreases after cessation of treatment, indicating the activity of cellular repair mechanisms. However, no specific DNA damage and repair pathways seem to be induced as demonstrated by a significant down-regulation of genes involved in DNA damage and repair on the transcriptional level. Results furthermore suggest that although the cellular repair machinery is able to cope with estragole DNA adducts, formation of the adducts is not fully reversible pointing at a role for persistence of low levels of adducts in the MOA. Results also reveal that at concentration levels and exposure time duration where DNA adduct formation is strongly elevated also cytotoxicity and apoptosis occur. Overall, both formation of DNA adducts together with a toxicity-mediated biological response may be necessary for the initiation and development of liver tumors by estragole.

5.1 Introduction

Estragole (4-methoxyallylbenzene) is a flavouring compound which occurs in a variety of spices and herbs including tarragon, sweet basil, sweet fennel, anise and star anise (EC-SCF, 2001; Smith *et al.*, 2002). Through the use of these herbs and spices and their essential oils in a variety of foods, cleaning agents, and cosmetic products, human exposure to estragole is widespread. Estragole has been repeatedly reviewed by expert committees. Because of its metabolic activation to a DNA reactive metabolite and evidence of hepatocarcinogenicity at high doses in mice, it has been classified as a genotoxic carcinogen. Reductions in exposure have been recommended (EU-SCF, 2001).

The metabolism of estragole is complex and is thought to drive its genotoxic/carcinogenic activity (Drinkwater *et al.*, 1976; Miller and Miller, 1983; Wiseman *et al.*, 1987). Estragole is rapidly absorbed by the oral route and metabolized in the liver by various phase I and phase II enzymes (Punt *et al.*, 2008; Smith *et al.*, 2002). *O*-demethylation of the p-methoxy substituent of estragole yields the corresponding phenolic derivative, which may be excreted as sulfate- or glucuronic acid conjugate (Anthony *et al.*, 1987; Solheim and Scheline, 1973; Zangouras *et al.*, 1981). This pathway was reported to be prevalent at low dose in humans and in rodents (Anthony *et al.*, 1987). Epoxidation of the side chain alkene yields the 2'-3'-epoxide that is subject to detoxification by epoxide hydrolase (EH) and glutathione s-transferase (GST) (Luo and Guenthner, 1995, 1996; Luo *et al.*, 1992). An additional documented pathway is oxidation of the allyl-group into 1',2'-unsaturated carboxylic acid. Such a pathway seems mainly active in humans and leads to detoxification (Phillips *et al.*, 1981; Punt *et al.*, 2009). The main metabolic pathway responsible for bioactivation of estragole to its genotoxic and carcinogenic metabolite is hydroxylation generating 1'-hydroxyestragole (1'-HE) and subsequently sulfooxyestragole through the action of sulfotransferases (Figure 5.1). The sulfate ester formed is prone to spontaneous heterolytic cleavage releasing a reactive electrophilic intermediate (carbocation) that can bind to hepatic proteins, DNA and RNA (Miller and Miller, 1983; Smith *et al.*, 2002). A major DNA adduct formed is N^2-(trans-isoestragole-3-yl)-2'-deoxyguanosine (E-3'-N^2-dG) (Phillips *et al.*, 1981; Randerath *et al.*, 1984), which can arise after an allylic shift of the carbocation prior to the reaction with the exocyclic group of 2'-deoxyguanosine (Phillips *et al.*, 1981; Phillips *et al.*, 1984).
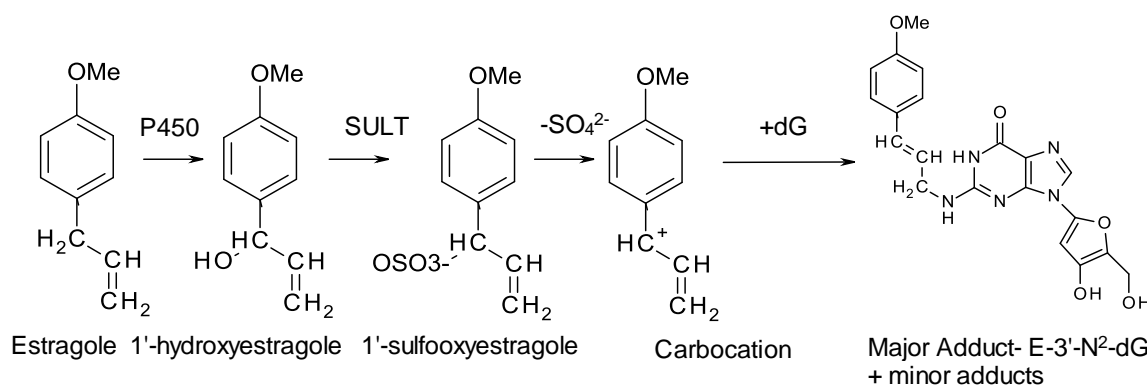

Figure 5.1. Estragole metabolic pathway leading to DNA adduct formation, and representation of the chemical structure of E-3'-N^2-dG, a major DNA adduct formed via hydroxylation and sulfation on the allyl-side chain.

For several reasons, to interpret the data on metabolism and DNA-adduct formation in the perspective of the potential carcinogenicity of low levels of estragole exposure is still not straightforward. First of all, the profile of the metabolites produced and the rate of bioactivation have been shown to be dose-dependent (Anthony *et al.*, 1987; Luo and Guenthner, 1995; Sangster *et al.*, 1987; Solheim and Scheline, 1973). It is currently thought that at low doses estragole is mainly *O*-demethylated (Anthony *et al.*, 1987), while at increasing doses, the 1'-hydroxylation pathway may became more important, due to saturation of the *O*-demethylation pathway in lungs and kidneys (Punt *et al.*, 2008, Punt *et al.*, 2009). Secondly, data are available providing evidence for the possibility of adduct elimination and DNA repair (Phillips *et al.*, 1981; Randerath *et al.*, 1984). In addition, it is important to keep in mind that mutagenic effects of estragole have not yet been fully demonstrated in animal studies *in vivo* and that carcinogenic doses were always associated with the expression of significant hepatotoxicity. To fully understand the mode of action involved in estragole carcinogenicity, additional work is therefore necessary, in particular the better integration of the dose-responses of metabolic pathways, DNA-adduct formation, DNA repair and toxicity. It is widely acknowledged that risk assessment would significantly benefit from elucidation of the Mode of Action (MOA) involved in estragole carcinogenicity.

5.2 Materials and Methods

5.2.1 Chemicals and reagents

Estragole was obtained from Acros Organics (Geel, Belgium). 1,2,3,7,9-^{15}N$_5$-2′-Deoxyguanosine (^{15}N$_5$-dG) was obtained from Cambridge Isotope Laboratories (Cambridge, MA). ITS+ (Insulin, Transferrin, and Selenous acid), L-glutamine and Matrigel were obtained from Collaborative Biomedical Products (Bedford, MA). Penicillin/streptomycin was purchased from Gibco (Paisley, UK). Fetal bovine serum (FBS) was purchased from Hyclone (Logan, Utah). Earle's balanced salt solution (EBSS), William's E medium, dexamethasone, ethylene glycol tetra acetic acid (EGTA), collagenase from *Clostridium hystoliticum* type IV-S, dimethyl sulfoxide (DMSO), Hepes, CaCl$_2$*2H$_2$O, MgCl$_2$*6H$_2$O, trypan blue, methanol, zinc sulphate (heptahydrate), phosphodiesterase I from *Crotalus adamanteus* (venom phosphodiesterase), phosphodiesterase II from bovine spleen (spleen phosphodiesterase), and alkaline phosphatase were purchased from Sigma (Schnelldorf, Germany). Aflatoxin B1, trans-anethole, 2′-deoxyguanosine and RIPA buffer were purchased from Sigma (Buchs, Switzerland). Acetonitrile, ethylenediamine tetra acetic acid (EDTA) and ethanol were purchased from Merck (Darmstadt, Germany). Nuclease P1 was obtained from MP Biochemicals (Aurora, OH), staurosporine from Cell Signaling Technologies (Danvers, MA). Antibodies for Gadd45α (C20) sc-792 were purchased from Santa Cruz (Santa Cruz, CA). Phospho-Histone H2A.X (Ser139) antibody #2577 and poly (ADP-ribose) polymerase (PARP) antibody #9542 were from Cell Signaling technologies (Danvers, MA). Histone H2A.X antibody #ab11175 was obtained from Abcam (Cambridge, UK).

1'-Hydroxyestragole (1'-HE) was synthesized as described previously in Chapter 2. Synthesis of E-3'-N^2-deoxyguanosine (E-3'-N^2-dG) and (^{15}N$_5$) E-3'-N^2-deoxyguanosine ((^{15}N$_5$) E-3′-N^2-dG) was done as reported in Chapter 2.

CAUTION! 1'-hydroxyestragole and aflatoxin B1 are known to be hepatocarcinogenic and must be handled accordingly.

5.2.2 Preparation and culture of primary rat hepatocytes

White male Sprague-Dawley rats, 8 weeks old, with a weight of 200-250 g were used to isolate fresh primary hepatocytes by perfusion, as described in Cavin *et al.*, (2007), based on a protocol first described by Sidhu *et al.* (1993). Viability of the isolated hepatocytes was determined by a trypan blue test, and was at least 90%. Cells were seeded at a density of $3,5*10^6$ cells/60 mm (6 cm ø) culture dish in 3.5 mL William's E medium containing phenol red, supplemented with 2 mM L-glutamine, 10 mM Hepes pH 7.4, 1% ITS+, 100 U/ml penicillin/streptomycin, 100 nM dexamethasone and 5% FBS. Hepatocytes were allowed to attach (at 37°C with 5% CO_2) for two to three hrs and then washed with EBSS to remove unattached cells. Fresh serum-free medium containing 25 nM dexamethasone was added and matrigel (233 µg/mL) was then applied. Cells were kept overnight at 37°C with 5% CO_2 before treatment with test compounds.

5.2.3 DNA adduct formation and extended time course for DNA repair in rat hepatocytes

DNA adduct formation was analyzed after incubating rat primary hepatocytes with 1, 10, and 50 µM 1'-HE or with 500 µM of estragole. Incubation time was 2 hrs or 24 hrs at 37°C. Additionally, a time course of DNA adduct formation in primary rat hepatocytes was performed: cells were exposed to 50 µM 1'-HE for 2 hrs, after which the medium was replaced with 1'-HE-free culture medium. Cells were allowed to recover for 5, 10, 15 and 30 min after which they were harvested for measurement of DNA adduct levels. To obtain a sufficient amount of DNA all concentrations of 1'-HE were tested in triplicates using hepatocytes from the same liver, and pooled before the extraction step. For biological replicates, hepatocytes isolated from four individual perfusions were used. The supernatants of the incubations were used to measure cytotoxicity by determining lactate dehydrogenase (LDH) activity.

5.2.4 DNA extraction from primary hepatocytes and enzymatic digestion

DNA was extracted from primary rat hepatocytes, as described previously (Chapter 2), using the Get pure DNA Kit-Cell (Dojindo Molecular Technology Inc., Kumamoto, Japan) for $3*10^6$ to $1*10^7$ cells (following the manufacturer's instructions). The final DNA pellet was dissolved in 100 µL MilliQ water. Digestion to release the nucleoside E-3'-N^2-dG was performed according to method described in chapter 2. The hydrolyzed sample was evaporated to dryness and reconstituted in 50 µL water.

5.2.5 LC-MS/MS method for detection and quantification of E-3'-N^2-dG

LC-MS/MS analysis was performed on a Perkin Elmer 200 Series HPLC System (Perkin Elmer, Waltham, Massachusetts) coupled to a API 3000 system (Applied Biosystem, Foster City, California). Samples were injected on an Agilent Zorbax Extend-C18 column, 2.1*50 mm, 3.5 Micron 80 Å (Basel, Switzerland), with a Zorbax guard column. The gradient and instrument conditions were set as reported in Chapter 4. Quantification of nucleoside E-3'-N^2-dG by isotope dilution was done as reported in Chapter 2. The amount of E-3'-N^2-dG detected in the samples was related to the total amount of digested DNA detected in each sample and adjusted for the average MW of DNA monophosphorylated nucleotides (nt) of 327 g/mol, in order to quantify the number of E-3'-N^2-dG adducts per 1000 nt.

5.2.6 RNA extraction, quantification and quality control

Total RNA from primary hepatocytes exposed to 1'-HE, estragole, trans-anethole (negative control), and aflatoxin B1 (positive control) were isolated using the NucleoSpin RNA Kit (Macherey-Nagel) following the manufacturer's protocol. Two dishes (6 cm ø) containing $3.5*10^6$ cells from the same liver were pooled after treatment. For biological replicates, hepatocytes isolated from three individual perfusions were used. Total RNAs were treated with DNAse I to remove genomic DNA. RNA concentration was measured with the RiboGreen RNA quantification Kit (Molecular Probes, Eugene, OR) by fluorescence using Polar star optima (BMG, Labtech) according to the manufacturer's instructions. Assessment of RNA quality and measurement of the 28S to 18S ratio were performed by dynamic gel electrophoresis using the Agilent RNA 6000 Nano assay (Agilent Biotechnologies, Germany).

5.2.7 DNA damage and repair arrays

RT^{2}Profiler^{TM} PCR arrays were purchased from SA Biosciences (Lucerna Chem, Luzern, CH). The 'Rat DNA damage signaling PCR array', profiling the expression of 84 genes involved in DNA damage signaling pathways was chosen for the analysis. The RT-PCR method was performed as indicated by the supplier. Briefly, cDNA was synthesized from RNA of primary rat hepatocytes. Genomic DNA was eliminated using a 2 µL mixture of GE (DNA elimination buffer) added to 1 µL of each RNA sample and 7 µL nuclease free water were added. To this mixture 10 µL of RT cocktail (SA Bioscience) were added and incubated for 15 min at 42° C, then immediately stopped by heating to 95° C for 5 min. To 20 µL of the cDNA synthesis reaction, 91 µL of nuclease free water was added. The experimental cocktail contained: 102 µL of cDNA mixture to which were added 1350 µL of RT^{2}Real Time SYBER Green/ROX PCR master mix (SA Bioscience) and 1248 µL nuclease free Water. 25 µL of the experimental cocktail were added to each well of the 96 well plate using a Corbett Robot (Châtel St Denis, Switzerland). Real Time PCR was performed using an ABI Prism®7000 Sequence Detection System (Applied Biosystems, Weiterstadt, Germany). The following thermo cycler conditions for amplification were used: initial inactivation of the DNA polymerase for 10 min at 95°C, followed by 40 cycles at 95°C, each consisting of a denaturing step for 15 seconds at 95°C and an annealing and extension step for 1 min at 60°C. R. Relative quantification of the expression level of the PCR products was performed following the comparative Ct method ($2^{-[delta][delta]Ct}$ method; Yuan *et al.*, 2006), which involves relative quantification using the Ct values of the samples of interest with the non-treated control sample (calibrator). The Ct values of both the calibrator and the samples of interest are normalized to the average of the endogenous housekeeping genes present on the array.

5.2.8 Real Time polymerase chain reaction (TaqMan RT-PCR)

RNA was reverse transcribed into cDNA using the 'Superscript First-Strand Synthesis for RT-PCR' kit (Invitrogen Life Technologies, Karlsruhe, Germany). cDNA synthesis was performed using a Thermal Cycler®9700 (Applied Biosystem, Weiterstadt, Germany); the thermal sequence selected was 10 min at 25°C, 30 min 48°C and a final inactivation step of 5 min at 95°C. Samples in triplicates were amplified in a 96 well plate using 1 µL of cDNA. Real Time PCR was performed using an ABI Prism®7000 Sequence Detection System (Applied Biosystems, Weiterstadt, Germany). The following thermo cycler conditions for amplification were used: 2 min at 50°C and 10 min at 95°C, followed by 40 cycles, each consisting of a

denaturing step for 15 seconds at 95°C and an annealing and extension step for 1 min at 60°C. Relative quantification of amplified PCR products was performed using ABI Prism®7700 Sequence Detection System software 1.1 (Applied Biosystems) normalized to the rat 18S rRNA gene as internal control. Furthermore, blanks were run with primers adding water instead of template.

5.2.9 Protein extraction and Western Blot

Protein expression was analyzed by Western blot (Invitrogen) as described by the supplier. Briefly, the cells were lysed by adding 100 µL of mixture (cell lysing buffer 10x, Cell Signaling Technologies, with antiphosphatase and antiprotease, Roche) and incubated on ice for 5 min. Cells were gently scraped and transferred to a 1.5 mL Eppendorf tube. Cells were sonicated and centrifuged at 14.000 g for 10 min at 4°C. The supernatant was snap frozen in liquid nitrogen and stored at -80°C. Thawed samples were centrifuged for 10 min at 8000 rpm; 1 µL was taken to measure the protein concentration in each sample using Biorad Protein assay kit (Bio-Rad, Richmond CA). A calibration curve was made using BSA and measured colorimetrically at 595 nm wavelength (Unikon XL, Bio Tek instrument). Using the MiniCell XCellSureLock system (Invitrogen), 25-40 µg of protein was loaded in the NuPage®Bis-Tris-Pre-Cast Gel 4-12% System (Invitrogen). Protein was transferred to nitrocellulose membrane (0.2 µm, Invitrogen) for 1 h at 30V. Membranes were first blocked using 5% of milk-TBST for 3hrs at room temperature, after washing, antibodies were added for overnight incubation at 4ºC. After washing, the second antibody anti-rabbit (Cell Signaling Technologies) was added in 5% milk-TBST for 1 h, after which membranes were washed. After a final washing step, chemiluminescence detection of the immunoblots was performed using the ECL solution (Pierce, Rockford, IL) for approximately 40 min. Membranes were wrapped in polyethylene film and exposed to Kodak films using the Curix 60 processor (AGFA).

5.2.10 Cytotoxicity assay

Cytotoxicity was determined by measuring the activity of cytoplasmic lactate dehydrogenase (LDH) in cell culture supernatants reflecting leakage from the cytoplasm of damaged cells after 2hrs or 24hrs of treatment with test compounds. The test was done using ENZYLINE™ LDH Optimise 10 (BioMerieux® SA, Lyon, France). The samples were measured with the Roche Cobas Mira plus analyzer (Minnesota, USA). LDH activity was analyzed by following the conversion of NADH to NAD^+ during the conversion of pyruvate to lactate. Absorbance of NADH was recorded at a wavelength of 340 nm at 37°C, with an extinction coefficient of 6.22 mM^{-1} cm^{-1} (at 340 nm and pH 7.1). In order to validate the measurements, commercially available quality controls were freshly prepared and run in parallel. The instrument quality controls used were: zymotrol™ (BioMerieux® SA, Lyon, France), duotrol™, and duotrol abnormal™ (Biomed, Germany).

5.2.11 ApoTox-Glo™ Triplex Assay

The ApoTox-Glo™ Triplex Assay (Promega, Madison, WI USA) was used to analyze cytotoxicity, viability, and apoptosis in treated cells seeded to 96 well plates. Analysis was performed following the protocol of the ApoTox-Glo™ Triplex Assay. Samples were analyzed measuring fluorescence (Unikon XL, Bio Tek instrument) at two wavelengths 400/505 nm (Viability) and 485/520 nm (Cytotoxicity). For each individual concentration the analysis was based on the average of four replicate wells. Two individual experiments

were performed from independent perfusions. A concentration curve with staurosporine was used as positive control for apoptosis (data not shown).

5.2.12 Statistical analysis

Statistical significance was tested where indicated using a Two Sample T-Test (Excel, Microsoft Office 2007).

5.3 Results

5.3.1 DNA adduct formation and elimination

Primary rat hepatocyte cultures were treated with either increasing concentrations (1, 10 or 50 µM) of 1'-hydroxyestragole (1'-HE), or with 500 µM estragole for 2 or 24 hrs. The DNA adduct E-3′-N^2-dG was analyzed by LC-MS/MS and quantified using sensitive isotope dilution methodology. Measurable amounts of DNA-adducts were found with each treatment regimen (Figure 5.2). Estragole was much less potent than 1'-HE at producing DNA-adducts. At 50µM 1'-HE a statistically significant concentration related increase in DNA adduct formation was observed at both time points tested. An impact of the duration of 1'-HE treatment on the number of DNA-adducts formed was also evident at the highest concentration tested (about 5-times higher levels of adducts at 24 hrs as compared to 2 hrs). Given that at 24 hrs the value was lower than proportional as compared to the value at 2 hrs the data were suggesting the presence of a cellular mechanism of elimination of DNA-adducts.

	Control DMSO	1µM 1'-HE	10µM 1'-HE	50µM 1'-HE	500µM ES
2 hrs (#adducts/1000nt)	0	0.193	0.337	1.338	0.175
24 hrs (#adducts/1000nt)	0	0.212	0.469	6.570	0.288
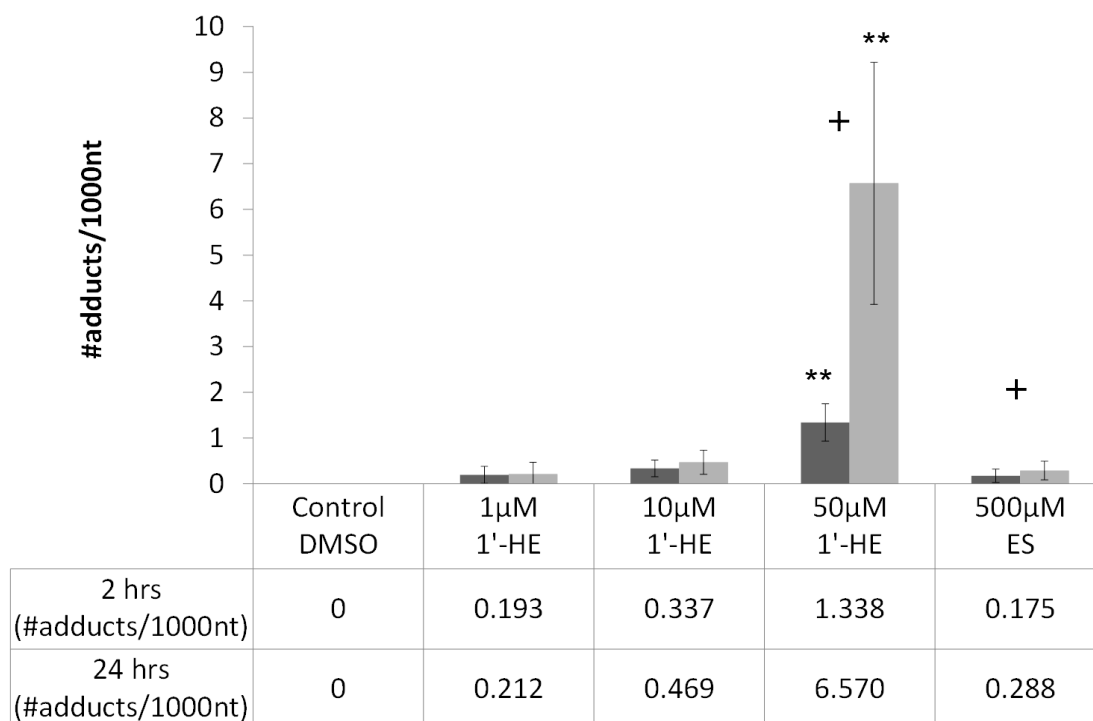
Figure 5.2. Concentration response of DNA adduct formation in primary rat hepatocytes exposed to 1µM, 10µM, and 50µM of 1'-hydroxyestragole (1'-HE) and 500µM estragole (ES) at 2hrs and 24hrs. The data represent mean and Stdev of 4 independent experiments. Statistical significance between time points (2 versus 24hrs) found only at 50µM of 1'-HE and 500µM ES : *p<0.05 (black cross). Black stars represents statistical significance in DNA adduct formation found between treatments (10µM versus 50µM) for both time points (2 and 24hrs): **p<0.01.

To further confirm the hypothesis of a cellular mechanism of DNA adduct elimination, primary hepatocyte cultures were treated for 120 min with 1, 10, and 50 µM 1'-HE and collected for DNA adduct measurement. The number of adducts measured after exposure to these concentration after 120 min were in line with previous data (Chapter 2). In an additional set of cultures, incubation media were replaced after 120 min (2 hrs) of treatment by fresh medium free of 1'-HE and the cells were collected 5, 10, 15 or 30 min later. DNA adducts were measured as described above. The data are depicted in Figure 5.3. After 120 min of treatment, the numbers of adducts measured confirmed the data shown in Figure 5.2. For all concentrations tested, a decline in the number of DNA adducts was observed after replacement of the incubation media with fresh media free of 1'-HE (Figure 5.3). The decline in DNA adducts was most significant for the sample treated with 50µM 1'-HE. However, after an initial fast decline a relatively stable and constant value of about 0.2-0.5 adducts/1000 nt was observed 30 min after the medium change.
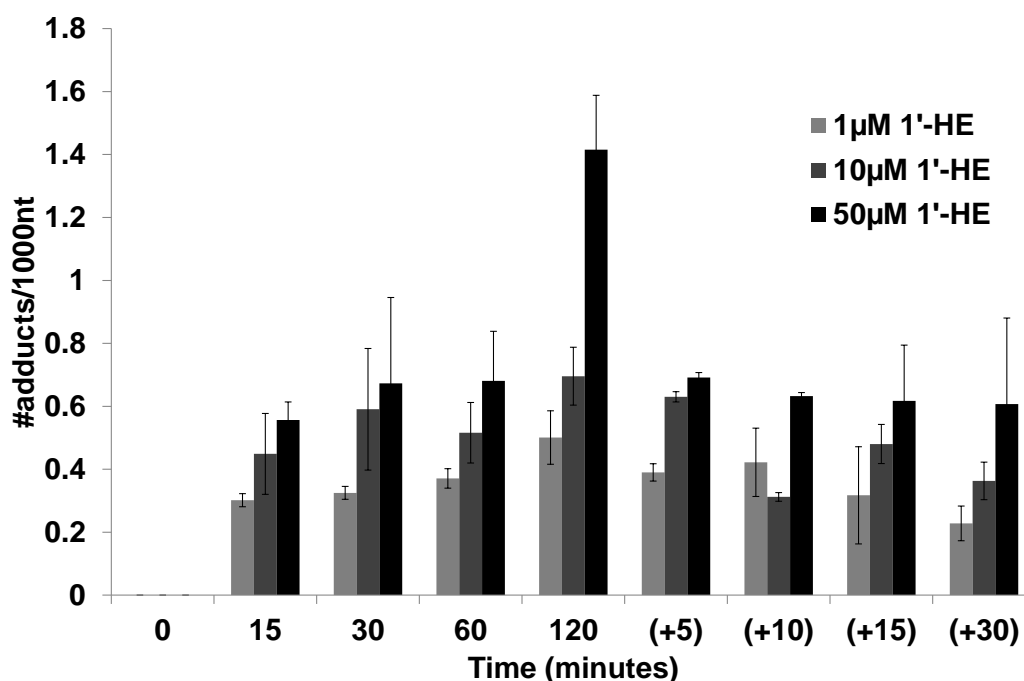
Figure 5.3. Time course of covalent DNA binding in primary rat hepatocytes exposed to 1, 10, and 50 µM of 1'-hydroxyestragole (1'-HE). After 2 hrs incubation of the cells with test compound the medium was replaced with 1'-HE-free medium and cells were collected after 5 min, 10 min, 15 min and 30 min for analysis of DNA adduct levels. The data represent mean and Stdev of 4 independent experiments. Black stars represents statistical significance in DNA adduct reduction at the different time points compared to the levels reached after 2hrs treatment: *p<0.05. Compared to the data at time 0 at all-time points the level of DNA adduct formation was statistically significantly increased (p<.0.05).

5.3.2 Transcriptional modulation of genes involved in the DNA damage response

In order to assess if the formation of DNA adducts was correlated with a global biological DNA damage response, the transcriptional expression of 84 genes involved in DNA damage and repair pathways was studied using RT²Profiler™ PCR arrays for Rat DNA damage signaling (SA Biosciences). Primary rat hepatocytes were exposed to the test compounds 1'-HE and estragole for either 2 or 24 hrs. In parallel, AfB1 was used as a positive control for genotoxicity through DNA-reactivity while trans-anethole was selected as a structural estragole analogue with no DNA reactivity. A heatmap depicting the up- and down-regulation of

gene expression from cells treated with 1'-HE, estragole, trans-anethole, and AfB1 for 2 hrs is shown in figure 5.4.
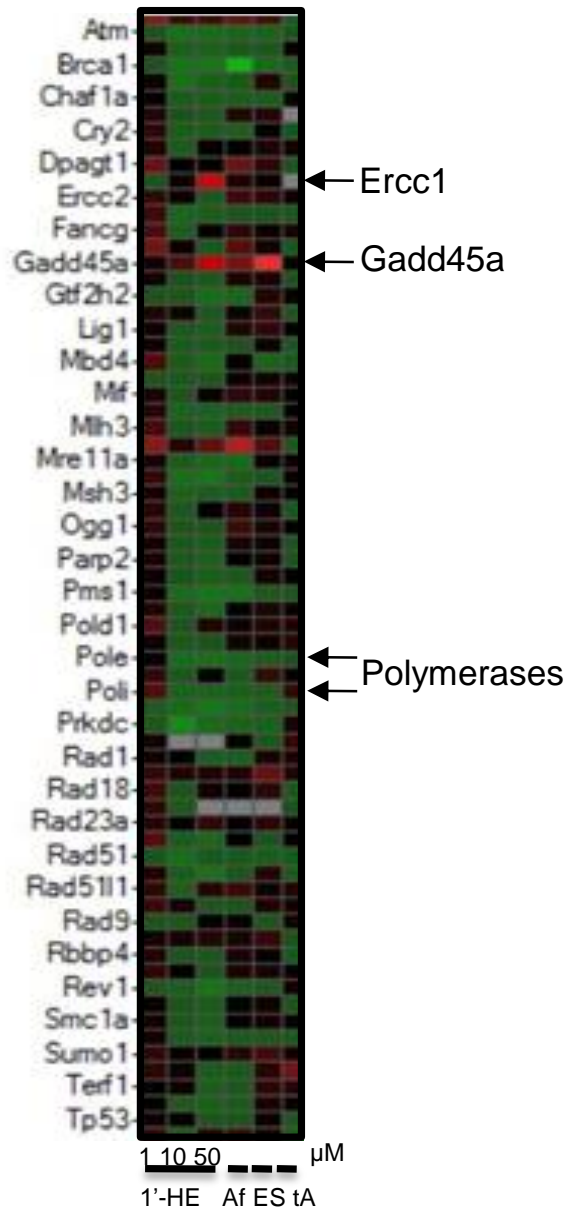
Figure 5.4. Heatmap-presentation of RT^{2}Profiler^{TM} PCR array results after treatment of primary hepatocytes for 2 hrs. Gene upregulations are indicated in red, downregulations in green. 1'-hydroxyestragole (1'-HE), alfatoxin B1 (AF), estragole (ES), trans-Anethole (tA).

The main effect induced by 1'-HE exposure was a concentration-related down-regulation of DNA repair-related genes. No modulation was identified with trans-anethole (500 μM). With the other compounds, the expression of a few genes appeared significantly changed after 2 hrs of treatment, but no such significant deregulation was noted after 24 hrs of treatment (data not shown). The most strongly up-regulated gene was the DNA damage marker Gadd45α, induced 9-fold with 50 μM 1'-HE. Gadd45α was also slightly induced as a result of treatment with 500 μM estragole (3.4-fold) and 0.5 μM AfB1 (2-fold). Another gene (Ercc1) was identified on the array to be highly up-regulated at 50 μM 1'-HE, but this could not be confirmed by TaqMan

PCR (data not shown). This gene was not investigated further. Interestingly, some significant (>2-fold) down regulations found at 2 hrs of treatment with 50 µM 1'-HE concerned several DNA repair polymerases. Some of them, i.e. members of the Y family of polymerases (such as Polκ, Polι and Rev1) belong to specialized low-accuracy, error-prone DNA-polymerases also known as translesion synthesis (TLS) polymerases. Because these polymerases are expected to play a role in DNA-adduct persistence, the potential effect of 1'-HE on their expression was further studied in an independent set of experiments and using TaqMan PCR as analytical method. Results are presented in Figure 5.5. A down-regulation in the expression of mRNAs specific for Polκ, Polε, Polη, Polι and Rev1 was observed in cultures treated with either 50 µM 1'-HE or 1 µM AfB1 for 2 hrs. On the contrary, at 24 hrs of treatment, a moderate up-regulation of these genes was found.
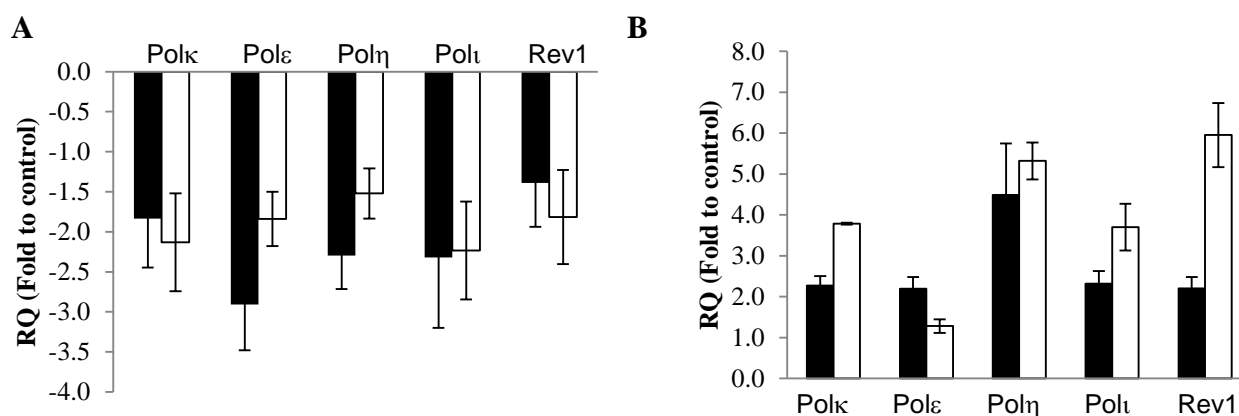
Figure 5.5. Taqman RT-PCR confirmation of polymerase genes modulated in primary rat hepatocytes. Hepatocytes were exposed for 2 hrs (A) and 24 hrs (B) to 50 µM of 1'-HE (white bars) and 1 µM of AfB1 (black bars). Data represent mean and Stdev of 2 independent experiments.

5.3.3 Genotoxic stress response

A striking effect of 1'-HE and estragole on gene expression identified with the application of the RT^{2}Profiler^{TM} PCR array was an early induction of Gadd45α. This gene is involved in multiple functions related to DNA repair, regulation of cell cycle and cell survival. It is often up-regulated in response to various physiological and environmental stresses. Gadd45α has been considered as a sensor of DNA-damage as well as a reliable biomarker of genotoxic stress. To confirm the validity of the result obtained with the array method, additional analyses were conducted and gene expression was measured using TaqMan PCR. Data obtained with the array were confirmed by the results obtained with the TaqMan PCR. A strong, concentration-dependent induction of Gadd45α mRNA was found after 2 hrs exposure to 1'-HE (Figure 5.6A). Slight inductions were found with the lower concentrations of 1'-HE, AfB1 and 500 µM estragole, but induction was not found with tA. To ascertain the biological relevance of the effects measured at RNA level, Western blot analysis was performed (Figure 5.6B). The protein expression data obtained were consistent with the RNA expression, although quantitatively RNA and protein expression were not fully correlated. Interestingly, with each compound tested, the Gadd45α protein induction was transient, clearly visible at 2 hrs, but not persisting until 24 hrs. The transient increase in Gadd45α expression observed above suggested a possible mobilization of a genotoxic stress response. To further characterize this response, downstream markers of genomic damage were analyzed.

A

B
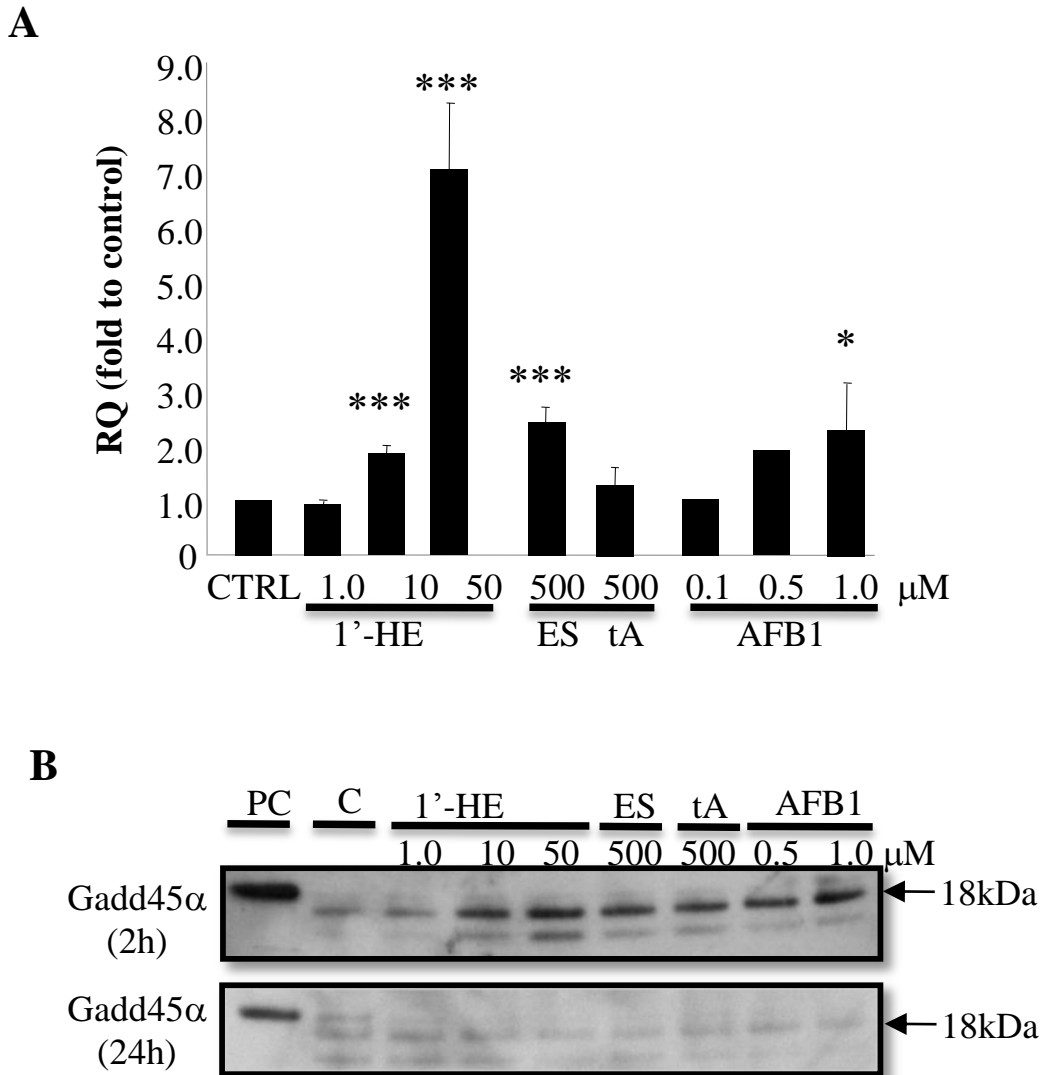
Figure 5.6. Modulation of Gadd45α expression in rat primary hepatocytes. (A) Taqman RT-PCR of RNA extracted from hepatocytes exposed to the indicated concentrations of test compounds for 2 hrs. Statistical significance of treatment versus control: *p<0.05;**p<0.01;***p<0.001. (B) Western blot analysis of Gadd45α protein expression after 2 hrs and 24 hrs exposure to the same compounds, the figure depicts one representative Western blot out of three replicates. (PC = protein control, C = control, 1'-HE = 1'-hydroxyestragole, ES = Estragole, tA = trans-anethole, AFB1 = Aflatoxin B1).

Histone H2A.X is a 15 kDa member of the histone family. In response to DNA-damage, it is rapidly phosphorylated into gamma histone H2A.X (γ-H2A.X). Analysis of γ-H2A.X expression is increasingly used to detect the genotoxic effect of toxic substances. Data on expression of H2A.X and γ-H2A.X are provided in Figure 5.7. After 2 hrs of incubation a slight induction of the protein H2A.X was observed with 1'-HE, estragole and AfB1 (Figure 5.7A). Although background levels were higher than at 2 hrs, no differences related to treatment were recorded on the expression of H2A.X at 24 hrs (Figure 5.7B). Very little expression was noticed for γ-H2A.X at 2 hrs of treatment, except possibly for 50 μM 1'-HE and 1 μM AfB1 where a very faint band may be visible (Figure 5.7A).
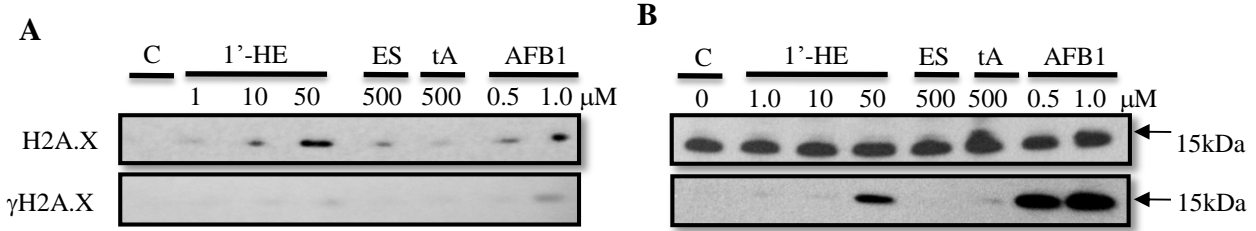
Figure 5.7. Concentration-response of the effect of 1'-HE on Histone (H2A.X) protein expression and phosphorylation. Western blot analysis of cell lysates from rat primary hepatocytes exposed for 2 hrs or 24 hrs to the indicated concentrations of test compounds using antibodies to H2A.X and γ-H2AX. The figure shows one representative blot out of the three replicates. (C = control, 1'-HE = 1'-hydroxyestragole, ES = Estragole, tA = trans-anethole, AFB1 = Aflatoxin B1).

However, at 24 hrs of treatment, a strong expression of γ-H2A.X was observed with 1'-HE (50 μM) and AfB1 (0.5 and 1 μM). No effect was detected with the lower concentrations of 1'-HE, estragole or trans-anethole. PARP-1 is a nuclear protein of 116 kDa, the main role of which is to detect and assist in the repair of DNA strandbreaks. Interestingly, when DNA damage is extensive, PARP-1 is inactivated by caspase cleavage releasing to two fragments of 89 and 24 kDa, respectively. The analysis of the fragments provides insight on the extent of DNA-damage involved. At 2 hrs of treatment, none of the treatments produced any effect on either PARP-1 expression or PARP-1 cleavage (Figure 5.8). Although no striking effect on PARP-1 expression was observed after 24 hrs of treatment with any of the treatment administered, PARP-1 cleavage was evident with 1'-HE (50 μM) and AfB1 (0.5 and 1 μM) as shown by an increased signal for the 89 kDa fragment (Figure 5.8).
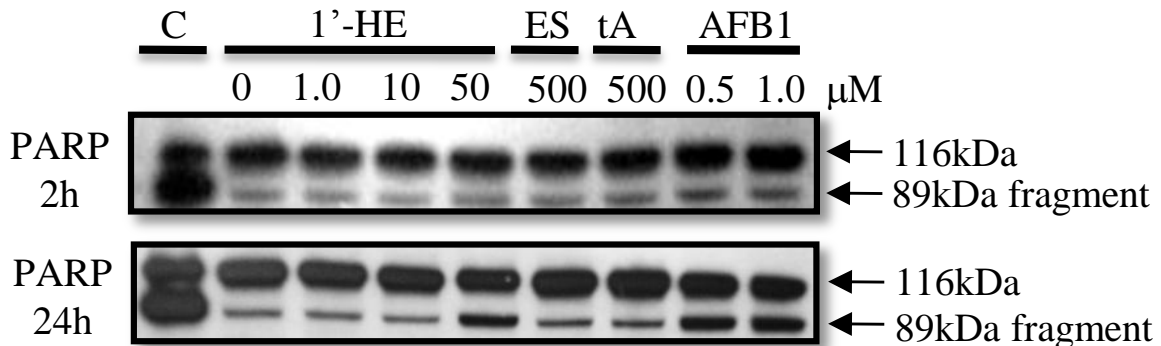
Figure 5.8. Concentration-response of the effect of 1'-HE on PARP protein expression and cleavage. Western blot analysis of cell lysates from rat primary hepatocytes exposed for 2 hrs or 24 hrs to the indicated concentrations of test compounds using PARP antibody. The figure depicts one representative Western blot out of three independent experiments. (C = control, 1'-HE = 1'-hydroxyestragole, ES = Estragole, tA = trans-anethole, AFB1 = Aflatoxin B1).

5.3.4 Toxicological consequences

The results described above suggest that a 50 μM concentration of 1'-HE produces severe genotoxic stress. In theory this may result in cell death, either through necrosis or apoptosis. In order to study the toxicological profile of the different treatment regimens applied, primary hepatocyte cultures were treated for 2 or 24 hrs

and then analyzed using both an LDH leakage test and the Apo Tox-Glo[TM] Triplex Assay. As reported previously (Chapter 2), no cytotoxicity was observed at any concentration after 2 hrs of treatment as assayed by the LDH assay. In contrast, after 24 hrs of exposure a 6-fold increase in LDH activity was measured in the supernatant of cells treated with 50 µM 1'-HE as compared to the non-treated controls (data not shown) indicating cytotoxicity. Viability, cytotoxicity and apoptosis induced by the test- (1'-HE, estragole) and the control- (AfB1 and trans-anethole) compounds were assessed by the Apo Tox-Glo[TM] Triplex Assay. Results are shown in Figure 5.9. At 2 hrs of treatment, no effect was found with 1'-HE and AfB1 (Figure 5.9A). The same was true for estragole and trans-anethole (data not shown). After 24 hrs of incubation with the test compounds (Figure 5.9B), cytotoxicity was increased at the highest concentrations tested of both 1'-HE and AfB1, while an increase in apoptosis was already evident at the second highest concentration of both 1'-HE and AfB1. Neither cytotoxicity nor increased apoptosis were observed with estragole or trans-anethole in rat primary hepatocytes.
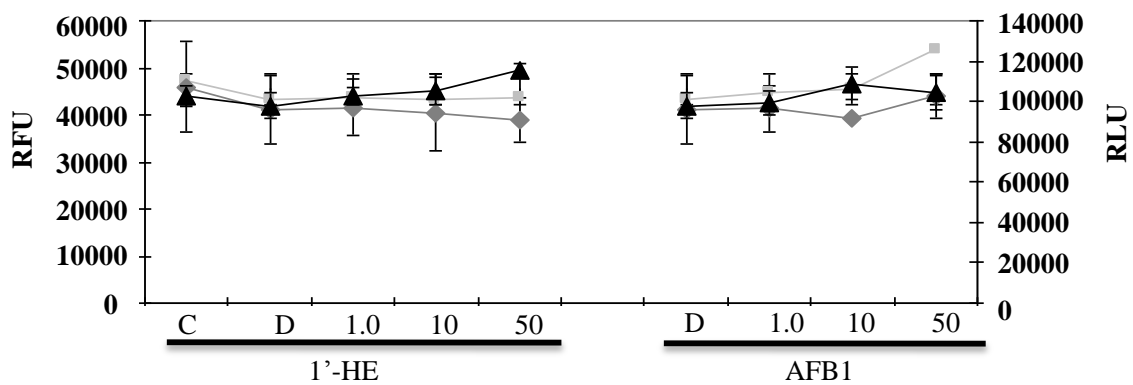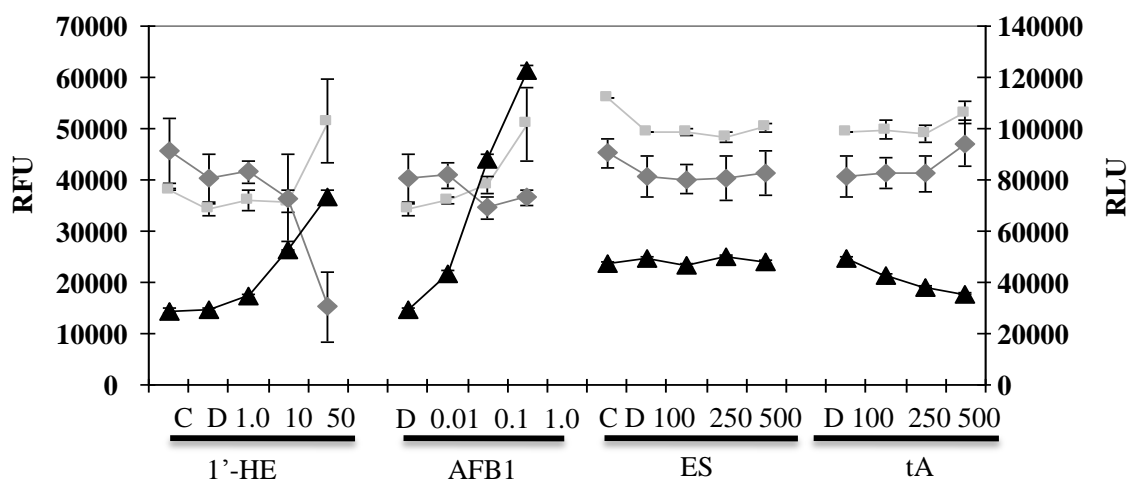
Figure 5.9. Viability (♦), cytotoxicity (■) and apoptosis (▲) as assessed by the Apo Tox-Glo[TM] Triplex Assay. Data represent the mean and Stdev of two biological replicates, based on the average of four technical replicates, from hepatocytes exposed to 1'-HE, AfB1, estragole (ES) and trans-anethole (tA) for 2 hrs (A) and 24 hrs (B). (C = control, D = DMSO control, 1'-HE'= 1'-hydroxyestragole, ES = Estragole, tA = trans-anethole, AFB1 = Aflatoxin B1).

5.4 Discussion

Estragole is a naturally occurring compound widespread in the human diet. Estragole is known to be hepatocarcinogenic at high doses in CD-1 and B6C3F1 mice (Miller *et al.,* 1983). Recent results have also indicated a potential for neoplastic transformation in rat liver (NTP, 2011; Ishii *et al.*, 2011). It is currently thought that the mechanism of estragole carcinogenicity involves primarily bioactivation into 1'-hydroxyestragole (1'-HE) leading after further metabolic transformation by sulfotransferases to the formation of 1'-sulfooxyestragole and DNA adducts. This specific pathway is expected to become relatively more important at high doses (Anthony *et al.*, 1987; Smith *et al.*, 2002). An impaired DNA adduct elimination and DNA repair may also play a role in the estragole carcinogenic process. Previous *in vivo* studies in adult rodents described a time-dependent decrease in total adducts formed in the liver exposed to a single dose of estragole. However, a residual amount of adducts was found to remain at constant level over time, suggesting incomplete DNA repair (Phillips *et al.* 1981; Randerath *et al.*, 1984). In pups, DNA adducts were found to be more persistent indicating reduced capacity of DNA repair which possibly could explain the higher susceptibility of young mice to the carcinogenic effect of estragole and 1'-HE (Phillips *et al.,* 1984). To fully understand the Mode of Action (MOA) involved in estragole carcinogenicity requires also to take into account that tumors are likely to develop only at toxic doses. In the present study primary hepatocytes from male Sprague-Dawley rats were used to evaluate the time and concentration dependent formation of DNA adducts *in vitro* after exposure to estragole or its proximate genotoxic metabolite 1'-HE. Stop-experiments were also conducted to assess the stability of the DNA adducts over time following cessation of exposure. Using a non-genotoxic (trans-anethole) and a DNA-reactive genotoxic compound (AfB1) as controls, we furthermore investigated whether the formation of DNA adducts was correlated with a specific cellular DNA damage and repair response and/or with cytotoxicity and apoptosis. Time course analysis of DNA adduct formation over 2 hrs and 24 hrs showed that at lower concentrations there was only a limited increase over time, whereas with 50 µM 1'-HE, the levels of adducts formed at 24 hrs were significantly higher than at 2 hrs although the increase was less than proportional when compared to the adducts measured at 2 hrs. This suggests that like in mature liver cells *in vivo*, a mechanism eliminating the DNA-adducts is active in the hepatocytes in culture. At low concentrations, such a mechanism is able to balance the formation of DNA adducts. At the highest concentration tested, the elimination mechanism appears to be overwhelmed resulting in the continued accumulation of DNA adducts. Further studies focusing on stability of DNA adducts, gene expression, and post-translational effects as well as on parameters for cytotoxicity were performed. Primary hepatocytes are metabolically active and efficiently metabolize estragole and 1'-HE, similar to the situation *in vivo.* Our previous experiments have established a half-life of 1'-HE in the cell culture supernatants of approximately 1 hour. After 2 hrs of exposure, a large proportion of dose is, therefore, already converted to the glucuronic acid conjugate (Chapter 2). This can contribute to the less than proportional difference in DNA adduct levels between 2 hrs and 24 hrs, because the concentration in the medium likely decreased in the first hour to lower levels. In stop-experiments, the fate of DNA adducts formed over 2 hrs as a result of treatment with 1'-HE was studied by replacing media containing 1'-HE by fresh medium free of 1'-HE. Over the initial 15 min after medium change, a rapid loss of the DNA adducts was observed reaching constant low levels after 30 min. These data confirm the presence of a mechanism of DNA-adduct elimination in the hepatocytes and are consistent with the available *in vivo* data in adult mice

(Phillips *et al.* 1981; Randerath *et al.,* 1984). Interestingly, in both *in vivo* and our *in vitro* experimental settings, after a rapid decrease in DNA adduct levels, low levels persisted over time. The mechanism of persistence is not known but results of the present study suggest that it may involve the action of translesion synthesis (TLS) polymerases. TLS is a DNA damage repair process by which a DNA lesion is bypassed by the incorporation of a nucleotide opposite to the lesion, allowing the replication on damaged DNA-substrates (Friedberg, 2005; Friedberg *et al.*, 2005; Luch, 2005; Prakash *et al.*, 2005; Waters *et al.*, 2009). TLS is known to play a role in adduct persistence. The polymerase data obtained for hepatocytes exposed to 50 µM 1'-HE suggest a potential modulation of polymerases involved in translesion synthesis, notably an increase in mRNA expression at 24 hrs of treatment. Based on the current data available, the actual biological significance of such an effect cannot be interpreted. However, a stimulation of translesion synthesis would be compatible with the hypothesis that the cells under genotoxic stress induced by 1'-HE at levels that induce significant DNA adduct formation may trigger a tolerance response to favor survival. This level of exposure may also result in DNA adduct persistence and possibly increased incidence of mutations. Results of the present study showed that AfB1 produced a similar pattern of effects on the expression of TLS polymerases. Interestingly, persistence of AfB1 DNA adducts is well documented and thought to play a role in the carcinogenicity of this mycotoxin (Croy and Wogan, 1981). To address the role of TLS polymerases in the mode of action of estragole carcinogenicity deserves further attention. As discussed above, cell treatment with high concentration of 1'-HE resulted in damage to DNA and most likely to other macromolecules such as proteins. The accumulation of damage was expected to lead to a global biological response involving the induction of multiple genes related to DNA damage and repair. To assess the validity of this hypothesis, the transcriptional expression of 84 genes involved in DNA damage and repair pathways was studied using the RT^{2}Profiler^{TM} PCR arrays for rat DNA damage signaling. The main effect of 1'-HE on gene expression was a clear down-regulation of many genes involved in DNA-repair processes. Interestingly, similar results obtained with the same PCR array were observed recently in rats administered high doses of methyleugenol (ME) (Ding *et al.*, 2011). These data suggest that exposure to 1'-HE as reported for high doses of ME is associated with suppression of DNA repair gene expression. The most striking effect identified through the application of the DNA damage array was an early (at 2 hrs of treatment) and transient induction of mRNA specific for Gadd45α. This effect was observed with all compounds, exception was trans-anethole. The biological significance of this transcriptional activation was confirmed by a concomitant induction at protein level. Gadd45α has been implicated in stress signaling in response to physiological and environmental stressors, which result in cell cycle arrest, DNA repair, cell survival and/or senescence or apoptosis. Gadd45α has been advocated as an early biomarker of genotoxicity, acting also as a cellular genotoxicity sensor (Liebermann and Hoffman, 2008; Rosemary and Richardson, 2009). In the present study, Gadd45α induction was exclusively associated with DNA-reactivity since no statistically significant induction was observed for trans-anethole which is considered to be non-genotoxic. At protein level, there was no simple correlation between DNA adduct levels and the extent of Gadd45α induction. As compared to data obtained with 50 µM 1'-HE, estragole at 500 µM produced a much smaller number of DNA adducts but a similar induction of Gadd45α. The analysis of additional biomarkers of genotoxic stress, indicated a clear, somehow delayed, DNA-damage response. At 24 hrs of treatment with either 50 µM 1'-HE or high concentration of AfB1, a significant increase in the expression of phosphorylated histone H2A.X (γ-

H2A.X) was measured. Such an effect was not observed with lower concentrations of 1'-HE suggesting a correlation with formation of significant levels of DNA adducts. The same conclusion can be drawn from the data on PARP-1. With either 50 µM 1'-HE or high concentration of AfB1, the significant release of the 89 kDa PARP-1 fragment is strongly indicative of severe DNA damage. The formation of DNA-adducts and the biological response induced by high concentrations of 1'-HE indicate the presence of severe genotoxic stress and DNA damage. This may have various consequences either favoring cell survival or triggering cell death. For example, it has been hypothesized that the extent of cellular DNA damage determines the association of Gadd45 proteins with specific partner proteins resulting into either survival or apoptosis (Lieberman and Hofmann, 2008). Data showing increased PARP-1 fragmentation support the hypothesis that at high concentrations of 1'-HE, cells do not repair and induce cell death. This is strongly confirmed by data showing that similar to high concentrations of AfB1, at 50 µM of 1'-HE, cytotoxicity and apoptosis were induced and cell viability decreased.

In conclusion, treatment of primary hepatocytes from adult rats with 1'-HE leads to the formation of DNA adducts. At low concentrations (up to 10 µM), a mechanism of adduct elimination/repair balanced the formation of adducts resulting in the establishment of a steady state low level. At such steady state low levels of adducts, no striking DNA-damage response, toxicity or apoptosis was observed indicating that the cells are able to cope with this stress and favor tolerance and repair. This may also be explained by the metabolic competence of primary hepatocytes to efficiently and quickly detoxify 1'-HE by glucuronidation, which may lead to only a short period of significant exposure to 1'-HE at the low concentrations, while at the high concentration the 1'-HE levels may remain above a critical level for a longer time resulting in longer exposure duration and higher adduct levels. At relatively higher levels of 1'-HE statistically significantly increased levels of DNA adduct formation can be detected. Interestingly, the mechanism of adduct elimination was not complete, some DNA adducts persisting even after terminating the treatment. At the 1'-HE concentration, that resulted in significant levels of DNA adducts, the elimination mechanism was overloaded resulting in a statistically significant increased number of adducts. This is likely to lead after 24 hrs to the initiation of cell death and apoptosis. The 500 µM of estragole was associated with the formation of a low number of DNA adducts shown to be insufficient to trigger a significant biological response. This is likely to be a consequence of the low metabolic rate of transformation of estragole to 1'-HE and subsequent sulfation in primary hepatocytes *in vitro* (Chapter 2), which reflects the situation reported previously (Punt *et al.*, 2008). It is concluded that the cellular repair machinery is able to cope with estragole DNA adducts to a certain level, but that formation of the adducts is not fully reversible pointing at a role for persistence of low levels of adducts in the MOA. The results also reveal that at concentration levels and exposure time duration where DNA adduct formation is strongly elevated also cytotoxicity and apoptosis occur. It is important to note that also *in vivo* studies reveal that estragole carcinogenicity is observed at doses associated with liver toxicity. The present study corroborates that both formation of DNA adducts together with a toxicity-mediated biological response may be necessary for the initiation and development of liver tumors by estragole.

Reference

Anthony A, Caldwell J, Hutt AJ, and Smith RL. (1987) Metabolism of estragole in rat and mouse and influence of dose size on excretion of the proximate carcinogen 1'-hydroxyestragole. Food Chem Toxicol 25: 799-806.

Cavin C, Delatour T, Marin-Kuan M, Holzhäuser D, Higgins L, Bezencon C, Guignard G, Junod S, Richoz-Payot J, Gremaud E, Hayes JD, Nestler S, Mantle P, and Schilter B. (2007) Reduction in antioxidant defenses may contribute to ochratoxin a toxicity and carcinogenicity. Toxicol. Sci. 96 (1): 30–39.

Croy RG and Wogan GN. (1981) Quantitative comparison of covalent aflatoxin-DNA adducts formed in rat and mouse livers and kidneys. J Natl Cancer Inst. 66(4):761-8.

Ding W, Levy DD, Bishop ME, Lascelles ELC, Kulkarni R, Chang CW, Aidoo A, Manjanatha MG. (2011) Methyleugenol Genotoxicity in the Fischer 344 rat using the Comet   Assay and Pathway-focused Gene Expression Profiling. Toxicological Sciences, 123(1):103-112.

Drinkwater NR, Miller EC, Miller JA, and Pitot HC. (1976) Hepatocarcinogenicity of estragole (1-allyl-4-methoxybenzene) and 1'-hydroxyestragole in the mouse and mutagenicity of 1'-acetoxyestragole in bacteria. J Natl Cancer Inst 57: 1323-1331.

EC-SCF. (2001) Opinion of the scientific committee on food on estragole (1-allyl-4-methoxybenzene). http://eceuropaeu/food/fs/sc/scf/out104_enpdf.

Friedberg EC. (2005) Suffering in silence: the tolerance of DNA damage. Nat Rev Mol. Cell Biol. 6: 943-953.

Friedberg, EC, Lehmann AR, Fuchs RP. (2005). Trading places: how do DNA polymerases switch during translesion DNA synthesis? Mol. Cell 18: 499-505.

Ishii Y, Suzuki Y, Hibi D, Jin M, Fukuhara K, Umemura T, Nishikawa A. (2011) Detection and quantification of specific DNA adducts by liquid chromatography-tandem mass spectrometry in the livers of rats given estragole at the carcinogenic dose. Chem Res Toxicol. 24(4): 532-41.

Liebermann DA, and Hoffman B. (2008) Gadd45 in stress signaling. J. Mol. Signal. 3:15.

Luch A. (2005) Nature and nurture - lessons from chemical carcinogenesis. Nat. Rev. Cancer 5: 113-125.

Luo G, and Guenthner TM. (1995) Metabolism of allylbenzene 2',3'-oxide and estragole 2',3'-oxide in the isolated perfused rat liver. J. Pharmacol. Exp. Ther. 272: 588-596.

Luo G, and Guenthner, TM. (1996) Covalent binding to DNA in vitro of 2',3'-oxides derived from allylbenzene analogs. Drug Metab. Dispos. 24: 1020-1027.

Luo G, Qato MK, and Guenthner TM. (1992) Hydrolysis of the 2',3'-allylic epoxides of allylbenzene, estragole, eugenol, and safrole by both microsomal and cytosolic epoxide hydrolases. Drug. Metab. Dispos. 20: 440-445.

Miller EC, Swanson AB, Phillips DH, Fletcher TL, Liem A, and Miller, JA. (1983) Structure-activity studies of the carcinogenicities in the mouse and rat of some naturally occurring and synthetic alkenylbenzene derivatives related to safrole and estragole. Cancer Res. 43: 1124-1134.

Miller JA, and Miller EC. (1983) The metabolic activation and nucleic acid adducts of naturally-occurring carcinogens: recent results with ethyl carbamate and the spice flavors safrole and estragole. Br. J. Cancer 48: 1-15.

NTP U.N.T.P. (2011) NTP Technical Report on the 3 month Toxicity Studies of Estragole - Draft peer revied Toxicity Report Series 82.

Phillips DH, Hanawalt PC, Miller JA, and Miller EC. (1981) The in vivo formation and repair of DNA adducts from 1'-hydroxysafrole. J Supramol Struct Cell Biochem 16: 83-90.

Phillips DH, Reddy MV, and Randerath K. (1984) P-32 Post-Labeling Analysis of DNA Adducts Formed in the Livers of Animals Treated with Safrole, Estragole and Other Naturally-Occurring Alkenylbenzenes .2. Newborn Male B6c3f1 Mice. Carcinogenesis 5: 1623-1628.

Prakash S, Johnson RE, and Prakash L. (2005) Eukaryotic translesion synthesis DNA polymerases: specificity of structure and function. Annu Rev Biochem 74: 317-353.

Punt A, Freidig AP, Delatour T, Scholz G, Boersma MG, Schilter B, van Bladeren PJ, and Rietjens IMCM.   (2008) A physiologically based biokinetic (PBBK) model for estragole bioactivation and detoxification in rat. Toxicology and Applied Pharmacology 231: 248-259.

Punt A, Paini A, Boersma MG, Freidig AP, Delatour T, Scholz G, Schilter B, van Bladeren, PJ, and Rietjens, IMCM. (2009) Use of Physiologically Based Biokinetic (PBBK) Modeling to Study Estragole Bioactivation and Detoxification in Humans as Compared with Male Rats.   Toxicological Sciences 110: 255-269.

Randerath K, Haglund RE, Phillips DH, and Reddy MV. (1984) P-32 Post-Labeling Analysis of DNA Adducts Formed in the Livers of Animals Treated with Safrole, Estragole and Other Naturally-Occurring Alkenylbenzenes .1. Adult Female Cd-1 Mice. Carcinogenesis 5: 1613-1622.

Rosemary SA, and Richardson DR. (2009) Growth arrest and DNA damage-45 alpha (GADD45a). Int. J. Biochem. & Cell Biol 4(1): 986-989.

Sangster SA, Caldwell J, Hutt AJ, Anthony A, and Smith RL. (1987) The metabolic disposition of [methoxy-14C]-labelled trans-anethole, estragole and p-propylanisole in human volunteers. Xenobiotica 17: 1223-1232.

Sidhu JS, Farin FM, and Omiecinski CJ. (1993) Influence of extracellular matrix overlay on Phenobarbital-mediated induction of CYP 2B1, 2B2 and 3A1 genes in primary adult rat hepatocyte culture. Arch. Biochem. Biophys. 301: 103–113.

Smith RL, Adams TB, Doull J, Feron VJ, Goodman JI, Marnett LJ, Portoghese PS, Waddell WJ, Wagner BM, Rogers AE, Caldwell J, and Sipes IG. (2002) Safety assessment of allylalkoxybenzene derivatives used as flavouring substances - methyl eugenol and estragole. Food Chem Toxicol 40: 851-870.

Solheim E, and Scheline RR. (1973) Metabolism of alkeneilbenzene derivatives in the rat. I. p-Methoxyallylbenzene (Estragole) and p-methoxypropenylbenzene (Anethole). Xenobiotica 3: 493-510.

Waters LS, Minesinger BK, Wiltrout, ME, D'Souza, S, Woodruff, RV, and Walker GC. (2009) Eukaryotic translesion polymerases and their roles and regulation in DNA damage tolerance. Microbiol Mol Biol Rev 73: 134-154.

Wiseman RW, Miller EC, Miller JA, and Liem A. (1987) Structure-activity studies of the hepatocarcinogenicities of alkenylbenzene derivatives related to estragole and safrole on administration to preweanling male C57BL/6J x C3H/HeJ F1 mice. Cancer Res 47: 2275-2283.

Yuan JS, Reed A, Chen F, and Stewart CN Jr. (2006) Statistical analysis of real-time PCR data. BMC Bioinformatics. 7:85.

Zangouras A, Caldwell J, Hutt AJ, Smith RL. (1981) Dose dependent conversion of estragole in the rat and mouse to the carcinogenic metabolite, 1'-hydroxyestragole. Biochem Pharmacol 30: 1383-1386.

Chapter 6

Based on:

Quantitative comparison between *in vivo* DNA adduct formation from exposure to selected DNA-reactive carcinogens, natural background levels of DNA adduct formation and tumor incidence in rodent bioassays

By

Paini A, Scholz G, Marin-Kuan M, Schilter B, O'Brien J, van Bladeren PJ, Rietjens, IMCM.

Abstract

This study aimed at quantitatively comparing the occurrence/formation of DNA adducts with the carcinogenicity induced by a selection of DNA-reactive, genotoxic carcinogens. Contrary to previous efforts, we used a very uniform set of data, limited to *in vivo* rat liver studies in order to investigate whether a correlation can be obtained, using a benchmark dose approach. Dose response data on both carcinogenicity and *in vivo* DNA adduct formation were available for six compounds, i.e. 2-acetylaminofluorene, aflatoxin B1, methyleugenol, safrole, 2-amino-3,8-dimethylimidazo[4,5-f]quinoxaline and tamoxifen. BMD_{10} values for liver carcinogenicity were calculated using the EPA benchmark dose software. DNA adduct levels at this dose were extrapolated assuming linearity of the DNA adduct dose response. In addition, the levels of DNA adducts at the BMD_{10} were compared to available data on endogenous background DNA damage in the target organ. Although for an individual carcinogen the tumor response increases when adduct levels increase, our results demonstrate that when comparing different carcinogens no quantitative correlation exists between the level of DNA adduct formation and carcinogenicity. These data confirm that the quantity of DNA adducts formed by a DNA-reactive compound is not a carcinogenicity predictor but that other factors such as type of adduct and mutagenic potential may be equally relevant. Moreover, comparison to background DNA damage supports the notion that the mere occurrence of DNA adducts above or below the level of endogenous DNA damage is neither correlated to development of cancer. These data strongly emphasize the need to apply the mode of action framework to understand the contribution of other biological effect markers playing a role in carcinogenicity.

6.1 Introduction

Cancer induced by exogenous as well as endogenous sources of chemicals acting through genotoxic mechanisms is a multi-step process which needs a number of critical events before the adverse effect is developed (Hanahan and Weinberg, 2000). Briefly, it involves an initiation step damaging the DNA and/or forming DNA adducts, followed by at least one round of DNA synthesis to fix the genetic damage. The promotion stage which is a reversible step is characterized by genetic instability and clonal expansion (Maley *et al.*, 2004) stimulating the induction of cell proliferation, resulting in the formation of an identifiable focal lesion. Progression, considered an irreversible process is the final step characterized by accumulation of additional genetic damage and cell proliferation. Formation of endogenously damaged DNA bases has been measured and quantified in various experimental studies. This damage has been reported to result from damage induced by oxidative stress, with reactive oxygen species being a major source for formation of damaged DNA bases (De Bont and van Larebeke, 2004). Furthermore, DNA damage may result from adduct formation by endogenous alkylating electrophiles, such as by-products resulting from lipid peroxidation (De Bont and van Larebeke, 2004). In addition to these endogenous factors, an important factor contributing to the occurrence of DNA damage can be found in exposure to exogenous DNA-reactive carcinogens. DNA adduct formation, although involved in the process of cancer formation, is generally considered a biomarker of exposure (La and Swenberg, 1996; Swenberg *et al.*, 2008; Brink *et al.*, 2009) rather than a biomarker of effect although it is also well recognized that increased levels of DNA adduct formation reflect a risk factor for cancer development. Progress has been made in understanding the mode of action (MOA) of DNA-reactive carcinogens but still not all pathways are clearly defined. The formation of DNA adducts is considered a prerequisite of cancer induction by DNA-reactive, genotoxic carcinogens, which, with or without metabolic conversion to a reactive metabolite can react with DNA to form adducts resulting in mutation and eventually carcinogenic transformation (Williams, 2001). Several attempts have been made to correlate the occurrence of DNA adducts with the carcinogenic outcome, but the significance of their formation in the risk assessment, especially with respect to the discussion and justification of possible thresholds is a matter of ongoing debate (Jarabek *et al.*, 2009; Neumann, 2009).

As reported by Boobis et al. (2009), there are several critical key events in the MOA of DNA reactive carcinogens: (i) exposure of the target cells to the ultimate reactive and mutagenic species, (ii) reaction with DNA in the target cells, (iii) misreplication or misrepair of the lesion, (iv), mutations in critical genes in replicating target cells etc. (clonal expansion, further mutations, uncontrolled growth, progression, malignancy). DNA-reactive carcinogens, directly or upon metabolic activation, can covalently bind to cellular DNA. DNA adducts occur at nucleophilic sites in the DNA strands (La and Swenberg, 1996), and this process can result in the formation of different types of adducts (La and Swenberg, 1996). DNA adduct formation can be a reversible process, since living organisms contain DNA repair mechanisms able to repair DNA damage induced by endogenous and exogenous electrophiles. These DNA repair mechanisms are supported by about 130 genes involved in different distinct repair processes (Wood *et al.*, 2001), including for example, direct repair, mismatch repair (MMR), base excision repair (BER), nucleotide excision repair (NER), and homologous recombination repair (de Laat *et al.*, 1999; Wood *et al.*, 2001; Stojic *et al.*, 2004).

If not repaired, DNA lesions can be misread by DNA polymerases, leading to heritable mutations (La and Swenberg, 1996). While DNA adducts are a biomarker of exposure (La and Swenberg, 1996; Swenberg *et al.*, 2008; Brink *et al.*, 2009), mutations are considered biomarkers of effect (Swenberg *et al.*, 2008). In an attempt to fill the gap between DNA adduct formation as a biomarker of exposure and tumor incidences as a biomarker of effect the aim of the present paper was to make a quantitative comparison between data on *in vivo* DNA adduct formation and on tumor incidences taking into account reported endogenous background levels of DNA adduct formation.

6.2 Methodology
6.2.1 Compound Selection

DNA-reactive carcinogens included in the present study were selected based on the following criteria: i) available data on *in vivo* DNA adduct formation and ii) available dose response data for tumor induction, both in the same target tissue, the liver, for the same species, the rat, and for the same gender, after oral administration (by gavage, feed or water). Data were searched using the ISI Web of Science (ISI Web of Knowledge), PubMed (PubMed), the Carcinogenic Potency Database (CPDB) (Berkeley; Gold *et al.*, 1999; Gold *et al.*, 2005) and the data base of the US National Toxicology Program (NTP).

6.2.2 Benchmark Dose Software

The tumor incidence data obtained were modeled with the BMD software version 2.1.1 developed by the US Environmental Protection Agency (EPA). The BMD methodology was developed by Crump (1984) and is based on statistically fitting a dose response model to experimental data. The advantage of applying the BMD software in analyzing tumor incidence data is that all information of the dose response curve is taken into account (EPA; Crump, 1984; Slob, 2002). The BMD level thus defined is not limited to an experimental dose level and is defined as the dose producing a defined change in response, for example 10% response, above background level defined as the Benchmark Response 10% (BMR 10%). The parameters for the computer modeling, using dichotomous models, were set as default predefined in the EPA software: 95% confidence limit, extra risk, and the BMR value set at 0.1. The BMD_{10} values were expressed as mg/kg bw/day for each mathematical model. The following dichotomous models were selected: Gamma, Logistic, Log-Logistic, Log-Probit, Multistage, Probit, Quantal-linear and Weibull. These models are each represented by a specific mathematical equation (EPA; Crump, 1984; Slob, 2002). Models were accepted or rejected based on the log-likelihood. The log-likelihood ratio test is based on the log-likelihood value associated with a fitted model compared with, and tested against, the log-likelihood value associated with the so-called "full model" (EPA; Crump, 1984; Slob, 2002). The full model simply consists of the observed (mean) responses at each applied dose (EPA; NTP). Hence, the number of parameters equals the number of dose groups. If a model fit is not significantly worse than that of the full model, then the model may be accepted (EPA; Crump, 1984; Slob, 2002). Furthermore, an extra criteria for accepting or rejecting the models was the p-value. When the p-value was greater than 0.1 the models were accepted (EPA; Crump, 1984; Slob, 2002), and only those BMD_{10} values were further used to estimate DNA adduct levels. In the case that several models

provide an adequate fit to a given data set, the goodness-of-fit was further evaluated on the basis of the Akaike Information Criterion (AIC) value. The AIC is a deviant of the log-likelihood and penalizes a model for having too many parameters (i.e. degrees of freedom), thus allowing to compare the goodness-of-fit between different models. Lower AIC values indicate a better fit within a dataset (EPA; Crump, 1984; Slob, 2002).

6.2.3 Aspects related to ^{32}P-Postlabeling

In order to use data set as uniform as possible experimental studies using similar analytical methods for detection and quantification were applied. For four carcinogens, data on total DNA adduct levels were available generated using ^{32}P-postlabeling followed by TLC separation; for ME the separation step was not specified. The types of adduct(s) formed were in most cases not characterized. ^{32}P-postlabeling is a highly sensitive method which needs only small amounts of DNA (Randerath *et al.*, 1981; Himmelstein *et al.*, 2009) and it has been the most widely used method for the detection of DNA adducts. However a limitation of the ^{32}P-postlabeling method is the potential for underestimation of the adduct levels due to incomplete DNA digestion, submaximal efficiency of adduct labeling by polynucleotide kinase and/or loss of adducts during enrichment and chromatography stages (Phillips and Arlt, 2007). For AfB1, available data were generated using ^{3}H-HPLC, the N-7 guanine is the predominant adduct formed by AfB1, which is poorly labeled by ^{32}P-postlabeling technique (Phillips and Arlt, 2007).

6.2.4 Dose adjustment for cancer bioassays

In order to correct the doses and the duration of treatment to the standard lifespan (2 years or 104 weeks by convention), we followed the recommendations of Peto et al. (1984) and Gold et al. (1984). Two principal situations of dose adjustments exist: in the first situation, administration of the test compound is discontinued before the terminal sacrifice after completion of the full duration of 2 years. In this case the dose is adjusted by multiplying with f=(period of active treatment)/(actual time on test i.e. 104 wk). This was the case for the highest dose group in the ME study, which was stopped after 53 weeks due to toxic side effects and continued to 104 weeks without treatment (26). This dose was, therefore, adjusted for f=(53/104). In the second principal situation both the treatment and the study are terminated before completion of the standard lifespan, e.g after 52 weeks. In this case the f^2 correction factor is used where f=(experiment time)/(standard lifespan). This was the case for the AfB1 study, where all except the lowest dose groups were terminated 'prematurely' between 54 and 93 weeks due to mortality (Peto *et al.*, 1984; Benford *et al.*, 2010). For the 'mixed' situation, where the study is terminated before completion of the 104 weeks, and treatment is even shorter, the adjustment was done by correcting for [(period of active treatment)/(standard lifespan)]×[(experiment time)/(standard lifespan)]. Thus in cases where treatment time equals study duration this corresponds exactly to the f^2 approach. When dosing was done during only 5 days of the week, as was the case for methyleugenol, the dose was corrected for f=5/7.

6.3 Results

6.3.1 Compound Selection

DNA-reactive carcinogens in the present study were selected based on i) available data on *in vivo* DNA adduct formation and ii) available dose response data for tumor induction, both in the same target tissue, the liver, for the same species, the rat, and for the same gender. *In vivo* DNA adduct formation data were available for a large number of carcinogens. However, the number of *in vivo* studies on tumor formation in the same species, sex and target tissue for which data also on *in vivo* DNA adduct formation were available, were limited. Only six DNA-reactive carcinogens were identified for which data on both tumor incidence and *in vivo* DNA adduct formation in rat liver were available. The compounds selected were: 2-acetylaminofluorene (2-AAF) (CAS # 53-96-3); aflatoxin B1 (AfB1) (CAS # 1162-65-8); methyleugenol (ME) (CAS # 93-15-2); safrole (SA) (CAS # 94-59-7); 2-amino-3,8-methylimidazo[4,5-f]quinoxaline (MeIQx) (CAS # 77500-04-0) and tamoxifen (TAM) (CAS # 54965-24-1). Even though the compounds were selected as to obtain relatively uniform dataset regarding target tissue, species and gender, important variations were observed in the available information with respect to study design, such as duration (5 days up to 18 months), dosing (water, diet, gavage), group size (≥2) and analytical methods employed. This is especially relevant concerning the DNA adduct data, for which (in contrast to e.g., a 2 years cancer bioassay), no guideline study protocols exist.

6.3.2 Data on *in vivo* DNA adduct formation

Table 6.1 recapitulates the data collected for the dose dependent *in vivo* DNA adduct formation of the selected DNA-reactive carcinogens (2-AAF, AfB1, ME, SA, MeIQx, and TAM) focusing on liver as the target organ. All data sets collected for the individual carcinogens were from rats, with the data for five of the six carcinogens being obtained in male rat liver whereas those for TAM were obtained in female rat liver. Table 6.1 presents information on the data collected including information on dose in mg/kg bw/day, exposure route and duration, amount of DNA adducts formed, type of adduct detected, method of analysis, species and gender. Exposure duration, dose ranges applied and mode of administration appear to vary between the studies available for the different model compounds. For instance, study duration varies from as short as 5 days (SA) up to 18 months of exposure (TAM). Due to the paucity of available data on formation kinetics, DNA adduct levels were assumed to have reached near steady state and were used as such without any normalization or adjustments. Therefore, data from the longest available treatment duration were used. For SA the longest available treatment duration was 5 days and this may be borderline to our selection criteria. The steady-state level of DNA adducts are a function of dose and adduct produced in a cell, modulated by processes linked to drug-metabolizing enzymes that activate or detoxify the genotoxic compound. Furthermore steady state levels are influenced by the type of DNA adduct and the DNA adduct half-life (Walker *et al.*, 1992). However, using an unpublished physiologically based kinetic (PBK) model for safrole (Martati *et al.*), which is based on a published PBK model for the related alkenylbenzene estragole (Punt *et al.*, 2008; Punt *et al.*, 2009), it can be estimated that at the dose levels used for DNA adduct analysis by Daimon et al. (1998) of 62.5, 125 and 250 mg/kg bw, full conversion of safrole will be obtained in 60, 62, and 70 hrs respectively.

Furthermore Miller and Miller (1992) reported that the metabolite 1´-sulfooxysafrole has a half-life of 1 min and quickly binds to DNA. Therefore we conclude that the biological responses towards safrole may be rapid and may result in a steady state in DNA adduct levels in a relatively short period of time.

Table 6.1. Published DNA adduct data, including dose, exposure route, exposure duration, number of adducts detected in the liver, adduct type, method of detection, species and gender.

Compound	Daily dose (mg kg^{-1} d^{-1})	Exposure Route	Exposure duration	Number of adducts/10^{8}nt	Adduct type	Method	Species/Sex	Reference
2-AAF	0-0.0011-0.011-0.333$^{\$\$}$	Gavage	12 w*16w	4-9-40-8000	Total adducts	^{32}P-postlab-TLC	Rat/M	(Williams et al., 2004)
AfB1	2.2*10^{-6}-73*10^{-6}-2110*10^{-6}	Water	8 w	0.091-3.2-85	aflatoxin- DNA adducts	^{3}H/HPLC	Rat/M	(Buss et al., 1990)
ME	1-5-1950	Diet	28 d	0(ND)-1-50	Total adduct	^{32}P-postlab	Rat/M	(Ellis et al., 2006)
SA	0-1-10-100-250-500	Gavage	1d	7-9-36-163-303-720	Total adduct	^{32}P-postlab-TLC	Rat/M	(Daimon et al., 1998)
	0-62.5-125-250	Gavage	5 d	27-430-673-898	Total adduct	^{32}P-postlab-TLC	Rat/M	(Daimon et al., 1998)
MeIQx	0.0013-0.013-0.134-1.26$^{\$}$	Diet	1 w	0.399-2.81-33.6-390	Total adduct	^{32}P-postlab-TLC	Rat/M	(Yamashita et al., 1990)
	0.0023-0.023-0.235-2.2$^{£}$	Diet	12 w	1-10-100-1000	Total adduct	^{32}P-postlab-TLC	Rat/M	(Yamashita et al., 1990)
TAM1	0-20-40$^{££}$	Diet	18m	0-300-610	Total adduct	^{32}P-postlab-TLC	Rat/F	(Li et al., 1997)
TAM2	4-20-40$^{££}$	Diet	8w	225-1050-2000$^{\$}$	Total adduct	^{32}P-postlab- TLC	Rat/F	(Schild et al., 2005)

ND: not detected (<1/10^8 nt); M=male, F=female, d=days, w=weeks, m=months. $^{\$\$}$ converted from cumulative doses $^{\$}$ converted from total daily doses assuming a bw of 200g £ converted from total daily doses assuming a bw of 350g ££ converted from 50-250-500 ppm TAM in feed using 0.02 kg daily intake and 0.25 kg bw. $^{\$}$ estimated from a graph.

To allow comparison table 6.1 presents all data on adduct formation expressed as number of adducts in 10^8 nucleotides (nt). A graphical representation of the dose-response curves is shown in Figure 6.1 that appears to fit linear dose responses in accordance with the current scientific view on low dose linearity (Swenberg *et al.*, 2008; Neumann, 2009) (Figure 6.1). Therefore, and due to the lack of data points to perform a statistical curve fit with sufficient confidence, no non-linear curve fit was applied to the DNA adduct dose response data. Instead, linear regression through the origin was applied to all data sets without any transformation. The linear regression gave satisfactory results for all six compounds (p<0.005) based on the residual plot and the p-value from the run test (p>0.5). The data obtained allow comparison of the relative potency of the six DNA-reactive carcinogens to form DNA adducts. To allow such comparison normalization for dose was applied by calculating for all six compounds the expected levels of DNA adduct formation at a dose of 1 mg/kg bw/day using the dose response data plotted in Figure 6.1. These results in the following decreasing order for DNA adduct formation at a dose of 1 mg/kg bw/day: AfB1 (40480 adducts / 10^8 nt) > 2-AAF (24002 adducts / 10^8 nt) > MeIQx (159 adducts / 10^8 nt) > TAM (59 and 15 adducts / 10^8 nt, respectively) (Li *et al.*, 1997; Schild *et al.*, 2005)> SA (4 adducts / 10^8 nt) > ME (1 adducts / 10^8 nt). Assuming that the level of DNA adduct formation will increase over time in a linear way, with the number of adducts formed each day being equal to the number formed minus the number that are lost or repaired (Swenberg *et al.*, 2008), one could further normalize the data to a one day exposure, in order to be able to compare the relative potency between compounds. The values obtained above for the total number of adducts/10^8 nt at a dose of 1 mg/kg bw/day were thus converted to numbers of adducts/10^8 nt per day by dividing the total numbers by the exposure duration; resulting in the following decreasing potency order: AfB1 (723 adducts / 10^8 nt / day) > 2-AAF (214

adducts / 10^8 nt / day) > MeIQx (1.89 adducts / 10^8 nt / day) > TAM (1 adducts / 10^8 nt/day) (Schild *et al.*, 2005) > SA (0.82 adducts / 10^8 nt / day) >ME (0.035 adducts / 10^8 nt / day) > TAM (0.03 adducts / 10^8 nt / day) (Li *et al.*, 1997). Together these data point at a different potency for each individual compound to result in DNA adduct formation, with AfB1 and 2-AAF being at least 2 to 3 orders of magnitude more effective in forming DNA adducts than MeIQx and SA, and even 4 orders of magnitude more effective than ME and TAM. It should be noted that rats treated with TAM in the study by Li *et al.* (1997) had undergone partial hepatectomy before treatment, which, by inducing liver proliferation, may have influenced the levels of DNA adduct formation.
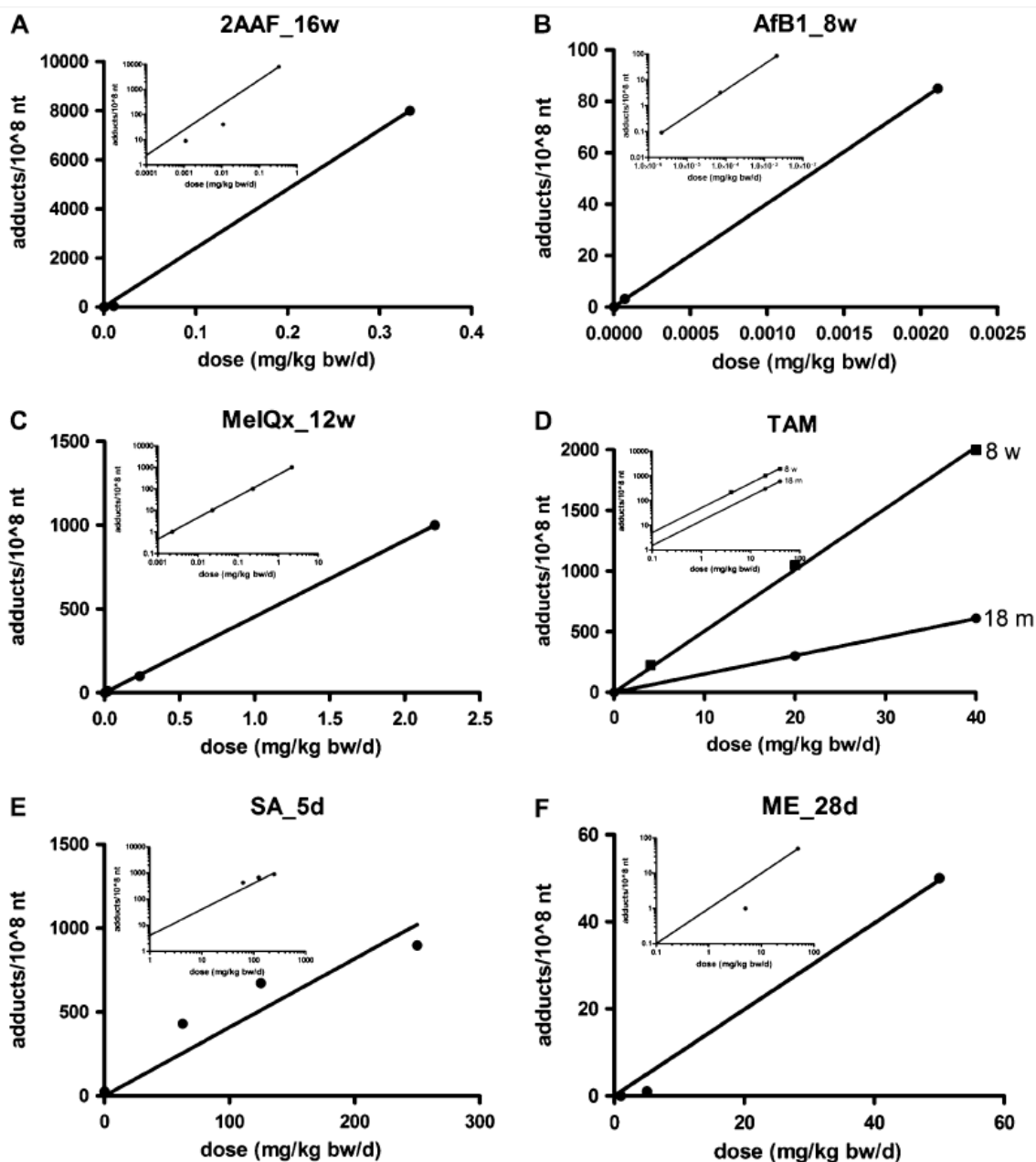
Figure 6.1. Dose dependent DNA adduct formation (number of adducts in 10^8 nt), in the liver as obtained from *in vivo* studies in male rats treated with: A) 2-AAF, B) AfB1, C) MeIQx, E) SA, and F) ME, and in female rats treated with D) TAM(Li *et al.*, 1997; Schild *et al.*, 2005). For all six DNA-reactive carcinogens linearity was assumed resulting in the following slope ((#adduct 10^8 nt)/(mg/kg bw/day)) factors: 2-AAF) m=24002; AfB1) m=40480; ME) m=0.9917; SA) m=4.0899; MeIQx) m=454.22; TAM) m=18.24; TAM) m=54.45. Inserts are log-log plots of doses and DNA adduct levels.

6.3.3 Tumor incidence data and BMD$_{10}$ calculation

To allow quantitative comparison of dose levels causing DNA adduct formation and dose levels causing a significant increase above background levels in tumor incidence, data from long term studies on tumor incidence induced by the selected set of model DNA-reactive carcinogens in rodent species were collected from the literature. Table 6.2 presents an overview of *in vivo* hepatic tumor incidence data obtained in rats as reported in the literature. Available tumor incidence data from carcinogenicity studies of the six DNA-reactive compounds (2-AAF, AfB1, ME, SA, MeIQx, and TAM) are presented including information on dose, exposure route and duration, liver tumor incidence, type of tumor lesion, and species/gender (Table 6.2).

Table 6.2. Published tumor incidence data, including dose, exposure route, exposure duration (w=weeks, m=months), the dose adjusted to 2 years of duration and exposure, tumor incidences in the liver, type of lesion), species and gender.

Compound	Dose (mg kg-1 d-1)	Exposure Route	Exposure Duration (weeks)	Time adjusted dose (mg kg^{-1} d^{-1})*	Liver Tumor incidence	Type of lesion in the liver	Species/ gender	Reference
2-AAF	0-0.32-1.6-8	Diet	104	0-0.32-1.6-8	0/30-3/29-26/28-23/23	hpc	Rat/M	(Ogiso et al., 1985)
AfB1	0-0.001-0.005-0.015-0.05-0.1	Diet	104-104-93-96-82-54	0-0.00004-0.00016-0.00051-0.00124-0.00108**	0/18-2/22-1/22-4/21-20/25-28/28	hpc	Rat/M	(Wogan et al., 1974)
ME	0-37-75-150-300	Gavage	104-104-104-104-53	0-26.4-53.6-107.1-101.85**	2/50-3/50-14/50-25/50-36/50	hpc	Rat/M	(Johnson et al., 2000)
SA	0-4-20-40-200	Diet	104	0-4-20-40-200	3/25-1/25-2/25-2/25-7/25	tum	Rat/M	(Long et al., 1963)
MeIQx	0-4-8-16	Diet	56	0-1.16-2.32-4.64	0/15-0/30-13/29-15/16	hpc	Rat/M	(Kushida et al., 1994)
TAM	0-5-20-35	Gavage	104-104-87-71	0-5-14-16.31	0/104-6/52-37/52-37/52	hpc	Rat/F	(Greaves et al., 1993)
TAM	0-11.3-22.6	Gavage	52	0-2.83-5.65	0/18-16/36-24/24	hpc	Rat/F	(Hard et al., 1993)

F = female and M= male, hpa: hepatocellular adenoma; hpc: hepatocellular carcinomas; tum: different liver tumor, w=weeks, m=months. * For each individual data set the dose was adjusted to the time of treatment (Benford *et al.*, 2010), to the duration of the *in vivo* study, and to the lifespan of rats of 104 w (for further explanations see text). ** Highest dose was not used when performing the BMD analysis.

Exposure to the compounds was via the diet with the exception of ME and TAM, which were dosed by gavage. In order to use datasets as uniform as possible, exclusively the development of hepatocellular carcinoma (hpc) was taken into consideration, since this endpoint was separately available for all compounds. Time of treatment was one year for MeIQx and longer than one year for the remaining carcinogens. All data sets collected were for male rats with the exception of TAM for which only female rat data were available. In a next step all data were modeled using the BMD software. The BMD$_{10}$ values thus obtained for the six selected DNA-reactive carcinogens, expressed in mg/kg bw/day, are reported in table 6.3. Each compound resulted in up to nine valid BMD$_{10}$ values, because of the number of models (9) used to calculate the BMD$_{10}$ (Table 6.3). The BMDL$_{10}$ values were also calculated but only the BMD$_{10}$ were used for further comparison; p-value, log likelihood and AIC are reported in table 6.3. Results obtained showed a large variation in the BMD$_{10}$ values for the six model DNA reactive carcinogens. For instance the upper value

of the BMD_{10} for AfB1 for male rats amounted to 0.00033 mg/kg bw/day. On the other hand, the highest BMD_{10} was found for male rats treated with SA and amounted to 169.1 mg/kg bw/day. The results from the BMD_{10} analysis show an increasing trend in the BMD_{10} value in the order AfB1 < 2-AAF < MeIQx < TAM < ME < SA. This order is identical to the order obtained on the basis of the carcinogenic potency estimates expressed as the TD_{50} that can be found in the Carcinogenic Potency Database (Berkeley). The TD_{50} is defined as the chronic dose rate (in mg/kg bw/day) which would halve the percentage of tumor-free animals at the end of a standard lifespan experiment time for the species (Peto *et al.*, 1984), or, simplified, represents the daily dose inducing tumors in half of the test animals (above background incidence). Based on the TD_{50} values the order in the carcinogenic potency of the six model carcinogens of the present study was AfB1 (0.0032 mg/kg bw/day) > 2-AAF (1.22 mg/kg bw/day) > MeIQx (1.66 mg/kg bw/day) > TAM (3.96 mg/kg bw/day) > ME (19.7 mg/kg bw/day) > SA (441 mg/kg bw/day) and thus similar to the order defined on the basis of the BMD_{10} approach in the present study, which is not surprising since dose response modeling and adjustments for exposure and experimental duration are also employed to derive the TD_{50} values in the CPDB (Gold *et al.*, 1984; Peto *et al.*, 1984). It can also be noted that this order of potencies is roughly similar to the order derived for their potency in inducing DNA adduct formation.

Table 6.3. Name of compound, sex, species, reference, p-Values, log-likelihood, Akaike's Information Criterion (AIC), degrees of freedom (d.f.), and BMD_{10} obtained with the different models using the EPA Benchmark dose software version 2.1.1 for the DNA-reactive compounds selected, and the extrapolated amount of DNA adducts formed for each individual BMD_{10} based on the regressions in Figure 6.1. The BMD_{10} are expressed as mg/kg bw.

2-Acetylaminofluorene (2-AAF), male rat (Ogiso *et al.*, 1985; Williams *et al.*, 2004).

Model	p-value	Log likelihood	AIC	d.f	BMD_{10}	number adducts in 10^8 nt
Full		-16.85				
Reduced		-76.08		3		
Gamma	1	-16.85	37.70	2	0.32	7561
Logistic	0.60	-17.67	39.34	2	0.45	10729
Log-Logistic	0.99	-16.86	37.73	2	0.32	7585
Log-Probit	0.999	-16.85	37.70	2	0.32	7585
Multistage	1	-16.85	37.70	2	0.31	7537
Multistage Cancer	1	-16.85	37.70	2	0.31	7537
Weibull	1	-16.85	37.70	2	0.31	7537
Probit	0.68	-17.45	38.90	2	0.41	9937
Quantal linear	0.067	-21.22	44.44	3		

Aflatoxin B1 (AfB1), male rat (Wogan *et al.*, 1974; Buss *et al.*, 1990).

Model	p-value	Log likelihood	AIC	d.f	BMD_{10}	number adducts in 10^8 nt
Full		-33.51				
Reduced		-63.98		4		
Gamma	0.25	-35.28	76.57	2	0.00043	17.56
Logistic	0.41	-35.15	74.31	3	0.00039	15.75
Log-Logistic	0.25	-35.28	76.56	3	0.00043	17.67
Log-Probit	0.41	-34.75	75.49	2	0.00045	18.37
Multistage	0.30	-35.49	74.98	3	0.00033	13.49
Multistage Cancer	0.30	-35.49	74.98	3	0.00033	13.49
Weibull	0.24	-35.27	76.55	2	0.00042	16.84
Probit	0.35	-35.19	74.37	3	0.00035	14.17
Quantal linear	0.085	-37.76	77.51	4		

Table 6.3.Continued. Name of compound, sex, species, reference, p-Values, log-likelihood, Akaike's Information Criterion (AIC), degrees of freedom (d.f.), and BMD_{10} obtained with the different models using the EPA Benchmark dose software version 2.1.1 for the DNA-reactive compounds selected, and the extrapolated amount of DNA adducts formed for each individual BMD_{10} based on the regressions in Figure 6.1. The BMD_{10} are expressed as mg/kg bw.

2-amino-3,8-dimethylimidazo[4,5-*f*]quinoxaline (MeIQx), male rat
(Yamashita *et al.*, 1990; Kushida *et al.*, 1994).

Model	p-value	Log likelihood	AIC	d.f	BMD_{10}	number adducts in 10^8 nt
Full		-23.69				
Reduced		-55.79		3		
Gamma	0.42	-24.79	53.59	2	1.59	721.6
Logistic	0.06	-26.44	56.87	2		
Log-Logistic	0.57	-24.44	52.87	2	1.65	748.7
Log-Probit	0.65	-24.27	52.54	2	1.62	736.2
Multistage	0.17	-28.04	58.07	3	1.04	473.7
Multistage Cancer	0.17	-28.04	58.07	3	1.04	473.7
Weibull	0.19	-26.09	56.17	2	1.44	651.9
Probit	0.09	-26.45	56.91	2		
Quantal linear	0.0019	-35.40	72.81	3		

Methyleugenol (ME), male rat (Johnson *et al.*, 2000; Ellis *et al.*, 2006).

Model	p-value	Log likelihood	AIC	d.f	BMD_{10}	number adducts in 10^8 nt
Full		-84.01				
Reduced		-106.63		3		
Gamma	0.24	-84.72	175.43	1	35.39	35.10
Logistic	0.21	-85.58	175.14	2	40.10	39.76
Log-Logistic	0.27	-84.65	175.30	1	35.16	34.87
Log-Probit	0.36	-84.44	174.87	1	35.84	35.54
Multistage	0.16	-84.99	175.98	1	35.70	35.41
Multistage Cancer	0.16	-84.99	175.98	1	35.70	35.41
Weibull	0.18	-84.97	175.94	1	34.20	33.92
Probit	0.27	-85.31	174.62	2	37.19	36.88
Quantal linear	0.09	-86.80	177.60	2		

Safrole (SA), male rat (Long *et al.*, 1963; Daimon *et al.*, 1998).

Model	p-value	Log likelihood	AIC	d.f	BMD_{10}	number adducts in 10^8 nt
Full		-42.13				
Reduced		-45.86		4		
Gamma	0.58	-42.70	91.40	2	158.80	649.5
Logistic	0.71	-42.79	89.58	3	117.31	479.8
Log-Logistic	0.58	-44.70	95.40	2	167.94	686.8
Log-Probit	0.58	-42.70	91.40	2	153.51	627.8
Multistage	0.77	-42.71	89.42	3	130.69	534.5
Multistage Cancer	0.77	-42.71	89.42	3	130.69	534.5
Weibull	0.58	-42.70	91.40	2	169.11	691.6
Probit	0.70	-42.81	89.62	3	112.66	460.8
Quantal linear	0.62	-42.97	89.94	3	91.20	372.9

Tamoxifen (TAM), female rat (Greaves *et al.*, 1993; Li *et al.*, 1997).

Model	p-value	Log likelihood	AIC	d.f	BMD_{10}	number adducts in 10^8 nt
Full		-81.07				
Reduced		-160.48		3		
Gamma	0.55	-81.67	167.35	2	4.56	69.31
Logistic	0.055	-84.77	173.45	2		
Log-Logistic	0.65	-81.57	167.02	2	4.60	69.92
Log-Probit	0.65	-81.50	167.01	2	4.66	70.83
Multistage	0.67	-81.86	165.72	2	4.44	67.49
Multistage Cancer	0.67	-81.86	165.72	2	4.44	67.49
Weibull	0.46	-81.86	167.72	2	4.39	66.73
Probit	0.10	-83.83	171.66	2	4.56	69.31
Quantal linear	0.018	-86.87	175.74	3		

Table 6.3.Continued. Name of compound, sex, species, reference, p-Values, log-likelihood, Akaike's Information Criterion (AIC), degrees of freedom (d.f.), and BMD_{10} obtained with the different models using the EPA Benchmark dose software version 2.1.1 for the DNA-reactive compounds selected, and the extrapolated amount of DNA adducts formed for each individual BMD_{10} based on the regressions in Figure 6.1. The BMD_{10} are expressed as mg/kg bw.

Tamoxifen (TAM), female rat (Hard *et al.*, 1993; Li *et al.*, 1997).

Model	p-value	Log likelihood	AIC	d.f	BMD_{10}	number adducts in 10^8 nt
Full		-24.73				
Reduced		-54.04		2		
Gamma	0.99	-24.76	51.51	2	2.12	32.22
Logistic	0.99	-24.73	53.46	2	2.54	38.61
Log-Logistic	0.99	-24.73	51.46	2	2.54	38.61
Log-Probit	0.99	-35.70	53.46	1	2.47	37.54
Multistage	0.33	-26.47	54.93	2	1.07	16.26
Multistage Cancer	0.33	-26.47	54.93	2	1.07	16.26
Weibull	0.99	-24.73	53.46	1	1.98	30.10
Probit	0.99	-24.73	53.46	1	2.27	34.50
Quantal linear	0.002	-54.04	63.39	2		

Tamoxifen (TAM), female rat (Greaves *et al.*, 1993; Schild *et al.*, 2005).

Model	p-value	Log likelihood	AIC	d.f	BMD_{10}	number adducts in 10^8 nt
Full		-81.07				
Reduced		-160.48		3		
Gamma	0.55	-81.67	167.35	2	4.56	230.5
Logistic	0.055	-84.77	173.45	2		
Log-Logistic	0.65	-81.57	167.02	2	4.60	232.5
Log-Probit	0.65	-81.50	167.01	2	4.66	235.5
Multistage	0.67	-81.86	165.72	2	4.44	224.4
Multistage Cancer	0.67	-81.86	165.72	2	4.44	224.4
Weibull	0.46	-81.86	167.72	2	4.39	221.5
Probit	0.10	-83.83	171.66	2	4.56	
Quantal linear	0.018	-86.87	175.74	3		

Tamoxifen (TAM), female rat (Hard *et al.*, 1993; Schild *et al.*, 2005).

Model	p-value	Log likelihood	AIC	d.f	BMD_{10}	number adducts in 10^8 nt
Full		-24.73				
Reduced		-54.04		2		
Gamma	0.99	-24.76	51.51	2	2.12	107.1
Logistic	0.99	-2473	53.46	2	2.54	128.4
Log-Logistic	0.99	-2473	51.46	2	2.54	125.4
Log-Probit	0.99	-35.70	53.46	1	2.47	124.8
Multistage	0.33	-26.47	54.93	2	1.07	54.08
Multistage Cancer	0.33	-26.47	54.93	2	1.07	54.08
Weibull	0.99	-24.73	53.46	1	1.98	100.1
Probit	0.99	-24.73	53.46	1	2.27	114.7
Quantal linear	0.002	-54.04	63.39	2		

6.3.4 Comparison of the BMD$_{10}$ data for cancer incidence to the data on *in vivo* DNA adduct formation

The quantitative BMD$_{10}$ values defined from the tumor incidence data were compared to the dose response curves for DNA adduct formation. To illustrate this comparison Figure 6.2 presents the dose response curves for DNA adduct formation already presented in Figure 6.1, but now including the range of accepted BMD$_{10}$ values obtained for each carcinogen focusing on the same gender for which the DNA adduct levels were reported. The results obtained reveal that generally the BMD$_{10}$ values (Figure 6.2, dashed lines) fall within the *in vivo* experimental dose ranges enabling detection of DNA adduct formation. This also allowed the calculation of the number of DNA adducts expected to occur at each BMD$_{10}$, using the linear extrapolation curves for the *in vivo* data for DNA adduct formation and these values are reported in table 6.3. The different data sets resulted in different models exhibiting the best fit (Table 6.3). Therefore, none of the models was appropriate to model all datasets.
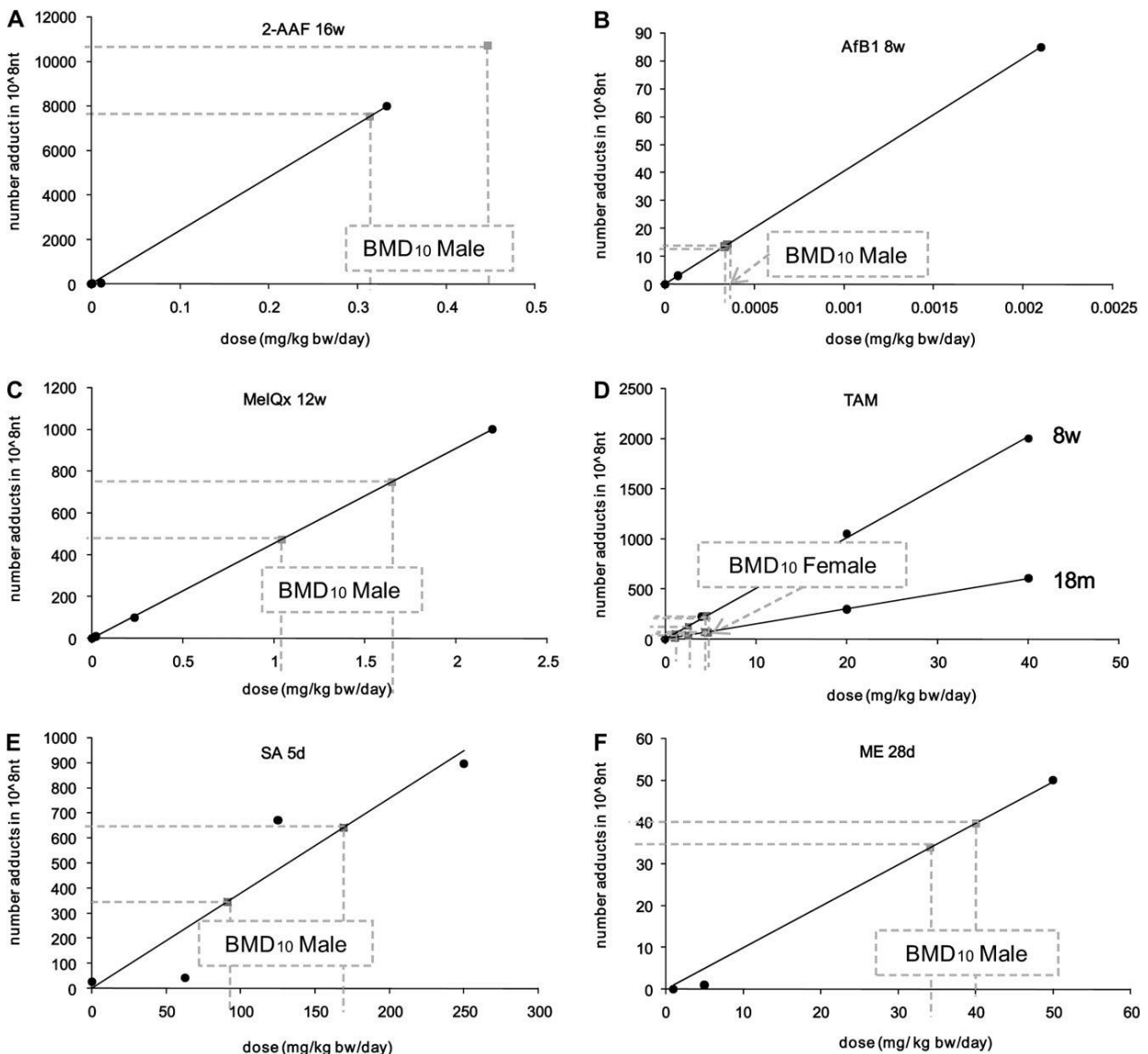

Figure 6.2. Illustration of the dose response curves for DNA adduct formation with the range of accepted BMD10 values (dashed lines) derived from in vivo data on liver tumor incidence, representing the data for male rats treated with: A) 2-AAF, B) AfB1, C) MeIQx, E) SA, F) ME, and female rats treated with D) TAM (Li *et al.*, 1997; Schild *et al.*, 2005).

In order to avoid averaging across the different BMD_{10} values obtained with the different models (as suggested in (Benford *et al.*, 2010), based on (Wheeler and Bailer, 2007)), accepted BMD_{10} values were computed and used individually in order to extrapolate DNA adduct levels, and for visualization in Figure 6.3. This approach also provided a good visual indication of values obtained using the BMD software. It can be concluded that at BMD_{10} levels for tumor induction significant levels of DNA adduct formation can be detected for all six DNA-reactive carcinogens. The highest amount of DNA adducts formed at the BMD_{10} was found for male rats exposed to 2-AAF followed by male rats exposed to MeIQx > male rats exposed to SA > male rats exposed to AfB1 > male rats exposed to ME. The amount of DNA adducts formed at the BMD_{10} for female rats exposed to TAM was comparable to the level found for ME in male rats.

The results also show that the number of adducts covers a range of 20-11000 adducts in 10^8 nt at the dose levels causing 10% increase in tumor incidence above background levels. i.e. less than 3 orders of magnitude, while the carcinogenic potencies (based on TD_{50}) covers more than 5 orders of magnitude. The data also lead to the conclusion that for all six DNA-reactive carcinogens, the actual level of DNA adducts formed at the BMD_{10}, do not vary by more than about three orders of magnitude. This may be related to the fact that genotoxic electrophiles can react at different sites within the DNA, resulting in the formation of different types of adducts. Together these results quantitatively support the conclusions that all individual DNA-reactive selected compounds 2-AAF, AfB1, MeIQx, TAM, SA, and ME give rise to DNA adducts with a 10-100 fold different potential to result in mutations and ultimately cancer.

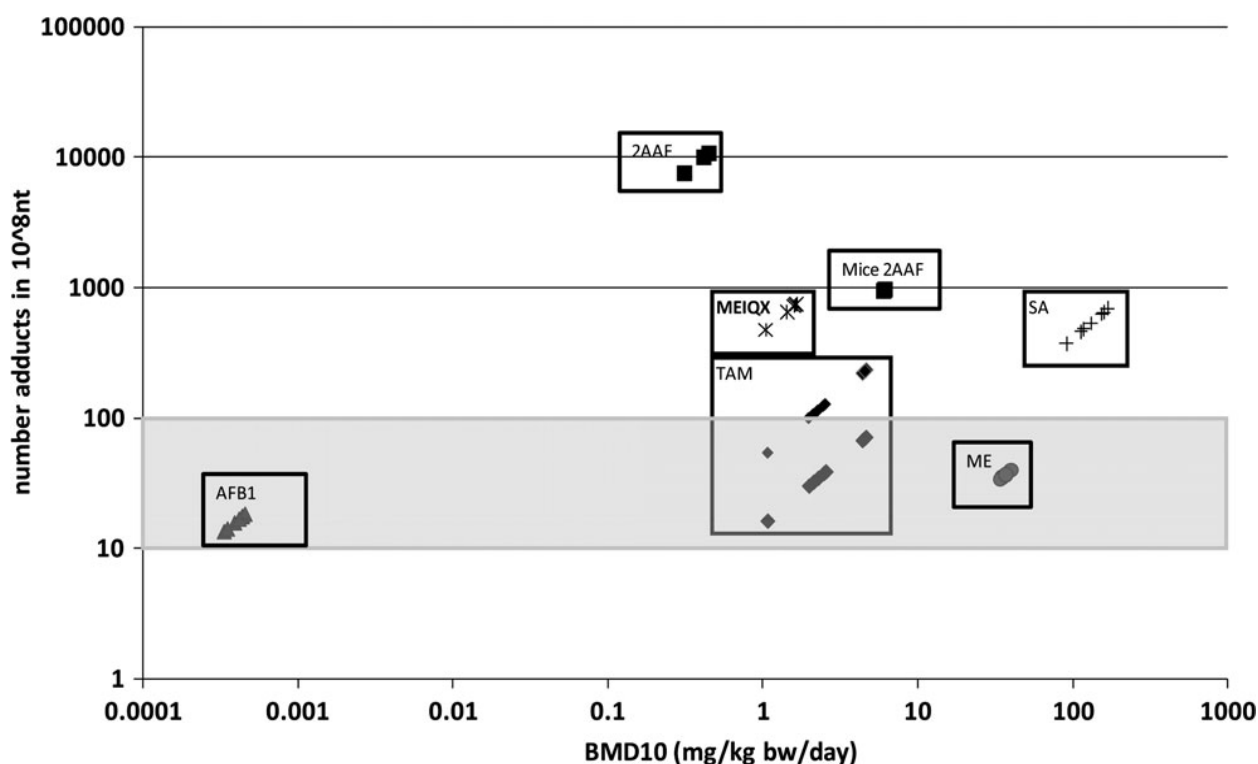Figure 6.3. Levels of DNA adduct formation at the BMD10 for liver tumor formation by the six model compounds as related to endogenous DNA adduct levels (10 to 100 adducts in 10^8 nt, gray shadow) in liver. The individual data points represent the outcome of each individual mathematical model for male rats treated with: 2-AAF, AfB1, MeIQx, SA, ME, and female rats treated with TAM, and male mice treated with 2-AAF.

6.3.5 Species differences in 2-AAF DNA adduct formation

Figure 6.4 presents the dose dependent DNA adduct formation measured in liver of mice chronically exposed to 2-AAF (Poirier *et al.*, 1991). In addition, literature data on tumor formation in the liver of mice dosed with 2AAF (Staffa and Mehlman, 1979) were used to determine the BMD_{10} value (Figure 6.4). For both studies the feed concentrations in ppm were converted to the following dose range: 0, 0.65, 1.3, 1.95, 3.9, 5.85, 7.8, 9.75, 13 and 19.5 mg/kg bw/day.
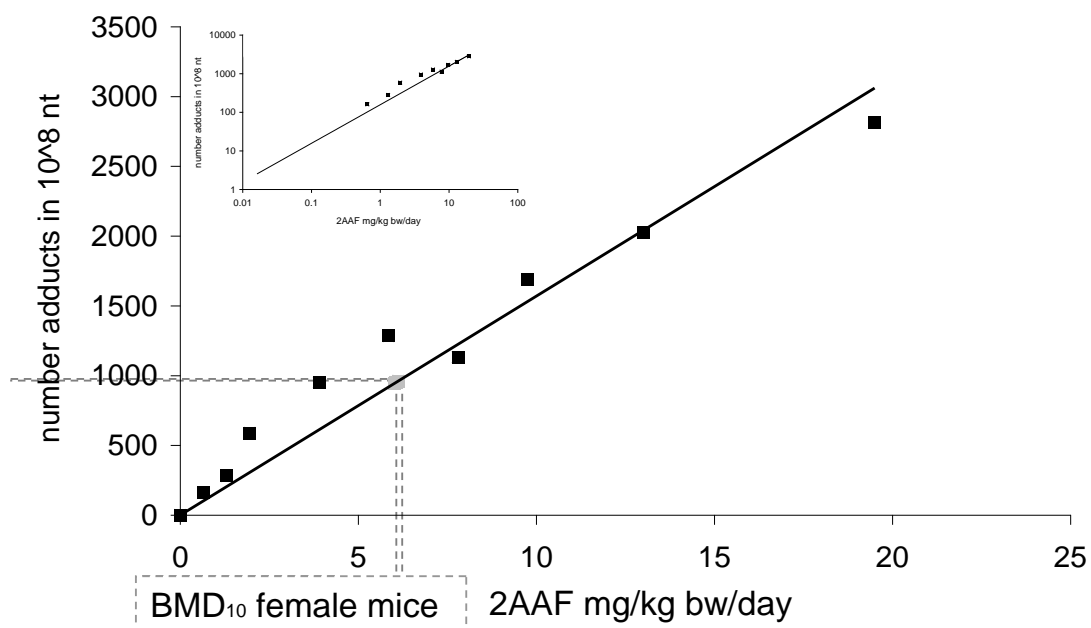

Figure 6.4. Dose dependent DNA adduct formation (number of adducts in 10^8 nt) in the liver as obtained from *in vivo* studies in male mice treated with 2-AAF, giving the following slope ((#adduct 10^8 nt)/(mg/kg bw/day)): m=156.96, the range of accepted BMD_{10} values derived from mice *in vivo* data on liver tumor incidence. Inserts are log-log plots of doses and DNA adduct levels.

DNA adduct levels at 1 mg/kg bw/day, the average BMD_{10} and the average DNA adduct formation at the BMD_{10} are displayed in table 6.4. When comparing the average DNA adduct levels at the average BMD_{10} it was found that at the BMD_{10} DNA adduct formation in rat was 8 fold greater than in mouse. Previous data derived for DNA adduct levels in rats and mice at the TD_{50} value were in line with this result (Pereira *et al.*, 1981).

Table 6.4. Species differences in response to 2-Acetylaminofluorene (2-AAF): female mice versus male rats (Ogiso *et al.*, 1985; Williams *et al.*, 2004).

Model	Number adducts in 10^8 nt for 1 mg/kg/ bw/day	Average BMD_{10}	Average number adducts in 10^8 nt
Mice	157.0	6.07	953.0
Rat	24002	0.343	8250

6.3.6 Endogenous DNA adduct levels

Endogenous or background DNA damage occurs constantly in all human and animal tissues, induced, for instance, through oxidative stress, the formation of radicals or reactive, alkylating metabolites. The targets of these 'stressors' are numerous and can be the deoxyribose-phosphodiester backbone, the glycosidic linkages connecting the nucleobases to the DNA backbone or the nucleobases itself, leading to a plethora of different possible primary and secondary modifications (Gates, 2009) that can have profound biological consequences. For the purpose of this manuscript, we use the term 'background' or 'endogenous DNA adduct' for measurable, specific covalent modifications of the nucleobases (including oxidatively damaged nucleobases) in order to define a background level for comparison with exogenous carcinogen specific adduct formation that principally attack similar atoms of the nucleobases. Reports in the literature on endogenous levels of DNA adducts are varied and address both animal and human tissues. Historically, difficulties were encountered concerning the performance of analytical methods. For instance, the determination of oxidatively damaged guanine (8-oxo-7,8-dihydroguanine, 8-oxo-dG) led to important overestimations due to artifactual DNA oxidation during the analytical sample workup (Gedik *et al.*, 1998; Moller *et al.*, 1998; Collins *et al.*, 2004; Valavanidis *et al.*, 2009). Due to the heterogeneity of adducts and available methods and the fact that most recent comprehensive reviews focus on human endogenous DNA adducts (Povey, 2000; De Bont and van Larebeke, 2004), detailed knowledge on endogenous DNA adduct formation in rat tissues is actually limited. Representative data on levels of the most studied endogenous adducts, in human and rat liver, were extracted from the literature and are summarized in table 6.5. Though not being exhaustive, the list provides a reasonable indication of the overall endogenous adduct levels. It is obvious that, even within the same species and organ, levels of a specific adduct can easily vary by more than one order of magnitude (e.g. in rats: 8-oxo-dG, $23-480/10^8$ nt and M1G, $1-52/10^8$ nt). The results presented in table 6.5 revealed that oxidative damage usually exceeds other endogenous DNA adducts induced by alkylation or lipid oxidation which is in agreement with previous reviews (Gupta and Lutz, 1999; Povey, 2000; De Bont and van Larebeke, 2004). In addition, endogenous DNA adduct levels tend to be somewhat higher in humans than in rats, probably due to non-controllable and lifestyle factors such as unknown dietary and environmental sources of exposure to alkylating agents, smoking or oxidative/metabolic stress as compared to the controlled housing conditions of laboratory animals. In general it has been reported that endogenous DNA adduct levels are present in 100 adducts in 10^8 nt (Swenberg *et al.*, 2008), and additionally, the level was reported by Farmer (2004; 2008) to be generally 10-100 adduct in 10^8 nt for low molecular weight alkylating electrophiles. Based on these data in the present manuscript the background of the alkylating endogenous DNA adduct level was defined at 10-100 adducts in 10^8 nt and used as the relevant background level for endogenous DNA adduct formation. This level of endogenous DNA adduct formation was also previously used to compare estragole DNA adduct formation predicted by our physiologically based biodynamic (PBBD) model for DNA adduct formation in male rat liver after exposure to estragole (Chapter 2).

Table 6.5. Quantitative information on endogenous DNA adduct levels limited to liver of humans and rats.

Adduct	affected nucleo-base position	Quantity /10^6 nt*	Method	Source (h, human ; r, rat) (no of samples)	Reference
Oxidation					
8-oxo-dG	C8	0.51	HPLC/EC[§]	r (3?)	(Hofer and Moller, 1998)
8-oxo-dG	C8	0.84-1.14	HPLC[§]	r (32)	(Moller *et al.*, 1998)
8-oxo-dG	C8	1.8-4.8[$]	LC-MS/MS	r (3)	(Singh *et al.*, 2009)
8-oxo-dA	C8	0.23-0.34[$]	LC-MS/MS	r (3)	(Singh *et al.*, 2009)
Lipid peroxidation					
M1G	N1	0.5-1.1	GC-MS	h (6)	(Farmer and Shuker, 1999)
M1G	N1	0.14	P^{32}/HPLC	h (?)	(De Bont and van Larebeke, 2004)
M1G	N1	0.9	GC/EC NCI/MS	h (?)	(De Bont and van Larebeke, 2004)
M1G	N1	0.01	LC-MS/MS	r (4)	(Jeong *et al.*, 2005)
M1G	N1	0.52	GC/ECNCI MS	r (6)	(Jeong *et al.*, 2005)
7-HEG	N7	3.0	GC-HRMS	h (9)	(Farmer and Shuker, 1999)
7-HEG	N7	0.06-0.09	^{32}P-pl	r (?)	(Zhao *et al.*, 1999)
7-HEG	N7	0.29	^{32}P-pl	h (?)	(Boysen *et al.*, 2009)
7-HEG	N7	0.013	LC-MS/MS	r (3)	(Marsden *et al.*, 2006; Marsden *et al.*, 2007)
7-HEG	N7	0.025	LC-MS/MS	r(12)	(Marsden *et al.*, 2006; Marsden *et al.*, 2007)
7-CEG	N7	0.05	LC-MS	h (24)	(Cheng *et al.*, 2010)
7-EtG	N7	0.0084	LC-MS	h (25)	(Boysen *et al.*, 2009)
Cyclic adducts	N^2,C3	0.02	LC-MS	h (1)	(Farmer and Shuker, 1999)
εG	N^2,C3	0.012	IA-GC/HRMS	r (8)	(Morinello *et al.*, 2002)
εG	N^2,C3	0.007	IA-GC/HRMS	r (7)	(Morinello *et al.*, 2002)
εG	C1,N^6	0.001-0.002	IA ^{32}P-pl	r (3)	(Navasumrit *et al.*, 2001)
εdA	C1,N^6	0.006	IA ^{32}P-pl	h (10)	(Barbin *et al.*, 2003)
εdA	C3,N^4	0.006-0.008	IA ^{32}P-pl	r (3)	(Navasumrit *et al.*, 2001)
εdC	C3,N^4	0.007	IA ^{32}P-pl	h (10)	(Barbin *et al.*, 2003)
εdC	C1,N^2	0.0006-	HPLC/P^{32}-pl	h (?)	(De Bont and van Larebeke, 2004)
HNE-dG	C1,N^2	0.0018	HPLC/P^{32}-pl	h (?)	(De Bont and van Larebeke, 2004)
Acr-dG		0.06-0.4			
Alkylation					
7-MG	N7	0.21-0.25	^{32}P-pl	r (?)	(Zhao *et al.*, 1999)
7-MG	N7	0.27	^{32}P-pl	r (?)	(Zhao *et al.*, 1999)
O^6-MeG	O^6	0.022-0.13	PREPI	h (?)	(De Bont and van Larebeke, 2004)
O^4-MeT	O^4	0.003-0.42	PREPI	h (?)	(De Bont and van Larebeke, 2004)
O^4-EtT	O^4	0.015-4.24	PREPI	h (?)	(De Bont and van Larebeke, 2004)
Abasic sites	-	8-9	ASB	h (?)	(De Bont and van Larebeke, 2004)

IA, immunoaffinity purification; PREPI, ^{32}P-postlabelling (^{32}P-pl) followed by HPLC and immunoprecipitation; ASB, combination of aldehyde reactive probe and slot blot techniques; HRMS, high resolution mass spectrometry; HNE, 4-hydroxynonenal; Acr, acrolein; ECNCI, electron capture negative chemical ionization.

*In part corrected from the number of adducts per normal parent base by using a content of 22% G or C and 28% of A or T in mammalian DNA.

[§] Improved workup to minimize artifactual formation.

[$] Depending on extraction procedure (chaotropic extraction or anion exchange, respectively).

In a next step the DNA adduct levels calculated at the BMD_{10} (Table 6.3) were compared to reported endogenous levels of DNA adduct formation (Table 6.5). The value of 10-100 adducts in 10^8 nt was included resulting in Figure 6.3, which allows comparison of the DNA adduct levels at the BMD_{10} to the endogenous DNA adduct levels in rat liver. When comparing the levels between genotoxic compounds it appears that the number of DNA adducts in 10^8 nt formed at the highest BMD_{10}, for 2-AAF, MeIQx, SA, TAM were 100, 7.5, 6.9, 2.3 fold higher than the highest value set for the endogenous DNA adduct levels (100 adduct in 10^8 nt). For AfB1 and ME, the predicted levels of DNA adduct formation at the BMD_{10} was within the background

level of 10-100 adducts 10^8 nt. In the specific case of TAM the amount of DNA adducts at the BMD_{10} resulted in four different sets of values (Figure 6.3), since two studies on DNA adduct formation and two tumor incidence studies were available for this compound. Two data sets falling within the endogenous background level while one data set was above the endogenous background and the fourth data set was partially above the back ground level. When the TAM-adducts calculated at the BMD_{10} were based on data generated using different analytical methods (Schild *et al.*, 2005) the values obtained did not vary by more than a factor of 2 (not shown), which is much less than the differences observed between different animal studies.

6.4 Discussion

In the present chapter a comparison was made between *in vivo* DNA adduct formation, cancer induction and background DNA adduct formation using a series of selected DNA reactive carcinogens: 2-acetylaminofluorene (2-AAF), aflatoxin B1 (AfB1), methyleugenol (ME), safrole (SA), 2-amino-3,8-methylimidazo[4,5-f]quinoxaline (MeIQx), and tamoxifen (TAM), as model compounds. The aim of this study was to use a uniform dataset on DNA-reactive, genotoxic carcinogens that induce, with or without metabolic activation, DNA adducts which can lead to hepatocellular carcinogenic transformation, in order to analyze if a correlation between the formation of DNA adducts and cancer incidences in the target organ can be obtained. A decade ago, Otteneder and Lutz (1999), making a similar effort, indicated that there was a need of more data on DNA adduct levels in target tissues of rodents and human. After more than 10 years little progress has been made, since a thorough literature search revealed only six DNA-reactive carcinogens for which in addition to tumor data also data on *in vivo* DNA adduct formation in the same target tissue, species and gender were available. Otteneder and Lutz (1999) used carcinogen-DNA adduct levels associated with a 50% tumor incidence, using data from both mice and rats, males and females. In the present manuscript we used data on DNA adducts and cancer incidences exclusively for rat, within the same gender, and dose responses for cancer incidences were modeled using a Benchmark dose (BMD) approach. In addition, data were compared to endogenous DNA adduct levels. Although for an individual carcinogen the tumor response increases when adduct levels increase, our results demonstrate that when comparing different carcinogens no quantitative correlation exists between the level of DNA adduct formation and carcinogenicity. Assuming that DNA adduct have a role in cancer development, the data corroborate that the different DNA adduct have different mutagenic and carcinogenic potential. The evaluation of DNA adduct data represents a particular difficulty, especially in risk assessment (Jarabek *et al.*, 2009). Jarabek *et al.* (2009) defined mutagenic efficiency to be: "the probability that a DNA adduct or an adduct load converts a normal cell to a viable cell containing a heritable alteration in the DNA (i.e., a mutation)"; the efficiency of conversion of a promutagenic DNA adduct to a mutation depends on a wide range of factors including the type and chirality of the adduct; the cell-, tissue-, or organ-specific DNA repair and metabolism; the local DNA sequence context of the adduct; the lability/stability of the adduct; the extent of disruption induced in the helix structure; the capacity of the affected cell to replicate to form a clone; and other cellular processes such as the frequency of cell replication. All these parameters must be considered when dealing with DNA adducts in risk assessment. Furthermore is important to underline that unlike the rodent two years cancer bioassay, that is conducted according to guideline protocols since considerable time, with agreed procedures as to adjust doses for

exposure and treatment duration in order to allow comparability between studies and compounds, analyses of in vivo DNA adduct formation have variable study designs, are usually done for very specific purposes, with particular dosing regimens and duration depending on the question asked. Therefore, we corrected for these diverting factors as much as possible.

Thus various DNA reactive carcinogens for which data on *in vivo* DNA adduct formation were available, such as for example dimethylnitrosamine (DMN), 2-Amino-3-methylimidazo[4,5-f]quinolone (IQ), and 2,4-diaminotoluene (DAT), which were used in Otteneder and Lutz (Otteneder and Lutz, 1999) did not have tumor incidence data meeting the criteria set in this manuscript. And for many other DNA reactive compounds for which long term carcinogenicity data are available, data on *in vivo* DNA adduct formation are lacking. The selection of the compounds in the present study was done following the following criteria: i) available data on *in vivo* DNA adduct formation and ii) available dose response data for tumor induction, both in the same target tissue, the liver, and for the same species, the rat, and for the same gender. In further analysis of the results obtained it was important to take into account other critical steps underlined by Otteneder and Lutz (1999) such as: i) DNA adduct measurement is a balance between formation of the adduct, repair, cell death, and dilution of the adduct formed by DNA replication; ii) the period of treatment should be long enough to achieve a steady state; and iii) the relationship between DNA adducts detected and tumor incidence may be influenced by the time of sacrifice of the animal after administration of the compound. DNA adduct data obtained from literature revealed that all the experimental data sets , although limited, appear compatible with linearity to the origin, a finding that is in line with the current understanding of DNA-adduct dose-response behavior (Pottenger *et al.*, 2009). DNA-adduct levels detected can be expected to reflect a balance between DNA-adduct formation and DNA repair, cell death, and dilution of the adduct formed by DNA replication (Swenberg *et al.*, 1995).

The data obtained point at a different potency for each individual compound to result in DNA adduct formation, with AfB1 and 2-AAF being at least 2 to 3 orders of magnitude more effective in forming DNA adducts than MeIQx and SA, and even 4 orders of magnitude more effective than ME and TAM. Such differences can be expected to result for example from differences in the reactivity of the DNA-reactive intermediate formed, in the relative percentage of the dose that is actually converted to the DNA reactive metabolite and/or in the stability of the DNA adduct formed. DNA adducts are produced when electrophilic compounds covalently bind to a base of the DNA structure, forming different types of DNA adducts (Swenberg *et al.*, 2008). DNA adducts vary greatly in their half-lives, which depends on their chemical stability, their repair by DNA repair processes, and/or their elimination through apoptosis and/or cell death. The site of formation of the electrophilic metabolite, combined with its chemical stability, influences the cellular and tissue distribution of DNA adducts. For instance highly unstable electrophiles do not persist long enough to form adducts in tissues distant to the site of metabolic activation (Swenberg *et al.*, 2008). On the other hand relatively stable metabolites can circulate in the blood, and form DNA adducts in many tissues (Swenberg *et al.*, 2008). Furthermore, tissue specific possibilities for DNA repair can greatly affect the amount of DNA adducts present in a tissue. In a repair proficient tissue the amount of DNA adduct rapidly decreases but if the tissue is deficient in repair mechanisms then the amount of DNA adducts remains unaffected (Swenberg *et al.*, 2008).

Furthermore, as outlined by Otteneder and Lutz (1999), it is important to note that, when comparing the relative potency of the different model compounds to form DNA adducts, the period of treatment underlying the data for which the comparison is made should be long enough to achieve a steady state. Steady state levels are reached when the number of DNA adducts formed are equal to the number that are destroyed and repaired, and this may be achieved either after a single exposure, or only after repeated exposure to a DNA reactive compound, the latter leading to an increase in DNA adduct formation over time. For highly unstable or rapidly repaired DNA adducts (such as N-3 methyladenine or N7 estrogen adducts on adenine) steady state may be reached as quickly as following the first daily dose (Swenberg et $al.$, 2008). However, in other cases (i.e. N7-alkylguanine adducts) a steady state may only be achieved in 7-10 days, whereas more persistent adducts (such as O4-ethyl thymidine) can accumulate over a period of 4 weeks (Swenberg et $al.$, 2008).

In the present paper we have normalized the data either only with respect to the dose or with respect to both the dose and duration of exposure. Some data are available that could provide at least some insight into the actual influence of dose and duration of exposure on the normalized levels of DNA adduct formed. For example for SA, DNA adduct levels were measured after one injection and after 5 repeated daily injections. The DNA adduct levels at the same dose (1 mg/kg bw/day) for the single exposure, amounted to $1.40 \cdot 10^8$ nt / day, whereas it amounted to a normalized value of $0.8 \cdot 10^8$ nt /day after 5 daily injections, indicating that the repeated daily exposure gave a somewhat lower amount of DNA adducts formed when normalized to 1 day. Similar for MeIQx DNA adduct measurements obtained after 1 week and 12 week administration of the same dose level revealed that after normalization, the longer treatment period (12 weeks) resulted in a lower number of DNA adducts amounting to $1.89 \cdot 10^8$ nt / day than the 1 week exposure period, which resulted in $8.8 \cdot 10^8$ nt/day. Clearly, however, these differences due to varying duration of the dosing remain within an order of magnitude and are thus smaller than the differences in the levels of DNA adduct formation at a dose of 1 mg/kg bw/day obtained for the model compounds of the present study. Furthermore the amount of DNA adducts detected may be influenced by the time of sacrifice of the animal after administration of the compound (Williams, 2008). Therefore, it could be important to take into account the time period between the last treatment and sacrifice when analyzing DNA adducts levels in $vivo$. In the studies discussed in the present manuscript two studies reported that the period between dosing and sampling was 24 hours (Daimon et $al.$, 1998; Williams et $al.$, 2004), whereas for the remaining studies this time was not specified, hampering further evaluation of this possible factor of influence. In the special case of 2AAF complete data sets (DNA adducts and tumor incidence in liver) were available for both rats and mice. Analysis of these data revealed that at the BMD_{10} the levels of DNA adduct formation in rat appeared to be 8 fold higher than the level in mouse. This suggests that, for this compound, there is a species dependent difference in sensitivity with rats requiring higher levels of DNA adducts formation for a similar level of tumor formation, and the difference between species (rat versus mice) indicating that mice are more sensitive to this compound than rats.

The present manuscript also focuses on the possible role of DNA adduct formation in the mode of action (MOA) of the different DNA reactive carcinogens and the endogenous DNA adduct levels. With respect to these MOAs, it has been reported for example that DNA adduct formation by AfB1 produces 8,9-dihydro-8-(N7-guanyl)-9-hydroxy AfB1 (AfB1-N7-Gua), which is converted naturally to two secondary lesions, an

apurinic site and an AFB1-formamidopyrimidine (AfB1-FAPY) adduct. AfB1-FAPY is detected at near maximal levels in rat DNA days to weeks after AfB1 exposure, underscoring its high persistence *in vivo* (Smela *et al.*, 2001). Furthermore, the DNA adduct formation by AfB1 does not occur randomly within the DNA but rather at so-called mutational hot spots causing mutations with high frequency in the p53 gene (Mace *et al.*, 1997). It has been shown in humans that AfB1 acts preferably on codon 249 and 250 of the p53 gene, resulting in AGG to AGT and CCC to ACC transversions with a relative mutation frequency of 15×10^{-6} (Mace *et al.*, 1997). The putative hot spot in humans, codon 249, corresponds to codon 243 in the rat gene which is located in exon 6. Results suggested that mutation at the site corresponding to the hot spot codon 243 in the rat gene is rare (Hulla *et al.*, 1993). Given however, that the occurrence of these mutational hotspots for AfB1 may not occur in rats (Hulla *et al.*, 1993) the first explanation pointing at high persistence of the AfB1 DNA adducts may provide an alternative explanation for their high mutagenic and carcinogenic potential compared to that of endogenous DNA. Reduction of aflatoxin-DNA adduct levels by chemopreventive agents could reduce the number of foci present and could be used as predictive of cancer preventive efficacy (Kensler *et al.*, 1986; Kensler *et al.*, 1987). For TAM mutations are found in the liver, including predominantly GC→TA transversions (Phillips, 2001), and Liapis et al. (Liapis *et al.*, 2008) predicted, using an *in silico* model, GC→TA mutational hotspots for TAM at codons 244 and 273 of p53. Among the 393 codons of the human p53 gene, 222 are the targets of 698 different mutational events (Beroud *et al.*, 1996). By reacting at different spots the ability of different genotoxic carcinogens to result in tumor formation can be expected to differ. Given this situation it is of interest to note that the actual levels of DNA adduct formation observed for the different DNA-reactive carcinogens at their BMD_{10} differ by only one to two orders of magnitude.

The general background level of DNA adducts was defined at 10-100 adducts in 10^8 nt (Swenberg *et al.*, 1995; La and Swenberg, 1996; Gupta and Lutz, 1999; Farmer, 2008). Based on the data obtained a comparison of the level of DNA adducts calculated to be observed at a dose level amounting to the BMD_{10} for tumor formation by the model carcinogens selected for the present study, to this endogenous DNA adduct levels in rat liver tissue could be made (Figure 6.3). For 2-AAF, 2-MeIQx and SA, DNA adduct formation at the BMD_{10} was above background levels for DNA adduct formation and may thus contribute to their mode of action (MOA). The levels of DNA adduct formation expected at the BMD_{10} were actually below or close to the background DNA adduct level set a 100 adduct in 10^8 nt for i) the study with female rats treated with TAM, ii) the study with ME in male rats, and iii) the study with male rats treated with AfB1. Theoretically this observation of DNA adduct formation at the BMD_{10} at levels that are below the background levels of DNA adduct formation might reflect that either the DNA adducts formed are far more mutagenic and carcinogenic than the type of lesions included in the background levels or it might imply that the mechanism underlying the tumor induction is not related to the DNA adduct formation but rather due to another mechanism of action such as for example cytotoxicity. Given the present proposals for the mode of action of ME, TAM and AfB1 one might conclude that the first explanation holds for AfB1 pointing at formation of DNA adducts that are more mutagenic than background type DNA lesions. The AfB1 mutation at high frequency in a hot spot in the p53 tumor suppressor gene (Mace *et al.*, 1997) and/or leading to DNA adducts with relatively high persistence (Jennings *et al.*, 1992) supports this hypothesis. An efficacy of at least one order of magnitude higher than the efficacy of background DNA lesions to result in tumor induction would already explain that

the level of adduct formation by AfB1 can result in tumor incidences above background level. Poirier and Beland (Poirier and Beland, 1992) reported that the high carcinogenic potency of AfB1 may result in tumor formation at concentrations that do not saturate metabolic pathways, stimulate cell proliferation, or induce extensive toxicity. For ME literature data point at a possible role for liver toxicity in the mechanism underlying tumor formation (FAO/WHO, 2010) and the results of the present analysis may corroborate involvement of another mechanism than merely DNA adduct formation in the MOA of this DNA-reactive carcinogen. Finally for the specific case of TAM there are still several options for the MOA of this genotoxic carcinogen. Formation of DNA adducts at mutational hot spots in the p53 tumor suppressor gene as suggested by Liapis et al. (2008) may support formation of DNA adducts with higher potency for tumor induction than background DNA adducts, whereas on the other hand involvement of the TAM or its metabolite 4-hydroxytamoxifen as a partial estrogen receptor alpha agonist (Liapis *et al.*, 2008) may point at a MOA including increased cell proliferation and tumor formation induced by estrogen receptor alpha agonist activity, representing a mode of action other than the association of hepatic tumors with accumulation of DNA adducts in the liver (Hard *et al.*, 1993). Estrogen receptor alpha activation may indeed play a role in hepatic tumor formation in rodents (Greaves *et al.*, 1993).

Overall the results of the present paper reveal that for some DNA reactive carcinogens the level of DNA adduct formation at the BMD_{10} for tumor formation does not significantly exceed endogenous DNA adduct levels, pointing at either the formation of DNA adducts that are more effective in inducing carcinogenesis than background DNA adducts or corroborating the involvement of other modes of action than DNA adduct formation underlying their carcinogenicity.

Reference

Barbin A, Ohgaki F, Nakamura J, Kurrer M, Kleihues P, and Swenberg JA. (2003) Endogenous deoxyribonucleic acid (DNA) damage in human tissues: A comparison of ethenobases with aldehydic DNA lesions. Cancer Epidemiology Biomarkers & Prevention 12, 1241-1247.

Benford D, Leblanc JC, and Setzer RW. (2010) Application of the margin of exposure (MoE) approach to substances in food that are genotoxic and carcinogenic Example: Aflatoxin B1 (AFB1). Food and Chemical Toxicology 48, S34-S41.

Berkeley Berkeley Potency Database, Website: http://potency.berkeley.edu/ visited in 2010.

Beroud C, Verdier F, and Soussi T. (1996) p53 gene mutation: Software and database. Nucleic Acids Research 24, 147-150.

Boobis AR, Daston GP, Preston RJ, and Olin SS. (2009) Application of Key Events Analysis to Chemical Carcinogens and Noncarcinogens. Critical Reviews in Food Science and Nutrition 49, 690-707.

Boysen G, Pachkowski BF, Nakamura J, and Swenberg JA. (2009) The formation and biological significance of N7-guanine adducts. Mutation Research-Genetic Toxicology and Environmental Mutagenesis 678, 76-94.

Brink A, Richter I, Lutz U, Wanek P, Stopper H, and Lutz WK. (2009) Biological significance of DNA adducts: Comparison of increments over background for various biomarkers of genotoxicity in L5178Y tk(+/-) mouse lymphoma cells treated with hydrogen peroxide and cumene hydroperoxide. Mutation Research-Genetic Toxicology and Environmental Mutagenesis 678, 123-128.

Buss P, Caviezel M, and Lutz WK. (1990) Linear Dose-Response Relationship for DNA Adducts in Rat-Liver from Chronic Exposure to Aflatoxin-B1. Carcinogenesis 11, 2133-2135.

Cheng GA, Wang MY, Villalta PW, and Hecht SS. (2010) Detection of 7-(2 '-Carboxyethyl)guanine but Not 7-Carboxymethylguanine in Human Liver DNA. Chemical Research in Toxicology 23, 1089-1096.

Collins AR, Cadet J, Moller L, Poulsen HE, and Vina J. (2004) Are we sure we know how to measure 8-oxo-7,8-dihydroguanine in DNA from human cells? Archives of Biochemistry and Biophysics 423, 57-65.

Crump KS. (1984). A New Method for Determining Allowable Daily Intakes. Fundamental and Applied Toxicology 4, 854-871.

Daimon H, Sawada S, Asakura S, and Sagami F. (1998) In vivo genotoxicity and DNA adduct levels in the liver of rats treated with safrole. Carcinogenesis 19, 141-146.

De Bont R, and van Larebeke N. (2004) Endogenous DNA damage in humans: a review of quantitative data. Mutagenesis 19, 169-185.

de Laat WL, Jaspers NGJ, and Hoeijmakers JHJ. (1999) Molecular mechanism of nucleotide excision repair. Genes & Development 13, 768-785.

Ellis JK, Carmichael PL, and Gooderham NJ. (2006) DNA adduct levels in the liver of the F344 rat treated with the natural flavour methyl eugenol. Mutagenesis 21, 291-292.

EPA B. s., website: http//www.epa.gov/ncea/bmds/index.htlm, visited in 2010.

FAO/WHO. (2010) Evaluation of certain Food Additives: sisty-ninth report of the joint FAO/WHO expert committee on Food Additives. WHO Technical Report 952.

Farmer P. (2008) Significance for risk assessment of increases in background levels of carcinogen-derived protein and DNA Aadducts. Toxicology Letters 180, S24-S24.

Farmer PB, Brown K, Corcoran E, Emms VL, Jones DJL, Singh R, and Phillips DH. (2004) DNA adducts: Mass spectrometry methods and future prospects. Toxicology and Applied Pharmacology 197, 164-164.

Farmer PB, and Shuker DEG. (1999) What is the significance of increases in background levels of carcinogen-derived protein and DNA adducts? Some considerations for incremental risk assessment. Mutation Research-Fundamental and Molecular Mechanisms of Mutagenesis 424, 275-286.

Gates KS. (2009). An Overview of Chemical Processes That Damage Cellular DNA: Spontaneous Hydrolysis, Alkylation, and Reactions with Radicals. Chemical Research in Toxicology 22, 1747-1760.

Gedik CM, Wood SG, and Collins AR. (1998) Measuring oxidative damage to DNA; HPLC and the comet assay compared. Free Radical Research 29, 609-615.

Gold LS, Manley NB, Slone TH, and Rohrbach L. (1999) Supplement to the Carcinogenic Potency Database (CPDB): Results of animal bioassays published in the general literature in 1993 to 1994 and by the National Toxicology Program in 1995 to 1996. Environmental Health Perspectives 107, 527-+.

Gold LS, Manley NB., Slone TH, Rohrbach L, and Garfinkel GB. (2005) Supplement to the Carcinogenic Potency Database (CPDB): Results of animal bioassays published in the general literature through 1997 and by the National Toxicology Program in 1997-1998. Toxicological Sciences 85, 747-808.

Gold LS, Sawyer CB, Magaw R, Backman GM, Deveciana M, Levinson R, Hooper NK, Havender WR, Bernstein, L, Peto R, Pike MC, and Ames BN. (1984) A Carcinogenic Potency Database of the Standardized Results of Animal Bioassays. Environmental Health Perspectives 58, 9-319.

Greaves P, Goonetilleke R, Nunn G, Topham J, and Orton T. (1993) 2-Year Carcinogenicity Study of Tamoxifen in Alderley-Park Wistar-Derived Rats. Cancer Research 53, 3919-3924.

Gupta RC, and Lutz WK. (1999) Background DNA damage from endogenous and unavoidable exogenous carcinogens: a basis for spontaneous cancer incidence? Mutation Research-Fundamental and Molecular Mechanisms of Mutagenesis 424, 1-8.

Hanahan D, and Weinberg RA. (2000) The hallmarks of cancer. Cell 100, 57-70.

Hard GC, Iatropoulos MJ, Jordan K, Radi L, Kaltenberg OP, Imondi AR, and Williams GM. (1993) Major Difference in the Hepatocarcinogenicity and DNA Adduct Forming Ability between Toremifene and Tamoxifen in Female Crl-Cd(Br) Rats. Cancer Research 53, 4534-4541.

Himmelstein MW, Boogaard PJ, Cadet J, Farmer PB, Kim JH, Martin EA, Persaud R, and Shuker DEG. (2009) Creating context for the use of DNA adduct data in cancer risk assessment: II. Overview of methods of identification and quantitation of DNA damage. Critical Reviews in Toxicology 39, 679-694.

Hofer T, and Moller L. (1998). Reduction of oxidation during the preparation of DNA and analysis of 8-hydroxy-2 '-deoxyguanosine. Chemical Research in Toxicology 11, 882-887.

Hulla JE, Chen ZY, and Eaton DL. (1993) Aflatoxin-B1-Induced Rat Hepatic Hyperplastic Nodules Do Not Exhibit a Site-Specific Mutation within the P53 Gene. Cancer Research 53, 9-11.

ISI Web of Knowledge, h. w. c., visited in 2010.

Jarabek AM, Pottenger LH, Andrews LS, Casciano D, Embry MR, Kim JH, Preston RJ, Reddy MV, Schoeny R, Shuker D, Skare J, Swenberg J, Williams GM, and Zeiger E. (2009) Creating context for the use of DNA adduct data in cancer risk assessment: I. Data organization. Critical Reviews in Toxicology 39, 659-678.

Jennings GS, Oesch F, and Steinberg P. (1992) Invivo Formation of Aflatoxin-B1 DNA Adducts in Parenchymal and Nonparenchymal Cells of Rat-Liver. Carcinogenesis 13, 831-835.

Jeong YC, Nakamura J, Upton PB, and Swenberg JA. (2005) Pyrimido[1,2-a]-purin-10(3H)-one, M(1)G, is less prone to artifact than base oxidation. Nucleic Acids Research 33, 6426-6434.

Johnson JD, Ryan MJ, Toft JD, Graves SW, Hejtmancik MR, Cunningham ML, Herbert R, and Abdo KM. (2000) Two-year toxicity and carcinogenicity study of methyleugenol in F344/N rats and B6C3F(1) mice. Journal of Agricultural and Food Chemistry 48, 3620-3632.

Kensler TW, Egner PA, Davidson NE, Roebuck BD, Pikul A, and Groopman JD. (1986) Modulation of Aflatoxin Metabolism, Aflatoxin-N7-Guanine Formation, and Hepatic Tumorigenesis in Rats Fed Ethoxyquin - Role of Induction of Glutathione S-Transferases. Cancer Research 46, 3924-3931.

Kensler TW, Egner PA, Dolan PM, Groopman JD, and Roebuck BD. (1987) Mechanism of Protection against Aflatoxin Tumorigenicity in Rats Fed 5-(2-Pyrazinyl)-4-Methyl-1,2-Dithiol-3-Thione (Oltipraz) and Related 1,2-Dithiol-3-Thiones and 1,2-Dithiol-3-Ones. Cancer Research 47, 4271-4277.

Kushida H, Wakabayashi K, Sato H, Katami M, Kurosaka R, and Nagao M. (1994) Dose-Response Study of Meiqx Carcinogenicity in F344 Male-Rats. Cancer Letters 83, 31-35.

La DK, and Swenberg JA. (1996) DNA adducts: Biological markers of exposure and potential applications to risk assessment. Mutation Research-Reviews in Genetic Toxicology 365, 129-146.

Li DH, Dragan Y, Jordan VC, Wang MY, and Pitot HC. (1997) Effects of chronic administration of tamoxifen and toremifene on DNA adducts in rat liver, kidney, and uterus. Cancer Research 57, 1438-1441.

Liapis E, McLuckie KIE, Lewis PD, Farmer PB, and Brown K. (2008) Mutagenicity of tamoxifen DNA adducts in human endometrial cells and in silico prediction of p53 mutation hotspots. Nucleic Acids Research 36, 5933-5945.

Long EL, Hansen WH, Nelson AA, and Fitzhugh OG. (1963) Liver Tumors Produced in Rats by Feeding Safrole. Archives of Pathology 75, 595-&.

Mace K, Aguilar F, Wang JS, Vautravers P, GomezLechon M, Gonzalez FJ, Groopman J, Harris CC, and Pfeifer AMA. (1997). Aflatoxin B-1-induced DNA adduct formation and p53 mutations in CYP450-expressing human liver cell lines. Carcinogenesis 18, 1291-1297.

Maley CC, Galipeau PC, Li XH, Sanchez CA, Paulson TG, Blount PL, and Reid BJ. (2004) The combination of genetic instability and clonal expansion predicts progression to esophageal adenocarcinoma. Cancer Research 64, 7629-7633.

Marsden D A, Farmer PB, Jones DJL, Lamb JH, Tompkins EM, Crookston RJR, and Brown K. (2006) Measurement of endogenous and exogenously derived N7-HEG adducts in ethylene oxide treated rats using LC-MS/MS. Mutagenesis 21, 293-293.

Marsden DA, Jones DJL, Lamb JH, Tompkins EM, Farmer PB, and Brown K. (2007) Determination of endogenous and exogenously derived N7-(2-hydroxyethyl)guanine adducts in ethylene oxide-treated rats. Chemical Research in Toxicology 20, 290-299.

Martati E, Boersma MG, Spenkelink A, Khadka DB, Punt A, Vervoort J, van Bladeren PJ, and Rietjens IMCM. A physiologically based kinetic (PBK) model for safrole bioactivation and detoxification in rat and comparison to those for estragole and methyleugenol. submitted to

Miller EC, and Miller JA. (1992). Studies on the mechanism of activation of aromatic amine and amide carcinogens to ultimate carcinogenic electrophilic reactants. Annals ENw York Academy of Sciences, 731-750.

Moller L, Hofer T, and Zeisig M. (1998). Methodological considerations and factors affecting 8-hydroxy-2 '-deoxyguanosine analysis. Free Radical Research 29, 511-524.

Morinello EJ., Ham AJL, Ranasinghe A, Nakamura J, Upton PB, and Swenberg JA. (2002) Molecular dosimetry and repair of N-2,3-ethenoguanine in rats exposed to vinyl chloride. Cancer Research 62, 5189-5195.

Navasumrit P, Ward TH, O'Connor PJ, Nair J, Frank N, and Bartsch H. (2001) Ethanol enhances the formation of endogenously and exogenously derived adducts in rat hepatic DNA. Mutation Research-Fundamental and Molecular Mechanisms of Mutagenesis 479, 81-94.

Neumann HG. (2009) Risk assessment of chemical carcinogens and thresholds. Critical Reviews in Toxicology 39, 449-461.

NTP U. N. T. P., http://ntp.nies.nih.gov/index.cfm, visited in 2010.

Ogiso T, Tatematsu M, Tamano S, Tsuda H, and Ito N. (1985) Comparative Effects of Carcinogens on the Induction of Placental Glutathione S-Transferase-positive Liver Nodules in a Short-term Assay and of Hepatocellular Carcinomas in a Long-term Assay. Toxicologic Pathology 13, 257-265.

Otteneder M, and Lutz WK. (1999) Correlation of DNA adduct levels with tumor incidence: carcinogenic potency of DNA adducts. Mutation Research-Fundamental and Molecular Mechanisms of Mutagenesis 424, 237-247.

Pereira MA, Lin LHC, and Chang LW. (1981) Dose-Dependency of 2-Acetylaminofluorene Binding to Liver DNA and Hemoglobin in Mice and Rats. Toxicology and Applied Pharmacology 60, 472-478.

Peto R, Pike MC, Bernstein L, Gold LS, and Ames BN. (1984). The TD50 - a Proposed General Convention for the Numerical Description of the Carcinogenic Potency of Chemicals in Chronic-Exposure Animal-Experiments. Environmental Health Perspectives 58, 1-8.

Phillips DH. (2001). Understanding the genotoxicity of tamoxifen? Carcinogenesis 22, 839-849.

Phillips DH, and Arlt VM. (2007). The P-32-postlabeling assay for DNA adducts. Nature Protocols 2, 2772.

Poirier MC, and Beland FA. (1992) DNA Adduct Measurements and Tumor-Incidence during Chronic Carcinogen Exposure in Animal-Models - Implications for DNA Adduct-Based Human Cancer Risk Assessment. Chemical Research in Toxicology 5, 749-755.

Poirier MC, Fullerton NF, Kinouchi T, Smith BA, and Beland FA. (1991) Comparison between DNA Adduct Formation and Tumorigenesis in Livers and Bladders of Mice Chronically Fed 2-Acetylaminofluorene. Carcinogenesis 12, 895-900.

Pottenger LH, Carmichael N, Banton MI, Boogaard PJ, Kim J, Kirkland D, Phillips RD, van Benthem J, Williams GM, and Castrovinci A. (2009) ECETOC workshop on the biological significance of DNA adducts: Summary of follow-up from an Expert Panel Meeting. Mutation Research/Genetic Toxicology and Environmental Mutagenesis 678, 152-157.

Povey AC. (2000) DNA adducts: Endogenous and induced. Toxicologic Pathology 28, 405-414.

PubMed http://www.ncbi.nlm.nih.gov/sites/entrez?db=pubmed, visited in 2010.

Punt A, Freidig AP, Delatour T, Scholz G, Boersma MG, Schilter B, van Bladeren PJ, and Rietjens IMCM. (2008). A physiologically based biokinetic (PBBK) model for estragole bioactivation and detoxification in rat. Toxicology and Applied Pharmacology 231, 248-259.

Punt A, Paini A, Boersma MG, Freidig AP, Delatour T, Scholz G, Schilter B, van Bladeren PJ, and Rietjens IMCM. (2009) Use of Physiologically Based Biokinetic (PBBK) Modeling to Study Estragole Bioactivation and Detoxification in Humans as Compared with Male Rats. Toxicological Sciences 110, 255-269.

Randerath K, Reddy MV, and Gupta RC. (1981) P-32-Labeling Test for DNA Damage. Proceedings of the National Academy of Sciences of the United States of America-Biological Sciences 78, 6126-6129.

Schild LJ, Phillips DH, Osborne MR, Hewer A, Beland FA, Churchwell MI, Brown K, Gaskell M, Wright E, and Poirier MC. (2005) Hepatic DNA adduct dosimetry in rats fed tamoxifen: a comparison of methods. Mutagenesis 20, 115-124.

Singh R, Teichert F, Verschoyle RD, Kaur B, Vives M, Sharma RA, Steward WP, Gescher AJ, and Farmer PB. (2009) Simultaneous determination of 8-oxo-2 '-deoxyguanosine and 8-oxo-2 '-deoxyadenosine in DNA using online column-switching liquid chromatography/tandem mass spectrometry. Rapid Communications in Mass Spectrometry 23, 151-160.

Slob W. (2002) Dose-response modeling of continuous endpoints. Toxicological Sciences 66, 298-312.

Smela ME, Currier SS, Bailey EA, and Essigmann JM. (2001) The chemistry and biology of aflatoxin B-1: from mutational spectrometry to carcinogenesis. Carcinogenesis 22, 535-545.

Staffa JA, and Mehlman MA. (1979) Innovations in cancer risk assessment (ED10 study). J. Environ. Pathol. Toxicol. 3, 1-246.

Stojic L, Brun R, and Jiricny J. (2004) Mismatch repair and DNA damage signalling. DNA Repair 3, 1091-1101.

Swenberg JA, Fryar-Tita E, Jeong YC, Boysen G, Starr T, Walker VE, and Albertini RJ. (2008) Biomarkers in toxicology and risk assessment: Informing critical dose-response relationships. Chemical Research in Toxicology 21, 253-265.

Swenberg JA, La DK, Scheller NA, and Wu KY. (1995) Dose-response relationships for carcinogens. Toxicology Letters 82-3, 751-756.

Valavanidis A, Vlachogianni T, and Fiotakis C. (2009) 8-hydroxy-2' -deoxyguanosine (8-OHdG): A Critical Biomarker of Oxidative Stress and Carcinogenesis. Journal of Environmental Science and Health Part C-Environmental Carcinogenesis & Ecotoxicology Reviews 27, 120-139.

Walker VE, Fennell TR, Upton PB, Skopek TR, Prevost V, Shuker DEG, and Swenberg JA. (1992) Molecular Dosimetry of Ethylene-Oxide - Formation and Persistence of 7-(2-Hydroxyethyl)Guanine in DNA Following Repeated Exposures of Rats and Mice. Cancer Research 52, 4328-4334.

Wheeler MW, and Bailer AJ. (2007) Properties of model-averaged BMDLs: A study of model averaging in dichotomous response risk estimation. Risk Analysis 27, 659-670.

Williams G, Iatropolous M, and Jeffrey A. (2004) Threshold for the effect of 2-Acetylaminofluorene in rat liver. Toxicology Pathology 32, 85-91.

Williams GM. (2001) Mechanisms of chemical carcinogenesis and application to human cancer risk assessment. Toxicology 166, 3-10.

Williams GM. (2008) Application of mode-of-action considerations in human cancer risk assessment. Toxicology Letters 180, 75-80.

Wogan GN, Paglialu S, and Newberne PM. (1974) Carcinogenic Effects of Low Dietary Levels of Aflatoxin-B1 in Rats. Food and Cosmetics Toxicology 12, 681-685.

Wood RD, Mitchell, M, Sgouros, J, and Lindahl, T. (2001). Human DNA repair genes. Science 291, 1284-+.

Yamashita K, Adachi M, Kato S, Nakagama H, Ochiai M, Wakabayashi K, Sato S, Nagao M, and Sugimura T. (1990) DNA Adducts Formed by 2-Amino-3,8-dimethylimidazo[4,5-f]quinoxaline in rat liver: Dose-Response on Chronic Administration. Cancer Science 81, 470-476.

Zhao CY, Tyndyk M, Eide I, and Hemminki K. (1999). Endogenous and background DNA adducts by methylating and 2-hydroxyethylating agents. Mutation Research-Fundamental and Molecular Mechanisms of Mutagenesis 424, 117-125.

Chapter 7

Summary, General Discussion, and Future Perspectives

7.1 Summary

Our food contains several compounds which, when tested in isolated form at high doses in animal experiments, have been shown to be genotoxic and carcinogenic. At the present state-of-the-art there is no scientific consensus on how to perform the risk assessment of these compounds when present at low dietary doses in a complex food matrix. In order to refine the evaluation of the risks associated with these food-borne genotoxic carcinogens, information on their mode of action (MOA) at low versus high doses, on species differences in toxicokinetics and toxicodynamics, including dose- and species- dependent occurrence of DNA damage and repair, and on effects on expression of relevant proteins, is required. For modern Toxicology it is of high interest to develop new methods for more accurate and science-based extrapolation of cancer incidences defined in animal experiments at high dose levels to the low dose human situation. Recently, physiologically based biokinetic (PBBK) models to predict detoxification and bioactivation of genotoxic carcinogens, using the alkenylbenzenes estragole, methyleugenol and safrole as model compounds, were developed (Punt et al, 2008; Punt et al., 2009; Martati et al., 2011; Al-Subeihi, et al., 2011). These PBBK models revealed that from dose levels as high as the BMD_{10} (benchmark dose causing 10% extra tumor incidence) down to the so-called virtual safe dose (VSD) (the dose resulting in one in a million extra tumor incidence upon life time exposure), formation of the ultimate carcinogenic metabolite of estragole and other alkenylbenzenes was linear, supporting that as far as toxicokinetics is involved linear extrapolation would be adequate. The PBBK models also revealed that species differences between rat and human were small. However these PBBK models do not take into account further biodynamic steps in the carcinogenic process including DNA adduct formation, DNA repair, mutagenesis and formation of neoplasms. Therefore, the aim of the present thesis was to extend the PBBK models previously defined for estragole to so-called physiologically based biodynamic (PBBD) models for DNA adduct formation taking the approach one step closer to the ultimate endpoint of tumor formation. Such models will facilitate risk assessment because they facilitate extrapolation from high to low dose levels, between species including human and between individuals. Furthermore, building the PBBD models predicting *in vivo* DNA adduct formation based on only *in vitro* parameters contributes to the 3Rs (Replacement, Reduction and Refinement) for animal testing.

In **Chapter 1** the aim of the thesis was introduced and background information on the mechanisms underlying DNA adduct formation by genotoxic carcinogens, the possible repair of these adducts, cancer risk assessment strategies, physiologically based biokinetic (PBBK) and physiologically based biodynamic (PBBD) models, and the food-borne genotoxic and carcinogenic model compound of the present thesis – estragole- was provided. Experimental work presented in this thesis was directed at better understanding and even predicting DNA adduct formation *in vitro* and *in vivo* in rat but also in human at realistic low dose exposure levels (**Chapter 2-4**), and also at better understanding the MOA of tumor induction by estragole (**Chapter 5**). In **Chapter 6** literature data available on DNA adduct formation and tumor incidences for a series of genotoxic liver carcinogens were analyzed to obtain insight into the relationships between DNA adduct formation and tumor incidence.

With the aim to ultimately model DNA adduct formation in the human population at realistic low dose exposure levels, a first step taken was to extend the previously develop physiologically based kinetic (PBBK)

model for bioactivation and detoxification of estragole in rats (Punt *et al.*, 2008) to a so-called physiologically based dynamic (PBBD) model able to predict DNA adduct formation in rat liver. The PBBK model enabled estimation of the dose-dependent formation of 1′-sulfooxyestragole, the reactive metabolite of estragole that is unstable and results in DNA and protein binding. The PBBK model, however, predicts only kinetic characteristics. **Chapter 2** of the present thesis describes the extension of this previously developed rat PBBK model to a PBBD model predicting the dose dependent *in vivo* DNA adduct formation of estragole in rat liver. This PBBD model was developed using *in vitro* data on DNA adduct formation determined in rat primary hepatocytes exposed to 1′-hydroxyestragole. Since hepatocytes are expected to display -in addition to formation of the ultimate carcinogenic metabolite 1′-sulfooxyestragole and DNA adducts- also DNA repair, this latter effect is included in the model. To define the PBBD model, the PBBK model was extended by linking the area under the curve for 1′-hydroxyestragole formation predicted by the PBBK model to the area under the curve for 1′-hydroxyestragole in the *in vitro* experiment. The performance of the newly developed PBBD model for rat could be evaluated based on data in mice, not rats, because for rats data on estragole dependent DNA adduct formation were not available. The PBBD model predicted that at a dose of 400 mg/kg bw/day the level of liver DNA adducts formed amounts to 40.000 in 10^8nt, whereas the value experimentally observed in mice amounted to 10.000 in 10^8 nt being in reasonable agreement given the species difference. Furthermore, the outcome of the PBBD model revealed a linear increase in DNA adduct formation with increasing estragole doses up to 100 mg/kg bw. At realistic estimated human intake levels of 0.01 mg/kg bw/day (Smith *et al.*, 2002) and 0.07 mg/kg bw/day estragole (SCF, 2001), the PBBD model predicted amounts of E-3′-N^2-dG DNA adducts formed amount to respectively 2 and 12.8 in 10^8 nt. These levels of adducts are 1 to 2 orders of magnitude below the background level of DNA damage of 100 adduct in 10^8 nt, which has been stated to be of no known consequence (Williams, 2008). Furthermore these levels are also 1 to 2 orders of magnitude lower than the background levels of DNA adducts formed by low molecular weight alkylating agents, like for example N-nitrosamines, that are in a range of 10–100 adducts in 10^8 nt (Farmer, 2005; Farmer, 2008). It was concluded that although DNA adduct formation of genotoxic carcinogens is generally seen as a biomarker of exposure rather than a biomarker of response, the PBBD model now developed is one step closer to the ultimate toxic effect of estragole than the PBBK model described previously. The PBBD model also provided a proof of principle for modeling a toxico-dynamic *in vivo* endpoint on the basis of solely *in vitro* experimental data, illustrating that PBBD modeling can contribute to the 3Rs (Replacement, Reduction and Refinement) for animal testing. Finally the model enabled prediction of levels of DNA adduct formation at low and realistic human exposure levels and this revealed that at these low exposure levels DNA adduct formation is far below the background level of DNA damage of 100 adduct in 10^8 nt, which has been stated to be of no known consequence.

Given that evaluation of the performance of the PBBD model had to be done based on data from mice because data on DNA adduct formation upon exposure of rats to estragole were not available, the objective of **Chapter 3** was to quantify the dose-dependent estragole DNA adduct formation in rat liver as well as the dose-dependent urinary excretion of 1′-hydroxyestragole glucuronide in order to better validate the physiologically based biodynamic (PBBD) model developed in Chapter 2. To this end groups of male outbred Sprague Dawley rats (n=10, per group) were administered estragole once by oral gavage at dose levels of 0

(vehicle control), 5, 30, 75, 150 and 300 mg/kg bw and sacrificed after 48hrs. Liver, kidney and lungs were analyzed for DNA adducts by LC-MS/MS. Results obtained revealed a dose-dependent increase in DNA adduct formation in the liver. In lungs and kidneys DNA adducts were detected at lower levels than in the liver confirming the occurrence of DNA adducts preferably in the target organ, the liver. The results obtained showed that the PBBD model predictions for both urinary excretion of 1′-hydroxyestragole glucuronide and the E-3′-N^2-dG DNA adduct formation in the liver were comparable within less than an order of magnitude to the values actually observed *in vivo*. The levels of urinary 1′-hydroxyestragole glucuronide were overestimated 4.6 to 7.7 fold and those of DNA adducts by only 1.9 to 2.3 fold. The results obtained provide the first data set available on estragole DNA adduct formation in rats and confirm their occurrence in metabolically active tissues, i.e. liver, lung and kidney, while the significantly higher levels found in liver are in accordance with the liver as the target organ for carcinogenicity. The development and validation of this PBBD model for DNA adduct formation of estragole in rats opened the way towards modeling the dose-dependent estragole liver DNA adduct formation in human, and this was done in **Chapter 4.**

In **Chapter 4** the levels of DNA adducts that could occur in human liver upon exposure to estragole at realistic human dietary intake levels were predicted, taking interindividual variability in bioactivation of estragole to its ultimate carcinogenic metabolite 1′-sulfooxyestragole within the human population into account. Estimates of DNA adduct formation in human liver upon exposure to estragole were made based on i) the previously defined PBBK model for estragole detoxification and bioactivation in humans (Punt *et al.*, 2009), on ii) data on interindividual variation in the kinetics for the major biotransformation enzymes influencing formation of 1′-sulfooxyestragole and on iii) an equation describing the relationship between 1′-sulfooxyestragole formation and DNA adduct formation obtained based on the rat PBBK model (Punt *et al.,* 2008) and the dose-dependent *in vivo* DNA adduct formation detected in rats (Chapter 3). Interindividual differences in the V_{max} and K_m for the major biotransformation enzymes influencing formation of 1′-sulfooxyestragole were determined using S9 liver samples from 22 individual donors. With the individual kinetic constants obtained differences in formation of 1′-sulfooxyestragole and DNA adduct formation could be modeled, indicating a 25-fold variation between the 22 individuals. In addition, a Monte Carlo simulation was performed to evaluate differences in formation of 1′-sulfooxyestragole and formation of estragole DNA adducts in the whole population. It was concluded that these analyses revealed that at an estimated daily intake of 0.01 mg/kg bw/day the DNA adduct levels are predicted to be within or even below the endogenous DNA adduct level of 10-100 adducts per 10^8 nt suggested before to be of no biological consequence, and also below the value of 490 adducts per 10^8 nt reported before as the value required for statistically significant tumorigenesis potential of alkenylbenzene DNA adducts. Thus, the results of Chapter 4 indicated a negligible risk for the average human population at the currently estimated daily intake levels.

It is important to emphasize that the validity and quality of the PBBK/BD model simulations depends on the corresponding model and it requires complete experimental data sets for both kinetic and dynamic processes that occur in biological systems. PBBK/BD models reflect the current scientific knowledge, and while some processes are known to be well characterized, information gaps may exist (Khalil and Laer, 2011). In chapter 4 for example an assumption was made that DNA repair in human would be comparable to that in rat to allow estimation of the levels of adducts formed at low estragole dietary human doses. This

assumption was made since there is no available information or experimental data on the difference between humans and rodents in DNA repair processes for estragole. In subsequent risk assessment such information gaps may be taken into account by using uncertainty factors. Thus, to overcome this information gap in chapter 4 the use of a 7.9 fold uncertainty factor for dynamic uncertainties was applied. Integration of additional information on human DNA repair mechanisms, for estragole DNA adducts could refine the model to a further extent.

Chapter 5 describes studies performed to obtain better insight in the possible role of the DNA adducts formed in the mode of action (MOA) of estragole. This MOA of estragole was further investigated *in vitro* using rat primary hepatocytes, studying the possible implications of DNA damage and repair mechanisms in the MOA of estragole and of its active metabolite 1'-hydroxyestragole. The results obtained revealed that significantly increased levels of DNA adducts were induced upon two hour incubation of primary rat hepatocytes with 1'-hydroxyestragole, and that the level of adducts rapidly decreased after cessation of treatment, indicating the activity of cellular repair mechanisms. However, no specific DNA damage and repair pathways appeared to be induced. The data obtained even revealed a significant down-regulation of genes involved in DNA damage and repair on the transcriptional level. The results furthermore suggested that although the cellular repair machinery is able to cope to some extent with estragole DNA adducts, formation of adducts is not fully reversible pointing at a role for persistence of low levels of estragole DNA adducts in the MOA. Results presented in **Chapter 5** also revealed that at concentration where DNA adduct formation is strongly elevated also cytotoxicity and apoptosis occurs. This indicates that it could be of interest to further explore a possible role for cytotoxicity in the MOA of estragole.

Finally in **Chapter 6** literature data available on DNA adduct formation and tumor incidences for a series of genotoxic liver carcinogens were analyzed to obtain insight into the relationships between DNA adduct formation and tumor incidence. Dose response data on both carcinogenicity and *in vivo* DNA adduct formation in the liver of rats were available for six compounds, i.e. 2-acetylaminofluorene (2AAF), aflatoxin B1 (AfB1), methyleugenol (ME), safrole (SA), 2-amino-3,8-dimethylimidazo[4,5-f]quinoxaline (MeIQX) and tamoxifen (TAM). Although a data set for estragole was not available, data sets for its related alkenylbenzenes methyleugenol (ME) and safrole (SA) (Figure 7.1) could be included in the analysis. BMD_{10} (benchmark dose causing 10% extra tumor incidence) values for liver carcinogenicity induced by the six compounds were calculated from *in vivo* tumor data using the EPA benchmark dose software (http//www.epa.gov/ncea/bmds/index.htlm, visited in 2010).
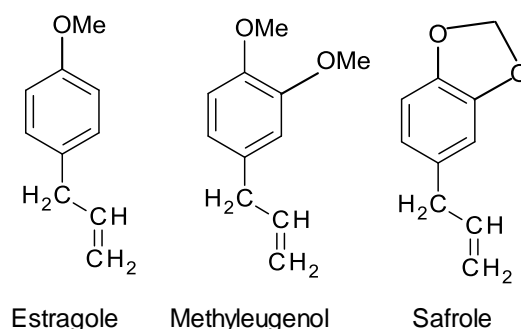

Figure 7.1. Structural formulas of the related alkenylbenzenes: estragole, methyleugenol, and safrole.

In a next step, using data available for dose-dependent DNA adduct formation in the liver, the level of DNA adducts at this BMD_{10} could be calculated. This enabled comparison of the levels of DNA adducts formed at the BMD_{10} for the different genotoxic carcinogens. It also enabled comparison of these levels of DNA adducts formed at the BMD_{10} to available data on endogenous background DNA damage in the target organ the liver. Although for an individual carcinogen the tumor response increases when adduct levels increase, the results obtained demonstrated that when comparing different carcinogens no quantitative correlation exists between the level of DNA adduct formation and carcinogenicity. These data confirm that the quantity of DNA adducts formed by a DNA-reactive compound is not a carcinogenicity predictor but that other factors such as type of adduct and mutagenic potential or other factors contributing to the MOA may be equally relevant. Moreover, comparison to background DNA damage revealed that although for some carcinogens (for example 2AAF) the level of DNA adduct formation at the BMD_{10} was far above background levels for DNA damage, for other gentotoxic carcinogens (for example AfB1 and ME) levels of DNA adducts detected at the BMD_{10} were within background levels. This suggests that the DNA adducts formed are either more mutagenic and carcinogenic than the type of background DNA adducts, or that other mechanisms than DNA adduct formation add to the MOA of the tumor formation. This result supports the notion that the mere occurrence of DNA adducts is not correlated to development of cancer in a uniform way and that the nature of the DNA adducts and/or their location within the genome needs to be taken into account when translating DNA adduct formation to cancer risk. This result strongly emphasizes the need to apply the MOA framework to understand the importance of DNA adduct formation in carcinogenicity.

7.2 DNA adduct formation at the BMD_{10} for tumor formation by estragole

As already indicated, a data set for dose-dependent tumor formation by estragole in rats is not available which implies that to enable estimation of DNA adduct formation in the liver at the BMD_{10} this BMD_{10} value has to be estimated in another way. To estimate the BMD_{10} for estragole dependent formation of liver tumors in the rat two approaches were taken. First, given that estragole and its level of bioactivation to 1'-sulfooxyestragole has been shown to be comparable to formation of the 1'-sulfooxy metabolite of the related alkenylbenzenes methyleugenol and safrole (Jeurissen *et al.,* 2007; Martati *et al.,* 2011) one could use the BMD_{10} values from rats for safrole amounting to 91-169 mg/kg bw/day, and for methyleugenol amounting to 35-40 mg/kg bw/day (Chapter 6), in the rat PBBD model (Chapter 2) to calculate the number of estragole adducts in liver tissue (Chapter 2). In the second approach the BMD_{10} for estragole dependent formation of liver tumors in the rat was estimated based on the BMD_{10} for estragole tumor formation in mice and a correction factor for the different sensitivity of mice and rats determined based on data sets available for the related alkenylbenzenes methyleugenol and safrole. The BMD_{10} values for safrole and methyleugenol in rats amount to respectively 91-169 mg/kg bw/day and 35-40 mg/kg bw/day (Chapter 6). Furthermore the BMD_{10} values for safrole and methyleugenol in mice amount to 9.4-16.4 mg/kg bw/day (based on data from the *in vivo* study performed by Boberg *et al.,* 1983) and to 3-4 mg/kg bw/day (based on data from the *in vivo* study performed by NTP, Johnson *et al.,* 2000). This implies that for these two related alkenylbenzenes the BMD_{10} in rats is on average 10 fold higher than that obtained in mice. Using this correction factor the BMD_{10} derived from a mouse study for estragole of 4.7-8 mg/kg bw/day (Van Den Berg *et al.*, 2011) can be converted to a value for rats between 47 and 80 mg/kg bw/day. Using these estimated BMD_{10} values and the PBBD model

derived in the present thesis the level of DNA adduct formation in the liver of male rat at the estimated BMD_{10} was calculated. The results thus obtained were included in the figure presenting the results for the six model compounds of Chapter 6 resulting in Figure 7.2.
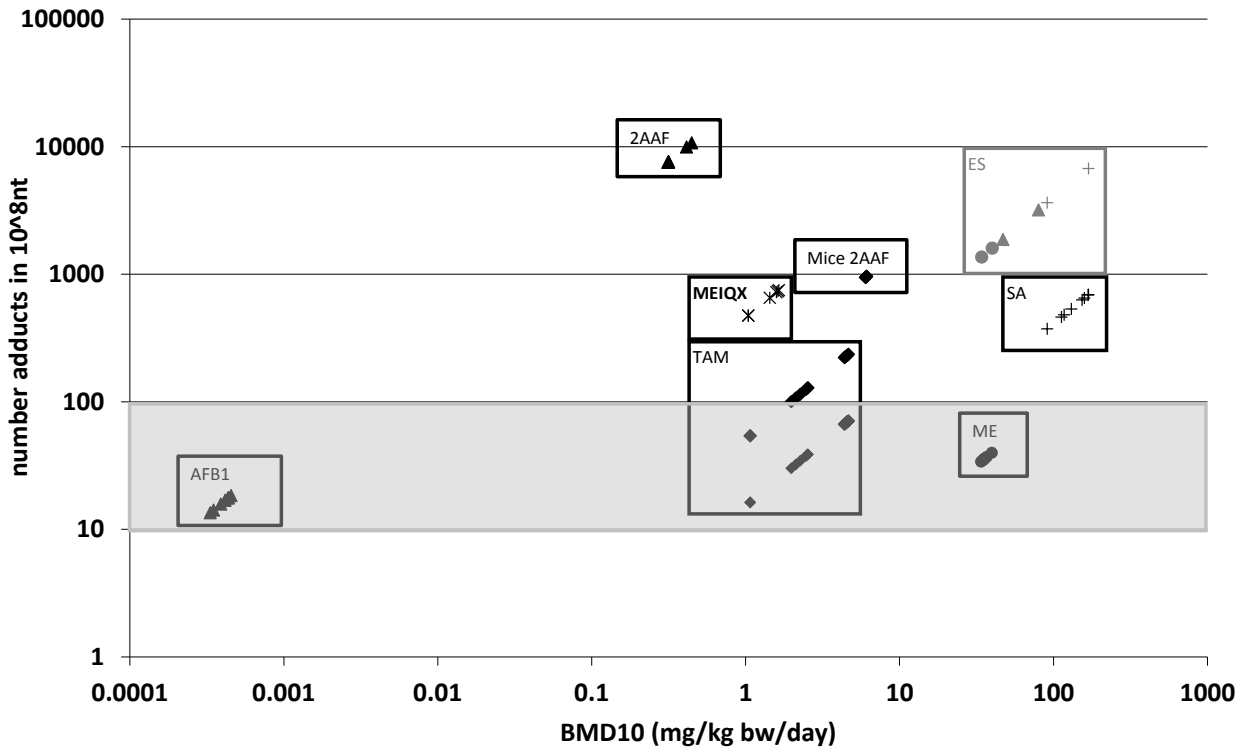

Figure 7.2. Levels of DNA adduct formation at the BMD_{10} for liver tumor formation by the six model compounds as related to endogenous DNA adduct levels (10 to 100 adducts in 10^8 nt, gray shadow; Williams, 2008; Farmer *et al.*, 2005; Farmer, 2008) in liver. The individual data points represent the outcome of each individual mathematical model for male rats treated with: 2-AAF, AfB1, MeIQx, SA, ME, and female rats treated with TAM, and male mice treated with 2-AAF (see chapter 6 for more details). In the grey box presented by grey crosses are the number of estragole adducts predicted to be formed when applying the BMD_{10} from rat *in vivo* data for safrole. The grey circles represent the number of estragole adducts predicted to be formed when applying the BMD_{10} from rat *in vivo* data for methyleugenol. Finally, the grey triangles are the number of estragole DNA adducts predicted to be formed at the BMD_{10} for estragole in rats estimated by multiplying the BMD_{10} in mice by a correction factor for the difference in species sensitivity (for further details see text).

The results presented in Figure 7.2. indicate that the number of DNA adducts formed at the BMD_{10} for estragole are predicted to be higher than the levels formed at the BMD_{10} values for safrole and methyleugenol, confirming the results found in mice in vivo by Randerath *et al.* (1983) reporting higher levels of DNA adduct formation of estragole than for safrole and methyleugenol at comparable dose levels. From this analysis it can be concluded that the data for estragole reveal that levels of DNA adduct formation at the BMD_{10} are predicted to be above the endogenous background levels (10-100 adducts in 10^8 nt, Williams 2008; Farmer et al., 2005; Farmer, 2008). This implies that at the BMD_{10} the levels of DNA adduct formed may contribute to the MOA of tumor formation by estragole.

7.3 Future Perspectives

Although the present thesis has extended the understanding and prediction of the dose-dependent bioactivation and detoxification of estragole, enabling prediction and understanding of the dose-dependent DNA adduct formation and elucidating the possible role of DNA adducts in the MOA of estragole by comparing their levels to endogenous levels for DNA damage, several issues remain to be elucidated to fully understand the implications of DNA adduct formation for tumor formation by estragole. The current section presents some considerations on future topics of importance in this field, including:

1) The matrix effect;

2) Use of DNA adduct data in cancer risk assessment;

3) Mode of action;

4) PBBD models for mutation and tumor formation.

7.3.1 The matrix effect

The present thesis focuses mainly on the formation of DNA adducts by exposure to estragole as a pure compound dosed by gavage. Also the results on tumor formation *in vivo* are generally obtained from studies with the pure compound dosed by gavage. In reality however, humans are mainly exposed to estragole via the diet, as a constituent of, for instance, herbs and spices. One could argue that dosing estragole as a pure compound by gavage does not reflect the human situation where estragole is consumed at low dose levels via the diet, and that it is essential to take the possible matrix effect into account in the risk assessment. In recent studies, for example, it was found that a methanolic basil extract was able to reduce the E-3′-N^2-dG adducts formation in HepG2 cells exposed to 1′-hydroxyestragole (Jeurissen *et al.,* 2007). Alhusainy *et al.* (2010) identified nevadensin (Figure 7.3) as the key compound present in basil extract responsible for this effect (Figure 7.4).
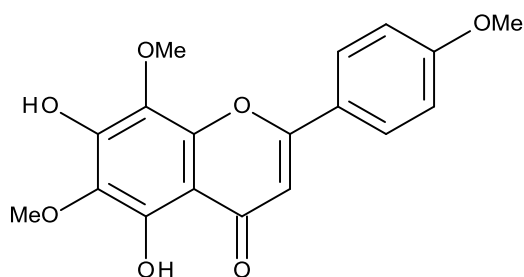

Fig. 7.3. Structural formula of nevadensin; the SULT inhibitor from basil (Alhusainy *et al.,* 2010).

This effect of nevadensin was shown to be due to inhibition of the sulfotransferase (SULT) mediated bioactivation of 1′-hydroxyestragole to 1′-sulfooxyestragole, leading to reduced formation of DNA adducts and increased chances for detoxification of 1′-hydroxyestragole via glucuronidaton or oxidation (Alhusainy *et al.,* 2010). Including the kinetics for SULT inhibition by nevadensin into the PBBK model for estragole bioactivation and detoxification revealed that co-administration of estragole at a level inducing hepatic tumors *in vivo* (50 mg/kg bw) with nevadensin at a molar ratio of 0.06, representing the ratio of their occurrence in basil, results in almost 100% inhibition of formation of the ultimate carcinogen 1′-sulfooxyestragole when assuming 100% uptake of nevadensin (Alhusainy *et al.*, 2010). Assuming 1% uptake of nevadensin, inhibition would still amount to more than 83%. It was concluded that the data point at a potential reduction of the cancer risk when estragole exposure occurs within a food matrix containing SULT inhibitors compared to what is observed upon exposure to pure estragole (Alhusainy *et al.*, 2010). Clearly future progress in the field of risk assessment of estragole will need to develop ways to take such matrix effects into account.
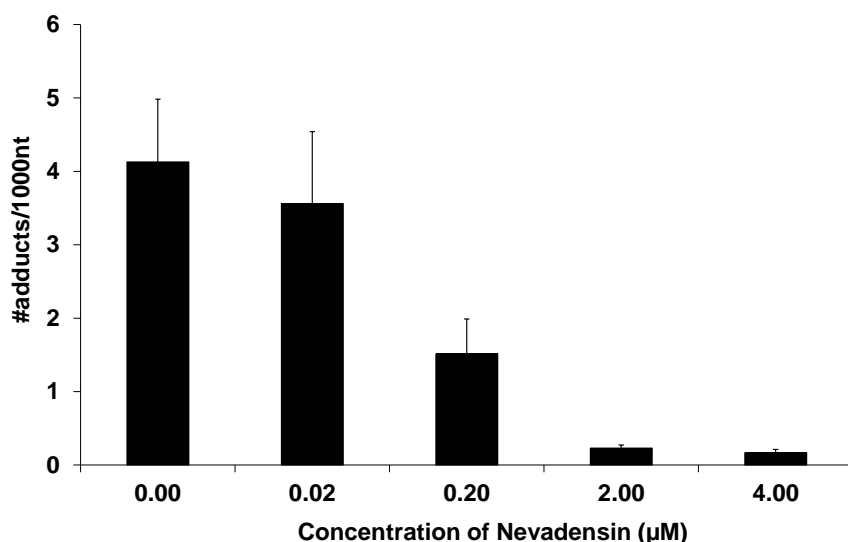

Figure 7.4. E-3′-N^2-dG formation in 10^3 nt in primary rat hepatocytes exposed for 4 h to 50 µM 1′-hydroxyestragole in the absence or presence of increasing concentrations (0–4 µM) of nevadensin. Data points represent mean (±Stdev) of triplicate measurements obtained in independent experiments (Alhusainy *et al.,* 2010).

7.3.2 Use of DNA adduct data in cancer risk assessment

A second item that needs to be further developed is how to use DNA adduct formation in future cancer risk assessment protocols. The potential use of DNA adduct data in risk assessment approaches was addressed in several workshops (Sander *et al.,* 2005; Pottenger *et al.,* 2009). Furthermore, a framework on how to organize and evaluate DNA adduct data in concert with data on subsequent key events in carcinogenicity was recently described (Jarabek *et al.,* 2009). This framework stresses that in risk assessment adduct data should not be considered in isolation, but in the context of other toxicological data, based on the current general knowledge of the carcinogenic process (Jarabek *et al.,* 2009). In an EFSA meeting in Brussels in 2005 no consensus was reached regarding the biological significance of low levels of DNA adducts, and the meeting rather identified the need for more experimental data and new approaches to enclose DNA adduct data into cancer risk assessment (EFSA, 2005). The aim of the present thesis was to develop new strategies to evaluate and even predict low dose effects of genotoxic carcinogens focusing especially on accurate and

realistic estimates of low dose DNA adduct formation and its possible biological relevance. However, important issues remain to be solved. In case of DNA reactive, genotoxic carcinogens, for example, it is often assumed that it is not possible to establish safe levels of exposure due to the lack of a threshold. Available data on the dose-dependent formation on DNA adducts *in vivo* can generally be described by a linear relation through the origin suggesting the absence of a threshold and low dose linearity for at least this part of the process leading to tumor formation (see also Figure 6.1 in **Chapter 6** of this thesis). This analysis is in line with the current ideas on this issue (Bolt *et al.,* 2004; EU-SCHER, 2009). However, close inspection of the data available reveals that the number of low dose data points included in these curves are generally limited with substantial experimental uncertainty. One could argue that more extended dose response curves with especially a larger number of low dose data points would be of use to judge whether there would be an apparent threshold (or not) for DNA adduct formation.

7.3.3 Mode of Action

Future studies should also be focused on elucidating the MOA of estragole in more detail putting emphasis on especially the nature, stability and location of adducts in the DNA, and a possible role for cytotoxicity. Results of the present thesis indicate that DNA adducts play a major role in the MOA of estragole mediated tumor formation. Future studies could focus on the location of these adducts, the possible occurrence of hot spots, and their repair. In Chapter 5 we describe that a significant increase in levels of DNA adducts formed was detected upon two hour incubation of primary rat hepatocytes with 1'-hydroxyestragole, and that the level of adducts rapidly decreased after cessation of treatment, indicating the activity of cellular repair mechanisms. In line with these findings it would be valuable to elucidate the mechanism of repair involved in the removal of the E-3′-N^2-dG adducts *in vivo*, using knockout rodents. Additionally, in Chapter 5 the persistence of low levels of adducts in the MOA of estragole was described and this result is in line with previously reported data for estragole showing persistency *in vivo* of estragole adducts (Phillips *et al.,* 1984). This estragole adduct persistency in time with repetitive dosing could lead to accumulation of adducts within the organ, and this corroborates a role for DNA adduct formation in the MOA of estragole. Results presented in Chapter 5 also revealed that at concentration where DNA adduct formation is strongly elevated also cytotoxicity and apoptosis occurs. This indicates that it could be of interest to further explore a possible role for cytotoxicity in the MOA.

7.3.4 PBBD models for mutation and tumor formation

Although the development of PBBD models for DNA adduct formation *in vivo*, as performed in the present thesis, takes the modeling approach one step beyond the kinetics for bioactivation and closer to the ultimate adverse effect of tumor formation, a real future challenge will be definition of models to predict tumor formation. To develop a systems biology PBBD approach that allows quantitative simulation of chemically induced carcinogenesis would be the ultimate goal. This approach should allow to make predictions on cancer development at different oral doses by simulating the sequence of events between initial exposure to the compound, its bioactivation and DNA adduct formation (as now achieved in the present thesis), but also the subsequent formation of mutations and neoplastic lesions. Such an approach would make testing for carcinogenicity less dependent on experimental animal studies and more directly relevant to the human situation. Punt (2011) describes how this approach might be made. A mathematic description of tumor

formation can be obtained with the Moolgavkar-Venzon-Knudson (MVK) multistage carcinogenesis model (Luebeck and Moolgavkar 2002). This model is based on the principle that cancer development is a multistage process in which normal cells transform into tumor cells via a series of transformations induced by sequential mutations in different tumor suppressor genes. This has been best characterized for colorectal cancer where mutations in the APC tumor suppressor gene have been linked to early stages in the carcinogenic process and mutations in K-ras and P53 tumor suppressor genes with malignant transformations that occur later in the carcinogenic process (Frank 2007). Coupling the MVK multistage carcinogenesis model for tumor progression with a physiologically based kinetic model that describes the absorption, distribution, metabolism, and excretion and the PBBD models that predict DNA adduct formation provides the opportunity to obtain a comprehensive simulation model of chemical carcinogenic (Conolly *et al.*, 1988). Although this conceptual model has been described before (Conolly *et al.*, 1988), it has so far not found any quantitative application in toxicological research. Limitations mainly occur in the parameterization of such models. *In vitro* experiments can play an important role to overcome this limitation. To date, the development of PBBK models based on *in vitro* data has been well established (Punt *et al.,* 2008, 2009, 2010; Al-Subeihi *et al.*, 2011; Martati *et al.*, 2011), but no experimental methods are presently available with which the death, division, and mutation rates of cells in different cancer stages and the effect of xenobiotic compounds on these rates can be determined. To determine the parameters needed for such models presents an important future challenge.

Another step to be included in these future models for tumor formation would be repetitive dose regimens, that may result in cumulative levels of DNA adducts in time. Whether this cumulative level is actually observed *in vivo* should be further investigated. Finally, gene and protein expression should be added to the *in silico* models to illustrate the cellular network response and make the approach a full system biology approach. This item could be explored following the approach described in Cucinotta *et al.* (2002). In this approach the mathematical description of mRNA and protein expression kinetics following DNA damage are described.

Taken altogether, these future challenges indicate that the approach described in the present thesis is an important step on the way from modeling kinetics in PBBK models to ultimately modeling tumor formation in PBBD models, since the results presented in the thesis model DNA adduct formation representing the first step beyond kinetics on the pathway to tumor formation. However, the future perspectives described above also illustrate that to finally reach a full system biology approach modeling of tumor formation at realistic low dose exposure levels *in vivo* on the basis of only *in vitro* data remains a real challenge. In spite of the difficulties of this challenge it is important to take the next steps on this pathway because it will ultimate contribute to science based risk assessment of the consequences of low dose exposure to genotoxic carcinogens preferably without the need for experimental animals studies.

Reference

Alhusainy WAAM, Paini A, Punt A, Louisse J, Spenkelink A, Vervoort J, Delatour T, Scholz G, Schilter, B, Adams T, van Bladeren PJ, and Rietjens IMCM. (2010) Identification of nevadensin as an important herb-based constituent inhibiting estragole bioactivation and physiology-based biokinetic modeling of its possible in vivo effect. Toxicology and Applied Pharmacology 245, 179-190.

Al-Subeihi AAA, Spenkelink B, Rachmawati N, Boersma MG, Punt A, Vervoort J, van Bladeren PJ, and Rietjens IMCM. (2011) Physiologically based biokinetic model of bioactivation and detoxification of the alkenylbenzene methyleugenol in rat. Toxicology in Vitro, 25(1), 267-285.

Boberg EW, Miller EC, Miller JA, Poland A, Liem A. (1983) Strong evidence from studies with brachymorphic mice and pentachlorophenol that 1'-sulfoöxysafrole is the major ultimate electrophilic and carcinogenic metabolite of 1'-hydroxysafrole in mouse liver. Cancer Res. Nov;43(11):5163-73.

Bolt HM, Foth H, Hengstler JG, and Degen GH. (2004) Carcinogenicity categorization of chemicals—new aspects to be considered in a European perspective. Toxicology Letters, 151, 29-41.

Conolly RB, Reitz RH, Clewell HJ, Andersen ME. (1988) Pharmacokinetics, biochemical mechanism and mutation accumulation: a comprehensive model of chemical carcinogenesis, Toxicol. Lett. 43 189–200.

Cucinotta FA, Dicello JF, Nikjoo H, and Cherubini R. (2001) Computational model of the modulation of gene expression following DNA damage. Radiation Protection Dosimetry. Vol. 99, (1–4), 85–90 (2002)

EFSA European Food safety Authority (2005). Opinion of the Scientific committee on a request of EFSA related to A harmonized approachfor Risk Assessment of substances which are both genotoxic andcarcinogenic. The EFSA journal, 282:1-31.

EU-SCHER (2009). Risk assessment methodologies and approaches for genotoxic and carcinogenic substances. Scientific Committee on Health and Environmental Risks (SCHER)- Scientific Committee on Consumer Products (SCCP)- Scientific Committee on Emerging and Newly Identified Health Risks (SCENIHR). http://ec.europa.eu/health/ph_risk/committees/04_scher/docs/scher_o_113.pdf

Farmer PB, Brown K, Tompkins E, Emms VL, Jones DJL, Singh R, and Phillips DH. (2005) DNA adducts: Mass spectrometry methods and future prospects Toxicology and Applied Pharmacology 207 (2005) S293 – S301.

Farmer PB. (2008) Significance for risk assessment of increases in background levels of carcinogen-derived protein and DNA Adducts. Abstracts / Toxicology Letters 180S (2008) S6–S27.

Frank SA. (2007) Dynamics of Cancer - Incidence, Inheritance, and Evolution Princeton (NJ): Princeton University Press.

Jarabek AM, Pottenger LH, Andrews LS, Casciano D, Embry MR, Kim JH, Preston RJ, Reddy MV, Schoeny R, Shuker D, Skare J, Swenberg J, Williams GM, and Zeiger E. (2009) Creating context for the use of DNA adduct data in cancer risk assessment: I. Data organization. Critical Reviews in Toxicology 39, 659-678.

Jeurissen SMF, Punt A, Boersma MG, Bogaards JJP, Fiamegos YC, Schilter B, van Bladeren PJ, Cnubben NHP, and Rietjens IMCM. (2007). Human cytochrome p450 enzyme specificity for the bioactivation of estragole and related alkenylbenzenes. Chemical Research in Toxicology 20, 798-806.

Johnson JD, Ryan MJ, Toft II JD, Graves SW, Hejtmancik MR, Cunningham ML, Herbert R. and Abdo KM. (2000) Two-Year Toxicity and Carcinogenicity Study of Methyleugenol in F344/N Rats and B6C3F1 Mice. J. Agric. Food Chem., 48 (8), pp 3620–3632

Khalil F, and Laer S. (2011) Physiologically Based Pharmacokinetic Modeling: Methodology, Applilcations, and Limitations with a Focus on its Role in Pediatric Drug Development. Journal of Biomedicine and Biotechnology (ahead of print) doi:10.1155/2011/907461.

Luebeck EG and Moolgavkar SH. (2002) Multistage carcinogenesis and the incidence of colorectal cancer. Proc. Natl Acad. Sci. USA, 99, 15095–15100.

Martati E, Boersma MG, Spenkelink A, Khadka DB, Punt A, Vervoort J, van Bladeren PJ, and Rietjens IMCM. (2011) A physiologically based kinetic (PBK) model for safrole bioactivation and detoxification in rat and comparison to those for estragole and methyleugenol.

Pottenger LH, Carmichael N, Banton MI, Boogaard PJ, Kim J, Kirkland D, Phillips RD, van Benthem J, Williams GM, and Castrovinci A. (2009) ECETOC workshop on the biological significance of DNA adducts: Summary of follow-up from an Expert Panel Meeting. Mutation Research/Genetic Toxicology and Environmental Mutagenesis 678, 152-157.

Phillips DH, Reddy MV, and Randerath K. (1984) P-32 Post-Labeling Analysis of DNA Adducts Formed in the Livers of Animals Treated with Safrole, Estragole and Other Naturally-Occurring Alkenylbenzenes. 2. Newborn Male B6c3f1 Mice. Carcinogenesis 5, 1623-1628.

Punt A, Freidig AP, Delatour T, Scholz G, Boersma MG, Schilter B, van Bladeren PJ, Rietjens IMCM. (2008). A physiologically based biokinetic (PBBK) model for estragole bioactivation and detoxification in rat. Toxicol. Appl. Pharmacol. 231:248-259.

Punt A, Paini A, Boersma MG, Freidig AP, Delatour T, Scholz G, Schilter B, van Bladeren PJ, Rietjens IMCM (2009). Use of physiologically based biokinetic (PBBK) modeling to study estragole bioactivation and detoxification in humans as compared with male rats. Toxicol. Sci. 110:255-269.

Punt A, Jeurissen SM, Boersma MG, Delatour T, Scholz G, Schilter B, van Bladeren PJ, Rietjens IMCM. (2010) Evaluation of human interindividual variation in bioactivation of estragole using physiologically based biokinetic modeling Toxicol. Sci. 113, 337– 348.

Punt A, (2011) Systems toxicology. Research Proposal for Veni Vernienwingsimplus grant.

Randerath K, Haglund RE, Phillips DH and Reddy MV. (1984) ^{32}P- Postlabelling analysis of DNA adducts formed in the livers of animals treated with safrole, estragole and other naturally-occurring alkenylbenzenes. I. Adult female CD-1 mice. Carcinogenesis, 5, 1613-1622.

Sander M, Cadet J, Casciano DA, Galloway SM, Marnett LJ, Novak RF, Pettit SD, Preston RJ, Skare JA, Williams GM, Van Houten B, and Gollapudi BB. (2005). Proceedings of a workshop on DNA adducts: Biological significance and applications to risk assessment Washington, DC, April 13-14, 2004. Toxicol. Appl. Pharmacol. 208: 1-20.

Smith RL, Adams TB, Doull J, Feron VJ, Goodman JI, Marnett LJ, Portoghese PS, Waddell WJ, Wagner B, Rogers AE, Caldwell J, and Sipes IG. (2002). Safety assessment of allylalkoxybenzene derivatives used as flavouring substances - methyl eugenol and estragole. Food Chem. Toxicol. 40: 851-870.

van den Berg S, Restani P, Boersma MG, Delmulle L, Rietjens IMCM. (2011) Levels of genotoxic and carcinogenic ingredients in plant food supplements and associated risk assessment. Food and Nutrition Sciences, Food and Nutrition Sciences, 2, 989-1010.

Williams GM. (2008). Application of mode-of-action consideration in human cancer risk assessment. Toxicol. Lett. 180: 75-80.

Chapter 8

NEDERLANDSE SAMENVATTING

8 SAMENVATTING

Onze voeding bevat verschillende stoffen die, als zij in geïsoleerde vorm worden getest in dierproeven, genotoxisch en carcinogeen blijken te zijn. Tot op dit moment is er geen wetenschappelijke consensus over de manier waarop de risicoschatting van deze stoffen moet worden uitgevoerd wanneer zij in lage doses in het dieet aanwezig zijn binnen een complexe voedingsmatrix. Om de evaluatie van de risico's, gerelateerd aan deze in voeding aanwezige genotoxische carcinogenen, te verbeteren is het noodzakelijk informatie te verkrijgen over de "mode of action" (MOA) bij lage doses versus hoge doses, over soortverschillen in toxicokinetiek en toxicodynamiek, inclusief dosis- en soortafhankelijke verschillen in DNA-schade en –herstel, en over effecten op expressie van relevante eiwitten. Voor de moderne Toxicologie is het van belang nieuwe methoden te ontwikkelen voor accuratere en meer wetenschappelijk gebaseerde extrapolatie van kankerincidenties, bepaald in dierproeven bij hoge doses, naar de mogelijke incidentie bij lage doses die relevant zijn voor blootstelling van de mens. Onlangs zijn zogenoemde "physiologically based biokinetic" (PBBK)-modellen ontwikkeld om voorspellingen te doen over detoxificering en bioactivering van de genotoxische carcinogene alkenylbenzenen estragol, methyleugenol en safrol als modelstoffen (Punt et al., 2008; Punt et al., 2009; Martati et al., 2011 Al-Subeihi et al, 2011). Deze PBBK-modellen maakten duidelijk dat, vanaf een hoog dosisniveau als de BMD_{10} (benchmarkdosis die 10% extra tumorincidentie veroorzaakt) naar een laag dosisniveau zoals de zogeheten virtual safe dose (VSD) (de dosis die resulteert in één op de miljoen extra tumorincidenties bij levenslange blootstelling), de vorming van de carcinogene metaboliet van estragol en andere alkenylbenzenen lineair was met de dosis. De PBBK-modellen lieten tevens zien dat soortverschillen tussen ratten en mensen klein zijn. Dit bevestigt dat, wat betreft de toxicokinetiek, lineaire extrapolatie van de kankerincidentie bij hoge doses in proefdieren naar de incidentie bij lage doses voor de mens, mogelijk zou zijn. De PBBK-modellen houden echter geen rekening met verdere biodynamische stappen in het carcinogene proces, zoals DNA-adductvorming, DNA-herstel, mutagenese en vorming van neoplasma's. Daarom was het doel van dit proefschrift de PBBK-modellen voor estragol uit te breiden naar zogeheten "physiologically based biodynamic" (PBBD- modellen voor DNA-adductvorming, en daarmee de modellen een stap dichter naar het ultieme eindpunt - tumorvorming- te brengen. Dergelijke modellen zullen risicobeoordeling ondersteunen omdat zij inzicht kunnen verschaffen in hoe te extrapoleren van hoge- naar lage dosisniveaus, tussen soorten, inclusief de mens, en tussen individuen. Bovendien draagt het bouwen van de PBBD-modellen die *in vivo* DNA-adductvorming voorspellen, gebaseerd op alleen *in vitro* parameters, bij tot de 3Rs (Replacement, Reduction en Refinement, ofwel vervanging, reductie en verfijning) van dierproeven.

In **Hoofdstuk 1** van dit proefschrift wordt het doel van het onderzoek geïntroduceerd en worden achtergrondgegevens verstrekt over de mechanismen die ten grondslag liggen aan DNA-adductvorming door genotoxische carcinogenen, het mogelijk herstel van deze adducten, strategieën voor kankerrisicoschatting, PBBK- en PBBD-modellen en de in voeding aanwezige genotoxische- en carcinogene modelstof -estragol- van het voorliggende proefschrift. Het doel van het experimentele werk dat in dit proefschrift wordt gepresenteerd, was een beter begrip, en zelfs het voorspellen, van DNA-adductvorming *in vitro* en *in vivo* in de rat, maar ook in de mens, bij blootstelling aan realistisch lage dosisniveaus (**Hoofdstuk 2-4**) en tevens een beter begrip van de MOA van tumorinductie door estragol (**Hoofdstuk 5**). In **Hoofdstuk**

6 worden beschikbare literatuurgegevens over DNA-adduct en tumorincidenties met betrekking tot een serie genotoxische levercarcinomen geanalyseerd, teneinde inzicht te verkrijgen in de relaties tussen DNA-adductvorming en tumorincidentie.

Met het doel om voor realistisch lage blootstellingsniveaus DNA-adductvorming te modelleren in de menselijke populatie, was een eerste stap het eerder ontwikkelde PBBK-model voor bioactivering en detoxificering van estragol in de rat (Punt et al., 2009) uit te breiden naar een PBBD-model dat in staat zou zijn DNA-adductvorming te voorspellen in de lever van de rat. Het PBBK-model maakt een schatting mogelijk van de dosis-afhankelijke vorming van 1'-sulfooxyestragol, de reactieve metaboliet van estragol, die instabiel is en resulteert in DNA- en eiwitbinding. Het PBBK-model voorspelt echter alleen kinetische eigenschappen en eindpunten. **Hoofdstuk 2** van dit proefschrift beschrijft de uitbreiding van het eerder ontwikkelde PBBK-model van de rat naar een PBBD-model dat de dosisafhankelijke *in vivo* DNA-adductvorming van estragol in de lever van de rat voorspelt. Dit PBBD-model werd ontwikkeld met gebruikmaking van *in vitro* data over DNA-adductvorming, bepaald met behulp van primaire rat-hepatocyten blootgesteld aan 1'-hydroxyestragol. Omdat hepatocyten, behalve de vorming van de carcinogene metaboliet 1'-sulfooxyestragol en DNA-adducten, ook DNA-herstel kunnen vertonen, is DNA-herstel impliciet opgenomen in het model. Om het PBBD-model te definiëren, werd het PBBK-model uitgebreid door het gebied onder de curve voor 1'-hydroxyestragol-vorming die werd voorspeld door het PBBK-model, te koppelen aan het gebied onder de curve voor 1'-hydroxyestragol in het *in vitro* experiment. De uitslag van het nieuw ontwikkelde PBBD-model voor de rat werd geëvalueerd op basis van gegevens in muizen, omdat voor de rat geen gegevens over estragol-afhankelijke DNA-adductvorming beschikbaar waren. Het PBBD-model voorspelde bij een dosis van 400 mg/kg lichaamsgewicht per dag vorming van lever DNA-adducten op een niveau van 40.000 in 10^8 nt, terwijl de waarde die in een experiment met muizen werd gevonden, 10.000 in 10^8 nt was. Deze data zijn in redelijke overeenstemming, zeker gegeven het verschil in diersoort. Bovendien liet het resultaat van het PBBD-model een lineaire toename van DNA-adductvorming zien, met oplopende estragol-doses tot 100 mg/kg lichaamsgewicht. Bij realistisch geschatte menselijke innameniveaus van 0.01 mg estragol/kg lichaamsgewicht per dag (Smith et al., 2002) en 0.07 mg estragol/kg lichaamsgewicht per dag (SCF, 2001) voorspelt het PBBD-model hoeveelheden van E-3'-N^2dG DNA-adductvorming van respectievelijk 2 en 12.8 in 10^8nt. Deze niveaus van adducten zijn 1 tot 2 orden van grootte lager dan het achtergrondniveau van DNA-schade van 100 adducten in 10^8 nt, waarvan is gesteld dat het geen consequenties heeft (Williams, 2008). Daarnaast zijn deze niveaus ook 1 tot 2 orden van grootte lager dan de achtergrondniveaus van DNA-adducten, gevormd door laag moleculaire alkylerende modelverbindingen, zoals N-nitrosaminen, die 10-100 adducten in 10^8 nt bedragen (Farmer, 2005; Farmer, 2008). De conclusie is dat, hoewel de DNA-adductvorming van genotoxische carcinogenen over het algemeen wordt gezien als een biomarker van blootstelling en niet als een biomarker van respons, het nu ontwikkelde PBBD-model een stap dichter bij het uiteindelijke toxische effect van estragol is dan het PBBK-model dat eerder werd beschreven. Het PBBD-model verschaft ook een "proof-of-principle" van modellering van een toxicodynamisch *in vivo* eindpunt op basis van uitsluitend *in vitro* experimentele gegevens. Dit toont aan dat PBBD-modellering kan bijdragen aan de 3Rs (Replacement, Reduction en Refinement) voor dierproeven. Ten slotte maakte het model voorspelling mogelijk van DNA-adductvorming bij lage en

realistische humane blootstellingniveaus en dit liet zien dat bij deze lage blootstellingsniveaus DNA-adductvorming ruim beneden het achtergrondniveau ligt van DNA-schade van 100 adduct in 10^8nt, waarvan is gesteld dat dit geen consequenties heeft.

Gegeven het feit dat de evaluatie van het resultaat van het PBBD-model moest plaatsvinden op basis van data van muizen omdat data van DNA-adductvorming bij blootstelling aan estragol van ratten niet beschikbaar waren, was het doel van **Hoofdstuk 3** zowel de dosis-afhankelijke estragol DNA-adductvorming in rattenlever als de dosis-afhankelijke urine-excretie van 1'-hydroxyestragol glucuronide te kwantificeren om zo het PBBD-model, dat in **Hoofdstuk 2** werd ontwikkeld, beter te kunnen valideren. In deze studie werd bij groepen mannelijke Sprague-Dawley ratten (n=10, per groep) eenmalig estragol toegediend via gavage met dosisniveaus van 0 (controlegroep), 5, 30, 75, 150 en 300 mg/kg lichaamsgewicht. Er werd urine opgevangen en na 48 uur werden de dieren opgeofferd en werden de lever, nieren en longen geanalyseerd op DNA-adducten door middel van LC-MS/MS. De verkregen resultaten lieten een dosis-afhankelijke toename van DNA-adductvorming zien in de lever. In longen en nieren werden DNA-adducten gevonden met lagere niveaus dan in de lever. Dit bevestigde de vorming van DNA-adducten in vooral het doelorgaan, de lever. De verkregen resultaten lieten zien dat de PBBD-modelvoorspellingen voor zowel excretie van 1'-hydroxyestragol glucuronide in de urine als voor de E-3'-N^2-dG DNA-adductvorming in de lever, vergelijkbaar waren binnen een orde van grootte met de waarden die *in vivo* werden gemeten. De niveaus van excretie van 1'-hydroxyestragol glucuronide in de urine waren 4.6 tot 7.7 keer overschat en die van de DNA-adducten slechts 1.9 tot 2.3 maal. De verkregen resultaten leveren de eerst beschikbare dataset op over estragol DNA-adductvorming in ratten en bevestigen hun aanwezigheid in metabool actief weefsel, zoals lever, long en nier, terwijl de hogere niveaus die werden gevonden in de lever in overeenstemming zijn met de lever als doelorgaan voor carcinogeniteit. De ontwikkeling en validatie van dit PBBD-model voor DNA-adductvorming van estragol in ratten, vormde de basis voor modellering van de dosisafhankelijke estragol DNA-adductvorming in de lever bij de mens, zoals is gebeurd in **Hoofdstuk 4**.

In **Hoofdstuk 4** zijn de niveaus van DNA-adducten voorspeld die bij blootstelling aan estragol bij een realistisch innameniveau van een humaan dieet zouden kunnen voorkomen in de humane lever, waarbij rekening is gehouden met interindividuele variaties binnen de humane populatie in de bioactivering van estragol tot zijn carcinogene metaboliet 1'-sulfooxyestragol. Schattingen van DNA-adductvorming in de menselijke lever bij blootstelling aan estragol werden gebaseerd i) op het eerder gedefinieerde PBPK-model voor estragol detoxificering en bioactivering in de mens (Punt et al., 2009), ii) op data over interindividuele variatie in de kinetiek voor de biotransformatie-enzymen met de meeste invloed op 1'-sulfooxyestragol vorming en iii) op een vergelijking die de relatie beschrijft tussen 1'-sulfooxyestragol-vorming en DNA-adductvorming welke is gebaseerd op het ratten-PBBK-model (Punt et al., 2008) en de dosisafhankelijke *in vivo* DNA-adductvorming zoals gevonden in ratten (**Hoofdstuk 3**). Interindividuele verschillen in de V_{max} en K_m voor de biotransformatie-enzymen met de meeste invloed op de vorming van 1'-sulfooxyestragol, werden bepaald door gebruik te maken van S9 leverpreparaten van 22 individuele donoren. Modellering op basis van de individuele kinetische constanten leverde informatie over de individuele verschillen in vorming van 1'-sulfooxyestragol en DNA-adducten en op deze wijze werd een 25-voudige variatie aangetoond tussen de 22 individuen. Daarenboven werd een Monte Carlo-simulatie uitgevoerd om verschillen te evalueren in de

vorming van 1'-sulfooxyestragol en de vorming van estragol DNA-adducten in de gehele populatie. Geconcludeerd werd dat deze analyses lieten zien dat bij een geschatte dagelijkse inname van 0.01 mg estragol/kg lichaamsgewicht per dag de DNA-adductniveaus binnen, of zelfs onder, het endogene DNA-adductniveau van 10-100 adducten per 10^8 nt bleven, een niveau waarvan eerder was gesuggereerd dat dit geen biologische consequenties zou hebben, en tevens beneden de waarde van 490 adducten per 10^8 nt die eerder werden gerapporteerd als de waarde die vereist was voor een statistisch significante tumorinducerende potentie van alkenylbenzeen DNA-adducten. Daarom toonden de resultaten van **Hoofdstuk 4** een te verwaarlozen risico aan voor de gemiddelde menselijke populatie bij de huidige ingeschatte dagelijkse innameniveaus van estragol. Het is belangrijk te benadrukken dat de validiteit en kwaliteit van PBBK/BD-modelsimulaties afhangt van het corresponderende model en dat het een volledige experimentele dataset vereist voor zowel kinetische als dynamische processen die zich voordoen in biologische systemen. PBBK/BD-modellen weerspiegelen de huidige wetenschappelijke kennis en terwijl sommige processen goed zijn beschreven, kan er voor andere aspecten gebrek aan gegevens zijn zodat aannames noodzakelijk zijn (Khalil en Lear, 2011). In **Hoofdstuk 4** bijvoorbeeld is een aanname gedaan dat DNA-herstel in de mens te vergelijken zou zijn met het herstel in de rat om de inschatting van de niveaus van adductvorming te maken bij lage estragoldoses in humaan dieet. Deze aanname is gedaan omdat er geen beschikbare informatie of experimentele data zijn over het verschil tussen mensen en knaagdieren in DNA-herstelprocessen voor estragol. In risicoschattingen kan met dergelijke informatieleemten rekening worden gehouden door onzekerheidsfactoren in te calculeren. Om die informatieleemte te ondervangen, is in **Hoofdstuk 4** een 7.9-voudige onzekerheidsfactor voor dynamische onzekerheden toegepast. Integratie van aanvullende informatie over humaan DNA-herstelmechanismen voor estragol DNA-adducten, zouden het model verder kunnen verfijnen.

Hoofdstuk 5 beschrijft studies die zijn uitgevoerd om beter inzicht te verkrijgen in de mogelijke rol van DNA-adducten in de "mode of action" (MOA) van estragol. De MOA van estragol werd *in vitro* verder onderzocht met gebruikmaking van primaire hepatocyten, waarbij de mogelijke implicaties van DNA-schade en –herstel na blootstellen van de cellen aan 1'-hydroxyestragol werden onderzocht. De verkregen resultaten toonden aan dat aanzienlijk toegenomen niveaus van DNA-adducten werden waargenomen na twee uur durende incubatie van primaire rat-hepatocyten met 1'-hydroxyestragol en dat het niveau van adducten snel verminderde na beëindiging van de behandeling, waarmee de activiteit van cellulaire herstelmechanismen werd aangetoond. Er werden echter geen specifieke DNA-schade- en herstelroutes geactiveerd. De verkregen gegevens toonden zelfs een significante afname van de expressie van genen die betrokken zijn bij DNA-schade en –herstel op transcriptioneel niveau. Voorts suggereerden de resultaten –hoewel de cellulaire herstelactiviteit tot op zekere hoogte in staat is estragol DNA-adducten te verwijderen- dat vorming van adducten niet volledig omkeerbaar is, getuige de rol van aanhoudend lage niveaus van estragol DNA-adducten in blootgestelde cellen, zelfs na een ruime blootstellingsvrije periode. Dit bevestigt een mogelijke rol van DNA-adducten in de MOA van estragol. Resultaten die in **Hoofdstuk 5** worden gepresenteerd, laten ook zien dat bij een concentratie van 1'-hydroxyestragole waar DNA-adductvorming in de cellen sterk stijgt, ook cytotoxiciteit en apoptose voorkomen. Dit betekent dat het van belang is verder onderzoek te doen naar een mogelijke rol van cytotoxiciteit in de MOA van estragol.

In **Hoofdstuk 6** tot slot, werden beschikbare literatuurgegevens geanalyseerd over DNA-adductvorming en tumorincidenties voor een reeks van genotoxische levercarcinogenen, om zo inzicht te verkrijgen in de relaties tussen DNA-adductvorming en tumorincidentie. Dosis-respons gegevens van zowel carcinogeniteit en *in vivo* DNA-adductvorming in de rattenlever waren beschikbaar voor zes stoffen, te weten: 2-acetylaminefluorene (2AAF),   aflatoxine B1 (AfB1), methyleugenol (ME), safrol (SA), 2-amino-3,8-dimethylimidazo[4,5-f]quinoxaline (MelQX) en tamoxifen (ATM). Hoewel een dataset voor estragol niet beschikbaar was, konden datasets voor de aan estragol verwante alkenylbenzenen methyleugenol (ME) en safrol (SA) (Figuur 8.1) worden meegenomen in de analyse. BMD_{10}-waarden (bench mark dosis die 10% extra tumorincidentie veroorzaakt) voor levercarcinogeniteit geïnduceerd door de zes stoffen, werden berekend uit *in vivo* tumorgegevens, waarbij gebruik werd gemaakt van de EPA benchmark dose software (http//www.epa.gov/ncea/bmds/index.htlm,visited in 2010).
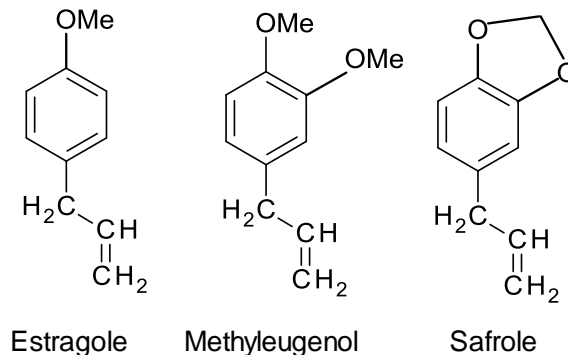

Figuur 8.1. Structuur formules van verwante alkenylbenzenen:
estragol, methyleugenol, en safrol.

Bij een volgende stap, waarbij gebruik gemaakt werd van beschikbare gegevens voor dosis-afhankelijke DNA-adductvorming in de lever, kon het niveau van DNA-adducten bij de BMD_{10} worden berekend. Dit maakte vergelijking mogelijk van de niveaus van DNA-adductvorming bij de BMD_{10} voor de verschillende genotoxische carcinogenen. Het maakte tevens vergelijking mogelijk van deze niveaus van DNA-adductvorming bij de BMD_{10} met beschikbare data over de endogene achtergrond van DNA-schade in het doelorgaan, de lever. Hoewel voor een individueel carcinogeen de tumorrespons toeneemt als de adductniveaus toenemen, toonden de verkregen resultaten aan dat –bij vergelijking van verschillende carcinogenen- geen kwantitatieve correlatie bestaat tussen het niveau van DNA-adductvorming en carcinogeniteit. Deze gegevens bevestigen dat de kwantiteit van DNA-adducten, gevormd door een DNA-reactieve stof, niet een bewijs is voor een bepaalde mate van carcinogeniciteit, maar dat andere factoren, zoals het type adduct, de mutagene potentie van het adduct of andere factoren die bijdragen aan de MOA, mogelijk net zo relevant zijn. Bovendien toonde vergelijking van de DNA-adductniveaus bij de BMD_{10} met achtergrond-DNA-schade aan dat, hoewel voor sommige carcinogenen (bijvoorbeeld 2AAF) het niveau van DNA-adductvorming bij de BMD_{10} ver boven de achtergrondniveaus ligt, de DNA-schade door andere genotoxische carcinogenen (bijvoorbeeld AfB1 en ME), bij de BMD_{10} binnen de achtergrondniveaus blijft. Dit suggereert voor de laatstgenoemde twee stoffen dat de gevormde DNA-adducten ofwel meer mutageen en

carcinogeen zijn dan het type van de achtergrond-DNA-adducten, ofwel dat andere mechanismen dan DNA-adductvorming bijdragen aan de MOA van de tumorvorming. Deze resultaten ondersteunen de notie dat het voorkomen van DNA-adducten, niet op een uniforme manier gecorreleerd is aan de ontwikkeling van kanker en dat de aard van de DNA-adducten en/of hun locatie binnen het genoom moeten worden meegewogen wanneer DNA-adductvorming wordt vertaald naar het risico op kanker. Dit resultaat benadrukt de noodzaak van toepassing van het MOA-raamwerk om het belang van DNA-adductvorming in carcinogeniteit te begrijpen.

Tenslotte wordt in **hoofdstuk 7** van het proefschrift een samenvatting gegeven van de resultaten en conclusies en worden zaken van belang voor toekomstig onderzoek beschreven. In dit hoofdstuk werd ook een analyse gemaakt van de mogelijke DNA adductvorming door estragol bij een geschatte BMD_{10} voor tumorvorming. Zoals al eerder vermeld, is er geen dataset beschikbaar voor dosisafhankelijke tumorvorming door estragol in ratten, hetgeen inhoudt dat –om in de lever een schatting van DNA-adductvorming bij de BMD_{10} mogelijk te maken- deze BMD_{10}-waarde op een andere manier moet worden geschat. Om de BMD_{10} voor estragol-afhankelijke vorming van levertumoren in de rat te schatten, zijn twee benaderingen toegepast. Ten eerste, gegeven het feit dat estragol en de omzetting ervan naar 1'-sulfooxyestragol aantoonbaar vergelijkbaar is met vorming van de 1'-sulfooxy metaboliet van de gerelateerde alkenylbenzenen methyleugenol en safrol (Jeurissen et al., 2007; Martati et al., 2011) zouden de BMD_{10} -waarden van ratten voor safrol, (91-169 mg/kg lichaamsgewicht per dag), en voor methyleugenol (35-40 mg/kg lichaamsgewicht per dag) (**Hoofdstuk 6**) gebruikt kunnen worden. Dan kan met behulp van deze waarden en het ratten PBBD-model (**Hoofdstuk 2**) het aantal estragol-adducten in leverweefsel bij de BMD_{10} berekend worden. In de tweede benadering werd de BMD_{10} voor estragol-afhankelijke vorming van levertumoren in de rat geschat gebaseerd op de BMD_{10} voor estragol-tumorvorming in muizen en werd een correctiefactor bepaald voor het verschil in gevoeligheid tussen muizen en ratten, gebaseerd op beschikbare datasets voor de gerelateerde alkenylbenzenen methyleugenol en safrol. De BMD_{10}-waarden voor safrol en methyleugenol in ratten bedragen 91-169 mg/kg lichaamsgewicht per dag en 35-40 mg/kg lichaamsgewicht per dag (**Hoofdstuk 6**). Verder bedragen de BMD_{10}-waarden voor safrol en methyleugenol in muizen 9.4-16.4 mg/kg lichaamsgewicht per dag (gebaseerd op data van de *in vitro* studie, uitgevoerd door Boberg et al., 1983) en 3-4 mg/kg lichaamsgewicht per dag (gebaseerd op data van de *in vivo* studie, uitgevoerd door NTP, Johnson et al., 2000). Dit houdt in dat voor deze twee gerelateerde alkenylbenzenen de BMD_{10} in ratten gemiddeld 10 maal hoger is dan die werd gevonden in muizen. Door gebruik te maken van deze correctiefactor en de BMD_{10}, ontleend aan een muizenstudie voor estragol van 4.7-8 mg/kg lichaamsgewicht per dag (Van den Berg et al., 2011) kan deze BMD_{10} worden omgezet naar een waarde voor ratten tussen 47 en 80 mg/kg lichaamsgewicht per dag. Door deze geschatte BMD_{10}-waarden te gebruiken in het PBBD-model, werd het niveau berekend van DNA-adductvorming in de lever van de mannelijke rat bij de geschatte BMD_{10}-waarden. De aldus verkregen resultaten voor estragol werden verwerkt in de figuur die de resultaten presenteert voor de zes modelstoffen van **Hoofdstuk 6**, resulterend in figuur 8.2.
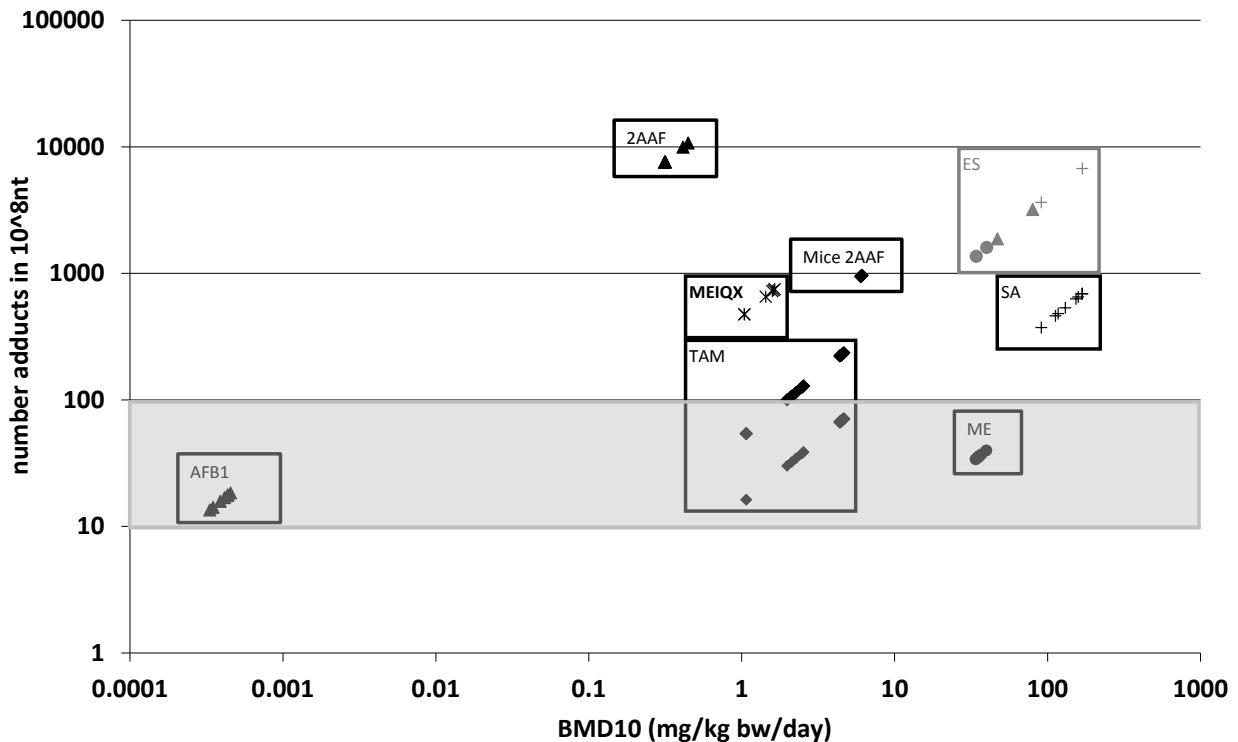
Figuur 8.2. Niveaus van DNA-adductvorming bij BMD_{10} voor tumorvorming in de lever van de zes modelstoffen gerelateerd aan endogene DNA-adduct niveaus (10-100 adducten in 10^8 nt, grijs gearceerd; Williams, 2008; Farmer *et al.*, 2005; Farmer, 2008) in de lever. De individuele datapunten geven de resultaten weer van elk individueel model voor mannelijke ratten blootgesteld aan: 2-AFF, AfB1, MelQx, SA, ME, en vrouwelijke ratten blootgesteld aan TAM, en mannelijke muizen blootgesteld aan 2-AFF (zie hoofdstuk 6 voor meer details). De grijs kruisen in het grijs vak geven de schatting weer van het aantal estragol adducten die worden gevormd, gebaseerd op *in vivo* data bij de BMD_{10} van ratten voor safrol. De grijs circels geven de schatting weer van het aantal estragol adducten die worden gevormd, gebaseerd op *in vivo* data bij de BMD_{10} van ratten voor methyleugenol. Tot slot geven de grijs driehoeken een schatting weer van het aantal estragol DNA-adducten die worden gevormd bij de BMD_{10} van estragol in ratten bij vermenigvuldiging de BMD_{10} in muizen met een correctiefactor voor het verschil in species gevoeligheid (voor verdere details zie tekst).

De resultaten zoals gepresenteerd in figuur 8.2, laten zien dat het aantal DNA-adducten, gevormd bij de BMD_{10} voor estragol, hoger zouden zijn dan de niveaus gevormd bij de BMD_{10}-waarden voor safrol en methyleugenol. Dit bevestigt de resultaten die gevonden zijn bij muizen *in vivo* door Randerath et al., (1983) waar bij vergelijkbare dosisniveaus hogere niveaus van DNA-adductvorming van estragol werden gerapporteerd dan voor safrol en methyleugenol. Uit de analyse kan worden geconcludeerd dat de data voor estragol laten zien dat niveaus van DNA-adductvorming bij de BMD_{10} boven de endogene achtergrondniveaus uit komen (10-100 adducten in 10^8 nt, Williams 2008, Farmer et al., 2005, Farmer, 2008). Dit betekent dat bij de BMD_{10} de gevormde niveaus van DNA-adducten mogelijk bijdragen tot de MOA van tumorvorming door estragol.

Al met al wordt geconcludeerd dat de benadering die in het huidige proefschrift is beschreven, een belangrijke stap is om van het modelleren van kinetiek in PBBK-modellen te komen tot het uiteindelijk modelleren van tumorvorming in PBBD-modellen. Dit omdat de resultaten van het proefschrift DNA-adductvorming modelleren en dit de eerste stap is in de route van kinetiek naar tumorvorming. Echter om uiteindelijk een volledige computergebaseerde modellering van tumorvorming *in vivo* bij realistische lage blootstellingsniveaus the realiseren op basis van alleen *in vitro* data, moeten ook nog andere mechanistische aspecten in de beschouwing worden meegenomen. Dit betreft bijvoorbeeld het matrixeffect, genexpressies en mutaties. Het is belangrijk deze volgende stappen in de modellering te zetten, omdat de benadering uiteindelijk zal bijdragen aan een op wetenschap gebaseerde risico-evaluatie van de consequenties van blootstelling aan lage doses genotoxische carcinogenen zonder de noodzaak voor experimentele dierstudies, en dus op die manier bijdraagt aan de 3R-benadering.

Referenties

Al-Subeihi AAA, Spenkelink B, Rachmawati N, Boersma MG, Punt A, Vervoort J, van Bladeren PJ, and Rietjens IMCM. (2011) Physiologically based biokinetic model of bioactivation and detoxification of the alkenylbenzene methyleugenol in rat. Toxicology in Vitro, 25(1), 267-285.

Boberg EW, Miller EC, Miller JA, Poland A, Liem A. (1983) Strong evidence from studies with brachymorphic mice and pentachlorophenol that 1'-sulfoöxysafrole is the major ultimate electrophilic and carcinogenic metabolite of 1'-hydroxysafrole in mouse liver. Cancer Res. Nov;43(11):5163-73.

EFSA European Food safety Authority (2005). Opinion of the Scientific committee on a request of EFSA related to A harmonized approachfor Risk Assessment of substances which are both genotoxic andcarcinogenic. The EFSA journal, 282:1-31.

EU-SCHER (2009). Risk assessment methodologies and approaches for genotoxic and carcinogenic substances. Scientific Committee on Health and Environmental Risks (SCHER)- Scientific Committee on Consumer Products (SCCP)- Scientific Committee on Emerging and Newly Identified Health Risks (SCENIHR). http://ec.europa.eu/health/ph_risk/committees/04_scher/docs/scher_o_113.pdf

Farmer PB, Brown K, Tompkins E, Emms VL, Jones DJL, Singh R, and Phillips DH. (2005) DNA adducts: Mass spectrometry methods and future prospects Toxicology and Applied Pharmacology 207 (2005) S293 – S301.

Farmer PB. (2008) Significance for risk assessment of increases in background levels of   carcinogen-derived   protein   and   DNA Adducts. Abstracts / Toxicology Letters 180S (2008) S6–S27.

Jeurissen SMF, Punt A, Boersma MG, Bogaards JJP, Fiamegos YC, Schilter B, van Bladeren PJ, Cnubben NHP, and Rietjens IMCM. (2007). Human cytochrome p450 enzyme specificity for the bioactivation of estragole and related alkenylbenzenes. Chemical Research in Toxicology 20, 798-806.

Johnson JD, Ryan MJ, Toft II JD, Graves SW, Hejtmancik MR, Cunningham ML, Herbert R. and Abdo KM. (2000) Two-Year Toxicity and Carcinogenicity Study of Methyleugenol in F344/N Rats and B6C3F1 Mice. J. Agric. Food Chem., 48 (8), pp 3620–3632

Khalil F, and Laer S. (2011) Physiologically Based Pharmacokinetic Modeling: Methodology, Applilcations, and Limitations with a Focus on its Role in Pediatric Drug Development. Journal of Biomedicine and Biotechnology (ahead of print) doi:10.1155/2011/907461.

Martati E, Boersma MG, Spenkelink A, Khadka DB, Punt A, Vervoort J, van Bladeren PJ, and Rietjens IMCM. (2011) A physiologically based kinetic (PBK) model for safrole bioactivation and detoxification in rat and comparison to those for estragole and methyleugenol.

Phillips DH, Reddy MV, and Randerath K. (1984) P-32 Post-Labeling Analysis of DNA Adducts Formed in the Livers of Animals Treated with Safrole, Estragole and Other Naturally-Occurring Alkenylbenzenes. 2. Newborn Male B6c3f1 Mice. Carcinogenesis 5, 1623-1628.

Punt A, Freidig AP, Delatour T, Scholz G, Boersma MG, Schilter B, van Bladeren PJ, Rietjens IMCM. (2008). A physiologically based biokinetic (PBBK) model for estragole bioactivation and detoxification in rat. Toxicol. Appl. Pharmacol. 231:248-259.

Punt A, Paini A, Boersma MG, Freidig AP, Delatour T, Scholz G, Schilter B, van Bladeren PJ, Rietjens IMCM (2009). Use of physiologically based biokinetic (PBBK) modeling to study estragole bioactivation and detoxification in humans as compared with male rats. Toxicol. Sci. 110:255-   269.

Punt A, Jeurissen SM, Boersma MG, Delatour T, Scholz G, Schilter B, van Bladeren PJ, Rietjens IMCM. (2010) Evaluation of human interindividual variation in bioactivation of estragole using physiologically based biokinetic modeling Toxicol. Sci. 113, 337– 348.

Randerath K, Haglund RE, Phillips DH and Reddy MV. (1984) [32]P- Postlabelling analysis of DNA adducts formed in the livers of animals treated with safrole, estragole and other naturally-occurring alkenylbenzenes. I. Adult female CD-1 mice. Carcinogenesis, 5, 1613-1622.

Smith RL, Adams TB, Doull J, Feron VJ, Goodman JI, Marnett LJ, Portoghese PS, Waddell WJ, Wagner B, Rogers AE, Caldwell J, and Sipes IG. (2002). Safety assessment of allylalkoxybenzene derivatives used as flavouring substances - methyl eugenol and estragole. Food Chem. Toxicol. 40: 851-870.

van den Berg S, Restani P, Boersma MG, Delmulle L, Rietjens IMCM. (2011) Levels of genotoxic and carcinogenic ingredients in plant food supplements and associated risk assessment. Food and Nutrition Sciences, Food and Nutrition Sciences, 2, 989-1010.

Williams GM. (2008). Application of mode-of-action consideration in human cancer risk assessment. Toxicol. Lett. 180: 75-80.

Appendix

Abbreviations

$^{15}N_5$-dG	1,2,3,7,9-$^{15}N_5$-2′-Deoxyguanosine ($^{15}N_5$-dG)
2-AAF	2-Acetylaminofluorene
AfB1	Aflatoxin B1
BER	Base Excision Repair
BMD	Benchmark Dose
BMR	Benchmark Response
DAD	Diode Array Detection
DDR	Direct damage reversal
DSBR	Double strand breaks repair
DSBs	Double strand breaks
dG	2'-deoxyguanosine
E-1'-N^2-dA	N^6-(trans-isoestragol-3′-yl)-deoxyadenosine
E-3'-7-dG	7-(trans-isoestragol-3′-yl)-deoxyguanosine
E-1'-N^2-dG	N^2-(estragol-1′-yl)-deoxyguanosine
E-3'-8-dG	8-(trans-isoestragol-3′-yl)-deoxyguanosine
E-3'-N^2-dG	N^2-(trans-isoestragol-3′-yl)-deoxyguanosine
EDI	Estimated Daily Intake
EFSA	European Food Safety Authority
Ercc1	Excision Repair Cross-Complementing, group 1
ES	Estragole
ESI	Electrospray Ionization
FEMA	Flavor and Extract Manufacturers Association
Gadd45α	Growth arrest and DNA damage 45-alpha
GC-MS	Gas Chromatography – Mass Spectrometry
GSH	Glutathione
GST	Glutathione-s-transferase
H2A.X	H2A histone family X
HE	1'-Hydroxyestragole
HEG	1'-Hydroxyestragole glucuronide
Hr	Hour
Hrs	Hours
HPLC	High Performance Liquid Chromatography
JECFA	Joint FAO/WHO Expert Committee on Food Additives
LDH	Lactate dehydrogenase
LC-MS	Liquid Chromatography – Mass Spectrometry
Min	Minute/s
ME	Methyleugenol

MeIQx	2-amino-3,8-methylimidazo[4,5-f]quinoxaline
MOA	Mode of Action
MOE	Margin of Exposure
NAD$^+$	Nicotinamide Adenine Dinucleotide
NADH	Reduced Nicotinamide Adenine Dinucleotide
NER	Nucleotide excision repair
nt	nucleotide
OE	1′-oxoestragole
P450	Cytochrome P450 enzyme
PAPS	3'-Phosphoadenosine-5'-phosphosulfate
PARP	Poly (ADP-ribose) Polymerase
PBBD	Physiologically based biodynamic
PBBK	Physiologically based biokinetic
PFS	Plant Food Supplements
SA	Safrole
SCF-EU	Scientific Committee on Food of the European Union
SD	Sprague Dawley
Stdev	Standard Deviation
SULT	Sulfotransferase
tA	trans-Anethole
TAM	Tamoxifen
TLS	Translesion synthesis
UV	Ultra-violet
VSD	Virtual Safe Dose

Acknowledgement

I owe special thanks to Ivonne for her inspiration, guidance, endless energy and passion for toxicology and science, and to Peter to have opened the doors to the most valuable research center where I was able to perform most of my experiments and build a large experience using various techniques. The experiments described in the thesis were mainly carried out at the Nestlé Research Center (NRC), Lausanne, Vaud, Switzerland.

I am indebted to my supervisors at the Nestlé Research Center from whom I have learned so much throughout my PhD project and who have helped paved the way for this thesis: Gabriele, Maricel, and Benoit.

Special thanks to the following scientists who have contributed directly or indirectly to this thesis, I am deeply grateful to each one of them: Thierry, Begona, Veronika, Ans, and Gerrit for brainstorming and constructive criticism.

In addition I would like to thank the people at the NRC: Gabriela, Clotilde, Dominique, Claudine, Helia, Patrick, Aurelien and Alexandra for their contribution to this thesis by explaining techniques, helping-out, and for coffee breaks *(what else?)*. My thanks also to Florian for introducing me to the world of synthesis, and to Eric for being patient and always in a good mood in explaining new LC-MS/MS instruments, software, and macro-systems. Bert, Hans, Laura, and Marelle for helping while I was performing experiments in the laboratories at Toxicology (TOX) in Wageningen. Rene and Bert for taking care of the *in vivo* part of the project at Wageningen. Special thanks to the administrative assistants, without whom trip planning and organization of meetings would have been difficult, Irene, and Gre (at TOX), Karin, Laurance, Fabiene and Christine (at NRC). Irene dank je wel for translating the summary of this thesis to Dutch.

Merel, Suzanne, Linda, Nynke to be great friends and perfect G.G. and for organizing the several TOX-ladies *chick flick*s movie nights. Thanks to Ana, David, Jochem, Wasma, Henrique, Niek, Si, Alexandros, Arif, Barae, Reiko, Walter, Marije, Samantha and Karsten, for sharing valuable experience. Thanks to all the PhD students and staff at the department of Toxicology for the time spent together over drinks and wonderful times spent during Lab trips and the PhD international excursion to Switzerland and Italy.

I would like to acknowledge my friends: Alessandra, Alessia, Begona, Claudia, Eveline, Flaminia, Imelda, Laetitia, Marie Emily, Nanna, Paola, Sophie, Veronika, Vera, Meindert's **A** friends, and "I mitici" for the wonderful time spent in Italy, the Netherlands, and Switzerland in these four years.
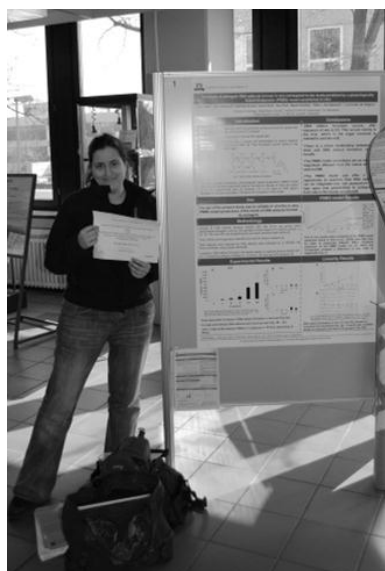
Finally, to my family: Anna, Marco, Isa, Giorgio, Adreo,zio Luca, Matteo, zio Marco. To my extended family Kent & Stefania and Valentina, Stefano, and Alberto. Special appreciations goes to my boyfriend Meindert and his family to whom I am grateful.

Thank you all for your encouragement and support during this long journey!

Alicia

About the Author

Alicia Paini was born on the 23rd of April 1980, in Ponte dell'Olio, Piacenza (I). After spending several years in the US, Australia, and New Caledonia, she graduated in 1999 from the Liceo Scientifico G. Marconi in Parma (Italy). She enrolled in 1999 in a 5 year study program in Food Science and Technology at the University of Parma (Italy). In 2004 she obtained a 7 months Erasmus scholarship to conduce part of her specialization thesis in Food Analytical Chemistry at the Department of Food Chemistry at Wageningen University (The Netherlands), in collaboration with Douwe Egberts under the supervision of Dr. Hank Schols. After obtaining the laurea in Food Science and Technology from the University of Parma, in 2006 she started the Master program in Food Safety at Wageningen University. She completed her studies in November 2007 after performing the Msc thesis within the Department of Toxicology under the supervision of Dr. Ans Punt and Prof. Ivonne M.C.M. Rietjens and her internship at the Nestlé Research Center in Lausanne (Switzerland) under the supervision of Dr. Gabriele Scholz and Dr. Benoit Schilter. From November 2007 to December 2011 she was appointed the PhD position at the Toxicology Department in collaboration with the Chemical Food Safety Group of the Nestlé Research Center under the supervision of Dr. Gabriele Scholz, Prof. Ivonne M.C.M. Rietjens and Prof. P.J. van Bladeren, on the project discussed in the present thesis. During her PhD she followed several postgraduate courses in Toxicology so she could register as a Toxicologist within the Netherlands Society of Toxicology. She attended several workshops and conferences during these 4 years and in March 2011 her work was awarded with the Mutagenesis/Oxford University Press Poster Award at the UKEMS/DUTCH EMS-sponsored Workshop on Biomarker of exposure and 7th GUM [32]Postalabelling workshop (Münster, Germany, 28-29 March 2011). After the end of her PhD thesis contract she collaborated on several projects at the Toxicology Department and she lectured on a one day course into LC-MS/MS techniques. On the 31st of January 2012 she was selected for a postdoc - grant holder position at JRC-IHCP, Ispra, Italy, to start in April 2012.

List of Publications

Alhusainy W, van den Berg SJPL, **Paini A,** Campana, A, Spenkelink A, Punt A, Scholz G, Schilter B, Adams TB, van Bladeren PJ, Rietjens IMCM. Matrix modulation of the bioactivation of estragole by different alkenylbenzene-containing herbs and spices and physiologically-based biokinetic modeling (PBBK) of possible *in vivo* effects (Submitted).

Paini A, Scholz G, Schilter B, van Bladeren PJ, Rietjens IMCM, Punt A. Evaluation of interindividual human variation in bioactivation and DNA binding of estragole in liver predicted by physiologically based biodynamic (PBBD) and Monte Carlo modeling (Submitted).

Paini A, Scholz G, Guignard G, Bezecon C, Dias Latado H, Schilter B, van Bladeren PJ, Rietjens IMCM, Marin-Kuan M. DNA damage response induced by 1'-hydroxyestragole in rat primary hepatocytes (Submitted).

Paini A, Gremaud E, Scholz G, Gerrit A, Punt A, Schilter B, van Bladeren PJ, Rietjens IMCM. Dose-dependent estragole DNA adduct formation in rat liver measured *in vivo* and predicted by physiologically based biodynamic (PBBD) modeling (Submitted).

Paini A, Scholz G, Marin-Kuan M, Schilter B, O'Brien J, van Bladeren PJ, Rietjens IMCM. (2011). Quantitative comparison between *in vivo* DNA adduct formation from exposure to selected DNA-reactive carcinogens, natural background levels of DNA adduct formation and tumor incidence in rodent bioassays. Mutagenesis 26, 5, 605-618.

Alhusainy W, **Paini A,** Punt A, Louisse J, Spenkelink A, Vervoort J, Delatour T, Scholz G, Schilter B, Adams TB, van Bladeren PJ, Rietjens IMCM. (2010). Identification of nevadensin as an important herb-based constituent inhibiting estragole bioactivation and physiology-based biokinetic modeling of its possible in vivo effect. Toxicology and Applied Pharmacology 245, 2, 179-190.

Paini A, Punt A, Viton F, Scholz G, Delatour T, Marin-Kuan M, Schilter B, van Bladeren PJ, Rietjens IMCM. (2010). A physiologically based biodynamic (PBBD) model for estragole DNA binding in rat liver on in vitro kinetic data and estragole DNA adduct formation in primary rat hepatocytes. Toxicology and Applied Pharmacology 245, 1, 57-66.

Punt A, **Paini A**, Boersma MG, Freidig AP, Delatour T, Scholz G, Schilter B, van Bladeren PJ, Rietjens IMCM. (2009). Use of physiologically based biokinetic (PBBK) modeling to study estragole bioactivation and detoxification in humans as compared with male rats. Toxicological Science 110, 2, 255-269.

List of Publication in Preparation

Alhusainy W, **Paini A,** Taylor S, Vervoort J, Scholz G, Schilter B, Adams T, van Bladeren PJ, Rietjens IMCM. (in preparation). Protective effect of nevadensin against estragole induced DNA adduct formation in male Sprague-Dawley rats.

Al-Subeihi A, **Paini A,** van Bladeren PJ, Rietjens IMCM. (in preparation). Inhibition of methyleugenol bioactivation by the herb-based constituent nevadensin and prediction of possible in vivo consequences using physiology based kinetic modelling.

van den Berg SJPL, Punt A, Soffers AEMF, **Paini A**, Spenkelink B, Ngeleja S, Rietjens IMCM. (in preparation). Physiologically based kinetic (PBK) models for the alkenylbenzene elemicin in rat and human.

Martati E, Boersma MG, Spenkelink A, Boonpawa R, **Paini A,** van Bladeren PJ , Punt A, Rietjens IMCM. (in preparation). Matrix effect of mace exract reducing safrole bioactivation and physiologically based biokinetic of its possible in vivo effect.

List of Abstract

Alhusainy W, Van den Berg SJPL, Campana, A, **Paini A,** Spenkelink A, Punt A, Scholz G, Schilter B, Adams TB, van Bladeren PJ, Rietjens IMCM. Matrix modulation by different alkenylbenzenes-containing herbs and spices of the bioactivation of estragole and physiologically-based biokinetic modeling of possible in vivo effects. Proceedings of the Annual Congress of The British Toxicology Society, Toxicology, 290, (2-3), 147–148, December 2011 (Poster Presentation).

Paini A, Gremaud E, Scholz G, Gerrit A, Punt A, Schilter B, van Bladeren PJ, Rietjens IMCM. The levels of estragole DNA adducts formed in vivo corresponds to the levels predicted by a physiologically based biodynamic (PBBD) model established *in vitro.* 8th Nestlé International Nutrition Symposium – NINS -, Nestlé Research Center, 19-21 October 2011. Lausanne, Switzerland (Poster Presentation).

Rietjens IMCM, Punt A, Alhusainy W, **Paini A**, Scholz G, Schilter B, Adams T, and van Bladeren PJ. Allylalkoxybenzenes: risk assessment of a class of food-borne genotoxic carcinogens. Abstract book –EUROTOX2011, August 2011. Paris, France (Oral Presentation).

Paini A, Scholz G, Schilter B, van Bladeren PJ, Rietjens IMCM. Estragole DNA adducts formed in vivo corresponds to the levels predicted by a physiologically based biodynamic (PBBD) model established *in vitro.* Toxicology PhD international trip symposium at Givaudan, June 2011. Kemptthal, Switzerland (Oral Presentation).

Paini A, Gremaud E, Scholz G, Gerrit A, Punt A, Schilter B, van Bladeren PJ, Rietjens IMCM. The levels of estragole DNA adducts formed in vivo corresponds to the levels predicted by a physiologically based biodynamic (PBBD) model established *in vitro.* Phd Days of the Netherlands Society of Toxicology, O1-P27. 17-18 May 2011. Zeist, The Netherlands (Oral & Poster Presentation).

Alhusainy W, Van den Berg SJPL, Campana, A, **Paini A,** Spenkelink A, Punt A, Scholz G, Schilter B, Adams TB, van Bladeren PJ, Rietjens IMCM. Matrix modulation by different alkenylbenzenes-containing herbs and spices of the bioactivation of estragole and physiologically-based biokinetic modeling of possible in vivo effects. Phd Days of the Netherlands Society of Toxicology, P1. 17-18 May 2011. Zeist, The Netherlands (Poster Presentation).

Paini A, Gremaud E, Scholz G, Gerrit A, Punt A, Schilter B, van Bladeren PJ, Rietjens IMCM. The levels of estragole DNA adducts formed in vivo corresponds to the levels predicted by a physiologically based biodynamic (PBBD) model established *in vitro.* Workshop Munster 28-29 March 2011, Mutagenesis 24, 5, 698. Munster, Germany (Poster Presentation).

Paini A, Scholz G, Bezecon C, Guignard G, Delatour T, Schilter B, van Bladeren PJ, Rietjens IMCM, Marin-Kuan M. Persistence of estragole DNA adduct in primary rat hepatocytes. IUTOX 2010 Abstract/Toxicology Letters 196S, S157 - P202, 2010. Barcelona, Spain (Poster Presentation).

Alhusainy W, **Paini A,** Punt A, Louisse J, Spenkelink A, Vervoort J, van den Berg S, Campana A, Scholz G, Schilter B, Adams T, van Bladeren PJ, Rietjens IMCM. Matrix modulation by different alkenylbenzenes-containing herbs and spices of the bioactivation of estragole and physiologically-based biokinetic modeling of possible in vivo effects. Phd Days of the Netherlands Society of Toxicology, O3-P1. 1st -2nd June 2010. Zeist, The Netherlands (Oral & Poster Presentation).

Paini A, Scholz G, Delatour T, Schilter B, van Balderen PJ, Rietjens IMCM. Low doses naturally genotoxic compounds and implication for risk assessment. Current Research 2010, Graduate School VLAG, 2010.

Alhusainy W, Louisse J, Punt A, Vervoort J, **Paini A,** Delatour T, Scholz G, Schilter B, Boersma M, van Bladeren PJ, Adams TB, Rietjens IMCM. Matrix effect on the bioactivation of estragole to its proximate carcinogen. 30th anniversary of the Netherlands Society of Toxicology: P09, 2009. Veldhoven, The Netherlands (Poster Presentation).

Paini A, Punt A, Scholz G, Delatour T, Schilter B, van Balderen PJ, Rietjens IMCM. A Physiologically based biodynamic (PBBD) model to assess 1'-hydroxyestragole metabolite-induced DNA adduct formation of estragole in rat liver. 30th anniversary of the Netherlands Society of Toxicology: P61, 2009. Veldhoven, The Netherlands (Poster Presentation).

Paini A, Scholz G, Delatour T, Viton F, Guignard G, Schilter B, van Bladeren PJ, Rietens IMCM. Low dose estragole and 1'-hydroxyestragole induced DNA adduct formation. EUROTOX 2008. Abstract /Toxicology Letters 180S S73 – R43, 2008. Rhodes, Greece (Poster Presentation).

Punt A, Carolus E, **Paini A**, Freidig AP, Delatour T, Scholz G, Schilter B, van Bladeren PJ and Rietjens IMCM. Development of Physiologically Based Biokinetic Model for Estragole in Man. Phd Days of the Netherlands Society of Toxicology . 12th -13th June 2007. Wageningen, The Netherlands (Poster Presentation).

Overview of completed training activity

Courses

General Toxicology, WUR, Wageningen,	2008
Animal Course Module I, CHUV, Lausanne,	2008
Mutagenicity and Carcinogenicity, PET, Leiden,	2009
Pathobiology, PET, Utrecht,	2009
Organ toxicology, PET, Utrecht,	2009
Physiologically Based Pharmacokinetic (PBPK) Modeling, Wageningen,	2009
Toxicogenomics, PET, Utrecht,	2010
Animal Course Dutch art.9, LAS, Utrecht,	2010
Immunotoxicology, PET, Utrecht,	2010
Risk Assessment, PET, Wageningen,	2010
Medical Forensic Toxicology and Regulatory Toxicology, PET, Utrecht,	2010
Ecotoxicology, PET, Utrecht/Wageningen,	2011

Specific Training Certified at the Nestlé Research Center (NRC)

Training in LC-MS/MS techniques, NRC, Lausanne,	2008
Training in perfusion & culture of rat primary hepatocytes, NRC, Lausanne,	2008

Meetings and Workshops

HESI Project Committee on the Biological Significance on DNA Adducts - Workshop, Cavtat,	2008
45th Congress of the European Society of Toxicology, Rhodes,	2008
30th Anniversary Meeting of the NVT, Veldhoven,	2009
8th International Comet Assay Workshop, Perugia,	2009
XII International Congress of Toxicology, Barcelona,	2010
UKEMS / Dutch EMS-sponsored Workshop on Biomarker of Exposure and Oxidative DNA Damage & 7th GUM 32P-postlabelling Workshop, Munster,	2011
NVT annual meeting and PhD student meeting, Zeist,	2011

General Courses, Meetings, and Activities

VLAG, AIO-week, Bilthoven,	2008
Techniques for Writing and Presenting Scientific Papers, WGS, Wageningen,	2008
Team Room Course, NRC, Lausanne,	2009
Hazard Chemical Safety Course, NRC, Lausanne,	2010
Waters Forum - analytical instruments- course update, NRC, Lausanne,	2010
Mini symposium 'How to write a world-class paper', WUR, Wageningen,	2010
Workshop "picture, tables, and info graph in your research", Wageningen,	2011

Optional

Preparation of Research Proposal	2008
Attending research discussion at Toxicology	2008-2011
Attending research discussion at Nestlé Research Center	2008-2011
Organization and participation at the international Toxicology PhD study tour	2011

Approved by Graduate School VLAG